# High Performance Materials from Renewable Aliphatic Polyesters

A DISSERTATION
SUBMITTED TO THE FACULTY OF THE GRADUATE SCHOOL
OF THE UNIVERSITY OF MINNESOTA
BY

Deborah Kay Schneiderman

IN PARTIAL FULFILLMENT OF THE REQUIREMENTS
FOR THE DEGREE OF
DOCTOR OF PHILOSOPHY

Marc A. Hillmyer, Advisor

August, 2016

# Acknowledgements

First and foremost, I would like to thank my advisor, Marc Hillmyer, for his exceptional guidance and support during my PhD work. I cannot imagine a more professional or knowledgeable advisor, and I am grateful for the opportunity to develop as a researcher under his direction.

Other professors who have taught me directly or inspired me in other ways during my graduate studies are Frank Bates, Chris Macosko, Jane Wissinger, Paul Dauenhauer, and Kechun Zhang.

The opportunity to visit APS on several occasions was facilitated by the Argonne Trip Planning Committee, made up of several students of the Lodge, Bates, and Hillmyer research groups. Although the composition of this group has shifted throughout my time at UMN, I would particularly like to thank Tim Gillard, Sangwoo Lee, Morgan Schulze, and Matt Irwin for making these trips both fun and productive. I would also like to thank Byeongdu Lee and Denis Keane of APS Beamlines 12-ID-B and DND-CAT, respectively, for training and assistance with experiments.

Further thanks to several members of the staff including, Letitia Yao and David Giles for training on NMR and rheology instruments, respectively, Kiley Schmidt for help with graphic design, and Laura Seifert for her extraordinary work as managing director of the CSP.

I have benefitted in many ways from collaborations with Mingyong Xiong, Chaoqun Zhang, Jiuyang Zhang, Tuoqi Li, Annabelle Watts, Katie Vinter, Jake Brutman, Charlie Spanjers, Ingrid Haugan Smidt, Marie Vanderlaan, Tessie Panthani, and Alex Mannion at UMN and Kyle O' Conner, Xiaopeng Yu, and Maria Sanford at Cornell. Much of the work described here would not have been possible without their help. Special thanks to the many undergraduate researchers I have mentored throughout my time here. These people are Erin Hill, Lindsay Davis, Ming Yu, Marcello Herrera, Cody Beam, Jay Wang, Derek Batiste, and Maggie Lau.

Many past graduate students and post-doctoral associates of the Hillmyer group have both assisted me with my research and enriched my graduate school experience. Most notably Mark Martello helped me get me started with my research project and provided several helpful and stimulating discussions. Other past and present members of the Hillmyer group who were particularly helpful during my time in the group are Paula Delgado, Henry Martinez, Josh Speros, Andrew Mullins, Jonathan Hollinger, Sam Dalsin, Justin Kennemur, and Alex Todd.

Lastly I would like to thank my parents, Judy and Richard Schneiderman. Among the many other reasons I have to thank them, they taught me the value of perseverance and of hard work.

# Dedication

This thesis is dedicated to Darren Olson, whose teaching inspired me to study chemistry, and to Ted Pappenfus, who guided me through my first encounter with research.

> "Aluminum beer cans, plastic spoons,
> plywood veneer, PVC pipe, vinyl seat covers,
> don't exactly burn, don't quite rot,
> flood over us,
>
> robes and garbs
> of the Kālī-yūga
>
>
> end of days."

—Gary Snyder, *LMFBR* in *Turtle Island*, 1974

# Abstract

Although synthetic polymers are essential to our society, their manufacture and disposal can be damaging to the environment. This dissertation is concerned with the development of new high performance sustainable polymers for a wide variety of applications. The first chapter gives a brief overview of the polymer industry and introduces past work in arena of sustainable polymers with a particular focus on poly(lactide). The remaining chapters discuss my research efforts to expand on earlier work to toughen poly(lactide) using a block polymer approach. Described first is the syntheses of renewable and degradable aliphatic polyester copolymers polyols containing ε-caprolactone. These statistical copolymers are used as building blocks to prepare mechanically tunable triblock and multiblock materials (Chapter 2). Following this, an efficient semisynthetic route to a branched lactone monomer, MVL, is presented and discussed. The potential of this monomer for the synthesis of block polymer and polyurethane materials is explored (Chapters 3 and 5, respectively). A large portion of each of these chapters is dedicated to exploring the relationship between aliphatic polyester structure and key physical parameters that influence material performance (summarized in Chapter 4).

# Table of Contents

viii

# List of Tables

# List of Figures

# List of Schemes

# Chapter 1. Background and Introduction

This chapter provides a brief overview of the current synthetic polymer industry, and includes a discussion of the major factors that have motivated the development of sustainable polymers. Examples of commercial bioplastics are briefly discussed, with special attention paid to the renewable compostable polyester poly(lactide). Finally, the major objectives of this research are outlined.

## 1.1 Background

### 1.1.1 Polymer Industry at a Glance

It would be difficult to overstate the importance of synthetic polymers to modern life. These versatile materials can be found in consumer products as deceptively simple as food packaging and bubble gum or as specialized as medical implants, bulletproof vests, and composites for aircraft. The remarkable commercial success of these synthetic materials is due to their low cost and amazing versatility. All polymers are giant chain-like molecules composed of small repeating subunits called monomers; however, different polymers vary in the type, number and arrangement of monomers in the polymer chain. Because the chemical structure of a polymer dictates its physical properties, chemists and engineers can design and make synthetic polymers with almost any desired combination of characteristics.

Two major types of polymers, thermosets and thermoplastics, are broadly defined by their ability to be reprocessed. Whereas thermosets are chemically crosslinked networks that are cured or set in a permanent shape, thermoplastics can be melted and reprocessed at elevated temperatures. While each class has its own advantages, by volume thermoplastics comprise the majority (approximately two-thirds) of the synthetic polymer industry, with nearly 300 million tons produced in 2015.[1] Perhaps as a consequence the terms plastic and polymer are often used interchangeably. The production history of the thermoplastics industry and the current market share of major commodity plastics are given in Figure 1.1.[1,2] Incredibly, the exponential growth

of industry means that by total volume more plastics have been produced in first 15 years of the 21$^{st}$ century than total in the entire 20$^{th}$ century.

Under the umbrella of thermoplastics, the highest volume plastics are, in order, polypropylene (PP), low-density and linear low-density polyethylene (LDPE and LLDPE, respectively), high-density polyethylene (HDPE), polyvinylchloride (PVC), polystyrene (PS), and polyethylene terephalate (PET). Together these polymers make up over 70% of all commodity plastics, a category that also encompasses other inexpensive high-volume polymers, including poly(methyl methacrylate) (PMMA).[2] In general commodity plastics are used for high volume, low-value applications where thermal and mechanical properties are not critical.



**Figure 1.1**

3
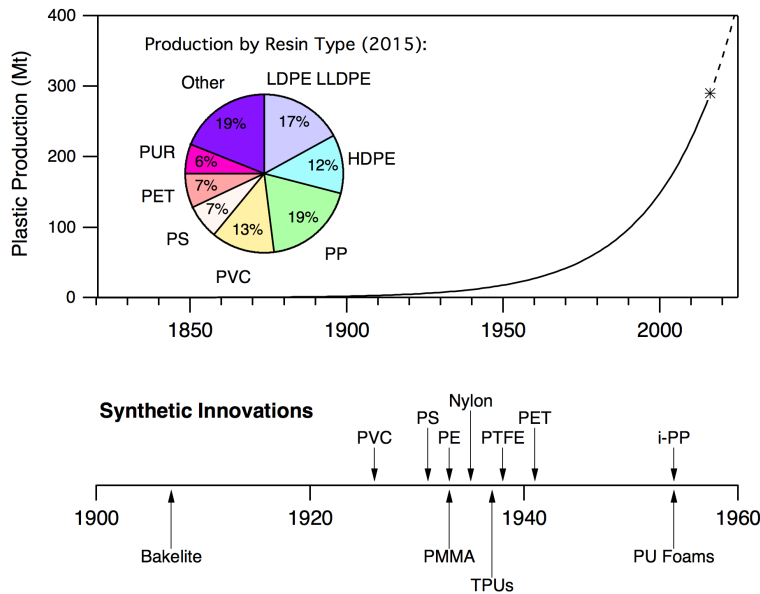
Compared to commodity materials, engineering plastics are produced on a much lower scale. This category includes high impact polystyrene (HIPS), acrylonitrile butadiene styrene (ABS), nylon, and polyurethanes (PUR), among others. Engineering plastics are more expensive to produce than commodity materials and are used for applications where improved mechanical or thermal performance is required (e.g., automobile parts and protective headgear).[3] Specialty plastics, such as polysulfones (PSU), polyether ether ketone (PEEK), and polybenzimidazole (PBI), are even more expensive to produce. These polymers and often have very high glass transition ($T_g$) or melting ($T_m$) temperatures. They are used for high-value niche applications, for example, fuel cell membranes, medical implants, and protective apparel.[4,5]
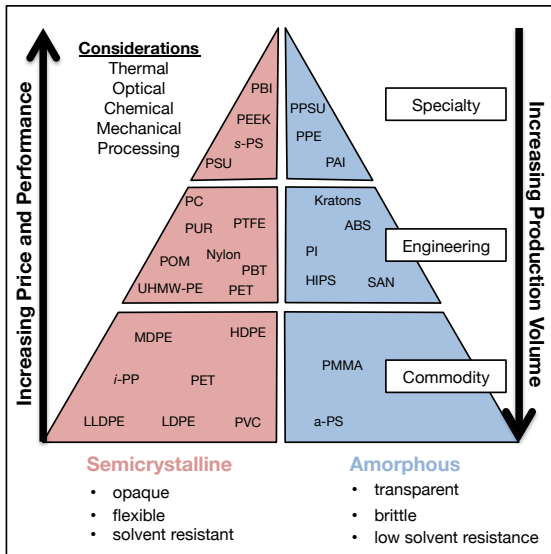


**Figure 1.2**

Value pyramid of commodity, engineering, and specialty plastics. Abbreviations of polymers not defined in the text are given at the end of the chapter, along with a list of the thermal properties of these polymers.

### 1.1.2 Social Benefits of Polymers

Polymers have many inherent advantages and can even be used improve the sustainability of consumer products. For example synthetic polymers can be used in vehicles to replace heavier materials like steel. This strategy can be used to increase fuel efficiency and reduce manufacturing costs. Indeed, while plastic components currently make up nearly 50% of the volume of a typical car, this equates to less than 10% of the total weight.[6] Though impressive this figure pales in comparison to airplanes, which are over 50% synthetic polymers by weight.[7] Similarly polymeric foams can be used to insulate buildings, which can directly reduce the costs and green house gas emissions associated with heating and air conditioning.

Even in seemingly trivial applications plastics can positively impact the environment and human heath. Used as food packaging, plastics can reduce waste by preventing spoilage. Additionally, packaged food and bottled water is often a crucial part of relief efforts following natural disasters. In medicine, plastic packaging keeps medical instruments sterile, forms the ubiquitous pill blister packs, and is used to store blood and plasma. Other medicinal uses for plastics include insulation on pacemakers, coatings for stents, resorbable sutures and bone screws, and carriers or excipients for drug delivery. More recently, polymers have even been used as pro-drugs or active pharmaceutical ingredients.[8]

In many contact sports polymers protect athletes from injury. For example, in football and cycling, polycarbonate helmets with polymer foam padding help prevent concussions and other head injuries. Other types of protective gear largely made from

polymers include shoulder padding, plastic mouth guards and shin guards. Even in non-contact sports plastics play an important role, improving performance and safety. In track and field, for example, runners race on a Tartan tracks with featherlight shoes made from ethylene-vinyl acetate; vaulters hurl themselves tremendous heights using poles made from polyacrylonitrile and fall safely on polyurethane foam padding.

The first full synthetic polymer was born out of necessity as the rise of the electronics industry created an appetite for insulating materials that natural resins alone could not sate. Today polymers are still an integral part of the electronics industry. To say nothing of the power grid itself, all consumer electronics are made using polymers. Mobile phones, for example, are over 40% plastic by mass, as are computers.[9] Polymers did not merely revolutionize the electronics industry; they facilitated its growth and expansion, and in so doing have changed the world dramatically.

### 1.1.3 Sources of Concern

It is undeniable that synthetic polymers provide many societal benefits. However, polymer prices often do not reflect the environmental costs associated with their manufacture and disposal.[10] The full scope of these negative externalities is not yet well understood and likely will not be for decades, if ever. Regardless, it is has now become clear to many that the current polymer industry is not sustainable. One major issue is most synthetic polymers share is that they are derived from non-renewable resources. In fact, as discussed in Appendix G., the birth of the polymer industry was closely tied

advancements in petroleum refining; both were direct consequences of the industrial revolution.

In the US and Europe coal surpassed biomass as an energy source in the 1880s, and was itself overtaken by oil in the late 1940s.[11] This change in energy sources is mirrored in the feedstocks used by the emerging polymer industry. The first plastics, Ebonite and Parkesine, were semisynthetic, respectively produced from chemical modification of natural rubber and cellulose. The first fully synthetic polymer, a thermosetting resin called Bakelite, was produced from phenol; a byproduct of the coal industry. Many of the synthetic polymers that today comprise the panoply of commodity thermoplastics were initially commercialized between 1930 and 1955, as cheap petroleum-derived monomers became available on an industrial scale.

Today the petrochemical industry is highly integrated. Whereas the cracking of naptha yields olefins (specifically, ethylene, propylene, as well as mixtures of $C_4$ and $C_5$ molecules), catalytic reforming is used to produce aromatics (namely, benzene, toluene, xylene, and napthalene). These platform chemicals are not only valuable precursors for the synthesis of a wide variety of complex chemical products but may also be useful monomers in their own right. For example, ethylene can be polymerized directly to produce polyethylene, but is also used for a precursor for the synthesis of other monomers including, ethylene oxide, dichloroethylene, tetrafluoroethylene, ethylene glycol, and vinyl acetate.

Likewise benzene, which is synthetically only two steps from styrene, is also a direct precursor for adipic acid, caprolactam, caprolactone, 1,6-hexane diol, bisphenol A, and variety of sulphone monomers. A small but non-negligible percentage of oil produced annually (8%) is currently consumed for the manufacture of polymers, with the amount being used directly in the synthesis of monomers roughly equal to the quantity consumed indirectly for production processes.[12] This number is expected to continue to grow; it is anticipated that by 2050, the plastics industry alone will use almost 20% of the total oil consumed annually.[7]

Because, polymers are directly derived from petroleum, the industry is sensitive to many of the same political and environmental concerns that plague fossil fuels. From an environmental standpoint, the nonrenewable energy sources consumed in the production of polymers lead to increases in greenhouse gasses and contribute to climate change. The large scale on which plastics are produced is concerning from an energy security standpoint for the simple reason that petroleum consumed in plastics production in generally not recovered. Public awareness of the greenhouse gas emissions and other forms of pollution associated with petroleum production has in recent years lead to an increased demand for renewable alternatives.

### 1.1.4 Plastics in the Environment

Synthetic polymers are lightweight and durable; while these characteristics are beneficial for many applications, it also means that polymeric materials take up significant portion of space in landfills and do not easily degrade. If improperly disposed of many can persist in the environment nearly indefinitely (experts have even

suggested that future archeologists will use plastic as a horizon marker for our current epoch, the Anthropocene).[13] Plastics can be produced on a large scale at low cost, which has contributed to their success in single-use products such as packaging. Although commodity thermoplastics can be recycled, the cost to do so is similar to the cost of the virgin resin, while the product is of lower value. In areas of the world with underdeveloped recycling and disposal facilities trash pickers have little incentive to recover these materials.[14,15]

Today, over 40% of plastic packaging is discarded in landfills while 32% escapes the collection system or is dumped illegally.[7] Only about 28% of plastic packaging is collected for energy recovery or recycling (the volume of each is roughly equal). Of the amount recycled, almost 30% is lost in sorting or is unusable material. Taking into account the recycled materials are of lower value, only 5% of the value of all packaging materials is actually recovered from first use cycle.[7] Although waste to energy (incineration) strategies can be used to help recover some value from post-consumer polymer products, this is expensive as extensive pollution control measures are necessary to prevent the release of hazardous atmospheric pollutants, including, HCl, dioxins, furans, as well as heavy metal and carbon particulates.[12] Because of this, and because most of the municipal waste collected has, on average, a lower energy density than plastic, waste–to energy facilities are typically more expensive to build and operate than traditional power plants.[16,17,18] Moreover, because most plastics are ultimately derived from petroleum, their incineration inevitably increases the level of atmospheric $CO_2$.

Plastic pollution gives rise to a host of environmental issues. On land it is mainly seen as an eyesore, yet it can significantly impact land use as well as animal and human health. Due to its low density and extreme durability, plastic often makes its way to the oceans over time. About 80% of marine litter is plastic, 20% of this results from ocean dumping from ships (both intentional and accidental) the vast majority results from land-based sources.[15] Plastic pollution can harm marine wild life through entanglement and ghost fishing and can result in economic losses for fisheries.[19]

Another serious problem is toxicity. While most synthetic polymers are chemically inert, many contain toxic residual monomers or plasticizers that can leach out over time. Moreover, plastics can actually increase in toxicity by picking up organic pollutants present in water.[20] Mechanical weathering causes plastics to break, forming fragments that are similar in size and shape to plankton and fish eggs. Although the effects of plastic on the food cycle are not yet well understood, laboratory studies indicate small molecule additives in plastic can be transferred to the blood and tissue of animals via ingestion.[21] Public awareness of the problem of plastic pollution in the ocean has increased in recent years, in part due media fascination with the Great Pacific Garbage Patch.[22]

## 1.2 The Bioplastics Industry

### 1.2.1 General Strategies

There are a number of factors driving the development of sustainable polymers. These include, increased consumer demand for biobased products, government labeling and

biopreferred incentives, and municipal restrictions on nondegradable plastics. The three basic approaches used in the development of sustainable polymeric materials: synthesis of conventional polymers from renewable resources, the synthesis of degradable polymers from renewable resources, and the synthesis of degradable polymers from petroleum sources. All three of these fall under the umbrella of the bioplastics industry. [23]

It is worth nothing that the drivers of the bioplasics industry have shifted significantly over the past 25 years. The original focus was on developing new biodegradable and compostable plastics for single use applications. In recent years, there has been an increased emphasis on the use of renewable resources to create drop in replacements to petrochemical plastics. Today, there has been a move toward durable, renewable plastics made from second-generation feedstocks.[23] These shifting market drivers are exemplified by commercially successful product like NatureWorks Ingeo and the Coca Cola Plant Bottle. These and a number of other examples of bioplastics are summarized in Table 1.1, below.

**Table 1.1**

**Examples of different kinds of BioPlastic**

|  | **Not biodegradable** | **Biodegradable** |
|---|---|---|
| **High Bio-content** | bio-PE[a]<br>bio-PP[a]<br>Nylon 11[b] | PHA[f]<br>PLA[g]<br>TPS[h] |
| **Medium Bio-content** | Bio-PET[c]<br>Nylon 6,10[d]<br>PTT[e] | PLA/AAC blend[i]<br>Starch/AAC blend[j] |
| **Non-Renewable** | Conventional Plastics<br>(LLDPE, LDPE,<br>UHMWPE, PP<br>PET, PS, PUR<br>TPUs, Kratons, etc) | AAC[k]<br>PBAT[l]<br>PBS[m]<br>PCL[n] |

[a]Ethylene sourced from renewable ethanol, is sold by Braskem under the trade name "I'm Green polyethylene"; Bio-PP is not yet commercialized. [b]Produced from ricinoleic acid (castor oil) by Arkema under the brand name Rilsan. [c]Currently, renewable ethylene glycol makes the Plant Bottle 30% biobased. Coca Cola has stated they are partnering with Virent to produce plant based Paraxylene by 2020.[24] [d]Produced from bio-sebacic acid by Akro-Plastic under the brand name Arkromid. [e]Polytrimethylene terephthalate from renewably sourced 1,3-propane diol (20 to 37% renewable content) by Du Pont under the brand name Sorona. [f]Medium-chain-length branched polyhydroxyalkanoates produced commercially by Meredian, Inc. (MHG) under the brand name Nodax. [g]Numerous companies produce poly(lactide) globally. The largest producers are NatureWorks, Evonik, and PURAC. [h]Thermoplastic starch [i]Blends of PLA and aliphatic-aromatic copolyester, examples include BASF's Ecovio, and CerePlast's Compostables. [j]Blends of Starch and aliphatic-aromatic copolyester, e.g., Novamont's Mater-Bi. [k]Aliphatic/aromatic copolyesters of various compositions. [l]Polybutyrate (brands include Ecoflex, Ecoworld, Eastar Bio, Origo-Bi).[m]Polybutylene succinate. Bioamber is attempting to commercialize bio-succinic acid; if they are successful this polymer could be partially renewable. [n]Polycaprolactone (derived from non-renewable cyclohexanone).

## 1.2.2 Why Renewable Monomers?

There are a number of reasons, aside from a desire to promote sustainability, why renewable feedstocks are attractive alternatives to petroleum. Historically, renewable feedstocks experience less price volatility than petroleum. As a specific example, during

the second Bush administration the price of oil more than tripled, from \$45 bbl$^{-1}$ in September of 2000 to \$145 bbl$^{-1}$ in September 2008. During the same period, growing demand for biofuels caused the price of corn to increase similarly, from \$1.61 bu$^{-1}$ to \$5.02 bu$^{-1}$. Although global corn syrup and sugar prices also increased, the change was much less dramatic (high fructose corn syrup increased from \$0.16 lb$^{-1}$ to \$0.28 lb$^{-1}$ and raw sugar increased from \$0.10 lb$^{-1}$ to \$0.15 lb$^{-1}$ over the same time period).

Agriculture is becoming increasingly productive, yet the total number of arable acres has not changed significantly since 1990. In the future, the total extent of cropland is expected to decrease in part due to global climate change. Advances in plant science and biotechnology will likely play a crucial role in bridging the gap. Concerns over food security are worth mentioning as they form the basis of consumer preference for inedible (second-generation) feedstocks in biorefinery processes. It is worth noting that the demand for monomers pales in comparison to the demand for fuel. The development of a biochemical industry is likely to have a major impact on rural economies. The low density of agricultural products makes the energy input and cost of shipping of renewable feedstocks nonegligible, meaning biorefineries are likely to be localized near crop production sites. This problem is exacerbated with second-generation feedstocks.

As mentioned previously, one approach that has attracted considerable research effort is the synthesis of traditional monomers and platform chemicals from renewable resources. Examples include: ethylene,[25] ethylene glycol,[26] terephthalic acid,[27] p-xylene,[28] benzene,[29] toluene,[30] xylene,[31] succinic acid,[32] and 1,4 butanediol.[33] An obvious

advantage of this approach is that these molecules are drop-in replacements, and are compatible with the current petrochemical infrastructure. Moreover, the markets for polymers derived from these monomers are already well established. The problem is that these bio-derived monomers must compete with their petrochemical counterparts in cost. As long as oil prices remain low is unlikely that renewable production methods will be cost competitive with steam cracking.

### 1.2.3 Renewable and Degradable Polymers

Although the creation of bioderived durable plastics will help meet consumer demand for renewable products these materials suffer from the same end of life issues as traditional petroleum-derived plastics. Bioderived compostable plastics have the potential to solve the disposal issues but come with their own unique set of challenges. Although a few biobased compostable polyesters have been commercialized, the development of this industry has been somewhat slow due to a lack of composting infrastructure. Other technical challenges include: removal of these new polymers from existing recycling streams (where they are essentially contaminants) and tuning their property profiles to match existing petroleum–derived polymers.

## 1.3 Properties and Limitations of PLA

Arguably the most successful bioplastic by commercial volume, poly(lactide) (PLA) is derived from lactic acid, a biorenewable produced by fermentation. This degradable polyester currently can be produced with only 15—25% surchage relative to poly(ethylene terephthalate), a price difference small enough to allow its use in commercial products such as textiles and disposable containers (e.g. bottles and cups).[34,35] Because lactide contains two chiral centers, four different PLA microstructures are possible. Atactic and heterotactic PLA are amorphous with glass transition temperatures close to 50 °C. The relatively low glass transition temperature of these variants severely limits their applications PLA. Isotactic and syndiotactic PLA are semicrystalline with melting points of 170 to 185 °C and 150 °C, making these forms more appropriate for use in applications where thermal stability is required.
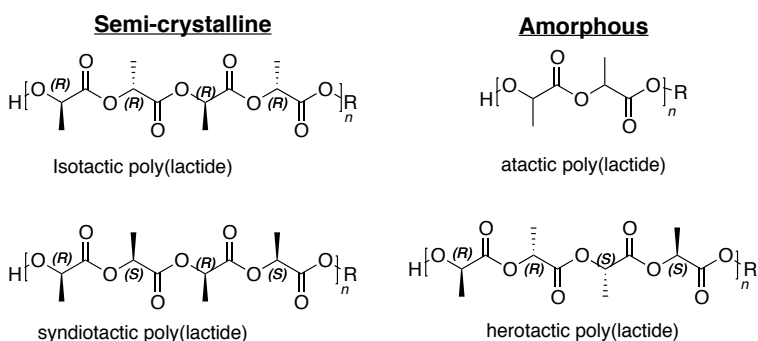


**Figure 1.3**

The four possible microstructures of poly(lactide).

15

Despite possessing a high tensile strength and elastic modulus, pristine PLA is intrinsically brittle, which prevents its use in such applications as packaging and films where toughness, impact resistance, and optical clarity are essential.[36,37] PLA is thus mechanically similar and shares many of the inherent limitations of the commodity thermoplastic poly(styrene) (PS). Appropriately, many of the stradegies that have been sucessfully employed to toughen polystyrene have also been investigated to alter the mechanical properties of PLA.

### 1.3.1 Statistical and Block Copolymers

The range of thermal and mechanical properties that may be accessed by a homopolymer, is largely dictated by its molecular size and architecture. An expanded range of property profiles can be obtained through the incorporation of one or more comonomers. Even when the number of different monomers is fixed at two (e.g., of type "A" and type "B"), a nearly infinite number of monomer arrangements or microstructures are possible. At one extreme the two comonomers are separated into distinct blocks (...-A-A-A-A-A-B-B-B-B-B-...), at the other they are randomly distributed along the polymer backbone (...-B-A-B-A-A-B-B-A-B-A-...).
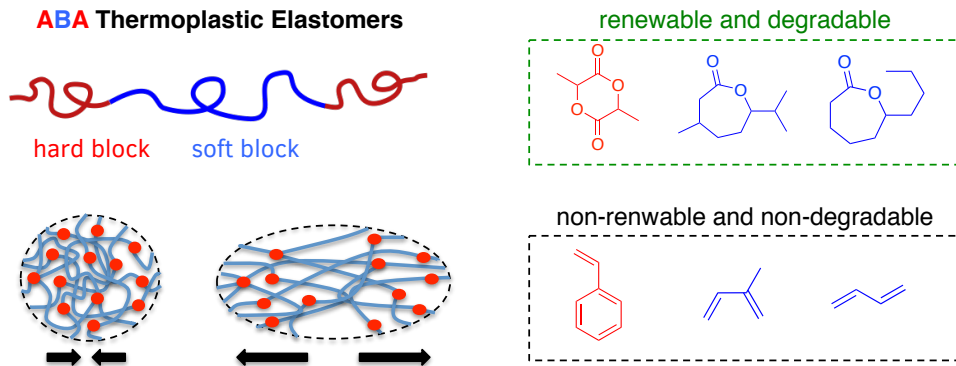
**Figure 1.4**

Cartoon showing the reversible deformation of physically crosslinked thermoplastic elastomers.

One particularly useful configuration is the ABA triblock architecture, which forms the basis for the commercially successful poly(styrene)-poly(diene) thermoplastic elastomers.[38] Provided the molar masses of the individual segments are high enough, the disparate blocks of the polymer tend to microphase separate to form nanoscopic structures. In these structures the rigid (glassy or semicrystalline) 'A' endblocks act as physical crosslinks that tether together the soft, low glass transition temperature ($T_g$), domains comprised of the center block 'B' component.[39,40,41,42] Prior to the onset of this study a number of PLA-containing polyester block polymer elastomers had been reported; several of these were shown to be flexible, tough, elastic, and hydrolytically degradable.[43,44,45,46] Unfortunately, the lactone monomers (exemplified in Figure 1.4 by ε-decalactone and menthide) utilized in these previous studies were either derived from fossil fuels or from prohibitively expensive natural products.

## 1.4 Thesis Overview

The desire to develop inexpensive degradable aliphatic polyesters for use in PLA block polymers provided the original motivation for the work discussed in subsequent chapters of this thesis. In Chapter 2, statistical copolymers are prepared using ε-decalactone and ε-caprolactone. These partially renewable gradient copolymers are used in conjunction with lactide to prepare polyester triblock and multiblock elastomers. Next, in Chapter 3, a branched lactone monomer, β-methyl-δ-valerolactone (MVL), is produced using an efficient semisynthetic route. This monomer is then polymerized to generate an amorphous polyester, poly(β-methyl-δ-valerolactone) (PMVL). A systematic comparison MVL and eleven other structurally similar lactones forms the basis of Chapter 4, in which where the effect of structure on lactone polymerizability and polyester performance are discussed. Finally, Chapter 5 discusses the synthesis and properties of PMVL-polyurethanes and also explores the chemical recycling of these high performance renewable materials.

**Table 1.2**

**Characteristics of Commodity, Engineering and Specialty Plastics**

| Polymer | $T_g$ (°C) | $T_m$ (°C) | Name | Density (g cm$^{-3}$) | Notes |
|---------|---------|---------|------|---------|-------|
| PVC | 81 | 227 | poly(vinyl-chloride) | 1.3-1.45 | atactic |
| a-PS | 100 | - | poly(styrene) | 0.96-1.04 | atactic |
| i-PS | 100 | 240 | poly(styrene) | 1.12 | isotactic |
| s-PS | 90 | 270 | poly(styrene) | 1.30 | syndiotactic (XAREC) |
| LLDPE | −110 | 126 | poly(ethylene) | 0.915-0.925 | linear low density |
| LDPE | −110 | 105-118 | poly(ethylene) | 0.91-0.94 | low density |
| MDPE | −110 | 120-125 | poly(ethylene) | 0.926-0.94 | medium density |
| HDPE | −110 | 126-135 | poly(ethylene) | ≥0.941 | high density |
| UHMWPE | −110 | 130-135 | poly(ethylene) | ≥0.941 | ultra high-molecular weight |
| PMMA | 105 | - | poly(methyl-methacrylate) | 1.18 | atactic |
| PET | 70-80 | >250 | poly(ethylene-terephthalate) | 1.38 | |
| i-PP | −10 | 173 | poly(propylene) | 0.946 | isotactic |
| ABS | 80-125 | - | acrylonitrile-butadiene-styrene | 1.05-1.1 | many types |
| HIPS | ~90 | - | poly(styrene)-*g*-poly(butadiene) | Variable | many types |
| Kratons | ~100 | - | styrenic block polymers | Variable | many types |

| | | | | | |
|---|---|---|---|---|---|
| Nylon 6 | 47 | 220 | poly(caprolactam) | 1.08 | |
| Nylon-6,6 | 70 | 243 | poly(hexamethylene-adipamide) | 1.14 | |
| PTFE | 117 | 326 | poly(tetrafluoro-ethylene) | 2.2 | |
| PC | 145 | 225 | poly(carbonate) | 1.22 | |
| PBT | 40 | 223 | poly(butylene terephthalate) | 1.3 | |
| POM | −30 | 175 | poly(oxymethylene) | 1.4 | |
| PI | 360-410 | | poly(imide) | 1.42 | (Kapton) |
| PSU | 170-185 | 330-370 | poly(sulfone) | 1.25 | many types |
| PEEK | 143 | 343 | poly(ether ether-ketone) | 1.32 | |
| PBI | 427 | 760 | poly(benzimidazole) | 1.30 | |
| PPE or PPO | 215 | - | poly(phenyl ether), poly(p-phenylene-oxide) | 1.20 | (Noryl) |
| PPSU | 220 | | poly(phenylsulfone) | 1.3 | (Radel) |
| PAI | 280 | - | poly(amide-imide) | 1.6 | (Torlon) |

## 1.5 References

(1) Thompsan, R.C.; Swan, S. H.; Moore, C. J.; vom Sall, F. S.  Our Plastic Age *Phil. Trans. Soc. B.* **2009,** *364,* (1973-1976)

(2) Plastics the Facts 2015 [Online] http://www.plasticseurope.org/plastics-industry/market-and-economics.aspx Accessed May 15th, 2016

(3) Research an Markets Reports Engineering Plastics Market by Type, Applications and Geography-Trends and Forecasts (2013-2018) [Online] http://www.researchandmarkets.com/reports/3446120/ Accessed May 29th, 2016

(4) Hammound, A. N.; Suthar, J.L. Characterization of Polybenzimidazole (PBI) Film at High Temperatures NASA Contractor Report # 189174, 1992

(5) Torlon® PAI Emco Industrial Plastics, Inc. 2016 [Online] http://www.emcoplastics.com/materials/torlon-pai/ Accessed May 4th, 2016

(6) Trucost  and UNEP Valuing Plastic: the business case for measuring, managing, and disclosing plastic use in the consumer goods industry June 2014 [Online] www.trucost.com/published-research/134/**valuing-plastic** Accessed May 19th, 2016

(7) World Economic Forum, Ellen MacArthur Foundation and McKinsey and Company, The New Plastics Economy Rethinking the Future of Plastics **2016**, http://www.ellenmacarthurfoundation.org/publications

(8) Thatte, S.; Datar, K.; Ottenbrite, R. M. Perpsectives On: Polymeric Drugs and Drug Delivery Systems *Journal of Bioactive and Compatible Polymers* **2005**, *20,* (585-601)

(9) Schuessler, H. Where it Goes; Breaking Down All Those Computers: Glass Over Here, Plastic There *The New York Times* November 23, 2000

(10) Trucost and TEEB for Business Coalition Natural Capital At Risk: The TOP 100 Externalities of Business April 15th, 2013 [Online] www.**naturalcapital**coalition.org/projects/**natural-capital-at-risk**.html Accessed May 20th, 2016

(11) U.S. Energy Information Administration Annual Energy Review 2011 [Online] http://www.eia.gov/totalenergy/data/annual/ Accessed May 1st, 2016

(12) Hopewell, J.; Dvorak, R.; Kosier, E. Plastics Recycling: Challenges and Opportunities *Philos. Trans. R. Soc. Lond. B Biol. Sci.* **2009,** *364,* (2115-2126)

(13) Corcoran, P. L.; Moore, C. J.; Jazvac, K. An Anthropogenic marker in the future rock record *GSA Today* **2013**, *24,* 4-8

(14) Kinnaman, T.C. The economics of municipal solid waste management *Waste Management* **2009***, 29,* (2615-2617)

(15) Ocean Conservancy Stemming the Tide: Land-based strategies for a plastic-free ocean [Online] http://www.oceanconservancy.org/our-work/marine-debris/mckinsey-report-files/full-report-stemming-the.pdf Accessed January 15th, 2016

(16) Lea, W. R. Plastic incineration verses recycling: a comparison of energy and landfill cost savings *Journal of Hazardous Materials* **1996,** 47, (295-302)

(17) Morris, J. Recycling verses incineration: an energy conservation analysis *Journal of Hazardous Materials* **1996,** *47,* (277-293)

(18) Funk, K.; Milford, J.; Simpkins, T. Waste Not, Want Not: Analyzing the Economic and Environmental Viability of Waste-to-Energy (WTE) Technology for Site-Specific Optimization of Renewable Energy Options NREL technical report (online) http://www.osti.gov/bridge accessed 2/25/2016

(19) Allsopp, M.; Walters, A.; Santillo, D.; Johnston, P. Plastic Debris in the World's Oceans **2006,** [report] Green Peace International

(20) Teuten, E. L.; Saquing, J. M.; Knappe, D. R. U.; Barlaz, M. A.; Jonsson, S.; Björn, A.; Rowland, S. J.; Thompson, R. C.; Galloway, T. S.; Yamashita, R.; Ochi, D.; Watanuki, Y.; Moore, C.; Viet, P. H.; Tana, T. S.; Prudente, M.; Boonyatumanond, R.; Zakaria, M. P.; Akkhavong, K.; Ogata, Y.; Hirai, H.; Iwasa, S.; Mizukawa, K.; Hagino, Y.; Imamura, A.; Saha, M.; Takada, H. Transport and release of chemicals from plastics to the environment and to wildlife *Phil. Trans. Royal Soc. B.* **2009,** *364,* (2027-2045)

(21) Rochman, C. M.; Browne, M. A. Classify plastic waste as hazardous *Nature* **2013,** *494,* (169-171)

(22) NOAA Office of Response and Restoration, 2016 Great Pacific Garbage Patch [Online] https://marinedebris.noaa.gov/info/patch.html Accessed May 29th, 2016

(23) The Society of Plastics Industry, Inc. **2012** [report] Bioplastics Industry Overview Guide

(24) Kable 2016, Coca-Cola's 100% Plant-Based Bottle, United States of America [Online] http://www.packaging-gateway.com/projects/-coca-cola-plant-based-bottle/ Accessed May 29th, 2016

(25) Fan, D.; Dai, D.J.; Wu, H.-S. Ethylene Formation by Catalytic Dehydration of Ethanol with Industrial Considerations *Materials* **2013,** *6,* (101-115)

(26) Ooms, R.; Dusselier, M.; Geboers, J. A.; de Beeck, B. O.; Verhaeven, R.; Gobechiya, E.; Martens, J. A.; Redl, A.; Sels, B. F. Conversion of sugars to ethylene glycol with nickel tungsten carbide in a fed-batch reactor: high productivity and reaction network elucidation *Green Chem.* **2014,** *16,* (695-707)

(27) Tachibana, Y.; Kimura, S.; Kasuya, K. Synthesis and Verification of Biobased Terephthalic Acid from Furfural *Sci. Rep.* **2015,** *5,* (8249)

(28) Wijaya, Y. P.; Suh, D. J.; Jae, J. Production of renewable p-xylene from 2,5-dimethylfuran via Diels-Alder cycloaddition and dehydrative aromatization reactions over silica-aluminum aerogel catalysts *Catalyst Communications* **2015,** *5,* (12-16)

(29) Xu, C.; Arancon, R. A. D.; Labidi, J.; Luque, R. Lignin depolymerization strategies: toward valuable chemicals and fuels *Chem. Soc. Rev.* **2014,** *43,* (7485-7500)

(30) Green, S. K.; Patent, R. E.; Nikbin, N.; Williams, C. L.; Chang, C.-C.; Yu, J.; Gorte, R. J.; Caratzoulas, S.; Fan, W.; Vlachos, D. G.; Dauenhauer, P. J. Diels-Alder cycloaddition of 2-methylfuran and ethylene for renewable toluene *Applied Catalysis B:Environmental* **2016,** *180,* (487-496)

(31) Williams, C. L.; Chang, C.-C.; Do, P.; Kikbin, N.; Caratzoulas, S.; Vlachos, D. G.; Lobo, R. F.; Fan, W.; Dauenhauer, P. J. Cycloaddition of Biomass-Derived Furans for Catalytic Production of Renewable p-Xylene *ACS Catal.* **2012,** *2,* (935-939)

(32) Cok, B.; Tsiropoulous, I.; Roes, A. L.; Patel, M. K. Succinic acid production derived from carobhydrates: An energy and greenhouse gas assessment of a platform chemical toward a bio-based economy *Biofuels, Bioproducts, and Biorefining* **2014**, *8,* (16-29)

(33) Yim, H.; Haselbeck, R.; Niu, W.; Pujol-Baxley, C.; Boldt, J.; Khandurina, J.; Trawick, J.D.; Osterhout, R.E.; Estadila, J.; Teisan, S.; Schreyer, H.B.; Andrae S.; Yang, T. H.; Lee, S. Y.l Burk, M. J.; Van Dien, S. Metabolic Engineering of Escherichia coli for direct production of 1,4-butanediol *Nat. Chem. Biol.* **2011**, *7,* (445-452)

(34) Liu, H.; Zhang, J. Research Progress in Toughening Modification of Poly(lactic acid) *Journal of Polymer Science Part B Polymer Physics* **2011**, *49,* (1051-1083)

(35) Miller, S. A. Sustainable Polymers: Opportunities for the Next Decade *ACS Macro Letters* **2013**, *2, (6),* (550-554)

(36) Anderson, K. S.; Schreck, K. M.; Hillmyer, M. A. Toughening polylactide *Polymer Reviews* **2008**, *48, (1),* (85-108)

(37) Perego, G.; Cella, G. D.; Bastioli, C. Effect of molecular weight and crystallinity on poly(lactic acid) mechanical properties *Journal of Applied Polymer Science* **1996**, *59, (1),* (37-43)

(38) Kraton Performance Polymers Inc. Product Families Kraton D SBS. http://www.kraton.com/products/Kraton_D_SBS.php.

(39) Bates FS, et al. Multiblock polymers: panacea or Pandora's box? *Science* **2012**, *336*, (434-440)

(40) Morton M Structure-Property Relations in Amorphous and Crystallizable ABA Triblock Copolymers. *Rubb Chem Technol* **1983**, *56, (1096-1110)*

(41) Schmalz H, Abetz V, Lange R Thermoplastic elastomers based on semicrystalline block copolymers. *Compos Sci Technol* **2003**, *63, (*1179-1186)

(42) Handlin D, Trenor S, Wright K *Applications of Thermoplastic Elastomers Based on Styrenic Block Copolymers. Macromolecular Engineering,* (Wiley-VCH Verlag GmbH & Co. KGaA), **2007**, (2001-2031)

(43) Olsén P, Borke T, Odelius K, Albertsson AC ε-Decalactone: A Thermoresilient and Toughening Comonomer to Poly(L-lactide). *Biomacromolecules* **2013**, *14,* (2883-2890)

(44) Lin JO, Chen WL, Shen ZQ, Ling J Homo- and Block Copolymerizations of ε-Decalactone with L-Lactide Catalyzed by Lanthanum Compounds. *Macromolecules,* **2013**, *46,* (7769-7776)

(45) Martello MT, Hillmyer MA Polylactide-Poly(6-methyl-ε-caprolactone)-Polylactide Thermoplastic Elastomers. *Macromolecules* **2011**, *44,* 8537-8545.

(46) Wanamaker CL, et al. Renewable-resource thermoplastic elastomers based on polylactide and polymenthide. *Biomacromolecules* **2007**, *8,* 3634-3640.

# Chapter 2. Block-Statistical Copolymers[*]

In this chapter batch ring opening transesterification copolymerization of ε-caprolactone and ε-decalactone is used to generate statistical copolymers over a wide range of compositions and molar masses. Reactivity ratios determined for this monomer pair, $r_{CL}$ = 5.9 and $r_{DL}$ = 0.03, reveal ε-caprolactone is added preferentially regardless of the propagating chain end. Relative to poly(ε-caprolactone) the crystallinity and melting point of these statistical copolymers were depressed by the addition of ε-decalactone; copolymers containing greater than 31 mol % (46 wt %) ε-decalactone were amorphous. Poly(lactide)-*block*-poly(ε-caprolactone-*co*-ε-decalactone)-*block*-poly(lactide) triblock polymers were also prepared and used to explore the influence of midblock composition on the temperature dependent Flory-Huggins interaction parameter (($\chi$). Finally, these triblocks were coupled to prepare linear (AB)$_n$ multiblock polymers. Uniaxial extension tests were used to determine the effects of midblock composition, poly(lactide) content, and molar mass on the mechanical properties of these new block polymer thermoplastic elastomers.

---

## 2.1 Introduction

Whereas the range of thermal and mechanical properties that may be accessed by a homopolymer is largely dictated by molar mass, architecture, and processing conditions, an expanded range of property profiles can be obtained through the incorporation of one or more comonomers. The physical characteristics of the resulting copolymer may be influenced greatly by the specific choice of monomers used, the composition, and the distribution of comonomers along the polymer backbone. In the case of a block polymer different comonomers are partitioned into distinct segments that can microphase separate to form ordered nanoscopic morphologies.[1,2] Microphase separated block polymers have been utilized for a number of innovative applications including gene and drug delivery,[3,4] energy capture and storage,[5,6,7] lithography,[8,9] and filtration membranes.[10,11] Despite remarkable advances in each of these areas, ABA styrenic block polymers elastomers—first commercialized over half a century ago—remain the cheapest, highest volume, commercial examples to date.

We and others have previously shown that a low glass transition temperature ($T_g$) midblock in combination with glassy poly(($\pm$)-lactide) (PLA) or semicrystalline poly(($-$)-lactide) (PLLA) endblocks can be used to prepare materials with mechanical properties similar to styrenic block polymers.[12,13,14,15,16,17,18,19,20] A number of previous studies have focused on developing sustainable poly(lactide) containing elastomers that are renewable [21,22] and degradable.[23,24,25,26] Polyester midblocks are particularly attractive for reasons of synthetic ease; triblock polymers can be synthesized by sequential monomer addition in a one pot approach.[18,19] The choice of a particular midblock may

not only influence the rheological, mechanical, and degradation behavior of the block polymer but also define processing and service temperatures.[27,20, 28] To strategically tune the properties of a block polymer it is desirable to select a midblock with a given combination of characteristics, e.g. melting point $(T_m)$,[29,30] entanglement molar mass $(M_e)$,[27] and glass transition temperature.[31] Because there are synthetic challenges associated with the efficient large-scale production of new monomers, the number of viable and practical homopolymer midblocks has been limited.

Others have previously studied block and multiblock polymers where at least one of the segments is a statistical copolymer.[32,29,33,34,35,36,37,38,39,40,41] In 2007 Staudinger *et al.* demonstrated using poly(styrene)-*block*-poly(styrene-*co*-butadiene)-*block*-poly(styrene) triblock polymers that the midblock composition could be used to tune the miscibility of the copolymer midblock and polystyrene endblock segments. At fixed molar mass, changes in midblock composition dramatically impacted both the phase behavior and mechanical properties of the material.[38] More recently, Widjaja *et al.* investigated poly((−)-lactide)-*block*-poly(caprolactone-*co*-trimethylene carbonate)-*block*-poly((−)-lactide) triblock polymers. In this system the soft segment composition dramatically impacted the thermal and mechanical properties of the material; triblocks with amorphous middle segments were less tough but exhibited better elasticity than those with semicrystalline midblocks containing a majority of poly($\varepsilon$-caprolactone) (PCL).[29]

We recently reported the synthesis and properties of amorphous poly((±)-lactide)-*block*-poly($\varepsilon$-decalactone)-*block*-poly((±)-lactide) (LDL) triblock and (LDL)$_n$ multiblock

elastomers.[20] Although ε-decalactone block and statistical copolymers containing pentadecalactone[42,43] and (−)-lactide[13,15,16] have also been reported, work on poly(ε-caprolactone-*co*-ε-decalactone) (PCD) statistical copolymers has been limited. Pitt and coworkers examined the impact of composition on the biodegradation of two semicrystalline PCD copolymers ($F_{CL}$ = 0.87 $F_{CL}$ = 0.92).[28] Glavas *et al* prepared block polymers micelles comprised of poly(ethylene oxide) (PEO) in combination with PLA, PCL, or PCD ($F_{CL}$ = 0.5).[44] They demonstrated that it was possible to tune the critical micelle concentration and micelle size by changing the composition of the polyester block. We posited that amorphous PCD copolymers could be used to prepare poly((±)-lactide)-*block*-poly(ε-caprolactone-*co*-ε-decalactone)-*block*-poly((±)-lactide) (LCDL) elastomers and that the ε-caprolactone content could be used to tune the miscibility of the midblock and endblock segments. We also predicted that the entanglement molar mass of the copolymer midblock would decrease with the addition of ε-caprolactone, which would lead to a substantial improvement in the mechanical performance of LCDL compared to LDL.[45,27,20]

In this work we utilize the Sn(Oct)₂ catalyzed batch ring opening transesterification polymerization (ROTEP) of ε-caprolactone and ε-decalactone to generate statistical copolymers that could be chain extended with lactide to prepare LCDL triblock polymers. We compare these LCDL block polymers to LDL and poly((±)-lactide)-*block*-poly(ε-caprolactone-*block*-poly((±)-lactide) (LCL) to determine the effects of midblock composition on segment-segment miscibility. Additionally, the mechanical properties of LCDL triblocks were evaluated using uniaxial extension and compared to chemically

similar polyester block polymers, poly((±)-lactide)-poly(menthide)-poly((±)-lactide) (LML),[18] poly((±)-lactide)-*block*-poly(6-methyl-ε-caprolactone)-*block*-poly((±)-lactide) (L6MCL),[16] and poly((±)-lactide)-*block*-poly(ε-decalactone)-*block*-poly((±)-lactide).[20] The general synthetic strategy used for this work is summarized in Scheme 2.1.

**Scheme 2.1**
**Synthesis of a PCD statistical copolymer midblock and subsequent chain extension to prepare the corresponding LCDL block-statistical copolymers.**
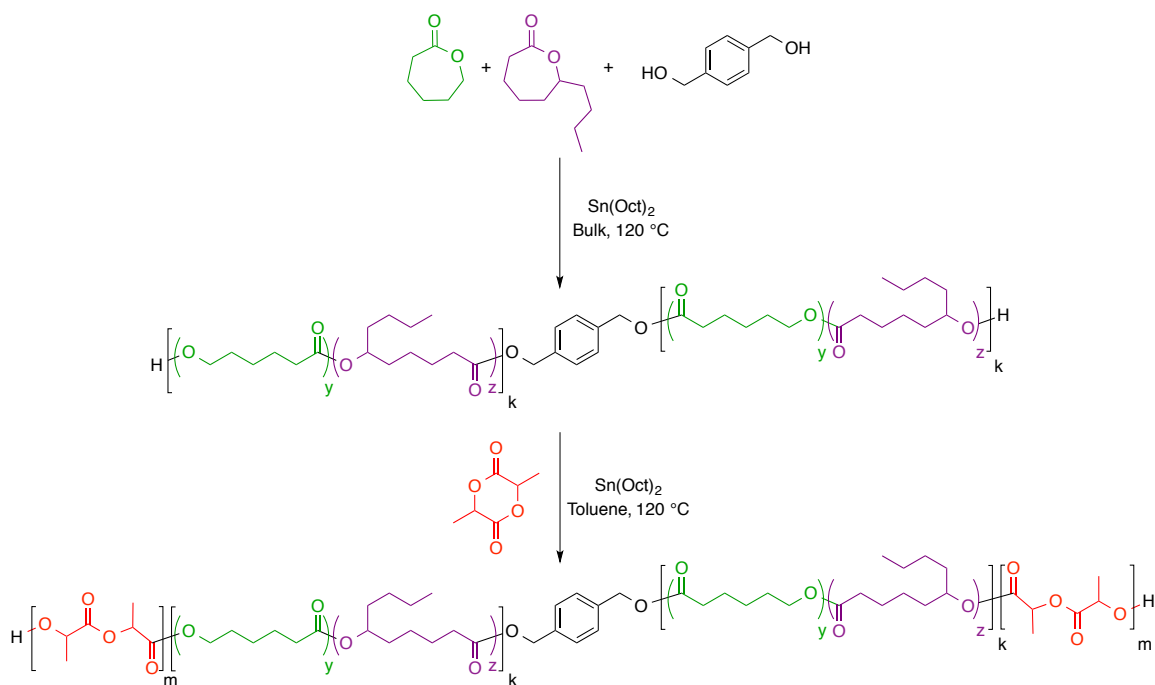
## 2.2 Results and Discussion

### 2.2.1 Copolymer Synthesis

We synthesized statistical copolymers using the bulk batch copolymerization of $\varepsilon$-caprolactone and $\varepsilon$-decalactone with catalytic $Sn(Oct)_2$ at 120 °C. 1,4 Benzene dimethanol (BDM) was added as an initiator to control the molar mass and end functionality. Typical of $Sn(Oct)_2$ catalyzed ROTEP, both PCD copolymers and similarly prepared PCL homopolymers exhibited relatively narrow dispersities ($1.05 \leq Đ \leq 1.20$).[13,20,46,47] The number average molar masses determined using proton nuclear magnetic resonance ($^1$H NMR) spectroscopy were in fair agreement with both the theoretical values and those ascertained using size exclusion chromatography with a multi-angle laser light scattering detector (MALLS-SEC). Since both adventitious initiation and transesterification are minimized, low dispersity linear telechelic polymers can be synthesized with control over molar mass and functionality. The characteristics of telechelic PCD and PCL polymers used in this work are summarized in Table 2.1.

**Table 2.1**

**Composition and thermal characteristics of telechelic PCL and PCD copolymers**

| Sample | $^a M_n^{NMR}$ (kg mol$^{-1}$) | $^b F_{CL}$ | $^c M_n^{SEC}$ (kg mol$^{-1}$) | $^c Đ$ | $^d T_g$ (°C) | $^d T_m$ (°C) | $^d X$ (%) |
|---|---|---|---|---|---|---|---|
| PCD66 (9.2) | 8.2 | 0.66 | 9.2 | 1.10 | −60 | | |
| PCD66 (10.2) | 9.7 | 0.66 | 10.2 | 1.20 | −63 | | |
| PCD65 (15.5) | 14.2 | 0.65 | 15.5 | 1.10 | −61 | | |
| PCD63 (18.3) | 18.3 | 0.63 | 18.3 | 1.13 | −62 | | |
| PCD69 (19.4) | 19.6 | 0.69 | 19.4 | 1.05 | −62 | | |
| PCD69 (83.4) | 96 | 0.69 | 83.4 | 1.16 | −62 | | |
| PCD78 (10.6) | 9.4 | 0.78 | 10.6 | 1.08 | −64 | 20 | 19 |
| PCD77 (12.5) | 11.4 | 0.77 | 12.5 | 1.05 | −64 | 16 | 16 |
| PCD76 (13.1) | 13.8 | 0.76 | 13.1 | 1.12 | −63 | 18 | 12 |
| PCD76 (17.0) | 15.0 | 0.76 | 17.0 | 1.08 | −65 | 16 | 15 |
| PCD77 (22.6) | 20.5 | 0.77 | 22.6 | 1.04 | −64 | 18 | 15 |
| PCL (10.8) | 11.1 | 1.0 | 10.8 | 1.06 | −62 | 55 | 52 |
| PCL(12.2) | 12.2 | 1.0 | 12.2 | 1.13 | −62 | 55 | 34 |
| PCL (11.6) | 10.1 | 1.0 | 11.6 | 1.06 | −60 | 54 | 50 |
| PCL (14.5) | 16.2 | 1.0 | 14.5 | 1.06 | −62 | 55 | 49 |
| PCL (15.7) | 16.0 | 1.0 | 15.7 | 1.13 | −64 | 55 | 59 |
| PCL (18.9) | 16.9 | 1.0 | 18.9 | 1.15 | −63 | 56 | 62 |
| PCL (18.1) | 18.8 | 1.0 | 18.1 | 1.18 | −62 | 55 | 53 |
| PCL (22.1) | 18.9 | 1.0 | 22.1 | 1.16 | −63 | 55 | 50 |

[a]Number average molar mass determined using $^1$H NMR spectroscopy. Calculated using initiator methylene protons as an internal standard. [b]Mole fraction of ε-caprolactone in the copolymer determined using $^1$H NMR spectroscopy. [c]Number average molar mass and dispersity determined using MALLS-SEC; d$n$/d$c$ was determined from the RI signal using the known concentration and the assumption of 100% mass recovery. [d]Glass transition temperatures and melting point values were determined by differential scanning calorimetry (DSC) and were taken on the second heating ramp with a rate of 5 °C min$^{-1}$. $T_m$ is taken as the peak maximum. Crystallinity was calculated using the reference enthalpy of fusion (139.5 J g$^{-1}$) for fully crystalline PCL.[48]

## 2.2.2 Reactivity Ratios

At high monomer conversions the compositions of PCD copolymers deviated only slightly from the feed. However, more significant differences were observed in polymerizations with lower monomer conversion. We used the dependence of instantaneous polymer composition (total monomer conversion < 10%) on feed composition to determine reactivity ratios for the bulk copolymerization of ε-caprolactone and ε-decalactone. The results of this experiment are shown in Figure 2.1. The relative reactivity of the two commoners tend to promote a gradient microstructure with longer initial runs of CL than DL emanating from the central difunctional initiator. Thus, the middle of midblock will be richer in CL whereas the ends of the midblock will be richer in DL.
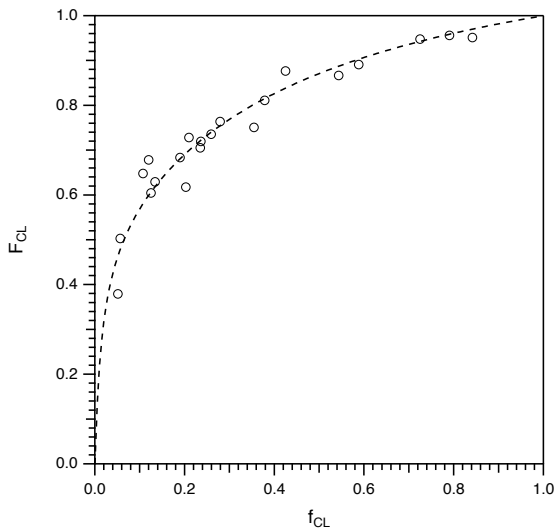


**Figure 2.1**

Dependence of polymer compostion (total monomer conversion < 10 %) on feed compostion (○). $F_{CL}$ and $f_{CL}$ are the mole fraction of caprolactone in the polymer and feed, respectively. Nonlinear least-squares fit (--) to copolymer equation used to find reactivity ratios $r_{CL} = 5.9 \pm 0.7$ and $r_{DL} = 0.03 \pm 0.01$.

### 2.2.3 Thermal Characteristics of Copolymer Midblocks

Differential scanning calorimetry (DSC) was used to analyze the impact of composition on the thermal properties of an array of statistical copolymers prepared using batch copolymerization of DL and CL. PDL is amorphous, PCL is semicrystalline with a melting temperature near 60 °C.[13,20,49] The crystallinity and melting point of PCD decreases with DL content, and at approximately 31 mol% (46 wt%) DL the polymers are amorphous. Representative thermograms are shown in Figure 2a, and data for several compositions of copolymers are summarized in Appendix B.

It is likely that the PCD crystallization behavior is impacted by both the copolymer composition gradient and size of the DL butyl substituent. Based on experimentally determined reactivity ratios the structurally similar copolymer poly(ε-methyl-ε-caprolactone)-co-poly(ε-caprolactone) (PCM) is predicted to have a much more random composition than PCD.[50] Although one would expect a random copolymer to display reduced crystallinity compared to a gradient copolymer, only PCM copolymers containing over 44 mol% (50 wt%) ε-methyl-ε-caprolactone are amorphous.[50] The probable reason for this discrepancy is that ε-methyl-ε-caprolactone is partially incorporated in the PCL crystal. [51,52] Due to the large size of the n-butyl substituent it is unlikely that PDL is included in the PCL crystal. In this way PCD copolymers are more similar to poly(γ-tert-butyl-ε-caprolactone)-co-poly(ε-caprolactone) copolymers.[53]

Because the glass transition temperatures of the corresponding homopolymers are similar ($T_g$ = −51 and $T_g$ = −61 °C for PDL and PCL, respectively), negligible variation in $T_g$ values was observed for the copolymer samples. This is in contrast to related works where lactide is used as a comonomer, e.g. poly(lactide)-*co*-poly(ε-decalactone),[13] and poly(lactide)-*co*-poly(ε-caprolactone).[54,50,41]
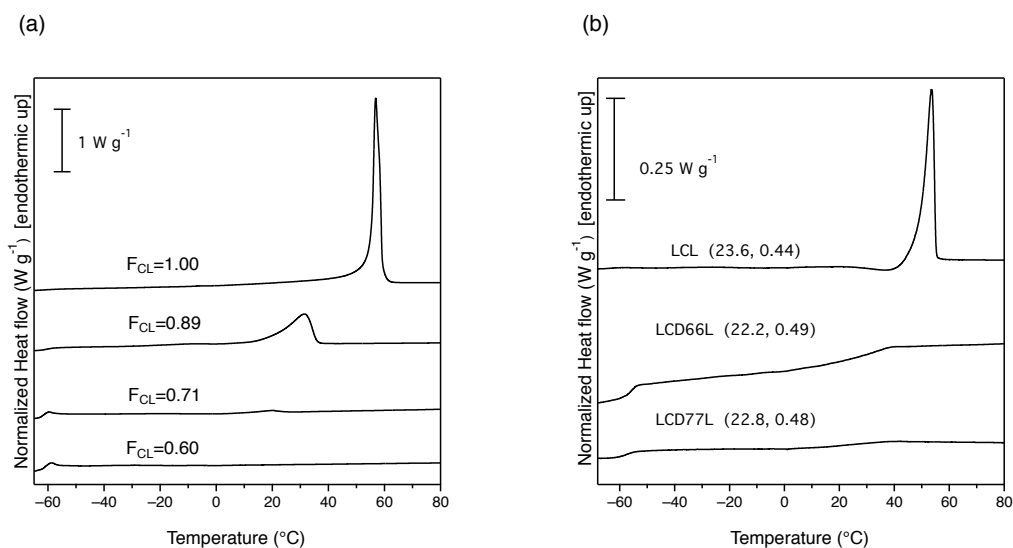


**Figure 2.2**

(a) DSC thermograms for PCL and representative PCD copolymers. To ensure consistent thermal histories all samples were heated to 100 °C (rate of 5 °C min⁻¹) and cooled at the same rate. Data were taken from the second heating ramp (5 °C min⁻¹) and are for polymers with molar masses near 20 kg mol⁻¹. Characteristics of these and other copolymer samples are given in Appendix B. (b) DSC thermograms for select LCL, LCD66L, and LCD77L triblock polymers described in Table 2.2. To ensure consistent thermal histories all samples were heated to 100 °C (rate of 5 °C min⁻¹) and cooled at the same rate. Data were taken from the second heating ramp (at a rate of 5 °C min⁻¹).

## 2.2.4 Triblock Synthesis and Characterization

The difunctional α,ω-hydroxyl telechelic polymers were used as macroinitiators for chain extension with (±)-lactide (LA). Similar conditions, 110–130 °C in toluene ($[LA]_0 \approx$ 1 M) with catalytic Sn(Oct)$_2$, were used regardless of midblock composition. As shown for representative samples in Figure 2.3, the SEC data of the triblock polymers indicated a clear increase in molar mass compared to the corresponding midblock. Additionally, there was minimal evidence of PLA homopolymer or residual macroinitiator. The $^{13}$C NMR spectra of triblocks samples revealed no significant transesterification between the midblock and poly(lactide) domains (this shown in further detail in Section 2.4). Together, these observations are consistent with the successful syntheses of the desired triblock polymers.
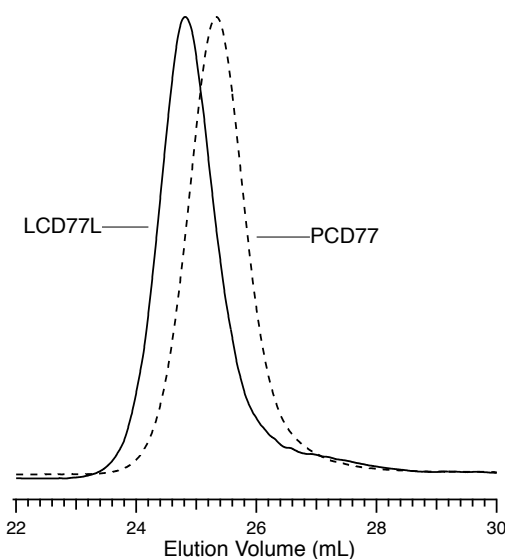


**Figure 2.3**

A representative example of size-exclusion chromatograms for a telechelic copolymer, PCD77 (22.6 kg mol$^{-1}$, $F_{CL}$ = 0.77), and the corresponding triblock, LCD77L (34.2 kg mol$^{-1}$, $F_{LA}$ = 0.30). Each chromatogram is shown for the purified polymers. Additional details for these midblock and triblock polymers are given in Table 2.1 and Table 2.2, respectively.

The thermal characteristics of the triblock polymer samples depended on composition. In the LCD77L triblock samples, crystallinity was suppressed at the molar masses and compositions investigated in this work. LCL samples exhibited significantly reduced crystallinity compared to parent macroinitiatiors, possibly the result of reduced chain mobility due to confinement.[55] As expected triblocks prepared using PCD69 macroinitiatiors were amorphous. In general, the LCDL triblocks exhibited two glass transition temperatures, one below −51 °C the other above 18 °C (more typically above 35 °C), consistent with microphase separation into PCD and PLA-rich domains, respectively. The thermograms of representative triblocks are shown in Figure 2.2b, compositions and thermal characteristics of several triblock samples are included Table 2.2.

**Table 2.2**

**Compositions and thermal characteristics of LCL and LCDL**

| Triblock | Block $M_n$ (kg mol$^{-1}$) | | [c]$N_{tot}$ | [d]$f_{PLA}$ | [f]$T_g$ (°C) | [f]$T_g$ (°C) | [f,g]$T_m$ (°C) | [g]X (%) | [h]$T_{ODT}$ (°C) |
|---|---|---|---|---|---|---|---|---|---|
| | [a]PLA | [b]PC(D) | | | | | | | |
| LCD65L (20.0, 0.49) | 5.4 | 9.2 | 250 | 0.49 | −58 | 26 | | | 65 |
| LCD66L (22.2, 0.49) | 6.0 | 10.2 | 280 | 0.49 | −56 | 31 | | | 92 |
| LCD67L (43.7, 0.49) | 9.1 | 15.5 | 420 | 0.49 | −57 | 37 | | | 126 |
| LCD63L (40.7, 0.5) | 11.2 | 18.3 | 510 | 0.50 | −59 | 49 | | | 170 |
| LCD69L (24.2, 0.17) | 2.5 | 19.4 | 320 | 0.17 | −52 | 18 | | | [i]nd |
| LCD69L (31.4, 0.33) | 6.0 | 19.4 | 400 | 0.33 | −59 | 30 | | | 95 |
| LCD69L (104, 0.17) | 10.5 | 83.4 | 1270 | 0.17 | −60 | 47 | | | >200 |
| LCD69L (113, 0.21) | 14.6 | 83.4 | 1320 | 0.21 | −60 | 50 | | | >200 |
| LCD69L (131, 0.32) | 24.0 | 83.4 | 1420 | 0.32 | −59 | 53 | | | >200 |
| LCD77L (22.8, 0.48) | 6.1 | 10.6 | 280 | 0.48 | −58 | 29 | | | 70 |
| LCD77L (27.1, 0.49) | 7.3 | 12.5 | 340 | 0.49 | −58 | 35 | | | 100 |
| LCD76L (28.7, 0.49) | 7.8 | 13.1 | 360 | 0.49 | −56 | 41 | | | 130 |
| LCD76L (39.4, 0.49) | 11.2 | 17.0 | 520 | 0.49 | −55 | 39 | | | 150 |
| LCD77L (34.2, 0.30) | 5.8 | 22.6 | 440 | 0.30 | −57 | 43 | | | 106 |
| LCL (23.6, 0.44) | 5.7 | 12.2 | 300 | 0.45 | −65 | | 54 | 33 | <60 |
| LCL 19.6, 0.50) | 4.4 | 10.8 | 250 | 0.50 | −63 | | 50 | 30 | 75 |
| LCL (24.2, 0.48) | 9.1 | 15.7 | 420 | 0.48 | −62 | | 54 | 36 | 112 |
| LCL (35.1, 0.53) | 10.3 | 14.5 | 430 | 0.53 | −63 | | 49 | 33 | 118 |
| LCL (34.3, 0.46) | 8.7 | 16.9 | 430 | 0.46 | −64 | | 54 | 35 | 119 |
| LCL (40.1, 0.48) | 10.6 | 18.9 | 500 | 0.48 | −63 | | 54 | 42 | 146 |
| LCL (43.1, 0.53) | 12.5 | 18.1 | 530 | 0.53 | −62 | | 51 | 35 | 174 |

[a]Molar mass of each PLA endblock calculated from the molar mass of the midblock and the PLA content by ^{1}H NMR. [b]Number average molar mass of the midblock determined using MALLS-SEC. Triblock dn/dc was determined form the RI signal using the known concentration with the assumption of 100% mass recovery. [c]Calculated from total molar mass (sum of block molar masses) using a reference volume of 118 Å$^3$ and room temperature densities of 1.248 g cm$^{-3}$ and 1.02 g cm$^{-3}$ for PLA and PCL or PCD, respectively.[56] [d]Volume fraction of poly(lactide) in the block polymer was calculated from composition by ^{1}H NMR spectroscopy. [f]Determined by DSC. To ensure consistent thermal histories all samples were heated to 100 °C (rate of 5 °C min$^{-1}$) and cooled at the same rate. Data reported were taken from the second heating ramp at 5 °C min$^{-1}$. [g]$T_m$ defined as the peak maximum. Crystallinity was calculated using a reference enthalpy of fusion of 139.5 J g$^{-1}$.[48] [h]Determined using DMA. [i]The $T_{ODT}$ could not be accurately identified using DMA.

### 2.2.5 PCL-PLA Interaction Parameter

Block polymer microphase separation is influenced by architecture, the volume fraction (*f*) of each component, and the segregation strength—a product of the segment-segment interaction parameter (*χ*) and the overall (reference volume averaged) degree of polymerization (*N*). By utilizing controlled polymerization strategies the majority of these parameters can be altered synthetically; however, *χ* is measure of relative incompatibility, a property inherent to any given polymer pair. On the basis of solubility parameter estimates the interaction parmeter for poly(lactide) with another polyester is generally expected to increase as the later becomes more aliphtic. In this work we assume that the temperature dependance of *χ* is inverse and can be described by Equation 2.1:

$$\chi(T) = \frac{\alpha}{T} + \beta \tag{2.1}$$

We used the order-to disorder transition temperatures ($T_{ODT}$) of several composisitionally symmetric ($f_{LA}$= 0.46-0.53) ABA triblocks and the mean field theoretical segregation strength ($xN$ = 17.996) at the lameller to disorder phase boundry to estimate the temperature dependence of $\chi_{PLA-PCL}$.[1] The $T_{ODT}$ values were determined using dynamic mechanical analysis (DMA),[57] and *N* was calculated from the overall molar mass using a reference volume of 118 $Å^3$. This is shown for LCL in Figures 2.4 a and 2.4 b. The interaction parameter of this system is compared to structurally similar

polyester block polymers in Table 2.3.[20,16] Our estimate of $\chi_{PLA-PCL}$ is consistent with prior reports regarding phase behavior of doubly crystalline poly((-)-lactide-*block*-poly(ε-caprolactone) (PLLA-PCL) block polymer samples;[58,59,60,61,62,63,64] and is also consistent with the observed behavior of poly((±)-lactide/poly(ε-caprolactone) blends.[65] However, to our knowledge this is the first estimate of $\chi_{PLA-PCL}$ determined using experimentally measured $T_{ODT}$ values.
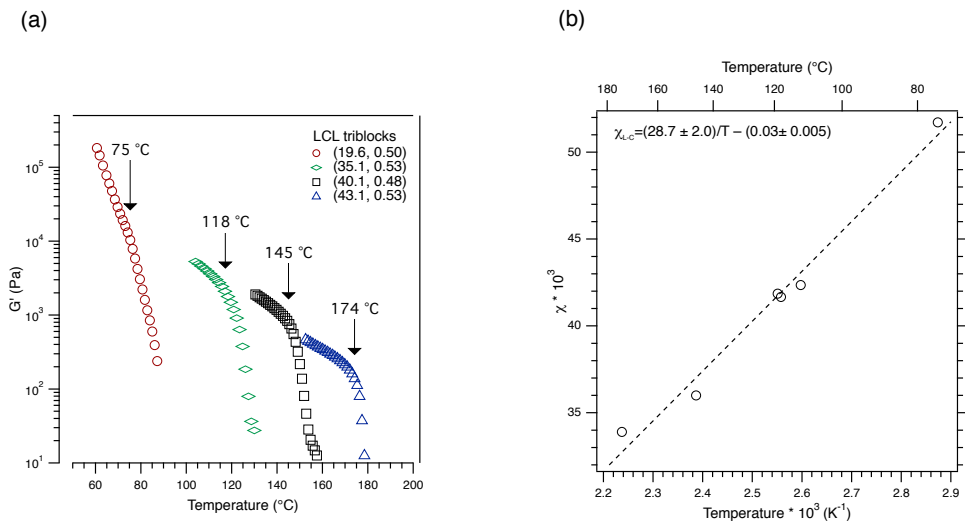


**Figure 2.4**

(a) Isochronal temperature ramp data on heating (1 rad s$^{-1}$, 1°C min$^{-1}$, 1% strain) for LCL triblock polymers LCL (19.6, 0.50)(○), LCL (35.1, 0.53)(◇), LCL (40.1, 0.48) (□), and LCL (43.1, 0.53) (△). (b) Inverse temperature dependence of $\chi_{PLA-PCL}$ and fit to equation 1. Two additional triblocks, LCL (24.2, 0.48) and LCL (34.3, 0.46) were excluded from (a) for clarity but are included in the fit shown in (b).

**Table 2.3**

Comparison of $\chi(T)$ for select aliphatic polyesters with poly(lactide)

| Polymer Pair | α | β | $\chi_{140\ °C)}$ | Reference: |
|---|---|---|---|---|
| PDL PLA | 69.1 ± 9.2 | −0.07 ± 0.03 | 0.1 | 20 |
| P6MCL PLA | 61.2 | −0.1 | 0.05 | 16 |
| PCD66 PLA | 56.3 ± 9.6 | −0.09 ± 0.03 | 0.05 | This work |
| PCD77 PLA | 45.8 ± 12.5 | −0.07 ± 0.03 | 0.04 | This work |
| PCL PLA | 28.7 ± 2.0 | −0.03 ± 0.005 | 0.04 | This work |

**2.2.6 Effect of Midblock Composition on Segregation Strength**

To determine the effect of midblock composition on the interaction parameter for block-statistical polymers containing PLA, we explored triblock polymers prepared from PCD66, and PCD77 midblocks. The results of this analysis are summarized in Table 2.3, corresponding DMA and linear fit data are shown in <u>Appendix E</u>. The reactivity ratios of DL and CL favor a gradient composition; therefore in LCDL triblocks the DL units are enriched near the junction of the PLA and CD copolymer blocks. The strength of this gradient depends details of the PCD synthesis, namely the initial feed composition and final conversion of each monomer. Theoretically a strong gradient could cause the measured value of $\chi_{PLA-PCD}$ to differ from that of polymer with a truly random PCD midblock. Beacuse the entropic terms are modest and because the enthalpic term is larger for $\chi_{PLA-PCD}$ than $\chi_{PLA-PCL}$, the segregation strength of LCL at high temperatures (T ≥ 180 °C) is predicted to be *higher* than LCDL block statistical polymers of the same overall degree of polymerization.

### 2.2.7 SAXS of Block Statistical Copolymers

Small-angle x-ray scattering (SAXS) was used to study the effects of midblock composition and crystallinity on the microphase separation of triblock samples. The SAXS data for lower molar mass samples at room temperature (20 °C), LCL (23.6, 0.44), LCD77L (22.8, 0.48), and LCD65L (20.0, 0.49), exhibited strong primary reflections but no distinct higher order reflections. These data are consistent with low segregation strength, microphase-separated materials that lack long-range order.[18,38,66,67] As shown for representative samples in Figure 2.5, compositionally symmetric LCDL and LCL triblocks with higher molar mass midblocks exhibit reflections indicative of the expected lamellar morphologies. Although the latter are semicrystalline, the $T_{ODT}$ values are higher than the crystallization temperature. When annealed above 60 °C then cooled the microstructure of the sample is preserved.

As shown in the inset of Figure 2.6, higher molar mass compositionally asymmetric samples, e.g. LCD69L (131, 0.32), exhibited intense principle peaks indicative of microphase separation; however, the morphology of these materials could not be definitively assigned due to the absence of well-defined higher order reflections. Although it was anticipated that LCD69 (131, 0.32) would adopt a cylindrical morphology, is likely the high molar mass samples are kinetically trapped in a poorly ordered state.[18] The SAXS data for a lower molar mass sample at, LCD77L (34.2, 0.30), exhibited several higher order peaks at ($q/q^* = 3^{\frac{1}{2}}, 4^{\frac{1}{2}}, 7^{\frac{1}{2}}, 9^{\frac{1}{2}}, 12^{\frac{1}{2}}$) consistent with the hexagonally close packed cylinders anticipated for polymers of this composition.[1] The

SAXS data for this triblock and low molar mass compositionally asymmetric samples are included in <u>Appendix E.</u>
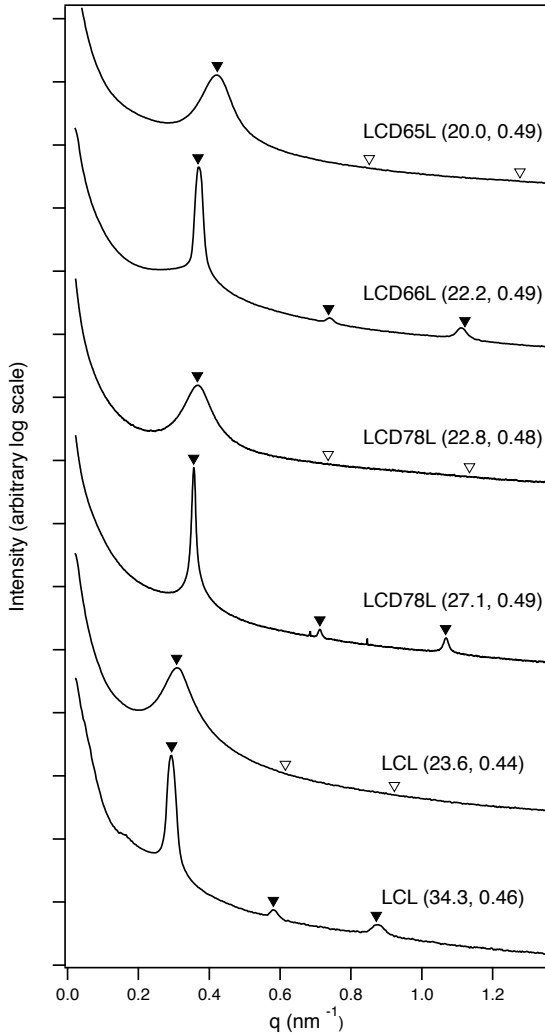


**Figure 2.5**

Room temperature SAXS data for of representative compositionally symmetric LCL and LCDL triblock samples. The principle peaks are marked with (▼). Calculated reflections for anticipated lamellar morphologies are also marked with (▼) and (▽) denoting reflections that are present, and absent respectively.
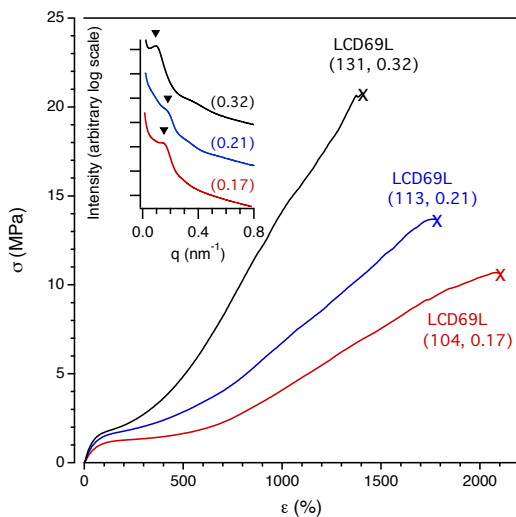
**Figure 2.6**

Representative examples of room temperature uniaxial extension of selected LCD69L triblock elastomers. Experiments were conducted with constant crosshead velocity of 50 mm min$^{-1}$. For each sample, average and standard deviation of a minimum of 5 specimens is reported in Table 4. The graph inset displays room temperature SAXS data of compression molded LCD69L elastomers prior to uniaxial extension test.

## 2.2.8 Tensile Properties of Triblock Samples

The tensile properties of LCDL triblocks, shown in Figure 6, were found to be qualitatively similar to other PLA containing polyester triblock elastomers.[16,20,19,18] Over the range of compositions investigated, Young's modulus ($E_y$) and ultimate tensile strength ($\sigma_b$) both increased with PLA content while the elongation at break ($\varepsilon_b$) decreased. At fixed PLA content LCD69L triblocks exhibited significant increases in stress at break compared to LDL; these data are provided in Table 4.[20] Interestingly, the elongation at break and ultimate tensile strength of high molar mass LCD69L triblocks are nearly the same as L6MCL triblocks of similar lactide content.[16] LCD69L and L6MCL, are both significantly tougher than LML of similar molar mass and

42

composition.[68] We believe the differences in the tensile behavior of these triblocks may be partially due to changes in the chain cross-section[69] and entanglement molar mass of the midblock.[27] From the plateau modulus of PCD69 ([Appendix F.](#)) we estimated the entanglement molar mass of PCD69 to be $M_e$ = 3.9 kg mol$^{-1}$. Whereas the reported entanglement molar mass of PM and PDL are both relativley high, ($M_e$ = 11-14 kg mol$^{-1}$ and $M_e$ = 5.9 kg mol$^{-1}$, respectively)[20,68] the entanglement molar mass of PCD69 is lower, closer to that of PCL (3.0 kg mol$^{-1}$) and P6MCL (3.0 kg mol$^{-1}$).[70] This is consistant with past reports regarding the relationship between composition and plateau modulus for random copolymers.[45]

**Table 2.4.**

**Mechanical Properties of Poly(lactide) Block Polymer Elastomers**

| Sample | $E_Y$ (MPa) | $\sigma_{300}$ (MPa) | $\sigma_b$ (%) | $\varepsilon_b$ (%) |
|---|---|---|---|---|
| LCD69L (104, 0.17) | 1.5 ± 0.3 | 1.3 ± 0.1 | 9.9 ± 0.6 | 2100 ± 100 |
| LCD69L (113, 0.21) | 2.0 ± 0.3 | 2.0± 1.2 | 13.5 ± 0.3 | 1690 ± 90 |
| LCD69L (131, 0.32) | 3.5 ± 0.3 | 2.9 ± 0.3 | 18 ± 4 | 1200 ± 100 |
| LCD69L (31.4, 0.33) | 1.1 ± 0.1 | 0.60± 0.1 | 0.9 ± 0.1 | 610 ± 20 |
| [a]LDL (136, 0.21) | 1.0 ± 0.1 | | 4.5 ± 0.3 | 1600 ±200 |
| [a]LDL(148, 0.27) | 1.1 ± 0.1 | | 9.4 ± 0.7 | 1310 ± 40 |
| [a]LDL (15.3, 0.30) | 4.5 ± 0.2 | | 0.24 ± 0.01 | 218 ± 9 |
| [c]LML (122, 0.15) | 0.45 ± 0.05 | | 0.03 | 630 ± 60 |
| [b]LML (48.2, 0.26) | 0.8 ± 0.1 | | 3.8 ± 0.2 | 872 ± 6 |
| [d]L6MCL (122, 0.18) | 1.87 ± 0.03 | | 10.2 ± 0.8 | 1880 ± 70 |
| [d]L6MCL (150, 0.31) | 31 ± 9 | | 14.0 ± 2 | 1400 ± 100 |

LCD69L samples were tested at room temperature with a constant crosshead velocity of 50 mm min$^{-1}$. [a]Information was taken from reference [20]. [b]Information was taken from reference 71. [c]Information for poly((±)-lactide)-poly(menthide)-poly((±)-lactide) (LML) was taken from reference [68]. Volume fractions were calculated using a room temperature of 0.975 g cm$^{-3}$ for poly(menthide) PM.[68] [d]Information was taken from reference 18. Volume fractions were calculated using a room temperature density of 0.97 for P6MCL.

### 2.2.9 Synthesis of Multiblock Polymers

At fixed composition the toughness of LCD69L triblocks decreased dramatically with molar mass. For example LCD69L (31.4, 0.33) exhibited a 95% reduction in ultimate tensile strength and a 63% decrease in elongation at break compared to LCD69L (131, 0.32). This is behavior similar to that of previously reported LDL and poly((±)-lactide)-poly(menthide)-poly((±)-lactide) (LML) triblocks.[71,20] We recently demonstrated that melt-processable $(LDL)_n$ multiblocks can be prepared by coupling low molar mass triblocks.[20] In every case the multiblocks were considerably tougher than the parent triblock; however, because the individual domains were unentangled, the elongation and stress at break were low compared to high molar mass LDL triblocks.[20] When designing these multiblocks, the upper molar mass of the AB repeat unit is limited by the segregation strength. Because $\chi_{PLA-PCD}$ is lower than $\chi_{PLA-PDL}$ it is possible to prepare multiblock polymers with higher molar mass segments while retaining an accessible $T_{ODT}$ values. To demonstrate this, a number of LCDL triblock polymers were coupled using diisocyanate coupling agent 4,4'-methylene bis(phenylisocyante) (MDI), in the presence of catalytic $Sn(Oct)_2$ as shown in Scheme 2.2, below.

## Scheme 2.2

**Synthesis of linear (LCDL)ₙ multiblock polymers**
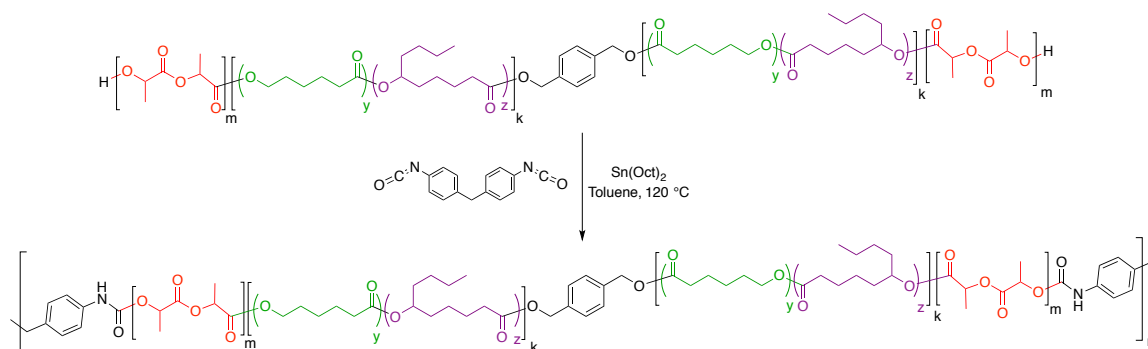


Notably, using the same catalyst for all three reactions ($\varepsilon$-CL/$\varepsilon$-DL copolymerization, lactide chain extension, and coupling) greatly simplifies the process because the multiblock can, in theory, easily be prepared in one pot without isolating intermediate products. In this work, the triblocks *were* isolated prior to coupling to allow characterization and mechanical testing of the parent material. As summarized in Table 2.5, below, the purified (LCDL)ₙ multiblocks by SEC showed an increase in $M_n$ and Đ upon coupling compared to the starting triblocks. The average number of triblock copolymers per multiblock chain, ‹$n$›, was calculated from the ratio of the $M_n^{SEC}$ of multiblock to $M_n^{SEC}$ of the triblock.[22] The values of ‹$n$› in this study is relatively low (2 ≤ ‹$n$› ≤ 4). This poor coupling efficiency may be due to stoichiometric imbalanced in the NCO:OH reactive group. However, it is also possible that the high molar mass of the telechelic prepolymers may also impact coupling. A number of multiblock samples prepared using the strategy are compared directly to their parent triblocks in Table 2.5 below.

**Table 2.5.**

**(LCDL)$_n$ multiblock polymers synthesized**

| Sample ID | Block $M_n$ (kg mol$^{-1}$) [a]PLA | [b]PCD | [c]$M_n^{SEC}$ (kg mol$^{-1}$) | [c]Đ | [d]\<n\> | [e]$f_{PLA}$ | [f]$T_g$ (°C) | [f]$T_g$ (°C) | [g]$T_{ODT}$ (°C) |
|---|---|---|---|---|---|---|---|---|---|
| LCD69L(24.2, 0.17) | 2.5 | 19.4 | 26.5 | 1.04 | - | 0.17 | −52 | 18 | nd |
| LCD69L(24.2,0.17)$_{3.46}$ | 2.5 | 19.4 | 91.8 | 1.41 | 3.46 | 0.17 | −52 | 30 | nd |
| LCD69L(31.4, 0.33) | 6.0 | 19.4 | 23.2 | 1.08 | - | 0.33 | −59 | 30 | 95 |
| LCD69L(31.4,0.33)$_{2.0}$ | 6.0 | 19.4 | 47.9 | 1.41 | 2.0 | 0.33 | −58 | 41 | 112 |
| LCD77L(34.2, 0.30) | 5.8 | 22.6 | 27.5 | 1.04 | - | 0.30 | −57 | 43 | 106 |
| LCD77L(34.2, 0.30)$_{2.0}$ | 5.8 | 22.6 | 54.7 | 1.33 | 2.0 | 0.30 | −56 | 47 | 120 |
| LCD69L (43.2, 0.5) | 11.9 | 19.4 | 19.4 | 1.06 | - | 0.50 | −51 | 38 | 190 |
| LCD69L(43.2, 0.5)$_{1.9}$ | 11.9 | 19.4 | 36.0 | 1.42 | 1.91 | 0.50 | −53 | 44 | >200 |

[a]Molar mass reported for PLA block, or ½ the total molar mass of PLA per triblock chain. This value was calculated from the molar mass of the midblock, determined using MALLS-SEC and the composition, determined using 1HNMR spectroscopy. [b]Number average molar mass of the midblock determined using MALLS-SEC [c]Determined using MALLS-SEC. [d]The average number of triblocks per multiblock chain, taken from the ratio of multiblock number average molar mass and triblock number average molar mass, determined using MALLS-SEC. [e]Volume fraction of poly(lactide) in the statistical block polymer determined using $^1$H NMR spectroscopy. [f]Glass transition temperatures were determined by DSC on the second heating ramp with a rate of 5 °C min-1. [g]Order to disorder transition temperatures were determined using DMA. Values for triblocks are reported for an isochronal (1 rad s$^{-1}$) temperature ramp at a rate of 1 °C and a constant strain of (1%). Values for multiblocks are reported for an isochronal (0.1 rad s$^{-1}$) temperature ramp at a rate of 0.2 °C and a constant strain of (1%).

**Table 2.6.**

**Mechanical Comparison of LCDL triblocks and (LCDL)$_n$ multiblocks**

| $^a$Sample | $E_Y$ (MPa) | $\sigma_{300}$ (MPa) | $\sigma_b$ (%) | $\varepsilon_b$ (%) |
|---|---|---|---|---|
| LCD77L (34.2, 0.30) | 7.1 ± 1.3 | 1.60 ± 0.05 | 1.7 ± 0.2 | 580 ± 60 |
| LCD69L (31.4, 0.33) | 1.07 ± 0.13 | 0.57 ± 0.06 | 0.9 ± 0.1 | 610 ± 20 |
| LCD69L (43.2, 0.50) | 47± 15 | | 2.9 ± 0.5 | 90 ± 30 |
| (LCD77L) (34.2, 0.30)$_{2.0}$ | 2.3 ± 04 | 1.86 ± 0.06 | 9.0 ± 0.3 | 1950 ± 70 |
| (LCD69L) (31.4, 0.33)$_{2.0}$ | 1.4 ± 0.4 | 1.61 ± 0.09 | 6.4 ± 0.2 | 1700 ± 100 |
| (LCD69L  (43.2, 0.50)$_{1.9}$ | 32 ±4 | 6.64 ± 0.60 | 8.5 ± 0.6 | 860 ± 60 |

Room temperature tensile properties of multiblock samples. $^a$All samples were prepared by compression molding and tested at room temperature with a constant crosshead velocity of 50 mm min-1. The data are the average and standard deviation for a minimum of 5 samples.

### 2.2.10 Mechanical Properties of Multiblock Polymers

In good agreement with previous work, each of the multiblock samples showed an increase in tensile strength relative to the corresponding low molar mass triblock precursor. For example, the multiblock sample (LCD77L)$_{2.0}$ (34.2, 0.30) was characterized a strain at break over three times larger and stress at break that was an order of magnitude higher than its precursor triblock, LCD77L (34.2, 0.30). These representative samples are shown in Figure 2.7, below. A similar trend was also observed for the other triblock-multiblock pairs. As anticipated, although the triblock precursors were of relatively high molar mass (25-35 kg mol$^{-1}$), the order-disorder transition temperatures of the multiblock samples still below the reversion temperature of the urethane linkage, a prerequisite for high sheer melt processing.[20]
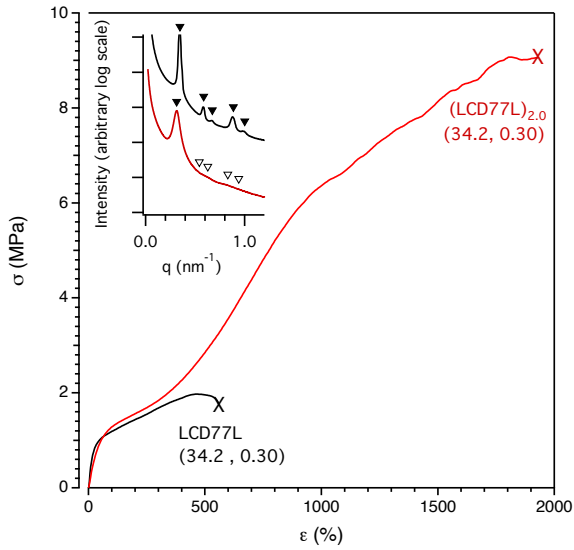
**Figure 2.7**

Representative examples of room temperature uniaxial extension of a LCD77L triblock and corresponding $(LCD77L)_n$ multiblock. Experiments were conducted with constant crosshead velocity of 50 mm min$^{-1}$. For each sample, average and standard deviation of a minimum of 5 specimens is reported in Table 2.6. The graph inset displays room temperature SAXS data of compression molded samples prior to uniaxial extension test.
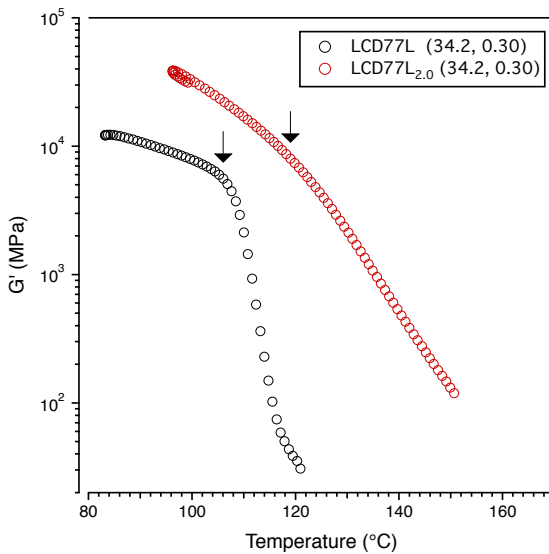


**Figure 2.8**

Isochronal temperature ramp data on heating (1 rad s$^{-1}$, 1°C min$^{-1}$, 1% strain) for LCD77L (34.2, 0.3). Isochronal temperature ramp data on heating (0.1 rad s$^{-1}$, 0.2°C min$^{-1}$, 1% strain) for multiblock $(LCD77L)_{2.0}$ (34.2, 0.3).

48

## 2.3 Conclusions

We have demonstrated that the batch melt copolymerization of ε-caprolactone and ε-decalactone can be utilized to generate α,ω-hydroxy telechelic statistical copolymers with good control over composition, molecular weight and dispersity. One advantage of this particular selection of comonomers is the ability to modify the degree crystallinity and melting temperature without affecting the glass transition temperature of the material. These α,ω-hydroxy telechelic polymers were used as macroinitiatiors for the synthesis well defined telechelic triblocks. The interaction parameter for the midblock with PLA was estimated from the $T_{ODT}$ values of microphase separated symmetric triblocks, and was found to be dependent on the composition of the midblock copolymer.

By varying midblock composition and lactide content it was possible to significantly alter the mechanical behavior of the corresponding block-statistical copolymers. At fixed midblock composition, tensile properties depended largely on molar mass and lactide content. Compared to triblock polymers with PDL midblocks, those prepared using PCD copolymers demonstrated significantly higher tensile stress at failure, an effect we attribute to the reduced entanglement molar mass relative to PDL. The facile synthesis, and tunable mechanical properties of PLA block-statistical triblock and multiblock polymers make these materials attractive new thermoplastic elastomers.

## 2.4 Experimental Section

### 2.4.1 Materials

ε-Caprolactone (Sigma-Aldrich), and ε-decalactone (Sigma-Aldrich) were each distilled under reduced pressure over calcium hydride and passed through a column of dry activated basic alumina (Sigma-Aldrich) without exposing to air. Tin(II) 2-ethylhexanoate (Sigma-Aldrich) was distilled (3×) under reduced pressure. 1,4-Benzenedimethanol (Sigma-Aldrich) was dried under reduced pressure at room temperature for 96 h. 4, 4'-Methylenebis(phenyl isocyanate) (Sigma-Aldrich) was stored in a -4°C freezer and used as received. Toluene (Fisher), used for triblock syntheses, was purified by passing though activated alumina columns (Glass Contour, Laguna Beach, CA) prior to use. D,L-Lactide, a kind gift from Ortec Inc (Easely, SC), was used as received. Chromium(III) acetylacetonate (Sigma-Aldrich) was purchased and used as received. All reagents mentioned were stored in a nitrogen-filled glovebox. Toluene (Fisher) used for large scale multiblock syntheses was distilled to remove the azotrope, stirred over calcium hydride for at least 24 hours, then distilled again under argon immediately prior to use. All other solvents were used as received without further purification.

Glass ampules, pressure vessels, Teflon caps, and Teflon-coated magnetic stir bars were dried in a 110 °C oven for a minimum of 6 hours prior to use. Pressure vessels, used for copolymer and block polymer syntheses, were charged and sealed in a glovebox under nitrogen then quickly removed and placed in a heating bath. Ampules, used for small-

scale copolymerization reactions, were also charged in an inert atmosphere then flame sealed under vacuum.

### 2.4.2 Nomenclature

In this work copolymer midblocks are named using a two-letter two-number code denoting the composition of the polymer. The letter codes are C and D for ε-caprolactone, and ε-decalactone, respectively. The number code is used to indicate the mole fraction of ε-caprolactone in the polymer. The number average molar mass is enclosed in parentheses following the name, e.g. CD77 (22.6) indicates a poly(ε-caprolactone-*co*-ε-decalactone) copolymer that is 22.6 kg mol$^{-1}$ and 77 mol% poly(ε-caprolactone) as determined by MALLS SEC and $^1$H NMR spectroscopy, respectively. Block-statistical copolymer triblocks are named using LXX##L, where XX## is the two-letter, two-number code of the midblock used to prepare the triblock. Block-statistical copolymer multblocks blocks are named (LXX##L)$_n$, where *n* is defined as the ratio of multiblock $M_n$ to triblock $M_n$ (both determined from MALLS SEC). For both triblock and multiblock polymers, the total molar mass and PLA volume fraction are included parenthetically following the letter/number code. Total triblock molar mass was calculated from the molar mass of the midblock, determined using MALLS-SEC and the composition, determined using $^1$H NMR spectroscopy.

### 2.4.3 Synthetic Methods

*Representative synthesis of poly(ε-caprolactone)-co-poly(ε-decalactone) statistical copolymer [PCD77 (22.6)]:* In a glovebox ε-decalactone (123 g, 0.71 moles), ε-caprolactone (185 g, 1.62 moles), $Sn(Oct)_2$ (0.9342 g, 2.306 mmol), and 1,4-benzenedimethanol (1.7513 g, 12.67 mmol) were added to a 500 mL pressure vessel equipped with a Teflon-coated magnetic stir bar. The sealed reaction vessel was placed in a 120 °C oil bath and stirred for 2 h before cooling to room temperature. A crude aliquot was taken to determine conversion, then the reaction solution was cooled to room temperature, diluted with dichloromethane, precipitated in methanol, and dried, yielding PCD77 (223.5 grams, 84% gravimetric yield). $^1$H NMR, $CDCL_3$: δ(ppm): 0.85-.91 (t, J=7.15, 115 H, -C**H**$_3$) 1.19 – 1.43 (m, 494 H,       -OC=O-CH$_2$CH$_2$C**H**$_2$CH$_2$CH(CH$_2$C**H**$_2$C**H**$_2$CH$_3$)-       and       -OC=O-CH$_2$CH$_2$C**H**$_2$CH$_2$CH$_2$-)       1.46-1.70       (m,       824       H,       -OC=O-CH$_2$C**H**$_2$CH$_2$C**H**$_2$CH(C**H**$_2$CH$_2$CH$_2$CH$_3$)-  and  -OC=O-CH$_2$C**H**$_2$CH$_2$C**H**$_2$CH$_2$-)       2.26-2.33  (m,  315  H,  -OC=O-C**H**$_2$CH$_2$CH$_2$CH$_2$CH(CH$_2$CH$_2$CH$_2$CH$_3$)-  and       -OC=O-C**H**$_2$CH$_2$CH$_2$CH$_2$CH$_2$-) 3.54-3.63 (m, 2.0 H, C**H**$_2$-OH) 3.98-4.14 (m, 250H, -OC=O-CH$_2$CH$_2$CH$_2$CH$_2$C**H**$_2$-)       4.79-4.91       (quin,       *J*=5.8       Hz,       37       H,       -OC=O-CH$_2$C**H**$_2$CH$_2$CH$_2$C**H**(CH$_2$CH$_2$CH$_2$CH$_3$)-) 5.10 (s, 4 H,       C**H**$_2$-O) 7.33 (s, 4 H, Ar-**H)**

*Representative synthesis of poly($_{D,L}$-lactide)-block-poly(ε-caprolactone)-co-poly(ε-decalactone)-block-block-statistical copolymer [LCD77L (34.2, 0.30)]:* In a nitrogen filled glovebox a 500 ml pressure vessel equipped with a Teflon-coated magnetic stir bar was charged with PCD (110 grams), (±)-lactide (58.716 grams, 0.407 moles), $Sn(Oct)_2$ (300 mg, 0.741 mmol), and toluene (300 ml). The vessel was capped, removed from the glovebox, and heated

in an oil bath to 60 °C. When the contents were dissolved, the vessel was transferred to a 120 °C oil bath and stirred for 2 hours (until the (±)-lactide conversion reached 83 %). At this time the reaction was cooled and precipitated in cold methanol. The isolated polymer was dried in a vacuum oven to obtain LCD77L (135 grams, 85% gravimetric yield). ^{1}H NMR, CDCL$_3$ δ(ppm): 0.85-.91 (t, J=7.15, 113 H, -C**H**$_3$) 1.19 – 1.43 (m, 488 H, -OC=O-CH$_2$CH$_2$C**H$_2$**CH$_2$CH(CH$_2$C**H$_2$**C**H$_2$**CH$_3$)- and -OC=O-CH$_2$CH$_2$C**H$_2$**CH$_2$CH$_2$-) 1.46-1.70 (m, 1346 H, -OC=O-CH$_2$C**H$_2$**CH$_2$C**H$_2$**CH(C**H$_2$**CH$_2$CH$_2$CH$_3$)- and -OC=O-CH$_2$C**H$_2$**CH$_2$C**H$_2$**CH$_2$- and - O-C=OCHC**H$_3$**-), 2.26-2.33 (m, 315 H, -OC=O-C**H$_2$**CH$_2$CH$_2$CH$_2$CH(CH$_2$CH$_2$CH$_2$CH$_3$)- and -OC=O-C**H$_2$**CH$_2$CH$_2$CH$_2$CH$_2$-) 3.98-4.14 (m, 245 H, -OC=O-CH$_2$CH$_2$CH$_2$CH$_2$C**H$_2$**-) 4.33-4.38 (m, 2.0 H, -C**H**-CH3-OH) 4.79-4.91 (quin, J=5.8 Hz, 37 H, -OC=O-CH$_2$CH**$_2$**CH$_2$CH$_2$C**H**(C**H$_2$**CH$_2$C**H$_2$**CH$_3$)-), 5.10 (s, 5.0 H, Ar-C**H$_2$**-O-) 5.11 - 5.26 (m, 145 H, - OC=O-C**H**(CH$_3$)-O-) 7.33-7.35 (s, 4 H, Ar–**H** initiator)

*Poly($_{D,L}$-lactide)-block-poly(ε-caprolactone)-co-poly(ε-decalactone)-block-poly($_{D,L}$lactide)* *multiblock statistical copolymer [(PCD77)$_{2.0}$ (34.2, 0.30)]:* To a 1 liter 3-necked round bottom flask was added 57.0 grams LCDL triblock polymer, the flask and its contents were dried in a vacuum oven overnight and then fitted with an overhead stir assembly, gas inlet, bubbler, and septum. The reaction was purged with argon for one hour then freshly distilled toluene (250 ml) was added to dissolve the block polymer. The reaction was heated to 110 °C in an oil bath and stirred while purging with argon for 1 hour, at this time Sn(oct)$_2$ (200 mg, 0.494 mmol) was injected. Following the introduction of the catalyst, the reaction was purged an additional 10 minutes then 4,4'-methylene bis(phenyl isocyante) (0.4050 grams, 1.6184 mmol) was added under a vigorous argon

flow. The reaction was stirred at 110 °C for 1 hour then cooled, precipitated in cold methanol, and dried to give (LCD77L)$_{2.0}$ (53 grams, 91% yield).

*Molecular Characteristics of Polymer Samples Included in Chapter 2.*

**Table 2.7**

**Telechelic PCL homopolymer midblocks used for this work.**

| Midblock | [a]$M_n^{NMR}$ (kg mol$^{-1}$) | [b]$M_n^{SEC}$ (kg mol$^{-1}$) | [b]Đ | [c]$T_g$ (°C) | [c]$T_m$ (°C) | [c]X (%) |
|---|---|---|---|---|---|---|
| PCL (10.8) | 11.1 | 10.8 | 1.06 | −62 | 55 | 52 |
| PCL(12.2) | 12.2 | 12.2 | 1.13 | −62 | 55 | 34 |
| PCL (11.6) | 10.1 | 11.6 | 1.06 | −60 | 54 | 50 |
| PCL (14.5) | 16.2 | 14.5 | 1.06 | −61 | 55 | 49 |
| PCL (15.7) | 16.0 | 15.7 | 1.13 | −64 | 55 | 59 |
| PCL (18.9) | 16.9 | 18.9 | 1.15 | −63 | 56 | 62 |
| PCL (18.1) | 18.8 | 18.1 | 1.18 | −62 | 55 | 53 |
| PCL (22.1) | 18.9 | 22.1 | 1.16 | −63 | 55 | 51 |

[a]Number average molar mass determined using ^{1}HNMR spectroscopy. Calculated using initiator methylene protons as an internal standard. [b]Number average molar mass and dispersity determined using MALLS-SEC; dn/dc was found from the RI signal using the known concentration and the assumption of 100% mass recovery. [c]Glass transition temperature values and melting point values were determined by DSC on the second heating ramp with a rate of 5 °C min$^{-1}$. Crystallinity was calculated using a reference enthalpy of fusion of 139.5 J g$^{-1}$ for fully crystalline PCL.

**Table 2.8**

**Telechelic PCD polymer midblocks used for this work.**

| Midblock | [a]$M_n^{nmr}$ (kg mol$^{-1}$) | [b]$F_{CL}$ | [c]$M_n^{SEC}$ (kg mol$^{-1}$) | [c]Đ | [d]$T_g$ (°C) | [d]$T_m$ (°C) | [d]X (%) |
|---|---|---|---|---|---|---|---|
| CD66 (9.2) | 8.2 | 0.66 | 9.2 | 1.10 | −60 | | |
| CD66 (10.2) | 9.7 | 0.66 | 10.2 | 1.20 | −63 | | |
| CD65 (15.5) | 14.2 | 0.65 | 15.5 | 1.10 | −61 | | |
| CD63 (18.3) | 18.3 | 0.63 | 18.3 | 1.13 | −62 | | |
| CD78 (10.6) | 9.40 | 0.78 | 10.6 | 1.08 | −64 | 20 | 19 |
| CD77 (12.5) | 11.37 | 0.77 | 12.5 | 1.05 | −64 | 16 | 17 |
| CD76 (13.1) | 13.8 | 0.76 | 13.1 | 1.12 | −63 | 18 | 12 |
| CD76 (19.0) | 15.0 | 0.76 | 17.0 | 1.08 | −65 | 16 | 15 |
| CD77 (22.6) | 20.5 | 0.77 | 22.6 | 1.04 | −64 | 18 | 15 |
| CD69 (19.4) | 19.61 | 0.69 | 19.4 | 1.05 | −62 | | |
| CD68 (42.5) | 41.5 | 0.68 | 42.5 | 1.10 | −63 | | |
| CD67 (48.5) | 45.1 | 0.67 | 48.5 | 1.30 | −61 | | |
| CD68 (50.1) | 54.5 | 0.68 | 50.1 | 1.41 | −61 | | |
| CD69 (83.4) | 95.8 | 0.69 | 83.4 | 1.16 | −62 | | |
| CD68 (86.5) | 104.5 | 0.68 | 86.5 | 1.44 | −61 | | |

[a]Number average molar mass determined using ^{1}HNMR spectroscopy. Calculated using initiator methylene protons as an internal standard. [b]Mole fraction of ε-Caprolactone in the copolymer determined using ^{1}H NMR spectroscopy. [c]Number average molar mass and dispersity determined using MALLS-SEC; d$n$/d$c$ was found from the RI signal using the known concentration and the assumption of 100% mass recovery. [d]Glass transition temperatures and melting point values were determined by DSC on the second heating ramp with a rate of 5 °C min$^{-1}$. Cystallinity was calculated using a reference enthalpy of fusion of 139.5 J g$^{-1}$ for fully crystalline PCL.

**Table 2.9**

**Telechelic LCL polymer triblocks used for this work.**

| Triblock | Block $M_n$ (kg mol$^{-1}$) [a]PLA | [b]PCL | [c]$N_{tot}$ | [d]$f_{PLA}$ | [e]D (nm) | [f]$T_g$ (°C) | [f]$T_m$ (°C) | [f]X % | [g]$T_{ODT}$ (°C) |
|---|---|---|---|---|---|---|---|---|---|
| LCL (23.6, 0.44) | 5.7 | 12.2 | 300 | 0.45 | 17 | −64 | 54 | 33 | <60 |
| LCL (19.6, 0.50) | 4.4 | 10.8 | 250 | 0.50 | 17 | −63 | 50 | 30 | 75 |
| LCL (24.2, 0.48) | 9.1 | 16.0 | 425 | 0.48 | 19 | −62 | 54 | 36 | 112 |
| LCL (35.1, 0.53) | 10.3 | 14.5 | 430 | 0.53 | 19 | −63 | 49 | 33 | 118 |
| LCL (34.3, 0.46) | 8.7 | 16.9 | 430 | 0.46 | 21 | −64 | 54 | 35 | 119 |
| LCL (40.1, 0.48) | 10.6 | 18.9 | 500 | 0.48 | 23 | −63 | 54 | 42 | 146 |
| LCL (43.1, 0.53) | 12.5 | 18.1 | 530 | 0.53 | 20 | −62 | 51 | 35 | 174 |

[a]Molar mass reported for PLA block, or ½ the total molar mass of PLA per triblock chain. This value was calculated from the molar mass of the midblock, determined using MALLS-SEC and the composition, determined using 1HNMR spectroscopy. [b]Midblock molar mass determined using MALLS-SEC. [c]Calculated from total molar mass (sum of block molar masses) using a reference volume of 118 Å and room temperature densities of 1.248 g cm$^{-3}$ and 1.02 g cm$^{-3}$ g cm$^{-3}$ for PLA and PCL midblock, respectively. [d]Volume fraction of poly(lactide) in the statistical block polymer determined using $^1$H NMR spectroscopy. [e]Principal domain spacing of the bulk sample determined by SAXS at room temperature. [f]Glass transition temperatures and melting point values were determined by DSC on the second heating ramp with a rate of 5 °C min-1. [g]Order to disorder transition temperatures were determined using DMA. Values are reported for an isochronal (1 rad s$^{-1}$) temperature ramps at a rate of 1 °C and a constant strain of (1%).

**Table 2.10**

**Telechelic LCDL polymer triblocks used for this work.**

| Triblock | Block $M_n$ (kg mol$^{-1}$) | | [c]$N_{tot}$ | [d]$f_{PLA}$ | [e]$D$ (nm) | [f]$T_g$ (°C) | [f]$T_g$ (°C) | [g]$T_{ODT}$ (°C) |
|---|---|---|---|---|---|---|---|---|
| | [a]PLA | [b]PCD | | | | | | |
| LCD65L (20.0, 0.49) | 5.4 | 9.2 | 250 | 0.49 | 15 | −54 | 26 | 65 |
| LCD66L (22.2, 0.49) | 6.0 | 10.2 | 280 | 0.49 | 17 | −56 | 31 | 92 |
| LCD67L (43.7, 0.49) | 9.1 | 15.5 | 420 | 0.49 | 20 | −57 | 37 | 126 |
| LCD63L (40.7, 0.5) | 11.2 | 18.3 | 510 | 0.50 | 24 | −59 | 49 | 170 |
| LCD78L (22.8, 0.48) | 6.1 | 10.6 | 280 | 0.48 | 17 | −58 | 29 | 70 |
| LCD77L (27.1, 0.49) | 7.3 | 12.5 | 340 | 0.49 | 18 | −58 | 35 | 100 |
| LCD76L (28.7, 0.49) | 7.8 | 13.1 | 360 | 0.49 | 20 | −56 | 41 | 130 |
| LCD76L (39.4, 0.49) | 11.2 | 17.0 | 520 | 0.49 | 22 | −55 | 39 | 150 |
| LCD69L (104, 0.17) | 10.5 | 83.4 | 1270 | 0.17 | 44 | −60 | 47 | >200 |
| LCD69L (113, 0.21) | 14.6 | 83.4 | 1320 | 0.21 | 34 | −60 | 50 | >200 |
| LCD69L (131, 0.32) | 24.0 | 83.4 | 1420 | 0.32 | 60 | −59 | 53 | >200 |

[a]Molar mass reported for PLA block, or ½ the total molar mass of PLA per triblock chain. This value was calculated from the molar mass of the midblock, determined using MALLS-SEC and the composition, determined using ^{1}HNMR spectroscopy. [b]Number average molar mass of the midblock determined using MALLS-SEC [c]Calculated from total molar mass (sum of block molar masses) using a reference volume of 118 Å and room temperature densities of 1.248 g cm$^3$ and 1.02 g cm$^{-3}$ g cm$^{-3}$ for PLA and copolymer midblock, respectively. [d]Volume fraction of poly(lactide) in the statistical block polymer determined using ^{1}H NMR spectroscopy. [e]Principal domain spacing of the bulk sample determined by SAXS at room temperature. [f]Glass transition temperatures and melting point values were determined by DSC on the second heating ramp with a rate of 5 °C min$^{-1}$. Crystallinity was estimated using a reference enthalpy of fusion of 139.5 J g$^{-1}$. [g]Order to disorder transition temperatures were determined using DMA. Values are reported for an isochronal (1 rad s$^{-1}$) temperature ramps at a rate of 1 °C and a constant strain of (1%).

**Table 2.11**

Hysteresis of block-statistical copolymer triblock and multiblock samples

| Sample | [a]Cyle1 (%) | [b]Cycle2 (%) |
|---|---|---|
| LCD69L (104, 0.17) | 26-28 | 15-17 |
| LCD69L (113, 0.21) | 24-27 | 11-14 |
| LCD69L (131, 0.32) | 34-37 | 19-20 |
| LCD77L (34.2, 0.30) | 55-57 | 36-38 |
| (LCD77L)$_{2.0}$ (34.2, 0.30) | 29-32 | 18-22 |

[a]Hysteresis tests were conducted at a constant crosshead velocity of 110 mm min$^{-1}$ and strain of 67%. The data is reported is the energy loss (%) on relaxation for the indicated cycle and is given as the measured range of three specimens.

### 2.4.4 Characterization Methods

All general characterization and instrumental methods are provided in Appendix A. Characterization methods specific to Chapter 2 are given in the sections below.

*$^1$H NMR Spectroscopy of Copolymer Samples*

Poly($\varepsilon$-caprolactone-*co*-$\varepsilon$-decalactone) copolymer composition and molar mass were estimated by $^1$H NMR using the following method: The singlet corresponding to the initiator methine (5.10 ppm) protons was used as an internal standard. The degree of polymerization of the PDL component, $N_{N(D)}$, was found using the integral of the peak corresponding to the PDL methine resonances in the region of 4.90–4.78 ppm (-OC=OCH$_2$CH$_2$CH$_2$CH$_2$**CH**(CH$_2$CH$_2$CH$_2$CH$_3$)O-). The degree of polymerization of the PCL component, $N_{N(C)}$, was calculated from one half the integral of the peak in the region of 4.0–4.11 ppm (-OC=OCH$_2$CH$_2$CH$_2$CH$_2$**CH$_2$**O-. Component molar masses found using the degree of polymerization times the mass of the respective repeat unit.

Number average molar mass was taken to be the sum of the two component molar masses.

Block-statistical copolymers composition and molar mass were estimated using the following method: The singlet representative of the initiator aromatic protons (7.34 ppm) was used as an internal standard. The degree of polymerization of the PLA block, $N_{N(LA)}$ was calculated using the integral of PLA methine protons in the region of 5.12 –5.35 ppm (-C**H**(CH$_3$)OC=O-). The midblock composition was estimated using the method outlined above. Number average molar mass was taken to be the sum of the component molar masses. The poly(lactide) volume fraction ($f_{PLA}$) was calculated from the composition using 1.248 g cm$^{-3}$ and 1.02 g cm$^{-3}$ for the midblock and PLA blocks, respectively. Total triblock molar mass was determined by using the number average mass of the midblock (determined using MALLS-SEC) and composition (determined by $^1$HMR spectroscopy) to calculate end block molar mass.
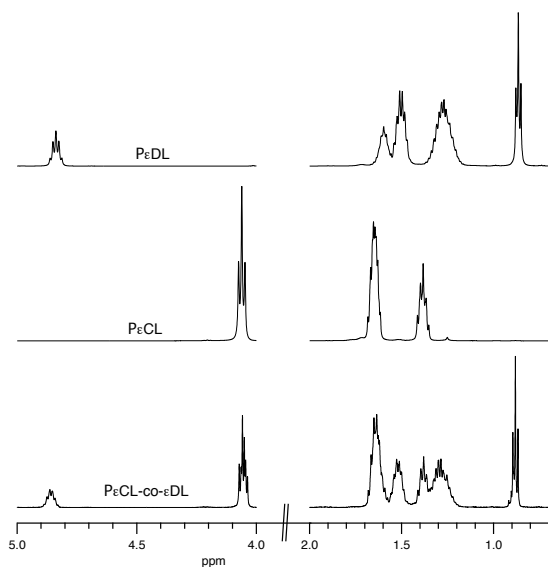
**Figure 2.9.**

$^1$H NMR spectra of poly(ε-decalactone), poly(ε-caprolactone), and poly(ε-decalactone-co-caprolactone) showing the resonances used to determine copolymer composition.

*Determination of Reactivity Ratios*

ε-Caprolactone and ε-Decalactone reactivity ratios were determined using catalytic Sn(Oct)$_2$ at 180 °C. Bulk polymerizations were run in 1 ml prescored glass ampoules equipped with magnetic stirbars. To ensure that the sample was heated uniformly the total reaction volume was less than 100 ml. Ampules were submerged in a 180 °C oil bath then removed, broken, and the sample diluted with cholorform. $^1$H NMR spectroscopy was used to determine the ε-CL composition of the feed and polymer, $f_{CL}$ and $F_{CL}$, respectively. Polymerization times were adjusted such that the total monomer conversion was less than 10%. The dependence of polymer composition on feed

60

composition was used to determine reactivity ratios, $r_C$ and $r_D$, using non-linear fit to the copolymer equation:

$$F_C = \frac{r_C f_C^2 + f_C f_D}{r_C f_C^2 + 2 f_C f_D + r_D f_D^2} \qquad (2.2)$$

In this equation $F$ and $f$ are the composition of the polymer and feedstock, respectively. The reactivity ratios, $r_C$ and $r_D$, are defined as the ratio of the rate constants for homopolymer propagation divided by cross propagation:

$$r_C = \frac{k_{CC}}{k_{CD}} \text{ and } r_D = \frac{k_{DD}}{k_{DC}} \qquad (2.3)$$

*$^{13}$C NMR Spectroscopy*

$^{13}$C NMR spectra were collected from CDCl$_3$ solution on a Varian INOVA-500 spectrometer operating at 126 MHz. Chemical shifts are referenced to the middle solvent peak at 77.36 ppm, respectively. The $^{13}$C NMR spectra show signals in the region of 169-170 ppm and 68.6-69.3 ppm consistent with carbonyl and methine resonances of poly(lactide) segments, respectively.

 For each of the poly(lactide) containing triblock polymers, the resonances in the methine region can be assigned to isi and iiisi, isiii, iii, isisi, iiisi, and isiii sterosequences, indicating minimal transesterification within the poly(lactide) block.[72] PCL-*block*-PDL-*block*-PCL, used as a reference spectrum, was synthesized using the procedure described in the methods section of this work except the chain extension was

conducted with ε-caprolactone rather than (±)-lactide. The spectrum of PCL-PDL-PCL exhibits resonances consistent with poly(ε-decalactone) and poly(ε-caprolactone) homopolymers but not poly(ε-decalactone-*co*-ε-caprolactone). Because no interblock transesterification is observed in this model system it seems likely that transesterication is minimal within the poly(CL-co-DL) copolymer midblocks.

An absence of signals from 172 to 172.5 ppm in the ^{13}C NMR spectrum of PLA-*block*-PCD-*block*-PLA suggest that interblock transesterification is suppressed.[73] The other poly(lactide)-containing polymers also show no evidence of significant transesterification between poly(lactide) endblocks and the homopolymer or copolymer midblock. The spectrum of PLA-*block*-PCL-*block*-PLA also indicates interblock transesterification is absent in these materials.[74,75,76] Taken together these results suggest the absence of transesterifiaction and sucessfull preservation of the desired triblock block architecture. Further information on these and other polyester copolymers and terpolymers are included in Appendix B.
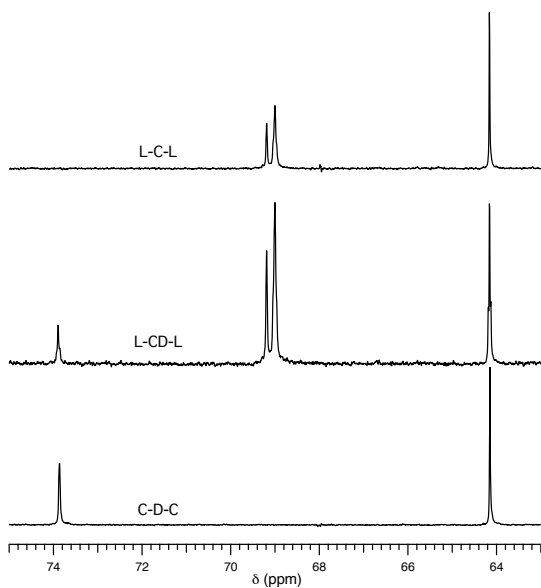
**Figure 2.10.**

^{13}C NMR spectra of representative triblock polymers showing resonances in the region characteristic of polyester methine or methylene carbons adjacent to the oxygen.
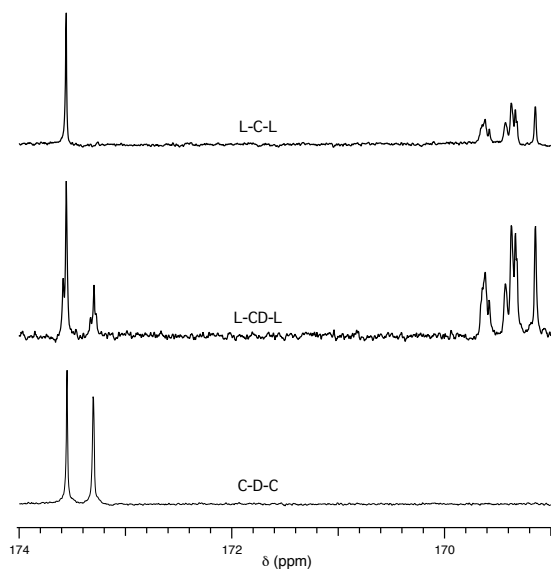


**Figure 2.11**

13C NMR spectra of representative triblock polymers showing resonances in the region (169–174 ppm) characteristic of the carbonyl carbons.

## 2.5 References

(1) Matsen, M.W. Effect of Architecure on the Phase Behavior of AB-Type Block Copolymer Melts *Macromolecules* **2012**, *45*, (2161-2165)

(2) Bates, F. S., and Fredrickson, G. H. Block Copolymers—Designer Soft Materials *Physics Today* **1999**, *52*, (32-38)

(3) Kataoka, K.; Harada, A.; Nagsaki, Y. Block copolymer micelles for drug delivery: design characterization, and biological significance *Advanced Drug Delivery reviews* **2001**, *47*, (113-131)

(4) Robertson, J.D.; Patikarnmonthon, N.; Joseph, A. S.; Battaglia, G. Block Copolymer Micelles and Vesicles for Drug Delivery In *Engineering Polymer Systems for Improved Drug Delivery* Bader, R. A., and Putnam, D. A., Ed. John Wiley and Sons, **2014**

(5) Guo, C.; Lin, Y.; Witman, M. D.; Smith, K. A.; Wang, C.; Hexemer, A.; Strzalka, J.; Gomez, E. D.; Verduzco, R. Conjugated Block Copolymer Photovoltaics with near 3% Efficiency through Microphase Separation *Nano Lett.* **2013**, *13*, (2957-2963)

(6) Young, W.; Kuan, W., and Epps, T. H., III, Block Copolymer Electrolytes for Rechargeable Lithium Batteries *Journal of Polymer Science B: Polymer Physics* **2014**, *52*, (1-16)

(7) Schulze, Morgan, W.; McIntosh, Lucas D.; Hillmyer, Marc A.; Ldge, Timothy P. - High-Modulus, High-Conductivity Nanostructured Polymer Electrolyte Membranes via Polymerization-Induced Phase Separation *Nano Lett.*, **2014**, *14*, (122-126)

(8) Fasolka, M. J.; Mayes, A. M. Block Copolymer Thin Films: Physics and Applications *Annu. Rev. Mater. Res.* **2001**, *31*, (325-355)

(9) Tseng, Y., Darling, S. B. Block Copolymer Nanostructures for Technology *Polymers* **2010**, *2*, (470-489)

(10) Phillip, W. A.; O' Neill, B.; Rodwogin, M.; Hillmyer, M. A.; Cussler, E. L. Self-Assembled Block Copolymer Thin Films as Water Filtration Membranes *ACS Appl. Mater. Interfaces* **2010**, *2*, (847-853)

(11) Jackson, E. A.; Hillmyer, M. A. Nanoporous Membranes Derived from Block Copolymers: From Drug Delivery to Water Filtration *ACS Nano* **2010**, *4*, (3548-3553)

(12) Lee, I.; Panthani, T. R.; Bates, F. S. Sustainable Poly(lactide-*b*-butadiene) Multiblock Copolymers with Enhanced Mechanical Properties. *Macromolecules* **2013**, *46*, (7387–7398)

(13) Olsén, P.; Borke, T.; Odelius, K.; Albertsson, A.-C. ε-Decalactone: A Thermoresilient and Toughening Comonomer to Poly(L-Lactide). *Biomacromolecules*, **2013**, *14*, (2883–2890)

(14) Zhang, Z.; Grijpma, D. W.; Feijen, J. Triblock copolymers based on 1,3-Trimethylene Carbonate and Lactide as Biodegradable Thermoplastic Elastomers *Macromol. Chem. Phys.* **2004**, *205*, (867-875)

(15) Lin, J. O.; Chen, W.; Shen, Z.; Ling, J. Homo- and Block Copolymerizations of ε-Decalactone with L-Lactide Catalyzed by Lanthanum Compounds. *Macromolecules* **2013**, *46*, (7769–7776)

(16) Martello, M. T.; Hillmyer, M. A. Polylactide-Poly(6-methyl-ε-caprolactone)-Polylactide Thermoplastic Elastomers *Macromolecules* **2011,** *44,* (8537-8545)

(17) Ryner, M.; Albertsson, A.-C. Resorbable and Highly Elastic Block Copolymers from 1,5-Dioxepan-2-One and L-Lactide with Controlled Tensile Properties and Hydrophilicity. *Biomacromolecules* **2002,** *3,* (601–608)

(18) Wanamaker, C. L.; O'Leary, L. E.; Lynd, N. A.; Hillmyer, M. A.; Tolman, W. B. Renewable-Resource Thermoplastic Elastomers Based on Polylactide and Polymenthide *Biomacromolecules* **2007,** *8,* (3634-3640)

(19) Xiong, M.; Schneiderman, D.K., Bates, F.S.; Hillmyer, M.A.; Zhang, K. Scalable production of mechanically tunable block polymers from sugar. Proceedings of the National Academy of Sciences, **2014,** *111,* (8357-8362)

(20) Martello, M. T.; Hillmyer, M. A.; Schneiderman, D. K. Synthesis and Melt Processing of Sustainable Poly(ε-decalactone)-block-Poly(lactide) Multiblock Thermoplastic Elastomers *ACS Sustainable Chemistry and Engineering* **2014,** *2,* (2519-2526)

(21) Yao, K; Tang, C. Controlled Polymerization of Next-Generation Renewable Monomers and Beyond *Macromolecules* **2013,** *46,* (1689-1712)

(22) Holmberg, A. L.; Reno, K. H., Wool, R. P.; Epps, T. H. Biobased building blocks for the rational design of renewable block polymers *Soft Matter* **2014,** *10,* (7405-7424)

(23) Tsui, A.; Wright, Z. C.; Frank, C. W. Biodegradable Polyesters from Renewable Resources *Annu. Rev. Chem. Biomol. Eng.* **2013,** *4,* (143-170)

(24) Hernández, N.; Williams, C.; Cochran, E. The battle for the "green" polymer. Different approaches for biopolymer synthesis: bioadvantaged vs .bioreplacement *Org. Biomol. Chem.* **2014,** *12,* (2834-2849)

(25) Harrane, A.; Leroy, A.;Nouailhas, H.; Garric, X.; Coudane, J.; Nottelet, B. PLA-based biodegradable and tunable soft elastomers for biomedical applications *Biomed. Mater.* **2011**, *6*, (1-11)

(26) Liu, Q.; Jiang, L.; Shi, R.; Zhang, L. Synthesis, preparation, in vitro degradation, and application of novel degradable bioelaastomers—A Review *Progress in Polymer Science* **2012,** *37,* (715-765)

(27) Tong, J.-D.; Jerôme, R. Dependence of the Ultimate Tensile Strength of Thermoplastic Elastomers of the Triblock Type on the Molecular Weight between Chain Entanglements of the Central Block. *Macromolecules* **2000,** *33,* (1479–1481)

(28) Pitt, C. G.; Gratzl, M. M.; Kimmel, G. L.; Surles, J.; Schindler, A. Aliphatic Polyesters II. The Degradation of Poly (D,L-lactide), Poly (ε-caprolactone), and Their Copolymers in Vivo *Biomaterials* **1981**, *2,* (215-220)

(29) Widjaja, L. K.; Kong, J. F. Chattopadhyay, S.; Lipik, V. T.; Liow, S. S.; Abadie, M. J. M.; Venkatraman, S. S. Triblock copolymers of ε-caprolactone, trimethylene carbonate, and L-lactide: Effects of using random copolymer as hard-block *Journal of the Mechanical Behavior of Biomedical Materials* **2012,** *6,* (80-88)

(30) Cohn, D.; Salomon, A. H. Designing biodegradable multiblock PCL/PLA thermoplastic elastomers *Biomaterials* **2005,** *26,* (2297-2305)

(31) Yu, J. M.; Dubois, P.; Jerome, R. Synthesis and Properties of Poly(isobornyl methacrylate (IBMA)-*b*-butadiene (BD)-*b*-IMBA Copolymers: New Thermoplastic Elastomers of a Large Service Temperature Range *Macromolecules* **1996,** *29,* (7316-7322)

(32) Widjaja, L. K.; Kong, J. F.; Chattopadhyay, S.; Lipik, V.T.; Liow, S. S.; Abadie, M. J. M.; Venkatraman, S. S.  Triblock copolymers of of ε-caprolactone, trimethylene carbonate, and L-lactide: Biodegradability and elastomeric behavior *Journal of Biomedical Materials Research A* **2011,** *99A,* (38-46)

(33) Lipik, V.T.; Widjaja, L. K.; Liow, S. S.; Venkatraman, S. S.; Abadie, M. J. M.  Synthesis of biodegradable thermoplastic elastomers (BTPE) based on ε-caprolactione *eXPRESS Polymer Letters* **2010,** *4,* (32-38)

(34) Ryynänen, T.; Nykänen, A., and Seppälä, J. V.   Poly(CL/DLLA-b-CL) multiblock copolymers as biodegradable thermoplastic elastomers *eXPRESS Polymer Letters* **2008,** *2,* (184-193)

(35) Andronova, N., and Albertsson, A.   Resilient Bioresorbable Copolymers Based on Trimethylene Carbonate, L-Lactide, and 1,5-Dioxepan-2-one  *Biomacromolecules* **2006,** *7,* (1489-1495)

(36) Kong, J. F.; Lipik, V.; Abadie, M. J.M.; Deen, G. R.; Venkatraman, Biodegradable elastomers based on ABA triblocks: influence of end-block crystallinity on elastomeric character S. S. *Polym. Int.* **2012,** *61,* (43-50)

(37) Zhang, Z.; Grijpma, D. W.; Feijen, J.  Thermoplastic elastomers based on poly(lactide)-poly(trimethylene carbonate-co-caprolactone)-poly(lactide) triblock copolymers and their stereocomplexes  *Journal of Controlled Release* **2006,** *116,* (e29-e31)

(38) Staudinger, U.; Satapathy, B. K.; Thunga, M.; Weidisch, R.; Janke, A., and Knoll, K.  Enhancement of mechanical properties of triblock copolymers by random copolymer midblocks *European Polymer Journal* **2007,** *43,* (2750-2758)

(39) Beckingham, B. S.; Register, R. A. Regular Mixing Thermodynamics of Hydrogenated Styrene–Isoprene Block–Random Copolymers *Macromolecules* **2013,** *46,* (3084-3091)

(40) Beckingham, B. S.; Burns, A. B., and Register, R. A. Mixing Thermodynamics of Ternary Block–Random Copolymers Containing a Polyethylene block *Macromolecules* **2013,** *46,* (2760-2766)

(41) Nakayama, Y.; Aihara, K.; Yamanishi, H.; Fukuoka, H.; Tanaka, R.; ZXhengguo, C.; Shiono, T.  Synthesis of Biodegradable Thermoplastic Elastomers from ε-Caprolactone and Lactide *Journal Polymer Science, Part A: Polymer Chemistry* **2015,** *53,* (489-495)

(42) Jasinska-Walc, L.; Hansen, M. R.; Dudenko, D.; Rozanski, A.; Bouyahyi, M.; Wagner, M.; Graf, R.; Duchateau, R.  Topological behavior mimicking ethylene-hexene copolymers using branched lactones and macrolactones *Polymer Chemistry* **2014,** *5,* (3306-310)

(43) Jasinska-Walc, L.; Bouyahyi, M.; Rozanski, A.; Gaf, R.; Hansen, M. R.; Duchateau, R.  Synthetic Principles Determining Local Organization of Copolyesters Prepared from Lactones and Macrolactones *Macromolecules* Advanced online publication. **2015,** *48,* (502-510)

(44) Glavas, L.; Olsén, P.; Odelius, K., and Albertsson, A.-C Achieving Micelle Control Through Core Crystallinity *Biomacromolecules* **2013,** *14,* (4150-4156)

(45) Lomellini, P.; Rossi, A. G. Effect of composition on the entanglement density in random copolymers *Makromol. Chem.* **1990,** *191,* (1729-1737)

(46) Kowalski, A.; Duda, A.; Penczek, S. Kinetics and Mechnaism of Cyclic esters polymerization initiated with tin(II) octoate, 1 *Marcomol. Rapid Commun.* **1998,** *19,* (567-572)

(47) Storey, R. F.; Sherman,  J. W. Kinetics and Mechanism of the Stannous Octoate-Catalyzed Bulk Polymerization of ε-Caprolactone *Macromolecules* **2002,** *35,* (1504-1512)

(48) Guo Q. and Groeninckx G., Crystallization Kinetics Poly(e-caprolactone) in Miscible Thermosetting Polymer Blends of Epoxy Resin and Poly (e-caprolactone), *Polymer*, **2001**, *42,* (8647-8655)

(49) Bittiger, H.; Marchessault, R. H. Crystal Structure of Poly(ε-Caprolactone) *Acta Cryst.* **1970**, *B26,* (1923-1927)

(50) Vion, J.-M.; Jérome, R.; Teyssié, P.; Aubin, M.; Prud'homme, R. E. Synthesis, Characterization, and Micibility of Caprolactone Random Copolymers *Macromolecules* **1986**, *19,* (1828-1838)

(51) Goulet, L.; Prud'homme, R. E. Crystallization Kinetics and Melting of Caprolactone Random Copolymers *Journal of Polymer Science: Part B: Polymer Physics* **1990**, *28,* (2329-2352)

(52) Vion, J.-M.; Jérome, R.; Teyssié, P.; Aubin, M.; Prud'homme, R. E. Synthesis, Characterization, and Micibility of Caprolactone Random Copolymers *Macromolecules* **1986**, *19* (1828-1838)

(53) Seefried, C.G.; Koleske, J.V.; Critchfield, F.E. Lactone Polymers. VIII. Dynamic Mechanical Properties of ε-Caprolactone and γ-(tert-butyl)-ε-Caprolactone Copolymers *Journal of Polymer Science Polymer Physics Edition* **1976**, *14,* (2011-2017)

(54) Darensbourg, D. J., and Karroonnirun, O. Ring-Opening Polymerization of L-Lactide and ε-Caprolactone of Utilizing Biocompatible Zinc Catalysts. Random Copolymerization of L-Lactide and ε-Caprolactone *Macromolecules* **2010**, *43,* (8880-8886)

(55) Nakagawa, S.; Tanaka, T.; Ishizone, T.; Nojima, S.; Kamimura, K.; Yamaguchi, K. Nakahama, S. Crystallization behavior of poly(ε-caprolactone) chains confined in lamellar nanodomains *Polymer* **2014**, *55,* (4394-4400)

(56) Henton, D. E.; Gruber, P.; Lunt, J.; Randall, J. Polylactic Acid Technology in *Natural Fibers, Biopolymers, and Biocomposites* Mohanty, A. K.; Misra, M.; Drzal, L. T., Ed.; CRC: Boca Raton, Fl **2005**, **(**527-528)

(57) Rosendale, J. H., and Bates, F. S. Rheology of ordered and disordered symmetric poly(ethylenepropylene)-poly(ethylethyene) diblock copolymers *Macromolecules* **1990**, 23, (2329-2338)

(58) Castillo, R. V.; Müller, A. J.; Raquez, J.-M.; Dubois, P. Crystallization Kinetics and Morphology of Biodegradable Double Crystalline PLLA-*b*-PCL Diblock Copolymers *Macromolecules* **2010**, *43,* (4149-4160)

(59) Hamely, I. W.; Castelletto, V.; Castillo, R. V., Müller, A. J.; Martin, C. M., Pollet, E.; Dubois, P. Crystallization in Poly(L-Lactide)-b-poly(ε-caprolactone) Double Crystalline Diblock Copolymers *Macromolecules* **2005**, *38,* (463)

(60) Hamely, I. W.; Parras, P.; Castelletto, V.; Castillo, R. V.; Müller, A. J.; Pollet, E.; Dubois, P.; Martin, C. M. Melt Structure and its Transformation by Sequential Crystallization of the Two Blocks within Poly(L-Lactide)-*block*-Poly(ε-Caprolactone) Double Crystalline Diblock Copolymers *Macromol. Chem. Phys.* **2006**, *207,* 941-953

(61) Ho, R.-M.; Hsieh, P.-Y.; Tseng, W.-H.; Lin, C.-C.; Huang, B.-H; Lotz, B. Crystallization-Induced Orientation of Poly(L-Lactide)-b-Poly(ε-Caprolactone) Diblock Copolymers *Macromolecules* **2003**, *36,* 9085-9092

(62) Kim, J. K.; Park, D. J.; Lee, M. S.; Ihn, K. J. Synthesis and crystallization behavior of poly(L-Lactide)-block-poly(ε-caprolactone) copolymer *Polymer* **2001**, *42,* 7429-7441

(63) Maglio, G.; Migliozzi, A.; Palumbo, R. Thermal properties of di- and triblock copolymers of poly(L-lactide) with poly(oxyethylene) or poly(ε-caprolactone) *Polymer* **2003**, *44,* 369-375

(64) Jeon, O.; Lee, S.-H.  Kim, S. H.; Lee, Y. M.; Kim, Y. H. Synthesis and Characterization of Poly(L-Lactide)-Poly(ε-caprolactone) Multiblock Copolymers *Macromolecules* **2003**, *36, (*5585-5592)

(65) Broz, M. E.; VanderHart, D.L.; Washburn, N. R. Structure and mechanical properties of poly(D,L-lactic acid)/poly(ε-caprolactone) blends *Biomaterials* **2003**, *24,* (4181-4190)

(66) Widin, J. M.; Schmitt, A. K.; Im, K.; Schmitt, A. L.; Mahanthappa, M. K. Polydispersity–Induced Stabilization of a Disordered Bicontinuous Morphology in ABA triblock copolymers, *Macromolecules,* **2010,** *43, (*7913-7915)

(67) Pitet, L. M.; Amendt, M. A.; Hillmyer, M. A. Nanoporous Linear Polyethyene from a Block Polymer Precursor *J. Am. Chem. Soc.* **2010**, *132,* (8230-8231)

(68) Shin, J.; Martello, M. T.; Shrestha, M.; Wissinger, J.E.; Tolman, W. B.; Hillmyer, M. A. Pressure-Sensitive Adhesives from Renewable Triblock Copolymers *Macromolecules* **2011,** *44,* (87-94)

(69) Vincent, P. I. A correlation between critical tensile strength and polymer cross-sectional area  *Polymer* **1972**, *13, (*558-560)

(70) Gimenez, J., Cassagnau, P., Michel, A. Bulk polymerization of ε-caprolactone: Rheological predictive laws. Journal of Rheology, **2000,** *44,* (527-547)

(71) Wanamaker, C. L.; Bluemle, M. J.; Pitet, L. M.; O'Leary, L. E.; Tolman, W. B.; Hillmyer, M. A. Consequences of Polylactide Stereochemistry on the Properties of Polylactide-Polymenthide-Polylactide Thermoplastic Elastomers *Biomacromolecules* **2009,** *10,* (2904-2911)

72 Thakur, K. A. M.; Kean, R. T.; Hall, E. S.; Kolstad, J. J.; Lindgren, T. A.; Doscotch, M. A.; Siepmann, J. I.; Munson, E. J.   High-Resolution 13C and 1H Solution NMR Study of Poly(lactide) *Macromolecules* **1997**, *30,* (2422-2428)

(73) Olsén, P.; Borke, T.; Odelius, K.; Albertsson, A.-C. ε-Decalactone: A Thermoresilient and Toughening Comonomer to Poly(L-Lactide). *Biomacromolecules,* **2013,** *14,* 2883–2890.

(74) Lipik, V. T., and Abadie, M. J. M  Synthesis of Block Copolymers of Varying Architecture Through Suppression of Transesterification during Coordinated Anionic Ring Opening Polymerization *International Journal of Biomaterials* **2012**, doi: 10.11555/2012/390947

(75) Duda, A.; Biela, T.; Libiszowski, J.; Penczek, S.; Dubois, P.; Mecerreyes, D.; Jérôme, R. Block and random copolymers of ε-caprolactone *Polymer Degradation and Stability* **1998**, *59,* (215-222)

(76) Veld, P. J.; Velner, E. M.; Van de Witte, P.; Hamhuis, J.; Dijkstra, P. J.; Feijen, J. Melt Block Copolymerization of ε-Caprolactone and L-Lactide *Journal of Polymer Science Part A. Polymer Chemistry*  **1997,** *35, (*219-226)

# Chapter 3. Mechanically Tunable Block Polymers From Sugar[†]

Development of sustainable and biodegradable materials is essential for future growth of the chemical industry. For a renewable product to be commercially competitive, it must be economically viable on an industrial scale and possess properties akin or superior to existing petroleum-derived analogs. Few biobased polymers have met this formidable challenge. To address this challenge, an efficient bio-based route to the branched lactone, β-methyl-δ-valerolactone (MVL) has been developed. This monomer can be transformed into a rubbery (i.e., low glass transition temperature) polymer (PMVL). The block copolymerization of MVL and lactide leads to a high performance polyesters with tunable mechanical properties. Key features of this work include the creation of a total biosynthetic route to produce MVL, an efficient semisynthetic approach that employs high yeilding chemical reactions to transform mevalonate to MVL, and the use of controlled polymerization stradegies to produce well defined P(L)LA-PMVL-P(L)LA triblock polymers. This comprehensive strategy offers an economically viable approach to sustainable plastics and elastomers for a broad range of applications.

---

## 3.1 Introduction

Polymeric materials account for nearly $400 billion in economic activity annually and represent the third largest manufacturing industry in the US.[1] Currently petroleum-derived polymers—for example polyethylene, polystyrene, and polyvinylchloride—dominate this market. Although these materials are widely useful, their manufacture and disposal present inescapable environmental challenges that are costly to correct and simply unsustainable in the long term. To ensure the continued vitality of the polymer enterprise, it is necessary to invent high performance polymers that are both sustainable and cost-competitive. In recent years, ingenious advances in synthetic biology have enabled the economical production of fuels[2,3,4,5,6,7] chemicals[8,9,10,11,12] and complex natural products[13,14,15,16] from renewable sugars. This elegant manipulation of existing organisms to efficiently produce valuable metabolites from inexpensive feedstocks represents a triumph of modern science and engineering and offers society the promise of renewable, environmentally compatible next generation materials.

While there has been steady scientific progress toward the production of synthetic polymers from renewable resources, the fraction of high-performing, biobased, degradable polymers on the market is today minuscule (1). Arguably the most successful example to date is poly(lactide) (PLA), a compostable aliphatic polyester derived from the fermentation product lactic acid. However, the brittle nature of PLA and other commercial aliphatic polyesters such as poly(butylene succinate) and poly(hydroxyalkanoate)s, has thwarted their broad-based utility. Expanded market

penetration will pivot on the development of products endowed with tunable combinations of properties, e.g., soft, ductile and tough.[17,18] Among myriad strategies that have been used to this end; PLA-containing block polymers represent a particularly attractive approach. These hybrid materials offer opportunities to easily tune a wide range of physical and mechanical properties by controlling molecular architecture, composition, and molar mass.

A specific example that illustrates the utility of this approach is ABA triblock thermoplastic elastomers. Here, rigid (glassy or semicrystalline) 'A' endblocks microphase separate to form nanoscopic domains that tether together the soft, low glass transition temperature $(T_g)$, regions comprised of the center block 'B' component.[19,20,21,22] This design results in outstanding mechanical properties and has been the basis for the commercially successful poly(styrene)-poly(diene) variants.[23] Many PLA-containing block polymers have been reported; several have been shown to be flexible, tough, elastic, and hydrolytically degradable.[24,25,26,27] Unfortunately the starting materials used to prepare these polymers are either derived from fossil fuels or from natural products that are prohibitively expensive. The development of an economically viable rubbery polymer that can be used in combination with PLA to prepare mechanically superior block polymers therefore is the grand challenge that must be addressed for these materials to be competitive with styrenic block polymers.

The need for an efficient, scalable, process to a methyl branched lactone suitable for ring-opening transesterification polymerization (ROTEP) led us to examine candidates that could be potentially produced by biosynthesis with both high titer and high yield. After

surveying the appropriate metabolic pathways, we identified β-methyl-δ-valerolactone (MVL) as an attractive target. Based on our experience with simple aliphatic polyesters we anticipated that poly(β-methyl-δ-valerolactone) (PMVL) could be used in conjuction with PLA segments to prepare block polymers with exceptional mechanical properties. [26,27] MVL can be generated by direct fermentation of glucose or through the production of the intermediate compound mevalonate. These two approaches to making MVL, one entirely biochemical and the other semisynthetic, represent facile chemical transformations (summarized in Figure 3.1).
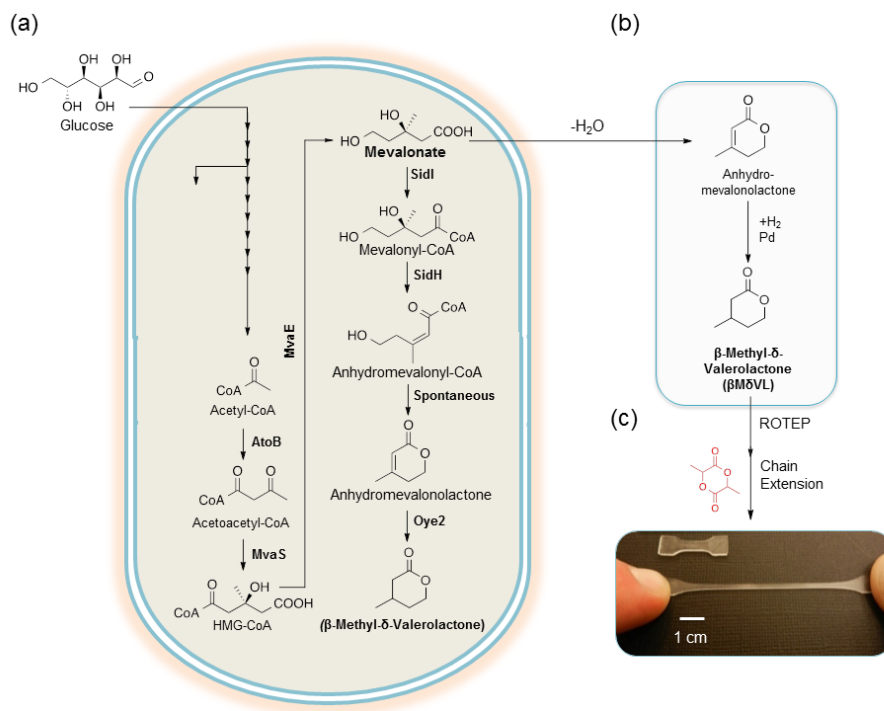


**Figure 3.1**

a) Total biosynthetic pathway for the production of β-methyl-δ-valerolactone. b) A semisynthetic route to produce β-methyl-δ-valerolactone from mevalonate. c) Conversion of β-methyl-δ-valerolactone to ABA triblock polymers with excellent mechanical properties.

Since the theoretical yield of this lactone monomer is 0.42 g/g glucose, we estimate that with further optimization it will be possible to produce MVL economically. Based on the prices of bio-derived commodity chemicals produced using similar processes, we estimate a production cost of less than $2 a kilogram (Table 3.1).

**Table 3.1.**

**The price of current bio-related commodities**

| Chemical | Titer (g L$^{-1}$) | Max. Yield (g g$^{-1}$ glucose) | Purification Method | Price ($ kg$^{-1}$) | Ref. |
|---|---|---|---|---|---|
| Ethanol | 150 | 0.51 | distillation | 0.4 | 28 |
| L-glutamate | 85 | 0.82 | ion-exchange | 1.5 | 28 |
| 1,3-propanediol | 72.2 | 0.84 | ion-exchange & distillation | 1.7 | 29, 30 |
| Succinate | 63.5 | 0.91 | crystallization | 0.7 | 31,32 |
| 1,4-butanediol | 18 | 0.50 | distillation | | 33 |
| Lactate | 200 | 1.0 | distillation | 0.8 | 34 |
| Mevalonate[a] | 88.3 | 0.55 | distillation | <2 | |
| MVL[b] | | 0.42 | distillation | <2 | |

[a]Mevalonate has a theoretical fermentation yield that is about half that for succinate and lactate, which leads us to estimate a production cost of approximately $1.5 kg$^{-1}$ following process optimization. The cost of cyclization through dehydration (over $H_2SO_4$) and subsequent hydrogenation leading to βMδVL are estimated to add roughly $0.2/kg and ~$0.1/kg to the overall production cost, respectively. [b]Direct fermentation to βMδVL eliminates the two finishing steps required to convert mevalonate to this product. Based on the theoretical yields for βMδVL and lactate, we estimate an optimized production cost of $1.9/kg for the fully biosynthetic route. Comparison with the overall cost of producing the monomer lactide must account for the expenses associated with dimerization of lactate, and the reduced effective yield due to the loss of two water molecules.

The bulk ROTEP of bioderived MVL proceeds at room temperature to high conversion yielding an amorphous polyester with $T_g$ = –51 °C.[26,35] These mild and solvent free conditions are synthetically convenient and attractive from both cost and environmental perspectives. The preparation of PLA containing block polymers in combination with PMVL requires only simple chain extension and thus the final ABA compounds can be readily prepared. The resultant mechanically tunable polymers possess outstanding properties not readily accessible in current aliphatic polyesters homopolymers.

## 3.2 Results and Discussion[‡]

### 3.2.1 Construction of a Nonnatural Metabolic Pathway

Because β-methyl-δ-valerolactone is not a natural metabolite, we constructed an artificial biosynthetic pathway to create an engineered *E. coli* strain (Figure 3.1a). Our biosynthetic strategy builds on the mevalonate pathway that has previously been engineered for the synthesis of artemisinin and terpenoids in *S. cerevisiae* and *E. coli*, respectively.[36,37] In this work we improved the production of mevalonate in *E. coli* and also expanded the pathway to synthesize MVL from this precursor.

---

[‡] All of the molecular biology and fermentation experiments discussed in this Chapter were conducted by Dr. Mingyong Xiong, while working in the Zhang group in the University of Minnesota Department of Chemical Engineering and Materials Science

The overall non-natural pathway has three components: (1) overexpression of the mevalonate producing enzymes; (2) introduction of the fungal siderophore proteins to synthesize anhydromevalonolactone (AML); (3) reduction of AML to MVL by enoate reductases.

To generate an acetoaceyl-CoA pool we employed the *E. coli* endogenous enzyme acetyl-CoA acetyltransferase AtoB. First HMG-CoA synthase (MvaS) and HMG-CoA reductase (MvaE) were cloned to provide a route for the production of mevalonate from this pool. To maximize mevalonate flux, the Protein-Protein Basic Local Alignment Search Tool (BlastP) was first used to identify MvaS and MvaE from various organisms: *E. faecalis*, *S. aureus*, *L. casei*, *M. maripaludis*, and *M. voltae*. Combinatorial tests were then used to identify the optimum set of MvaS and MvaE for mevalonate production (Fig. 3.2a). HPLC analyses indicated that, with the exception of MvaS from *M. maripaludis* and *M. voltae*, all heterologous enzymes were active in *E. coli*. The strain expressing both *mvaS* and *mvaE* genes from *L. casei* produced 14.6 g $L^{-1}$ mevalonate from 40 g $L^{-1}$ glucose, better than any other combination (V in Fig. 3.2a). The strain expressing the *L. casei* enzymes produced 50% more mevalonate than other engineered *E. coli* strains described in previous work.[37,38,39]
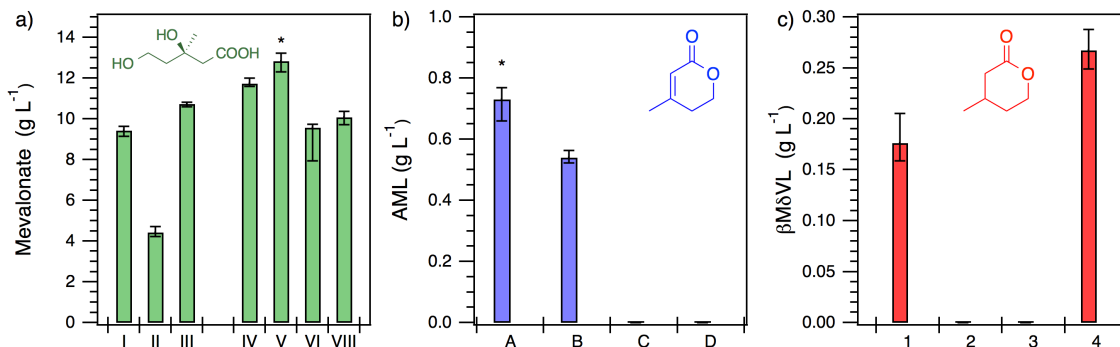
**Figure 3.2**

Biobased production of β-methyl-δ-valerolactone (total biosynthesis a-c; semisynthesis d-f). (a) Mevalonate fermentation with different combinations of MvaS and MvaE. MvaE from *E. faecalis* plus MvaS from: I, *E. faecalis*; II, *S. aureus*, III: *L. casei*. MvaS from *L. casei* plus MvaE from: IV, *S. aureus*; V, *L.casei*; VI, *M. maripaludis*; VII, *M. voltae*. (b) Anhydromevalonolactone fermentation with siderophore enzymes SidI and SidH: A, *A.fumigatus*; B, *N.crassa*; C, *P.nodorum*; D, *S.sclerotiorum*. (c) β-methyl-δ-valerolactone fermentation with enoate-reductase: 1, Oye2 from *S. cerevisiae*; 2, Oye3 from *S. cerevisiae*; 3, wild type YqjM from *B. subtilis*; 4: Mutant YqjM (C26D and I69T) from *B. subtilis*. For each plot the colored bars and error bars represent the median and range of three trials, respectively.

To biosynthesize anhydromevalonolactone from mevalonate, we explored the potential of siderophore pathway enzymes. In fungi acyl-CoA ligase SidI converts mevalonate to mevalonyl-CoA, and enoyl-CoA hydratase SidH transforms mevalonyl-CoA to anhydromevalonyl-CoA.[40] (33) We hypothesized that anhydromevalonyl-CoA could spontaneously cyclize into anhydromevalonolactone intracellularly. To test this hypothesis, we synthesized *sidH* and *sidI* genes based on *E. coli*-optimized codons for protein expression. Using BLASTP analysis, homologous SidI and SidH from *A. fumigatus*, *N. crassa*, *P. nodorum*, and *S. sclerotiorum* were chosen for fermentation experiments.[41] Results revealed that the strain expressing SidI and SidH from *A. fumigatus* produced 730 mg $L^{-1}$ anhydromevalonolactone; the strain carrying enzymes

76

from *N. crassa* could also produce 540 mg L$^{-1}$ anhydromevalonolactone (Figure 3.2b). The other two enzyme pairs did not function properly in *E. coli*.

To explore the reduction of anhydromevalonolactone to β-methyl-δ-valerolactone by enoate reductases, we cloned Oye2 and Oye3 from *S. cerevisiae*[42] (35), wild type and mutant YqjM (C26D and I69T) from *B. subtilis*.[43] The strains carrying the anhydromevalonolactone pathway and Oye2 or mutant YqjM successfully produced 180 or 270 mg L$^{-1}$ MVL, respectively, directly from glucose (Figure 3.2c). Thus we successfully constructed an artificial biosynthetic pathway to MVL from glucose.

### 3.2.2 A Semisynthetic Route to β-Methyl-δ-Valerolactone

While directed evolution approaches will undoubtedly improve the novel MVL biosynthetic pathway,[5] we also developed a semisynthetic approach for the immediate large-scale production of MVL. In this approach the fermented mevalonate is first dehydrated to anhydromevalonolactone, then reduced to MVL (Figure 3.1b). To scale up the production of mevalonate, the *E. coli* strain carrying genes from *L. casei* was tested for fermentation in a 1.3 L bioreactor. During the fermentation, the strain achieved a productivity of 2 g L$^{-1}$ h$^{-1}$ mevalonate with the final titer reaching 88.3 g L$^{-1}$ (Figure 3.3 a). The yield for this semibatch fermentation was 0.26 g/g glucose. To prepare anhydromevalonolactone we then added sulfuric acid directly to the fermentation broth and heated to reflux to catalyze the dehydration of mevalonate (Figure 3.3b). At a catalyst loading of 10% by volume, 98% of the mevalonate was reacted with a selectivity of 89% to produce anhydromevalonolactone. The resulting anhydromevalonolactone

was isolated by solvent extraction and hydrogenated to MVL using Pd/C as the catalyst (bulk, room temperature, 350 psi $H_2$, 12 h) at >99% conversion. The crude product could readily be purified by distillation into *polymer-grade* monomer (Figure 3.3 c).
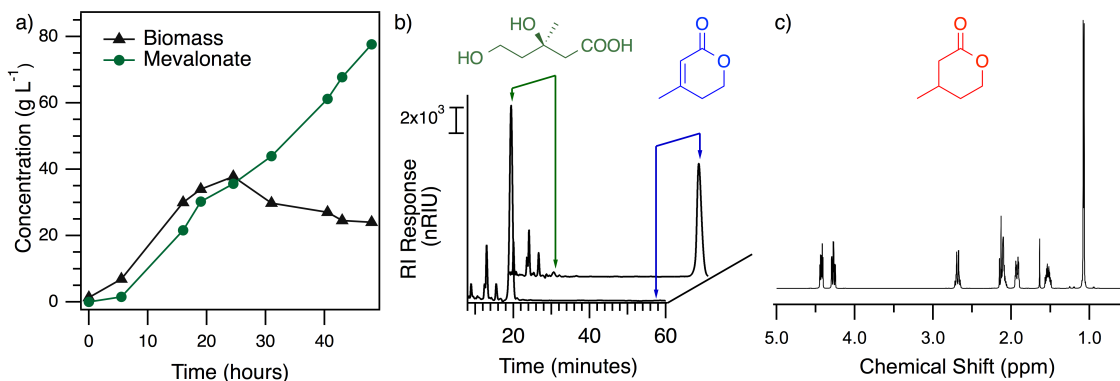


**Figure 3.3**

(a) Mevalonate fermentation in a 1.3 L bioreactor. (b) HPLC showing fermentation broth containing mevalonate and anhydromevalonolactone obtained after refluxing fementation broth with an acid catalyst. (f) $^1$H NMR spectrum of purified MVL prepared via hydrogenation of anhydromevalonolactone, the extraneous peak present at 1.56 ppm is from water present in the solvent ($CDCl_3$).

### 3.2.3 Polymerization of β-Methyl-δ-Valerolactone.

Based on previous work with alkyl-substituted δ-valerolactones we suspected the ceiling temperature for the polymerization of MVL might be low.[35,44,45] To favor high conversion we therefore conducted the polymerizations in bulk monomer at room temperature using the highly active organocatalyst triazabicyclodecene (TBD) (Scheme 3.1).[46]

**Scheme 3.1**

**Polymerization of β-Methyl-δ-Valerolactone to produce PMVL**
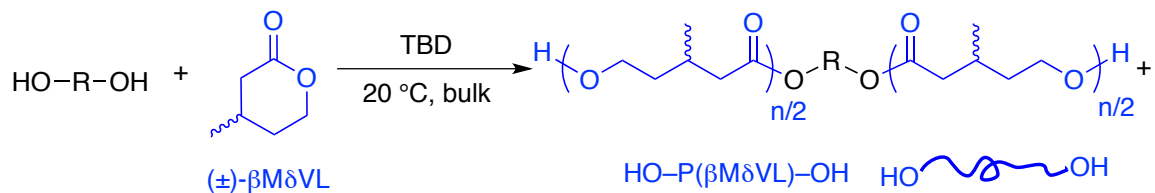


Initial experments demonstrated that addition of TBD to neat MVL in the presence of benzyl alcohol (BnOH) as the initiator ([MVL]/[TBD]/[BnOH]=492/1/1.7) resulted in the rapid production of PMVL—within one hour at room temperature (T= 18 °C) 75% of the monomer was consumed, within three hours the reaction approached equilibrium (Figure 3.4 a). Later investigations revealed that the equilibrium conversion is dependant upon both starting MVL concentration and temperature. We found that for the bulk polymerization the expermentally observed eqilibrium values are about 91% and 60% at 18 °C and 120 °C, respectively (see Chapter 4 for a more detailed discussion and Appendix D. for experimental information).

At 18 °C with as little as 0.05 wt% TBD, the bulk polymerization is well controlled with the conversion and ratio of monomer to added initiator dictating the molar mass of the polymer (Figure 3.4 b). As shown in Figure 3.5 a, by adjusting the ratio of MVL monomer to added alcohol initiator it is possible to access hydroxyl telechelic PMVL polyols with molar masses ranging from approximately 1 kg mol$^{-1}$ to nearly 100 kg mol$^{-1}$ (Figure 3.4). Practically, the accessible range of molar mass is limited on the upper range by monomer purity and on the lower range by the solubility of the initiator.
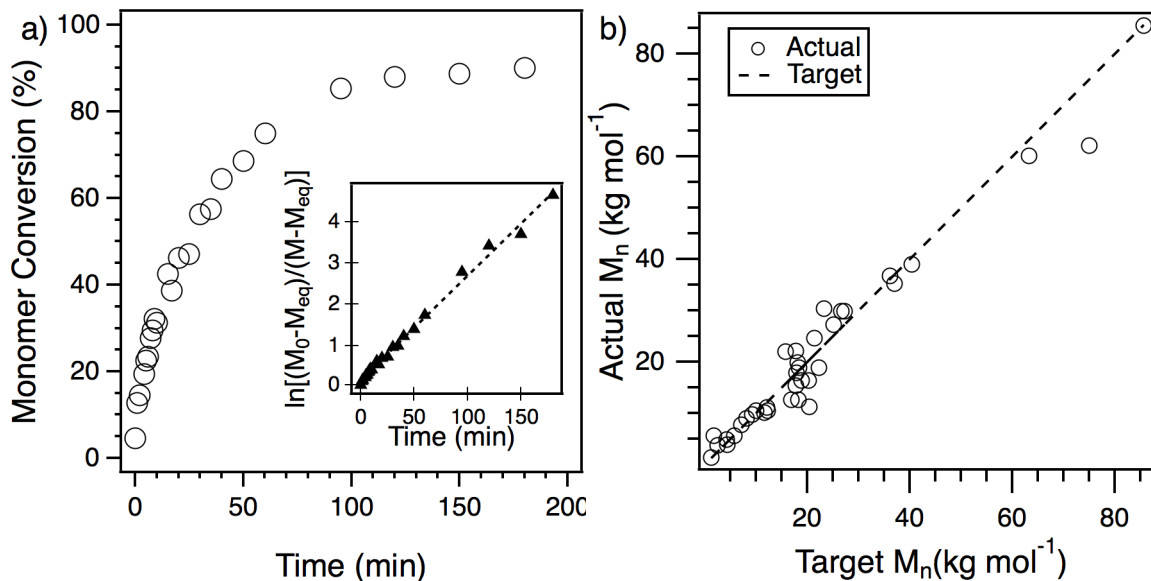
**Figure 3.4**

a) Conversion over time for bulk polymerization of βMδVL using TBD as a catalyst and psuedo-first-order kinetics plot for same kinetics data. $[M]_{eq}$ is the experimentally determined equilibrium monomer concentration of MVL (see Appendix D. for further details). This experiment was conducted at room temperature (18 °C) with [MVL]/[TBD]/[BnOH]=492/1/1.7. The inset shows a pseudo-first-order fit to the data. b) Molecular weight control for the bulk polymerization of MVL. The target molar mass was calculated as $M_n$ Target = 114.1 g mol$^{-1}$ * $[MVL]_0/[ROH]_0$*ρ. In this expresssion $[MVL]_0$ and $[ROH]_0$ are, respectively, the initial concentrations of monomer and initiator and ρ is the observed final conversion of MVL, determined using $^1$H NMR.

Small angle ossilitory shear experiments on a high molar mass sample of PMVL were conducted over a wide range of temperatures and the data were used to construct a master curve, shown in Figure 3.5, below. From the plateau modulus, we estimate an entanglement molar mass ($M_e$) of 4.3 kg mol$^{-1}$. Because of this relatively low entanglement molar mass, and its thermal characteristics—PMVL is amorphous with a low glass transition temperature ($T_g$ = −51 °C)—this renewable polyester can be considered a degradable analog of 1,4 polyisoprene. Indeed, it is worth noting that the alternating copolymerization of $CO_2$ and isoprene, followed by hydrogenation could, at

least in theory, be used to produce PMVL. Practically, the need to promote both perfect alternation between the two comonomers and precise control over the special configuration of isoprene represents an interesting (if somewhat daunting) synthetic challenge.
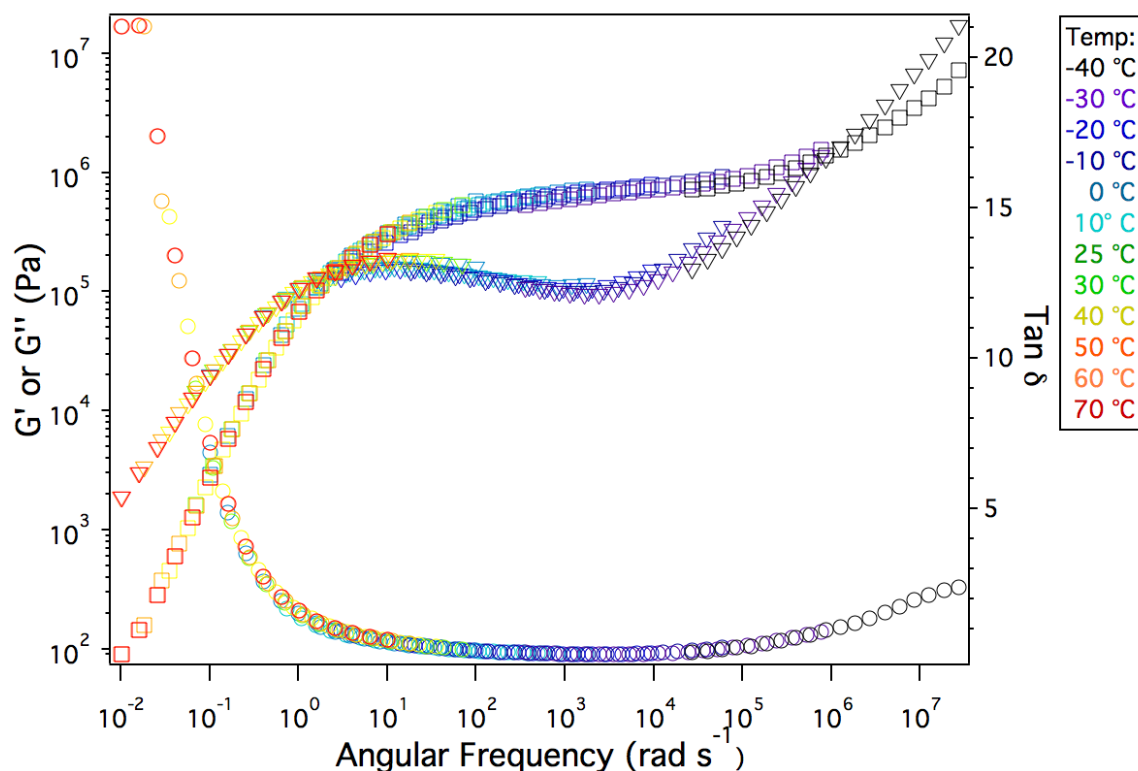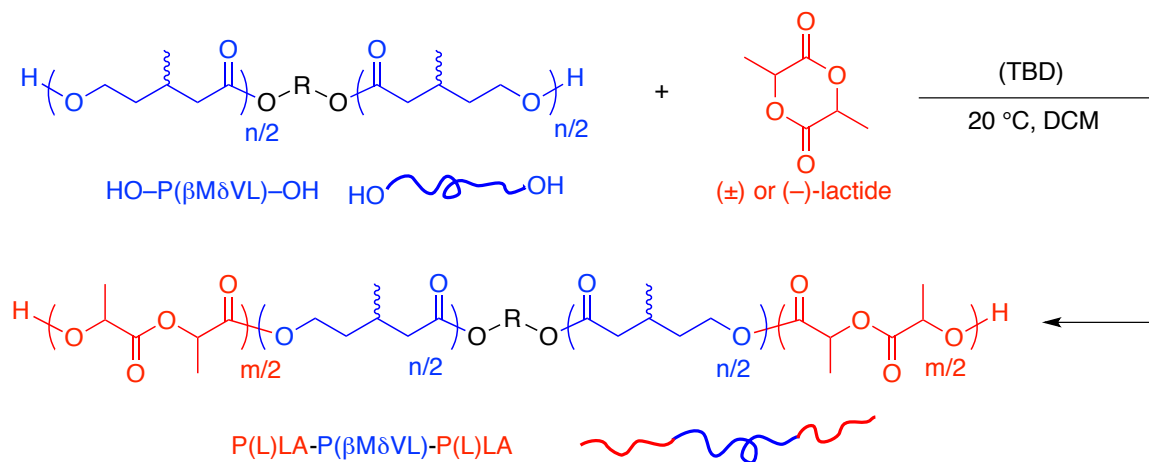


**Figure 3.5**

Pβ1 Master curve created using isothermal frequency sweeps (100 to 0.1 rad sec$^{-1}$). The reference temperature used is 25 °C. The shift factors were obtained by shifting tan δ and applied to G' and G". No vertical shifts were applied. Further information is given in Appendix F.

### 3.2.4 Synthesis and Mechanical Properties MVL TPEs

To explore the potential of this new aliphatic polyester as the soft segment thermoplastic elastomers we employed dihydroxy terminated PMVL samples (synthesized from MVL using 1,4-benzene dimethanol as the initator) to prepare triblock polymers with poly(lactide) endblocks (Scheme 3.2). This could be easily accomplished by adding a solution of (±) or (–)-lactide directly to a polymerization of MVL that was near equilibrium. Alternatively, purfied telechelic PMVL (free of residual monomer and catalyst) could be dissolved in a solution of lactide, and the polymerization initiated by addition of TBD. Although depolymerization can be problematic for PMVL when diluted in the presence of TBD, the conversion of MVL was virtually unchanged before and after the chain extenstion with lactide, this suggests that the addition of lactide to the end of the PMVL prevents significant depolymerization.

**Scheme 3.2**

**Chain extension of β-Methyl-δ-Valerolactone to produce poly(lactide)-block-PMVL-block-poly(lactide) triblock copolymers.**

Compared to the PMVL macroinitiators, polymers prepared using either extension strategy exhibited an increase in mass average molar mass ($M_m$) as determined by MALLS-SEC (Figure 3.6 a). In addition the $^{13}C$ NMR spectra of the resulting triblocks revealed no evidence of significant tranesterification between the PMVL and poly(lactide) blocks, consistent with clean formation of the desired ABA triblock architecture (Figure 3.6 b).
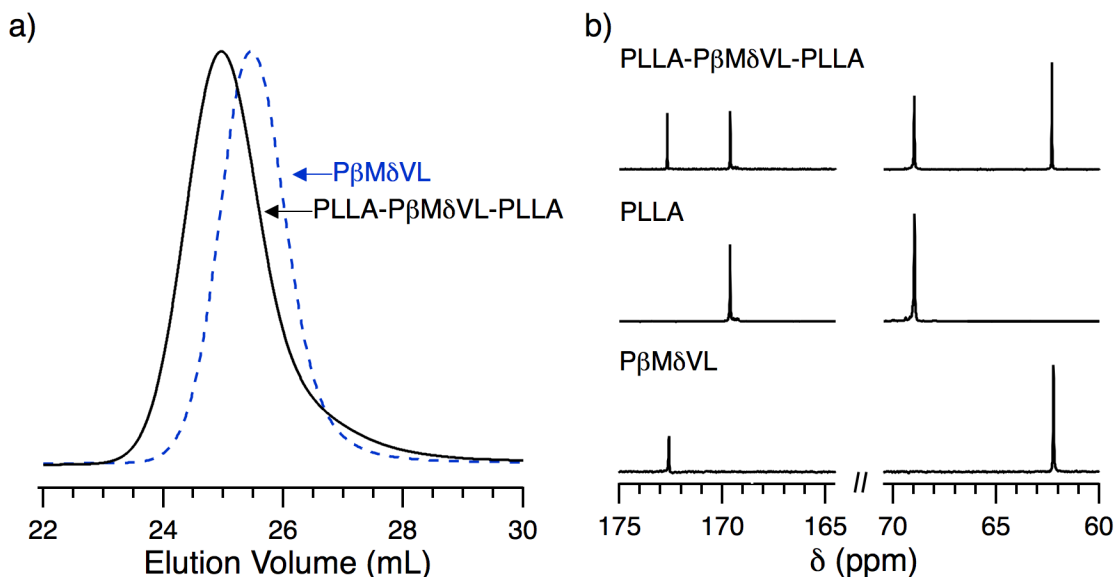


**Figure 3.6**

(a) Overlay of size exclusion chromatography traces for 20.0 kg mol-1 PMVL midblock and corresponding 9.1-20.0-9.1 kg mol-1 PLLA-MVL-PLLA triblock. (b) Overlay of 13C NMR spectra showing (bottom) 20.0 kg mol$^{-1}$ PMVL midblock (middle) 10.0 kg mol-1 PLLA, and (top) 9.1-20.0-9.1 kg mol-1 PLLA-PMVL-PLLA triblock.

### 3.2.5 Microphase Separation of PLA-PMVL-PLA block copolymers.

Despite the structural similarity of poly(lactide) and PMVL, P(L)LA-PMVL-P(L)LA triblock polymers readily microphase separate at only moderate molar masses as evidenced by differential scanning calorimetry (DSC) and small angle x-ray scattering (SAXS). Both PLA-PMVL-PLA (from (±)-lactide) and PLLA-PMVL-PLLA (from (-)-lactide) exhibit separate glass transitions for the midblock and endblock segments by DSC (Figure 3.7 a). In addition, the SAXS data from these triblocks include well-defined scattering peaks that correspond to d-spacings ranging from 20 to 50 nm; as is exemplified by the sample shown in Figure 3.7b.
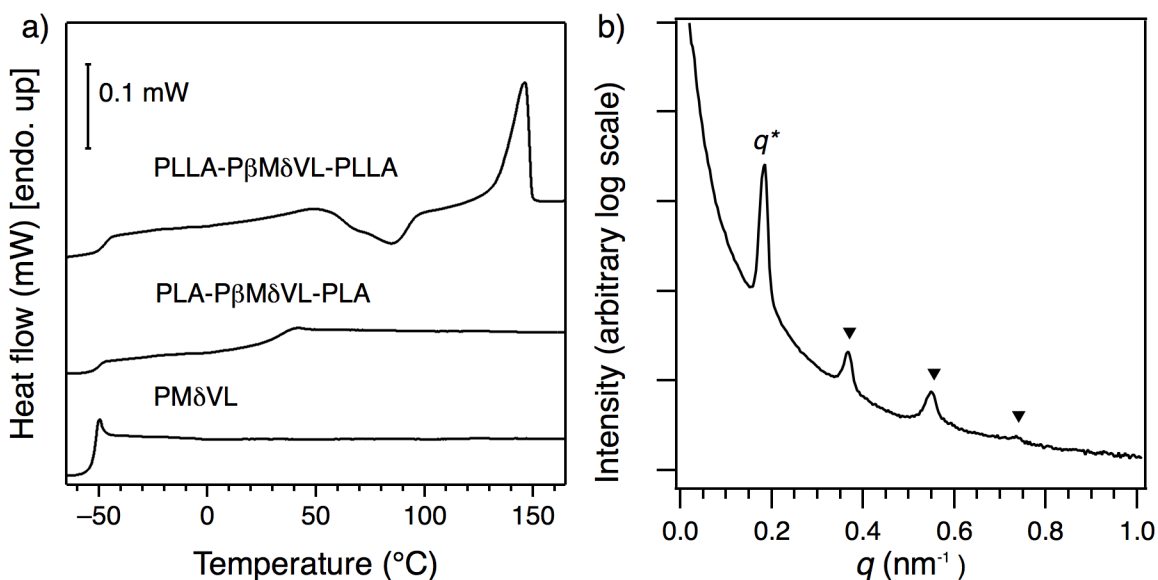


**Figure 3.7**

(c) DSC thermograms for (bottom) 20.0 kg mol-1 MVL midblock and corresponding (middle) 16.2-20.0-16.2 kg mol-1 PLA-MVL-PLA and (top) 9.1-20.0-9.1 kg mol-1 PLLA-MVL-PLLA triblocks. Data were taken on second heating at a rate of 5 °C min-1 after previously cooling from 200 °C at the same rate. (d) Room temperature 1-D SAXs data for 16.2-20.0-16.2 kg mol$^{-1}$ ($f_{LA}$=0.59) PLA-MVL-PLA triblock. The primary peak ($q^*$=0.185 nm$^{-1}$) was taken as the local maximum, the markers indicates calculated higher order reflections ($2q^*$, $3q^*$, and $4q^*$) expected for a lamellar structure with a domain spacing of 34.0 nm.

### 3.2.6 Mechanical Behavior of PLA-PMVL-PLA block copolymers.

Predictably, the mechanical and thermal properties of these ordered block polymers are influenced by molar mass, tacticity of the poly(lactide) segments, and composition. By changing the endblock from the minority component ($f_{LA}$=0.29) to the majority component ($f_{LA}$=0.59) it is possible to access either elastomers or tough plastics. Moreover, at a fixed composition and molar mass, the use of semi-crystalline PLLA endblocks leads to remarkably strong elastomers that rival commercially available petroleum based block copolymers in recoverability, tensile strength, and ultimate elongation (Figure 3.8a).[23]
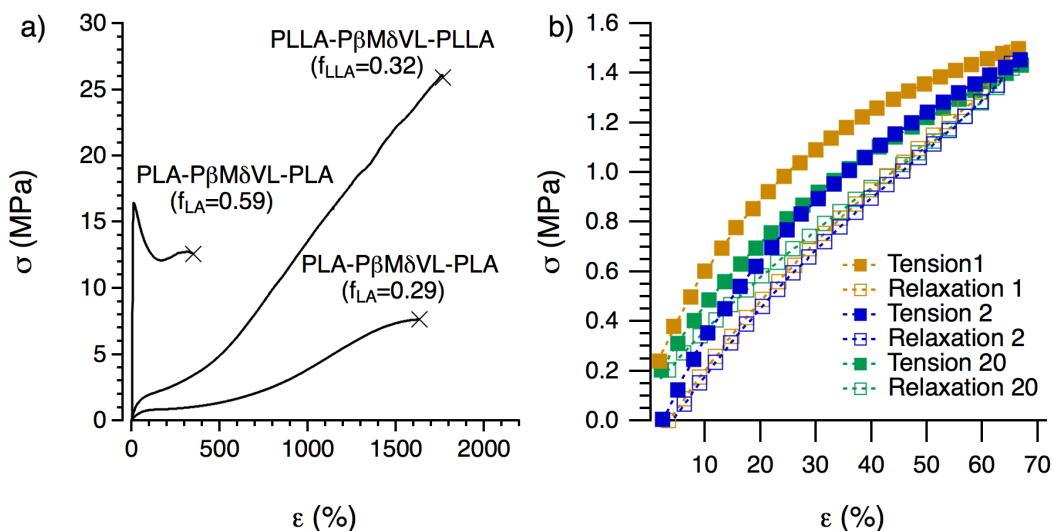


**Figure 3.8**

Representative (a) stress vs strain results in uniaxial extension for three P(L)LA-MVL-P(L)LA triblock copolymers with varying composition. PLA-MVL-PLA 16.2-20.0-16.2 kg mol$^{-1}$ ($f_{LA}$=0.59): E=229±54 Mpa, $\sigma_b$=12.5±1.1 MPa, $\varepsilon_b$=360±78%, $\sigma_y$=15.7±2.3 MPa; PLA-MVL-PLA 16.8-70.0-16.8 kg mol$^{-1}$ ($f_{LA}$=0.29): E=1.9±0.6 Mpa, $\sigma_b$=9.1±1.1 MPa, $\varepsilon_b$=1790±130%; PLLA-MVL-PLLA 18.6-70.0-18.6 kg mol$^{-1}$ ($f_{LLA}$=0.32): E=5.9±1.0 MPa, $\sigma_b$=28.0±3.4 MPa, $\varepsilon_b$=1718±140% (b) Stress verses strain for 18.6-70.0-18.6 kg mol$^{-1}$ PLLA-MVL-PLLA subjected to 20 cycles of tension and relaxation. For each cycle sample was pulled to 67% strain at a rate of 5 mm min$^{-1}$ then relaxed to 0% strain at the same rate. These results are competitive with commercially available elastomers and plastics.

## 3.3 Conclusions

In this work we have developed a semisynthetic approach to β-methyl-δ-valerolactone from glucose that relies upon the femenation of mevalonate and subsequent transformaiton of mevalonate to β-methyl-δ-valerolactone. The high titer of the fermentaion (88.3 g $L^{-1}$) and the efficiency of the chemical reactions used to produce to produce the final product make the overall process scalable and potentially commercially viable. We have also described a non-natural total biosynthetic pathway for the production of β-methyl-δ-valerolactone. Optimization of this novel all-biosynthetic pathway (i.e., titer and yield comparable to the semisynthetic route) would make additional chemical transformation unnecessary, further reducing the production cost of β-methyl-δ-valerolactone. This bioderived monomer can be readily converted from the neat state to a rubbery hydroxyl telechelic midblock using controlled polymerization techniques at ambient temperature; addition of either (±) or (-)-lactide to a living β-methyl-δ-valerolactone can be used to produce well defined ABA triblock polymers. We have demonstrated that the thermal and mechanical properties of these triblock polymers can be tuned by controlling molar mass, arcitecture, and endblock tacticity and have also prepared thermoplastic elastomers with properties similar to commercially availible styrenic block polymers. This work has therefore laid the foundation for the production of new biobased polymeric materials with a wide range of potential properties and applications.

## 3.4 Experimental Section

### 3.4.1 Materials

All reagents used for polymer synthesis were stored and handled in a glovebox under a nitrogen atmosphere. Triazobicyclodecene (TBD) (98%, Sigma-Aldrich) was purchased and purified by sublimation. 1,4-Benzene dimethanol (BDM) (99%, Acros Organics) and diphenyl phosphate (DPP) (99%, Sigma-Aldrich) were purchased and dried under vacuum at room temperature for a minimum of 48 hours prior to use. Benzyl alcohol (99%, Sigma-Aldrich) was purchased and used without additional purification. D,L-Lactide was a kind gift from Ortec Incorporated and was used as received. L-Lactide was a kind gift from Natureworks and was recrystallized twice from dry tolune and dried prior to use.

Tolune and dichloromethane (DCM) was passed through a home-built solvent purification system, which includes a column of activated alumina and a column of molecular sieves operated under a positive pressure of nitrogen gas. Anhydrous methanol (Sigma-Aldrich) and chloroform (Fisher) were purchased and used as received. Triethylamine (99.5%, Macron), and benzoic acid (99.5%, Fisher) used to quench DPP and TBD catalyzed reactions, respectively were also purchased and used as received. Glass and teflon components used for polymer synthesis were dried in an oven at 100 °C for a minimum of 6 hours immediately prior to use.

### 3.4.2 Molecular Biology and Fermentation Methods

*Bacterial and growth condition*

BW25113 ($rrnB_{T14}$ $\Delta$lacZ$_{WJ16}$ $hsdR514$ $\Delta araBAD_{AH33}$ $\Delta rhaBAD_{LD78}$) was used to produce mevalonate (MEV) and $\beta$-methyl-$\delta$-valerolactone ($\beta$M$\delta$VL or alternatively, MVL) (1). All cloning procedures were carried out in the *E. coli* strain XL10-gold (Stratagene). These *E. coli* strains were grown in test tubes at 37 $^{\circ}$C in 2XYT rich medium (16 g/L Bacto-tryptone, 10 g/L yeast extract and 5 g/L NaCl) supplemented with appropriate antibiotics (ampicillin 100 µg/mL and kanamycin 50 µg/mL) unless otherwise specified.

*Plasmids construction*

Three kinds of plasmids, shown in Figure 3.9 were constructed for the biosynthesis of $\beta$M$\delta$VL. The first plasmid, pMEV-1, is responsible for MEV production. The second plasmid, pAML-1, is used to produce anhydromevalonolactone (AML); the third plasmid is used to convert AML into $\beta$M$\delta$VL. Primers for plasmid construction are listed in Table 3.2.

**Table 3.2.**

**Primers used in the present study**

| Primer name | Sequence |
| --- | --- |
| atoBAcc-F | GGGCCC ggtacc atgAAAAATTGTGTCATCGTCAGTGC |
| atoBPst-R | GGGCCC ctgcag ttaATTCAACCGTTCAATCACCATCG |
| mvaSPst-F | GGGCCC ctgcag AGGAGAAATTAACT atgacaattgggattgataaaattag |
| mvaSBam-R | GGGCCC ggatcc ttagtttcgataagaacgaacggtat |
| mvaEBam-F | GGGCCC ggatcc AGGAGAAATTAACT atgaaaacagtagttattattgatgc |
| mvaEXba-R | GGGCCC tctaga ttattgttttcttaaatcatttaaaa |
| VecAcc-R | GGGCCC ggtacc tttctcctctttaatgaattcggtcagt |
| VecXba-F | GGGCCC tctaga ggcatcaaataaaacgaaaggctcagtc |
| SA.mvaSPst-F | GGGCCC ctgcag AGGAGAAATTAACTatgacaataggtatcgacaaaataaa |
| SA.mvaSBam-R | GGGCCC ggatcc ttactctggtctgtgatattcgcgaa |
| LC.mvaSPst-F | GGGCCC ctgcag AGGAGAAATTAACTatgaaaatcgggattgatgcaatcgc |
| LC.mvaSBam-R | GGGCCC ggatcc ttaccgctgctgatattgacgttctt |
| Mm.mvaSPst-F | GGGCCC ctgcag AGGAGAAATTAACTatgaaagaagtaggtattgtaggata |
| Mm.remPst-R | ttagcaccgatgatgtatgcagcaccacc Agcagcagcagtgtattcaagagcatctcc |
| Mm.remPst-F | ggagatgctcttgaatacactgctgctgc Tggtggtgctgcatacatcatcggtgctaa |
| Mm.mvaSBam-R | GGGCCC ggatcc ttacattctaattttttcctctgtatttc |
| Mv.mvaSPst-F | GGGCCC ctgcag AGGAGAAATTAACT atgaacgaagtgggtatcgtaggata |

| | |
|---|---|
| Mv.remPst-R | cctacaagtcccatacacatttgtatacc Agcagtacctgctttacaagcaaattctaa |
| Mv.remPst-F | ttagaatttgcttgtaaagcaggtactgc Tggtatacaaatgtgtatgggacttgtagg |
| Mv.mvaSBam-R | GGGCCC ggatcc ttacattctaatttttttctctgtatt |
| Sa.mvaEBam-F | GGGCCC ggatcc AGGAGAAATTAACT atgcaaagtttagataagaatttccg |
| Sa.mvaEXba-R | GGGCCC tctaga ttattgttgtctaatttcttgtaaaa |
| Lc.mvaEBam-F | GGGCCC ggatcc AGGAGAAATTAACT atgaaattttacgagttgtctccaga |
| Lc.mvaEXba-R | GGGCCC tctaga tTaatcccgattttcatcttttgatt |
| Mm.mvaEBam-F | GGGCCC ggatcc AGGAGAAATTAACT atggaaaataacgttaatattgaaga |
| Mm.mvaEXba-R | GGGCCC tctaga ttatcttccaagttcagaatgcgctt |
| Mv.mvaEBam-F | GGGCCC ggatcc AGGAGAAATTAACT atgaacaatataaaaaataataatga |
| Mv.mvaEXba-R | GGGCCC tctaga ttaccttcctaattccgaatgtgctt |
| SidHind-F | GGGCCCaagcttAGGAGAAATTAACTATGAGCACCGAGGCTCATCCTACTGT |
| SidHsal-R | GGGCCCgtcgacTTACAACTTGCTCGGGCGCCATTGCG |
| OYE2sal-F | GGGCCCgtcgacAGGAGAAATTAACTATGCCATTTGTTAAGGACTTTAAGCC |
| OYE2-Vec | gagcctttcgttttatttgatgcctctagaGCTAGCTTAATTTTTGTCCCAACCGAGTTT |
| OYE3sal-F | GGGCCCgtcgacAGGAGAAATTAACTATGCCATTTGTAAAAGGTTTTGAGCC |
| OYE3-Vec | gagcctttcgttttatttgatgcctctagaGCTAGCTtAGTTCTTGTTCCAACCTAAATC |
| yqjM-F | GGGCCCgtcgacAGGAGAAATTAACTatgGCCAGAAAATTATTTACACCTAT |
| yqjM-Vec | gagcctttcgttttatttgatgcctctagaGCTAGCttaCCAGCCTCTTTCGTATTGAAC |
| yqjMC26D-R | TTCCGTCCTTTTCATGAGAAGAATACATgtcCATTGGCGACATGACAATG-CGGTTTTTT |

| | |
|---|---|
| yqjMC26D-F | AAAAAACCGCATTGTCATGTCGCCAATGgacATGTATTCTTCTCATGAAA-AGGACGGAA |
| yqjMI69T-R | CGCTCCAAATGCCTAAGTCTTGGTCAGTcgtTCGTCCTTGAGGGTTAACCGCTGACGCC |
| yqjMI69T-F | GGCGTCAGCGGTTAACCCTCAAGGACGAacgACTGACCAAGACTTAGGCATTTGGAGCG |

To construct pMEV-1 (Figure 3.9), the gene fragment of *atoB* was amplified from *E. coli* genomic DNA with primers atoBAcc-F and atoBPst-R, and genes of *mvaS* and *mvaE* were amplified from *E. faecalis* genomic DNA with primers mvaSPst-F and mvaSBam-R, mvaEBam-F and mvaEXba-R. The vector fragment of pZE was amplified from plasmid pIVC3 (2) with primers VecAcc-R and VecXba-F. Then the gene fragments of *atoB*, *mvaS*, *mvaE* and pZE were digested with Acc65I/PstI, PstI/BamHI, BamHI/ XbaI, and Acc65I/ XbaI, respectively. These digested genes were ligated with T4 DNA ligase to form the plasmid pMEV-1.
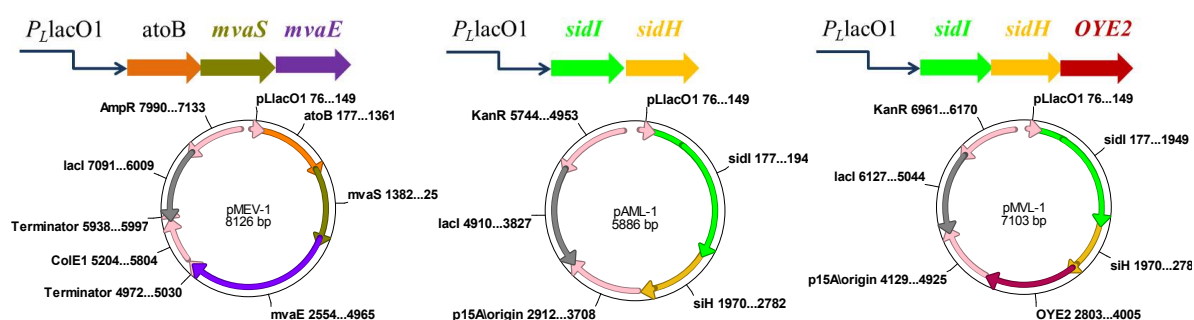


**Figure 3.9**.

**The three plasmids constructed for this study**

To build plasmids with combinations of different *mvaS* and *mvaE*, *mvaS* genes from *S. aureus*, *L. casei*, *M. maripaludis* and *M. voltae* were amplified from their corresponding genomic DNA with primer pairs SA.mvaSPst-F/SA.mvaSBam-R, LC.mvaSPst-F/LC.mvaSBam-R, Mm.mvaSPst-F/ Mm.remPst-R and Mm.remPst-F/Mm.mvaSBam-R, Mv.mvaSPst-F/Mv.remPst-R and Mv.remPst-F/Mv.mvaSBam-R, respectively. Then *mvaS* in plasmid pMEV-1 was replaced to form plasmids of pMEV-2, pMEV-3, pMEV-4 and pMEV-5.

Since the transformed *E. coli* strain with plasmid pMEV-3 produced the highest level of MEV, more plasmids were constructed with different *mvaE* based on pMEV-3. *mvaE* genes from *S. aureus*, *L. casei*, *M. maripaludis* and *M. voltae* were amplified from their corresponding genomic DNA with primer pairs Sa.mvaEBam-F/Sa.mvaEXba-R, Lc.mvaEBam-F/Lc.mvaEXba-R, Mm.mvaEBam-F/Mm.mvaEXba-R, and Mv.mvaEBam-F/Mv.mvaEXba-R, respectively. Then *mvaE* in plasmid pMEV-3 was replaced to form pMEV-6, pMEV-7, pMEV-8 and pMEV-9.

To build plasmids to synthesize AML, genes of *sidI* and *sidH* from *A. fumigatus*, *N. crassa*, *P. nodorum*, *S. sclerotiorum* (3) were codon-optimized and synthesized by GenScript company. Genes *sidI* and *sidH* were then digested with Acc65I/HindIII and HindIII/NheI, and inserted into pIVC1 (*2*) to form pAML-1, pAML-2, pAML-3 and pAML-4, respectively.

To build pMVL-1, genes *sidH* and *OYE2* were PCR amplified with primers of SidHind-F/SidHsal-R and OYE2sal-F/OYE2-Vec by using pAML-1 and *S. cerevisiae* genomic

DNA as templates. Then the PCR products were digested by HindIII/SalI and SalI/NheI and inserted into pAML-1 to form pMVL-1. The *OYE3* and *YqjM* genes were PCR amplified with primer pairs OYE3sal-F/OYE3-Vec and yqjM-F/yqjM-Vec by using genomic DNA of *S. cerevisiae* and *B. subtilis* as templates, and then *OYE3* and *yqjM* were used to replace *OYE2* of pMVL-1 to generate pMVL-2 and pMVL-3. To introduce two point mutations into *yqjM*, three fragments were PCR amplified with primers of yqjM-F/yqjMC26D-R, yqjMC26D-F/yqjMI69T-R and yqjMI69T-F/yqjM-Vec by using *B. subtilis* genomic DNA as the template, and another round PCR was carried out with primers of yqjM-F/yqjM-vec by using the last three PCR fragments as templates. The PCR product was inserted into pAML-1 to generate pMVL-4.

*Shake flask batch fermentation*

To carry out small-scale fermentation, 125 ml conical flasks with 0.5 g CaCO3 were autoclaved and dried. Then the flasks were filled with 5 ml M9 medium supplemented with 5 g $L^{-1}$ yeast extract, 40 g $L^{-1}$ glucose, and antibiotics. 200 µl of overnight cultures incubated in 2XYT medium were transferred into the flasks and placed in a shaker at a speed of 250 rpm. After adding 0.1 mM isopropyl-β-D-thiogalactoside (IPTG), the fermentation was performed for 48 hours at 30 °C. The fermentation results of mevalonate, AML and βMδVL in shake flasks are described in respective in Tables 3.3-3.5, below.

**Table 3.3**

**Batch fermentation results for mevalonate production**

| Strain | Acetate (g L$^{-1}$) | MEV (g L$^{-1}$) |
|---|---|---|
| BW25113 with pMEV-1 | 0.45±0.28 | 10.75±0.28 |
| BW25113 with pMEV-2 | 3.11±0.07 | 5.05±0.28 |
| BW25113 with pMEV-3 | 0.20±0.03 | 12.57±0.15 |
| BW25113 with pMEV-4 | 6.48±0.49 | 0 |
| BW25113 with pMEV-5 | 8.80±1.51 | 0 |
| BW25113 with pMEV-6 | 0.13±0.05 | 13.37±0.54 |
| BW25113 with pMEV-7 | 0.17±0.01 | 14.62±0.24 |
| BW25113 with pMEV-8 | 0.13±0.05 | 10.90±0.39 |
| BW25113 with pMEV-9 | 0.18±0.02 | 11.48±0.28 |

**Table 3.4.**

**Batch fermentation results for anhydromevalonolactone production**

| Strain | MEV (g L$^{-1}$) | AML (g L$^{-1}$) |
|---|---|---|
| BW25113 with pMEV-7 and pAML-1 | 12.36±1.18 | 0.73±0.06 |
| BW25113 with pMEV-7 and pAML-2 | 13.59±0.24 | 0.54±0.02 |

**Table 3.5.**

**Batch fermentation results for βMVL production**

| Strain | MEV (g L$^{-1}$) | AML (g L$^{-1}$) | βMδVL (g L$^{-1}$) |
|---|---|---|---|
| BW25113 with pMEV-7 and pMVL-1 | 10.19±0.61 | 0.34±0.03 | 0.18±0.03 |
| BW25113 with pMEV-7 and pMVL-2 | 6.77±0.58 | 0.48±0.03 | 0 |
| BW25113 with pMEV-7 and pMVL-3 | 8.85±0.56 | 0.55±0.01 | 0 |
| BW25113 with pMEV-7 and pMVL-4 | 9.39±0.48 | 0.31±0.01 | 0.27±0.02 |

*Fed-batch fermentation in bioreactor*

Fermentation media for bioreactor cultures contained the following composition: glucose, 10 g $L^{-1}$; $K_2HPO_4$, 7.5 g $L^{-1}$; citric acid monohydrate, 2.0 g $L^{-1}$; yeast extract, 0.5 g $L^{-1}$; $MgSO_4 \cdot 7H_2O$, 2.0 g $L^{-1}$; Thiamine hydrochloride, 0.008 g $L^{-1}$; D-(+)-biotin, 0.008 g $L^{-1}$; nicotinic acid, 0.008 g $L^{-1}$; pyridoxine, 0.032 g $L^{-1}$; ampicillin, 0.1 g $L^{-1}$; concentrated $H_2SO_4$, 0.8 mL; and trace metal solution 1 mL $L^{-1}$. The trace metal solution contained: NaCl, 10 g $L^{-1}$; Citric acid, 40 g $L^{-1}$; $ZnSO_4 \cdot 7H_2O$, 1.0 g $L^{-1}$; $MnSO_4 \cdot H_2O$, 30 g $L^{-1}$; $CuSO_4 \cdot 5H_2O$, 0.1 g $L^{-1}$; $H_3BO_3$, 0.1 g $L^{-1}$; $Na_2MoO_4 \cdot 2H_2O$, 0.1 g $L^{-1}$; $FeSO_4 \cdot 7H_2O$, 1.0 g $L^{-1}$; $CoCl_2 \cdot 6H_2O$, 1.0 g $L^{-1}$. The feed solution contained: glucose, 600 g $L^{-1}$; $K_2HPO_4$, 7.4 g L; and antifoam 10 mL.

Cultures of *E. coli* were performed in 1.3 L Bioflo 115 Fermenter (NBS, Edison, NJ USA) using an initial working volume of 0.5 L. The fermenter was inoculated with 10% of overnight pre-culture with 2XYT medium. The culturing condition was set at 34°C, dissolved oxygen level (DO) 30%, and pH 7.0. After $OD_{600}$ reached 5.2, 0.2 mM IPTG was added to produce MEV. The pH was controlled at 7.0 by automatic addition of 26% ammonia hydroxide. Airflow rate was maintained at 1 vvm in the whole process. DO was maintained about 20% with respect to air saturation by raising stirring speed (from 300 to 1200 rpm). The fed-batch rate of glucose was determined according to the glucose consumption rate manually. The fermentation process was stopped 2 days after IPTG addition. Fermentation culture was sampled periodically to determine cell density and production level. The detailed fermentation results are listed in Table 3.6.

**Table 3.6**

**Fed-batch fermentation results for the production of mevalonate in 1.3 L bioreactor**

| Time (h) | Biomass (g L$^{-1}$) | Glucose (g L$^{-1}$) | Acetate (g L$^{-1}$) | MEV (g L$^{-1}$) |
|---|---|---|---|---|
| 0 | 1.3 | 4.6 | 0.85 | 0 |
| 5.5 | 6.9 | 12.9 | 2.25 | 1.7 |
| 16 | 30.0 | 0 | 1.39 | 24.5 |
| 19 | 34.0 | 14.3 | 0.48 | 34.4 |
| 24.5 | 37.8 | 24.8 | 0.35 | 40.5 |
| 31 | 29.8 | 34.2 | 0.33 | 50.0 |
| 40.5 | 27.0 | 27.3 | 1.09 | 69.6 |
| 43 | 24.5 | 12.5 | 1.50 | 77.1 |
| 48 | 24.0 | 0 | 3.48 | 88.3 |

### 3.4.3 Synthetic Methods

The thermodynamics of MVL polymerization are discussed in Chapter 4 as are the DPP-catalyzed MVL polymerization kinetics studies. Relevant experimental details are included in [Appendix D.](#) and in, [Appendix C.,](#) respectively.

*Dehydration and extraction*

The fermentation broth from bio-reactor was harvested by centrifugation, then filtered through activated charcoal to remove colored contaminants. To determine the optimal level of catalyst for the dehydration reaction test tubes were filled with 5 ml fermentation broth and 0-12% concentrated $H_2SO_4$; these tubes were autoclaved for 1 hour (121 °C, 15 psi) to produce AML. The concentrations of MEV and AML were measured by HPLC. Immiscible organic solvents were used to extract AML from the reaction mixture. The results of dehydration and extraction are shown in Table 3.7.

**Table 3.7.**

Dehydration results by using different concentrations of $H_2SO_4$

| $H_2SO_4$ (%) | Mevalonate (g/L) | Anhydro-mevalonolactone (g/L) | Conversion (%) | Selectivity (%) |
|---|---|---|---|---|
| 0 | 88.3 | 0 | - | - |
| 2 | 67±4 | 2.5±0.7 | 24±5 | 16±1 |
| 4 | 55±2 | 24±2 | 38±2 | 92±1 |
| 6 | 10.6±0.1 | 52±2 | 88±0.1 | 88±3 |
| 8 | 2.7±0.1 | 56±0.7 | 97±0.1 | 86.0±0.9 |
| 10 | 1.7±0.01 | 58±0.6 | 98±0.01 | 88.8±0.9 |
| 12 | 1.6±0.02 | 58±3 | 98±0.02 | 89±4 |

*Hydrogenation*

Unreduced palladium on activated carbon (10% w/w Acros Organics) was purchased and dried in situ prior to use. Tetrahydrofuran (THF) (Fisher) was purchased and used as received. In a typical hydrogenation procedure, 10 g of catalyst were added to a 300 mL high-pressure reactor with jacketed temperature control and mechanical stirring. The palladium catalyst was held under vacuum at 80 °C for an hour, then cooled to ambient temperature. Separately, 50 ml of anhydromevalonate was transferred into a solution delivery vessel (SDV) and sparged with argon for at least 15 min. The SDV was attached to the reactor and 50 psig argon was applied to displace the contents into the

cooled reactor. Argon was released, and the SDV detached; at this time stirring was initiated, and the vessel charged with $H_2$ to a pressure of ~350 psig. The pressure in the vessel was replenished periodically as the hydrogenation progressed until the pressure remained static within the vessel. The reaction was then allowed to stir under $H_2$ at room temperature overnight to ensure quantitative conversion. Following depressurization, the reactor was flushed with argon and the reactor contents diluted with THF to facilitate total transfer. The catalyst was removed from the solution by filtration through a Millipore filter flask containing a 0.45 µm HVHP membrane. The THF was removed by rotary evaporation to obtain crude MVL in typical yields of ~93% (conversion >99% by ^{1}HNMR).

*MVL purification*

The crude MVL was dried over calcium hydride for 12 hours then distilled under vacuum (50 mTorr, 30°C); the distilled product was passed through dry basic alumina using dry cyclohexane as an eluent. The cyclohexane was removed under vacuum to obtain purified MVL.

*Polymerization kinetics experiment with TBD catalyst*

A kinetics experiment was conducted using the following method: In a glovebox with a nitrogen atmosphere TBD was added to a vial containing MVL and stirred to dissolve. At this time benzyl alcohol was injected and immediately mixed, starting the polymerization. The initial concentrations of monomer, catalyst, and initiator were $[MVL]_0$=9.16 M, $[TBD]_0$=0.019 M, $[BnOH]_0$=0.032 M. Aliquots were taken and

quenched with 1M benzoic acid before the addition of initiator (t=0) and periodically thereafter until the reaction reached 4 half-lives.

*Poly(β-methyl-δ-valerolactone)*

To synthesize PMVL a monofuntional (benzyl alcohol) or difunctional (1,4 benzene dimethanol) alcohol was added to monomer in a pressure vessel or glass vial and stirred with a magnetic stir bar until completely dissolved. The ratio of monomer to alcohol was varied to target polymers of different molecular weights. When the initiator was dissolved an appropriate amount of catalyst (~0.05-0.2 mol% TBD or ~0.5 mol% DPP) relative to monomer was added to initiate the polymerization. The reaction was stirred and the conversion monitored using $^1$H NMR of crude quenched aliquots dissolved in CDCl$_3$. To obtain PMVL homopolymer the reaction was quenched by the addition of 5 equivalents, relative to catalyst, of either 1M benzoic acid is chloroform (TBD catalyzed reactions) or triethylamine (DPP catalyzed reactions). The quenched polymer was diluted with chloroform, precipitated in cold methanol and dried for a minimum of 24 hours at room temperature in a vacuum oven.

*Poly((L)LA)-b-PMVL-b-poly((L)LA) : Addition of lactide to living polymerization*

To prepare poly((L)LA)-*b*-PVML-*b*-poly((L)LA) a solution of $_{D,L}$-Lactide or $_L$-Lactide in DCM (1M) was added slowly to a living TBD catalyzed polymerization at equilibrium while stirring manually with a glass stir rod. The amount of added lactide solution added depended on the target composition of the block polymer. To obtain purified polymers the samples were quenched with benzoic acid, diluted with chloroform, precipiated in methanol, and dried. It is worth noting that DPP is not capable of catalyzing the polymerization of lactide. Therefore, addition $_{D,L}$-Lactide in DCM PMVL in the presence of this catalyst resulted in depolymerization of PMVL rather than the synthesis of a block polymer.

*Poly((L)LA)-b-PMVL-b-poly((L)LA)-TBD catalyzed addition of lactide to purified telechelic PMVL in solution:* To prepare poly((L)LA)-*b*-PMVL-*b*-poly((L)LA) from a previously isolated and purified PMVL using TBD, the prepolymer was dissolved in a 1 M solution of D,L-Lactide or $_L$-Lactide in DCM, when fully dissolved 0.1 mol% TBD (relative to lactide) was added. The solution was stirred for 10 minutes, then quenched via the addition 5 equivalents of benzoic acid relative to TBD. To obtain purified polymers the samples were diluted with chloroform, precipiated in methanol, and dried.

**Table 3.8.**

**Molar mass control for synthesis of representative poly(βMδVL) homopolymers diols**

| Sample No. | [a]$M_n$ Theor. (kg mol$^{-1}$) | [b]Conversion (%) | [c]$M_n$ (kg mol$^{-1}$) | [d]$M_m$ (kg mol$^{-1}$) | [d]Đ | [e]$T_g$ (°C) |
|---|---|---|---|---|---|---|
| 1 | 4.1 | 64.1 | 4.2 | 5.3 | 1.08 | −51 |
| 2 | 4.3 | 79.1 | 4.3 | 4.1 | 1.06 | −50 |
| 3 | 7.2 | 89.0 | 7.2 | 8.3 | 1.08 | −51 |
| 4 | 10.1 | 79.6 | 10 | 11 | 1.05 | −52 |
| 5 | 12.1 | 90.2 | 12 | 12 | 1.05 | −52 |
| 6 | 18.4 | 46.0 | 19 | 18 | 1.05 | −50 |
| 7 | 19.0 | 88.0 | 21 | 20 | 1.06 | −51 |
| 8 | 74.9 | 86.0 | 100 | 70 | 1.13 | −51 |
| 9 | 94.1 | 89.9 | 85 | 65 | 1.07 | −49 |

[a]Conversion adjusted theoretical molar mass calculated using ratio of monomer to initiator and observed conversion. [b]Monomer conversion determined using $^1$H NMR of crude sample via comparision of residual monomer methylene signals to polymer methylene proton signals. [c]Number average molar mass of polymer sample determined using $^1$H NMR of purified polymer, the degree of polymerization was found by normalizing the spectrum to the initiator methylene protons. $M_n$ determined using this method is likely not accurate for high molecular weight polymers as the endgroup is insignificant compared to the polymer protons. [d]Mass average molar mass and dispersity were determined using LS-SEC with the assumption of 100% mass recovery to determine dn/dc of the polymer. [e]Glass transition temperatures determined using DSC with a heating ramp rate 5 °C min$^{-1}$, to ensure the samples had the same thermal history data were taken from second heating ramp.

*Poly((L)LA)-b-PMVL-b-poly((L)LA)–Sn(Oct)₂ catalyzed addition of lactide to purified telechelic poly(βMδVL) in melt/bulk:* To prepare poly((L)LA)-*b*-PVML-*b*-poly((L)LA) from a previously isolated and purified PMVL in the melt the prepolymer was added to an appropriate amount of D,L-Lactide or  ₗ-Lactide in a 5-necked kettle reactor fitted with  an overhead stir assembly,  thermometer, gas inlet,  bubbler, and septum. The contents were heated while stirring under constant argon flow until the internal temperature reached 180 °C. At this time the solution was stirred for an additional ½ hour to ensure the contentes were homogeneous then 0.05 mol% Sn(Oct)₂  (relative to lactide) was injected. After stirring ½ hour the reaction was cooled to ambient temperature. To obtain purified polymers the samples were diluted with chloroform, precipiated in methanol, and dried.

**Table 3.9.**

**Characteristics of selected Poly(LA-*b*-βδMVL-*b*-LA) Triblocks**

| [a]Composition | [b]Lactide (wt %) | [c]$f_{(L)LA}$ | [d]$T_g$ (°C) | [d]$T_g$ (°C) | [d]$T_m$ (°C) | [de]X (%) | [f]$T_{ODT}$ (°C) | [g]d (nm) |
|---|---|---|---|---|---|---|---|---|
| [h]LA-MVL-LA 2.9-4.9-2.9 | 54 | 0.51 | −13 | - | - | - | Dis. | Dis. |
| LA-MVL-LA 9.3-18.5-9.3 | 50 | 0.47 | −48 | 32 | - | - | 109 (105) | 22 |
| LA-MVL-LA 9.5-20.0-9.5 | 49 | 0.48 | −47 | 38 | - | - | 138 (140) | 27 |
| LLA-MVL-LA 9.0-20.0-9.0 | 47 | 0.44 | −47 | 42 | 134 | 20 | 150 (160) | 30 |
| [i]LA-MVL-LA 16.2-20-16.2 | 49 | .59 | −45 | 33 | - | - |  | 33 |
| [i]LA-MVL-LA 16.8-70.0-16.8 | 32 | 0.29 | −53 | 30 | - | - |  | 47 |
| LLA-MVL-LLA 18.6-70.0-18.6 | 35 | 0.32 | −51 | 43 | 150 | 10 |  | 48 |

[a]Composition calculated from the mass average molar mass of the corresponding midblock determined by LS-SEC   and the lactide content of the  purified triblock determined by ^{1}H NMR. [b]weight percent of lactide in triblock determined using ^{1}H NMR analysis. [c]Volume fraction of (L)LA blocks determined using densities of 1.248 g cm$^{-3}$ and 1.10 g cm$^{-3}$ for poly(lactide) and poly(δMVL), respectively. [d]Glass transition temperatures and melting points, and enthalpy of fusion were  determined using the second DSC heating ramp at a rate 5 °C min$^{-1}$ after previously cooling from 200 °C at the same rate. [e] Percent crystallinity for the entire triblock was calculated from the enthalpy of fusion and a reference heat of fusion (12) of 94 J/g for the α-form of crystalline PLLA.[47]  [f]Order to disorder transition temperatures determined by DMA temperature ramps  heating a a rate of 1 °C min$^{-1}$ with a constant frequency of 1 rad/s and a strain of 1%. Transition temperatures were also determined using variable temperature SAXS (listed in parentheses).  For samples 5, 7, and 8 the transition temperature was above the degradation temperature of the sample. [g]Domain spacing calculated from primary SAXS peak at room temperature (20 °C) after heating above the order to disorder transition and annealing in a vacuum oven  at 100 °C for a minimum of 12 hours prior to cooling. For samples with order to disorder transitions greater than 180 °C a film was prepared by casting from a solution of chloroform, dried and  annealed at 100 °C for 12 hours prior to cooling. [h] Sample is disordered by SAXS.  [i] Order to disorder transition not apparent by SAXS or rheology, likely >200 °C.

**Table 3.10.**

[a] **Mechanical properties of Poly(LA-*b*-MVL-*b*-LA) Triblocks**

| [a]Sample | [b]E (MPa) | [b]$\sigma_b$ (MPa) | [b]$\varepsilon_b$ (%) | [c]$f_{(L)LA}$ |
|---|---|---|---|---|
| LA-MVL-LA 16.2-20.0-16.2 | 229+54 | 12.5+1.2 | 350+80 | 0.59 |
| LLA-MVL-LLA 9.0-20.0-9.0 | 22+9 | 8.32+0.61 | 623+40 | 0.44 |
| LA-MVL-LA 9.5-20.0-9.5 | 54+12 | 1.65+0.91 | 190+30 | 0.46 |
| LLA-MV-LLA 18.6-70.0-18.6 | 5.92+0.95 | 28 +4 | 1720+140 | 0.32 |
| LA-MVL-LA 16.8-70.0-16.8 | 1.93+0.61 | 9.0+1.1 | 1790+130 | 0.29 |

[a]Details of the characteristics of these samples are provided in Table 3.8. [b] Determined by uniaxial extension at a constant deformation rate of 110 mm min$^{-1}$. [c]Volume fraction of P(L)LA blocks determined using densities of 1.248 g cm$^{-3}$ and 1.10 g cm$^{-3}$ for amorphous PLA and PMVL, respectively

*Poly($_L$-Lactide)*

Poly($_L$-lactide) was synthesized from lactide at room temperature using TBD as a catalyst and benzene dimethanol as an initiator. To a 1 M solution of lactide in DCM benzene dimethanol was added and stirred until fully dissolved. To initiate the polymerization 0.1 mol% TBD relative to lactide was added and the reaction stirred for 5 minutes. At this time the catalyst was quenched via the addition of 5 equivalents of benzoic acid. The polymers were subsequently isolated by precipitation in methanol and dried for 24 hours in a vacuum oven.

*PMVL Density Determination*

PMVL density was determined using the following method: Glycerol (99%, Riedel-de Haën), ethylene glycol (99% Mallinckrodt) were purchased and used with DI water to prepare several solutions with densities ranging from 1.25 and 1.0 g cm$^{-3}$. A small, bubble-free sample of PMVL ($M_m$= 30 kg mol$^{-1}$) was dropped into these solutions at room temperature. The density of the solution in which the sample appeared to achieve neutral buoyancy was taken to be the polymer density; this was determined to be 1.10 $\pm$0.05 g cm$^{-3}$ using a 0.989 cm$^{3}$ glass micropycnometer previously calibrated using room temperature deionized $H_2O$ (data are the average and standard deviation of 5 replicates).

### 3.4.4 Characterization Methods

All general characterization and instrumental methods are provided in . Characterization methods specific to Chapter 3 are given in the sections below.

*Metabolite analysis and cell dry weight determination*

Fermentation products were analyzed using an Agilent 1260 Infinity HPLC equipped with an Aminex HPX 87H column and a refractive-index detector. The mobile phase was 0.01N $H_2SO_4$ with a flow rate of 0.6 ml/min. The column temperature and detection temperature were 35°C and 50°C, respectively. Cell dry weight was determined by filtering 5ml culture through a 0.45 µm pre-weighed glass fiber filter. After removal of

medium, the filter was washed with 15ml of DDI water, dried in a microwave oven for 20 min at 300 W and then weighed. Cell dry weight was determined in triplicate.

## 3.5 References

(1) Miller S.A. Sustainable Polymers: Opportunities for the Next Decade. *ACS Macro Lett* **2015**, *2,* (550-554)

(2) Atsumi S.; Hanai T.; Liao J. C. Non-fermentative pathways for synthesis of branched-chain higher alcohols as biofuels. *Nature* **2008**, *451,* (86-89)

(3) Xu P., Gu, Q.; Wang, W.; Wong, L.; Bower, A. G.; Collins, C. H.; Koffas, M. A. Modular optimization of multi-gene pathways for fatty acids production in *E. coli. Nat Commun* **2013**, *4,* (1409-1417)

(4) Dellomonaco, C.; Clomburg, J.M.; Miller, E.N.; Gonzalez R. Engineered reversal of the beta-oxidation cycle for the synthesis of fuels and chemicals. *Nature* **2011**, *476,* (355-359)

(5) Bastian, S.; Liu, X.; Meyerowitz, J. T.; Snow, C. D.; Chen, M.M.; Arnold, F. H. Engineered ketol-acid reductoisomerase and alcohol dehydrogenase enable anaerobic 2-methylpropan-1-ol production at theoretical yield in *Escherichia coli. Metab Eng* **2011**, *13,* (345-352)

(6) Steen, E.J.; Kang, Y.; Bokinsky, G.; Hu, Z.; Schirmer, A.; McClure, A.; del Cardayre, S. B.; Keasling, J. D. Microbial production of fatty-acid-derived fuels and chemicals from plant biomass *Nature* **2010**, *463,* (559-562)

(7) Enquist-Newman M.; Faust, A. M.; Bravado, D. D.; Santos, C. N.; Raisner, R. M.; Hanel, A.; Sarvabhowman, P.; Le, C.; Regitsky, D. D.; Cooper, S. R.; Peereboom, L.; Clark, A.; Martinez, Y.; Goldsmith, J.; Cho, M. Y.; Donohoue, P. D.; Luo, L.; Lamberson, B.; Tamrakar, P.; Kim, E. J.; Villari, J. L.; Gill, A.; Tripathi, S. A.; Karamchedu, P.; Paredes, C. J.; Rajgarhia, V.; Kotlar, H. K.; Bailey, R. B.; Miller, D. J.; Ohler, N. L.; Swimmer, C.; Yoshikuni, Y. Efficient ethanol production from brown macroalgae sugars by a synthetic yeast platform *Nature* **2014**, *505,* (239-243)

(8) Yim H.; Haselbeck, R.; Niu, W.; Pujol-Baxley, C.; Burgard, A.; Boldt, J.; Khandurina, J.; Trawick, J. D.; Osterhout, R. E.; Stephen, R.; Estadilla, J.; Teisan, S.; Schreyer, H. B.; Andrae, S.; Yang, T. H.; Lee, S. Y.; Burk, M. J.; Van Dien, S. Metabolic engineering of *Escherichia coli* for direct production of 1, 4-butanediol. *Nat Chem Biol* **2011**, *7,* (445-452)

(9) Tseng H. C., Prather K. L. Controlled biosynthesis of odd-chain fuels and chemicals via engineered modular metabolic pathways. *Proc Natl Acad Sci USA* **2012**, *109,* (17925-17930)

(10) Achkar, J.; Xian, M.; Zhao, H.; Frost, J. W. Biosynthesis of phloroglucinol. *J Am Chem Soc* **2005**, *127,* (5332-5333)

(11) Causey, T.B.; Zhou, S.; Shanmugam, K.T.; Ingram, L.O. Engineering the metabolism of *Escherichia coli* W3110 for the conversion of sugar to redox-neutral and oxidized products: homoacetate production. *Proc Natl Acad Sci USA* **2003**, *100,* (825-832)

(12) Park S.J.; Kim, E. Y.; Noh, W.; Park, H. M.; Oh, Y. H.; Lee, S. H.; Song, B. K.; Jegal, J.; Lee, S. Y. Metabolic engineering of *Escherichia coli* for the production of 5-aminovalerate and glutarate as C5 platform chemicals. *Metab Eng* **2013**, *16*, (42-47)

(13) Ajikumar P.K.; Xaio, W.-H.; Tyo, K. E. J.; Yong, W.; Simeon, F.; Leonard, E.; Mucha, O.; Phon, T. H.; Pfeifer, B.; Stephanopoulos, G. Isoprenoid pathway optimization for Taxol precursor overproduction in *Escherichia coli*. *Science* **2010**, *330*, (70-74)

(14) Ma S.M.; Li, J. W.; Choi, J. W.; Zhou, H.; Lee, K. K.; Moorthie, V. A.; Xie, X.; Kealey, J. T.; Da Silva, N. A.; Vederas, J. C.; Tang, Y., Complete reconstitution of a highly reducing iterative polyketide synthase. *Science* **2009**, *326*, (589-592)

(15) Ro, D.K.; Paradise, E. M.; Ouellet, M.; Fisher, K. J.; Newman, K. L.; Ndungu, J. M.; Ho, K. A.; Eachus, R. A.; Ham, T. S.; Kirby, J.; Chang, M. C. Y.; Withers, S. T.; Shiba, Y.; Sarpong, R.; Keasling, J. D., Production of the antimalarial drug precursor artemisinic acid in engineered yeast. *Nature* **2006**, *440*, (940-943)

(16) Pfeifer, B.A.; Admiraal, S. J.; Gramajo, H.; Cane, D. E.; Khosla, C., Biosynthesis of complex polyketides in a metabolically engineered strain of *E. coli*. *Science* **2001**, 291, (1790-1792)

(17) Anderson K. S., Schreck K. M., Hillmyer M. A. Toughening polylactide *Polym Rev* **2008**, *48*, (85-108)

(18) Tsui A.; Wright, Z.C.; Frank, C.W. Biodegradable Polyesters from Renewable Resources. *Annu Rev Chem Biomol Eng* **2013**, *4*, (143-170)

(19) Bates, F.S.; Hillmyer, M. A.; Lodge, T. P.; Bates, C. M.; Delaney, K. M.; Fredrickson, G. H., Multiblock polymers: panacea or Pandora's box? *Science* **2012**, *336*, (434-440)

(20) Morton, M. Structure-Property Relations in Amorphous and Crystallizable ABA Triblock Copolymers. *Rubb Chem Technol* **1983**, *56*, (1096-1110)

(21) Schmalz, H.; Abetz, V.; Lange, R. Thermoplastic elastomers based on semicrystalline block copolymers. *Compos Sci Technol* **2003**, *63*, (1179-1186)

(22) Handlin, D.; Trenor, S.; Wright, K. *Applications of Thermoplastic Elastomers Based on Styrenic Block Copolymers. Macromolecular Engineering*, (Wiley-VCH Verlag GmbH & Co. KGaA), **2007**, (2001-2031)

(23) Kraton Performance Polymers Inc. Product Families Kraton D SBS. http://www.kraton.com/products/Kraton_D_SBS.php.

(24) Olsén P., Borke T., Odelius K., Albertsson, A. C. ε-Decalactone: A Thermoresilient and Toughening Comonomer to Poly(L-lactide) *Biomacromolecules* **2013**, *14*, (2883-2890)

(25) Lin, J.O.; Chen, W.L.; Shen, Z.Q.; Ling, J. Homo- and Block Copolymerizations of ε-Decalactone with L-Lactide Catalyzed by Lanthanum Compounds. *Macromolecules* **2013**, *46*, (7769-7776)

(26) Martello M.T.; Hillmyer M.A. Polylactide-Poly(6-methyl-ε-caprolactone)-Polylactide Thermoplastic Elastomers. *Macromolecules* **2011**, *44*, (8537-8545)

(27) Wanamaker, C.L.; O' Leary, L. E.; Lynd, N. A.; Hillmyer, M. A.; Tolman, W. B. Renewable-resource thermoplastic elastomers based on polylactide and polymenthide. *Biomacromolecules* **2007**, *8*, (3634-3640)

(28) Soetaert, W.; Vandamme, E. The impact of industrial biotechnology. *Biotechnol J* **2006**, *1(7-8)*, (756-769)

(29) Wu, Z.; Wang, Z.; Wang, G.; Tan, T. Improved 1,3-propanediol production by engineering the 2,3-butanediol and formic acid pathways in integrative recombinant Klebsiella pneumoniae.

*J Biotechnol* **2013,** *168(2),* (194-200)

(30) Posada, J.A.; Cardona, C. A.; Higuita, J. C.; Tamayo, J. A.; Pisarenko, Y. A. Design and economic analysis of the technological scheme for 1,3-propanediol production from raw glycerol. *Theor Found Chem Eng* **2013,** *47(3),* (239-253)

(31) Zhu, J.; Thakker, C.; San K.-Y.; Bennett, G. Effect of culture operating conditions on succinate production in a multiphase fed-batch bioreactor using an engineered Escherichia coli strain. *Appl Microbiol Biotechnol* **2011,** *92(3)*, (499-508)

(32) Orjuela A.; Orjuela A.; Lira, C. T.; Miller, D. J. A novel process for recovery of fermentation-derived succinic acid: Process design and economic analysis. *Bioresour Technol.* **2013,** *139, (*235-241).

(33) Yim, H.; Haselbeck, R.; Niu, W.; Pujol-Baxley, C.; Burgard, A.; Boldt, J.; Khandurina, J.; Trawick, J. D.; Osterhout, R. E.; Stephen, R.; Estadilla, J.; Teisan, S.; Schreyer, H. B.; Andrae, S.; Yang, T. H.; Lee, S. Y.; Burk, M. J.; Van Dien, S. Metabolic engineering of Escherichia coli for direct production of 1,4-butanediol. *Nat Chem Biol* **2011,** *7, (*445-452)

(34) Sanna T., Heikki, O. The Current Status and Future Expectations in Industrial Production of Lactic Acid by Lactic Acid Bacteria. **2013,** DOI: 10.5772/51282.

(35) Nakayama A., Kawasake, N.; Arvanitoyannis, I.; Iyoda, J.; Yamamoto, N. Synthesis and Degradability of a Novel Aliphatic Polyester - Poly(β-methyl-δ-valerolactone-co-L-lactide). *Polymer* **1995,** 36, (1295-1301)

(36) Paddon, C.J.; Westfall, P. J.; Pitera, D. J.; Benjamin, K.; Fisher, K.; McPhee, D.; Leavell, M. D.; Tai, A.; Main, A.; Eng, D.; Polichuck, D. R.; Teoh, K. H.; Reed, D. W.; Treynor, R.; Lenihan, J.; Jiang, H.; Fleck, M.; Bajad, S.; Dang, G.; Dengrove, D.; Diola, D.; Dorin, G.; Ellens, K. W.; Fickes, S.; Galazzo, J.; Gaucher, P.; Geistlinger, T.; Hepp, H. M.; horning, T.; Iqbal, T.; Kizer, L.; Lieu, B.; Melis, D.; Moss, N.; Regentin, R.; Secrest, S.; Tsuruta, H.; Vazquez, R.; Westblade, L. F.; Xu, L.; Yu, M.; Zhang, Y.; Zhao, L.; Lievense, J.; Covello, P. S.; Keasling, J. D.; Reiling, K. K.; Renninger, N. S.; Newman, J. D. High-level semi-synthetic production of the potent antimalarial artemisinin. *Nature* **2013,** *496,* (528-532)

(37) Martin V.J.; Pitera, D. D.; Withers, S. t.; Newman, J. D.; Keasling, J. D., Engineering a mevalonate pathway in *Escherichia coli* for production of terpenoids. *Nat Biotechnol* **2003,** *21,* (796-802)

(38) Yang J.; Xian, M.; Su, S.; Zhao, G.; Nie, Q.; Jiang, X.; Zheng, Y.; Liu, W. Enhancing production of bio-isoprene using hybrid MVA pathway and isoprene synthase in *E. coli. PLoS One* **2012,** *7,* (27-34)

(39) Tabata K.; Hashimoto S. Production of mevalonate by a metabolically-engineered *Escherichia coli. Biotechnol Lett* **2004,** *26, (*1487-1491)

(40) Yasmin S.; Alcazar-Fuoli, L.; Gründlinger, M.; Puempel, R.; Cains, T.; Blatzer, M.; Lopez, J. F.; Gimalt, J. O.; Bignell, E.; Haas, H. Mevalonate governs interdependency of ergosterol and siderophore biosyntheses in the fungal pathogen *Aspergillus fumigatus. Proc Natl Acad Sci USA* **2012***, 109,* (E497-504)

(41) Grundlinger, M.; Yasmin, S.; Lechner, B. E.; Geley, S.; Schretti, M.; Hynes, M.; Haas, H., et al. Fungal siderophore biosynthesis is partially localized in peroxisomes. *Mol Microbiol* **2013,** *88, (*862-875)

(42) Hall M.; Stueckler, C.; Hauer, B.; Stuermer, R.; Friedrich, T.; Breuer, M.; Kroutil, W.; Faber, K., Asymmetric Bioreduction of Activated C=C Bonds Using *Zymomonas mobilis* NCR

Enoate Reductase and Old Yellow Enzymes OYE 1–3 from Yeasts. *European J Org Chem* **2008**, *2008*, (1511-1516)

(43) Bougioukou, D.J.; Kille, S.; Taglieber, A.; Reetz, M.T. Directed Evolution of an Enantioselective Enoate-Reductase: Testing the Utility of Iterative Saturation Mutagenesis. *Adv Synth Catal* **2009**, *351*, 3287-3305

(44) Save, M.; Schappacher. M.; Soum, A. Controlled Ring-Opening Polymerization of Lactones and Lactides Initiated by Lanthanum Isopropoxide, 1. General Aspects and Kinetics. *Macromol Chem Phys* **2002**, *203*, 889-899

(45) Martello, M.T.; Burns, A.; Hillmyer, M. A. Bulk Ring-Opening Transesterification Polymerization of the Renewable δ-Decalactone Using an Organocatalyst. *ACS Macro Lett* **2011**, *1*, 131-135

(46) Kiesewetter, M. K.; Scholten, M. D.; Kirn, N.; Weber, R. L.; Hedrick, J. L.; Waymouth, R. M. Cyclic Guanidine Organic Catalysts: What Is Magic About Triazabicyclodecene? *J Org Chem* **2009**, *74*, (9490-9496)

(47) Boesel, L.F.; De Geus, M.; Thöny-Meyer, L. Effect of PLA crystallization on the structure of biomimetic composites of PLA and clay *J. Appl. Polym. Sci.* **2013**, *129*, 1109-1116

# Chapter 4. Aliphatic Polyester Design[§]

Aliphatic polyester block polymers constitute a highly useful and amazingly versatile class of self-assembled materials. Analogous to styrenic block polymers in both design and function, the property profiles of these degradable materials can be precisely tailored by altering the chemical structure of the components. In this chapter the impact of *n*-alkyl substituents on the polymerization thermodynamics and kinetics of substituted δ-valerolactone monomers is examined and critical structure property relationships in the resulting aliphatic polyesters are elucidated. Under bulk room temperature conditions the polymerization rate depends strongly on substituent position and exhibits a more modest dependence on alkyl length (from $-CH_3$ to $-(CH_2)_8CH_3$). The enthalpy and entropy of polymerization are significantly impacted by substituent position, but both are largely insensitive to *n*-alkyl length. Contrariwise, the physical properties of the resulting aliphatic polyesters depend much more on substituent length than on substituent position. Notably, that polymer entanglement molar mass and solubility parameter can be systematically tuned by changing the substituent length. As is discussed herein, these key structure property relationships can be used to inform the design of high performance sustainable materials.

---

## 4.1 Introduction

Few would argue synthetic polymers are indispensible to modern society. These durable and versatile materials are produced on a scale of hundreds of billions of kilograms annually for many diverse applications, including lightweighting transportation, insulating buildings, and packaging food and pharmaceuticals.[1,2] However, the widespread use of non-degradable, petroleum–derived plastics has created a massive waste management problem and left an indelible mark on the environment.[3,4] Increasingly, public awareness of the problem of plastic pollution has prompted municipal bans on, for example, plastic bags and single–use food packaging.[5,6] An important goal of contemporary polymer science is therefore to create renewable, degradable alternatives that can compete with existing polymers in  performance and, perhaps more importantly, cost.

Inspired by the incredible versatility of styrenic ABA triblock polymers, a number of researchers have investigated degradable analogs comprised of poly(lactide) (PLA) as the hard 'A' blocks and an amorphous aliphatic polyester homopolymer. [7,8,9,10,11,12,13,14,15,16,17] or statistical copolymer[18,19] as the soft 'B' block. These all-polyester materials are very attractive from a synthetic perspective, because ring opening transesterification polymerization (ROTEP) is generally very well controlled, the molecular architecture, composition, and molar mass of the block polymer can be easily adjusted to alter the properties of the material.[20] Structural variations in the midblock, such as changes in the substituent size or location, provide another mechanism for tuning the thermal, mechanical, and degradation behavior of the product block polymer.[13,21,22,19]

Although myriad aliphatic lactones with diverse structures have been polymerized, the majority of these monomers have been derived from fossil fuels or from prohibitively expensive natural products.[7,23] Recent advances in synthetic biology have enabled the microbial production of monomers, including lactones, from inexpensive renewable starting materials.[14,24,25,26] It is important, however, to consider whether the potential value of a new polymer justifies the cost and effort of developing an engineered organism. To help establish general design rules for aliphatic polyester block polymers, we examined how changing the position and size of an alkyl substituent influences lactone polymerizability and resultant polyester properties.

The thermodynamic polymerizability of cyclic monomers is strongly related to ring size.[27] The ring opening polymerization of small and medium sized cyclic monomers (3-14 membered rings) is typically enthalpically favored ($\Delta H_p^{\circ} < 0$) but entropically disfavored ($\Delta S_p^{\circ} < 0$). In practical terms, these thermodynamic characteristics can lead to low equilibrium conversions for monomers characterized by low ring strain. Specific to unsubstituted lactones, experimental and computational studies have revealed that ring strain is highest for β-propiolactone, (4 membered ring) and much lower for γ–butyrolactone (5 membered ring) and δ-valerolactone (6 membered ring).[28,29] Indeed, the former is nearly incapable of polymerization under typical conditions.[29,30,31,32] Although thermodynamic parameters have been reported for the polymerization of several substituted δ-valerolactone monomers, the effect of alkyl substituent size and location on the standard state enthalpy ($\Delta H_p^{\circ}$) and entropy ($\Delta S_p^{\circ}$) of polymerization has

114

not been experimentally studied in a systematic manner.[14,30,33,34] Importantly, when both $\Delta H_p^\circ$ and $\Delta S_p^\circ$ are negative (as is generally true for medium-sized lactones), the ratio of the two is proportional to the ceiling temperature ($T_c$). It is worth noting that $T_c$, the temperature above which a monomer will not polymerize at a given concentration in a specific solvent, is catalyst independent.

For prospective new monomers, favorable thermodynamics are absolutely necessary but not wholly sufficient; practically, the polymerization must reach high conversion within an operable time. Thermodynamic and kinetic polymerizability are not inherently linked, and the latter is intrinsically dependent on the catalyst used.[35,36] Multitudinous transition metal, enzymatic, and organic catalysts have been developed for the polymerization of lactones.[37,38,39,40,41] When monomer ceiling temperature is low it is imperative to conduct the polymerization at the lowest temperature and highest monomer concentration practically possible. However, with only few exceptions, kinetic experiments are typically conducted in solution using unsubstituted lactones such as ε-caprolactone or δ-valerolactone.[33,42,43,44,45] The effect of alkyl substituent size and location on bulk polymerization rate has not been systematically studied.

In this chapter, the impact of lactone structure on ROTEP of *n*-alkyl substituted δ–valerolactones is investigated. Using a series of twelve different δ-lactones, shown in Figure 4.1, we systematically analyze how changes in the position and length of a substituent influence both $\Delta H_p^\circ$ and $\Delta S_p^\circ$. With the same set of monomers, we study how monomer structure impacts the bulk polymerization kinetics. By comparing two

different aliphatic polyesters, poly(β-methyl-δ-valerolactone) (Pβ1, referred to in the previous chapter as MVL ) and poly(δ-pentyl-δ-valerolactone) (Pδ5), we also examine how polymer structure can impact key physical characteristics (e.g., solubility parameter ($\delta$) and entanglement molar mass ($M_e$)). We then discuss how degradable alkyl-substituted polyesters such as these can be used to prepare polyester block polymers suitable for a wide range of potential uses. This comprehensive study melds a fundamental study of lactone polymerizability with a detailed analysis of polymer structure–property relationships to establish guidelines for the design of future sustainable materials that are becoming more and more important for environmentally sound product applications.
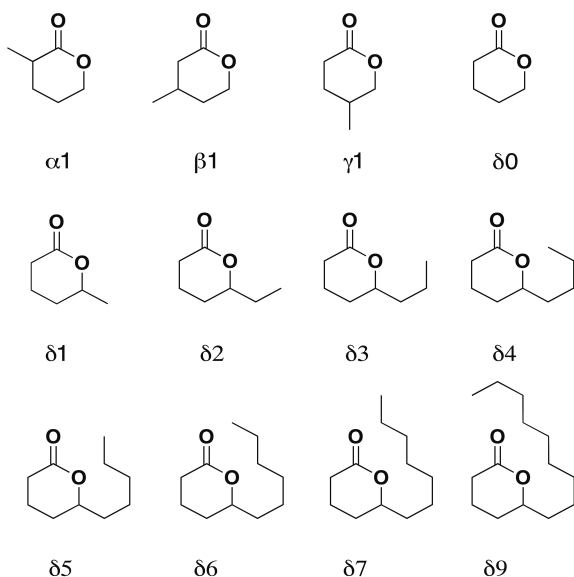


**Figure 4.1**

The *n*-alkyl-δ-valerolactone monomers studied in this work. All compounds studied were racemic.

## 4.2 Results

### 4.2.1 Kinetics of DPP Catalyzed ROTEP

The racemic monomers shown in Figure 4.1 were each polymerized in the bulk at room temperature (~27 °C) with the acid catalyst diphenyl phosphate (DPP). Benzyl alcohol (BnOH) was employed as an initiator to control the molar mass of the polymer. To stop the polymerization, excess triethylamine was added, this deactivates the DPP catalyst but does not appear to have any effect on the resulting polymer structure. Using $^{1}$H NMR spectroscopy of quenched aliquots, the initiation and polymerization reactions were independently monitored; this is shown for the monomer β1 in Figure 4.2 a. For this particular monomer, the initiator is fully consumed within minutes while the polymerization approaches equilibrium in a few hours. The chemical shift of the signal(s) corresponding to the δ methine or methylene proton(s) were slightly different for each of the monomers shown in Figure 4.1. As shown in Appendix C., it was possible to simultaneously monitor both initiation and polymerization by $^{1}$H NMR spectroscopy in all cases. Although individual monomer structure impacts both initiation and polymerization rates, in all cases studied the rate of initiation is at least ten times greater than the rate of propagation.
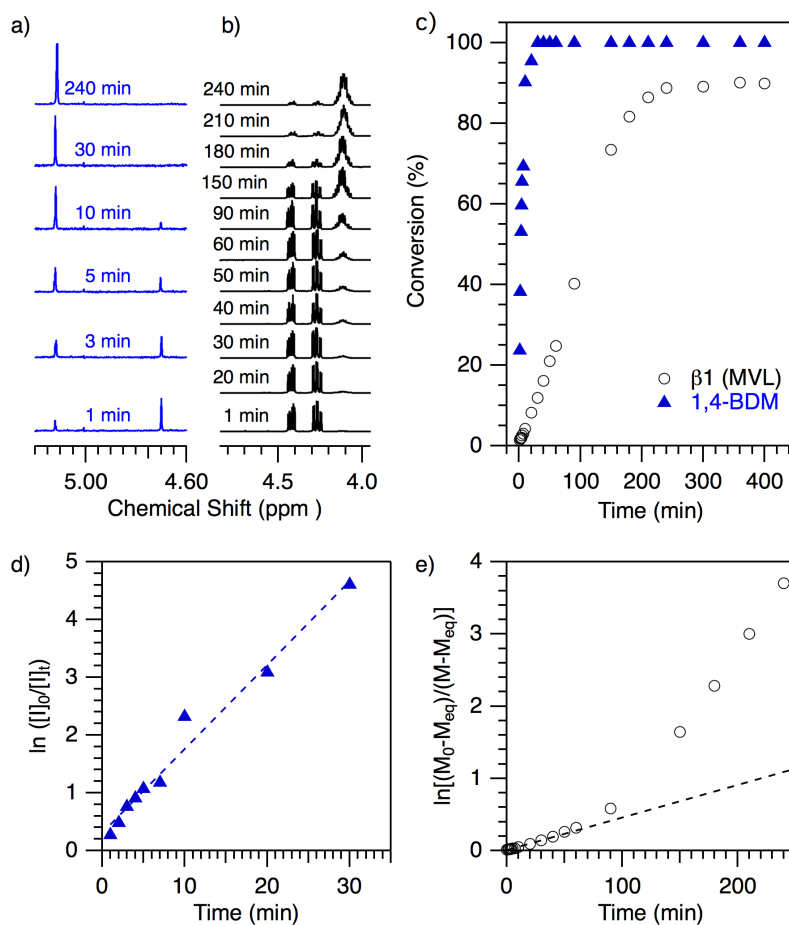
**Figure 4.2.**

Room temperature (~27 °C) polymerization of β1 with $[DPP]_0 = 0.045$ M   $[BnOH]_0 = 0.055$ M, and $[β1]_0 = 9.11$ M.   a) $^1$H NMR spectra overlay showing initiation. The benzyl methylene protons shift from 4.74 ppm in the free alcohol to 5.10 ppm in the initiated polyester. b) $^1$H NMR spectra overlay showing monomer consumption. The δ methylene protons, present at 4.25 ppm and 4.40 ppm in the lactone, coalesce and shift to 4.10 ppm in the polyester. **c)** Plot of the data in 2a and 2b showing BnOH (▲) and β1 (○) conversion over time c) Semi-logarithmic anamorphosis of BnOH consumption reveals initiation is first order in initiator concentration. d) Plot showing deviation from first-order polymerization of β1. Initial conditions were $[DPP]_0 = 0.045$ M $[BnOH]_0 = 0.055$ M, and $[β1]_0 = 9.11$ M.

As shown in Figure 4.2 c, the initiation reaction is first order in initiator. Initial rate studies, summarized in [Appendix C.](#), confirm the polymerization rate increases with both initiator and catalyst concentration. Interestingly, the rate of polymerization does not decrease as monomer is consumed. That is, the slope of monomer conversion over time is linear until the reaction approaches equilibrium. This is atypical for ROTEP polymerizations where, more commonly, the rate of polymerization decreases as the monomer is consumed (recall, for example, Figure 3.4 in the previous chapter). A semi-logarithmic anamorphosis, Figure 4.2 d, of the monomer conversion data in Figure 2 is concave up, indicating the reaction is pseudo-zero in monomer. The pseudo-zero monomer dependence is also evident by the linearity of the data shown in Figure 4.2 c. Although this peculiar observation has not previously reported for DPP catalyzed polymerizations, it has been observed for other cationic polymerizations where the monomer is more basic than the polymer.[46]

### 4.2.2 Impact of Lactone Structure on Polymerization Rate

At fixed initial monomer, catalyst, and initiator concentrations, the rate of polymerization is strongly dependent on monomer structure. Among the methyl–substituted lactones β1 and α1 exhibit polymerization rates that are similar to the unsubstituted parent δ-valerolactone (δ0) under identical conditions. Among the methyl-substituted monomers, δ1 is the slowest to polymerize with an observed polymerization rate constant about an order of magnitude smaller than that of the unsubstituted lactone. It is likely that this effect is partially caused by the relatively low reactivity of the propagating terminal secondary alcohol.[47,48] When the substituent

position is fixed, increasing the *n*-alkyl length decreases the polymerization rate, however it is worth noting that the bulk concentration also decreases as the side chain length is increased. On the basis of prior work, we expect a similar trend to hold, even if the polymerizations are conducted in solvent at fixed concentration.[42] Provided the catalyst and initiator loadings are fixed, the observed time required to reach 50% monomer conversion ($t_{1/2}$) allows a more direct comparison of all monomers; these data are summarized below in Figure 4.3.
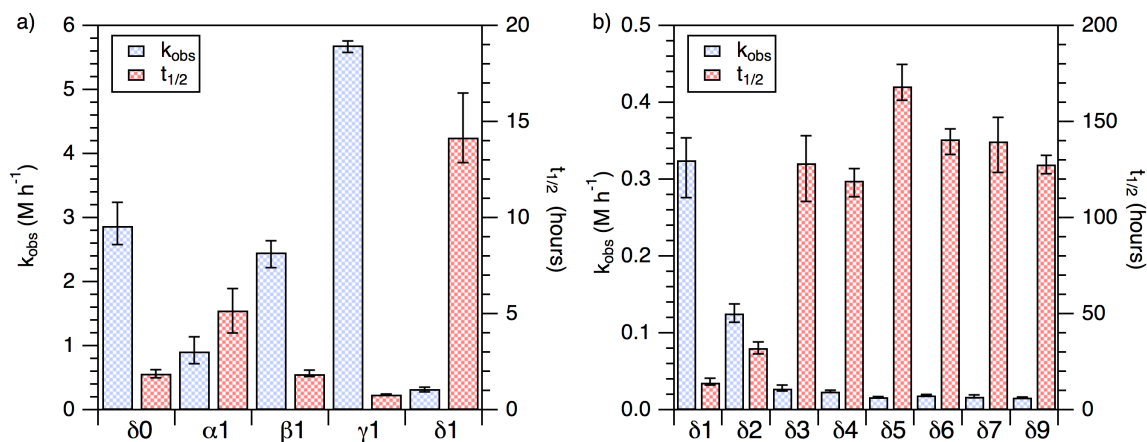


**Figure 4.3**.

Observed rate for the DPP catalyzed bulk polymerization of a) methyl-substituted δ-valerolactone derivatives and b) poly(*n*-alkyl-δ-valerolactones). The column bars and error bars show the median and range for three replicates, respectively. Polymerizations were conducted in the bulk at temperatures of 27 ± 2 °C using initial catalyst and initiator loadings of ($[M]_0$:$[DPP]_0 \approx 200$:1 and $[M]_0$:$[BnOH]_0 \approx 200$:1).

### 4.2.3 Impact of Lactone Structure on Polymerization Thermodynamics

As noted previously, the room temperature kinetics experiments approach an equilibrium monomer concentration ($[M]_{eq}$) over time. The residual monomer concentration is highly dependent on substituent location and reaction temperature.

Whereas the bulk room temperature polymerizations of α1 and of γ1 each approach 98% monomer conversion, the bulk polymerizations of β1 and of δ1 reach lower equilibrium conversion, 91% and 89%, respectively. Within the δ-substituted monomer series, the substituent length influences the equilibrium conversion very little. For all *n*-alkyl substituent lengths the room temperature equilibrium conversion is 89% ± 2%. To learn how monomer structure impacts polymerization thermodynamics, we used the temperature dependence of the equilibrium monomer concentration (i.e., Van't Hoff analysis) to estimate $\Delta H_p^\circ$ and $\Delta S_p^\circ$. This is shown for the methyl–substituted lactones in Figure 4.4, where the residual monomer concentration is fit to Equation 4.1:

$$ln\left(\frac{[M]_{eq}}{[M]_{ss}}\right) = \frac{\Delta H_p^\circ}{RT} - \frac{\Delta S_p^\circ}{R} \qquad\qquad (4.1)$$

In this expression $T$ is the temperature at which the polymerization is conducted and $[M]_{ss}$ is a standard state monomer concentration. A more detailed discussion, and Van't Hoff plots for the other *n*-alkyl substituted monomers are included in Appendix D.
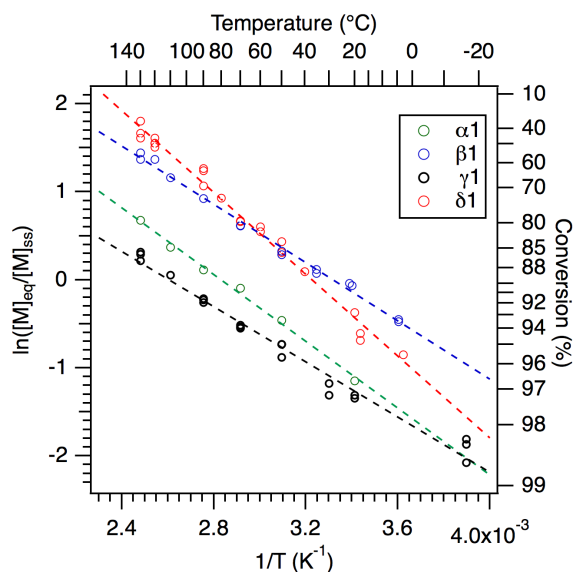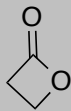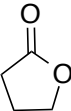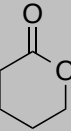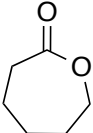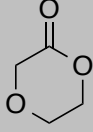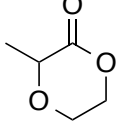
**Figure 4.4.**
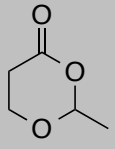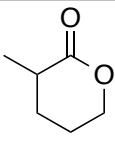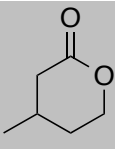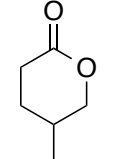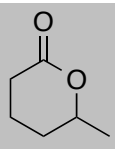
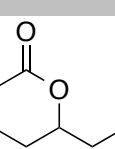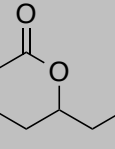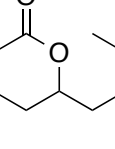Inverse temperature dependence of $\ln([M]_{eq}/[M]_{ss})$ fit to Equation 1. In this work the reference standard state concentration is defined as 1.0 M for convenience. Thermodynamic parameters, $\Delta H_p^{\circ}$ and $\Delta S_p^{\circ}$ for these and other monomers are summarized in Table 4.1. The bulk concentrations for the monomers analyzed in this work are given in Table 4.2.
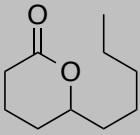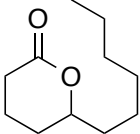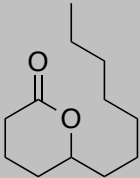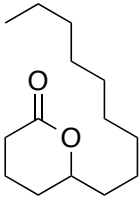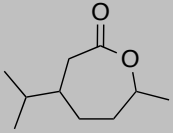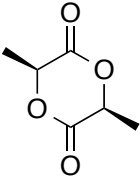
Comparing the methyl–substituted δ–valerolactones, the bulk polymerization of δ1 is both most exothermic and most entropically unfavored.[14,30] When the *n*-alkyl substituent position is fixed, increasing the length appears to have little effect on the thermodynamics of polymerization. These data are shown in Table 4.1. Increasing the substituent position from a methyl to a nonyl group produced minor changes in $\Delta S_p^{\circ}$ and $\Delta H_p^{\circ}$. However, the changes are minimal compared to the impact of substituent position. Indeed, we find that within error, δ7 has the same values of $\Delta S_p^{\circ}$ and $\Delta H_p^{\circ}$ as δ1.

**Table 4.1.**

Summary of the enthalpy ($\Delta H_p^\circ$) and entropy ($\Delta S_p^\circ$) of the ring-opening polymerization of various lactone structures.

| Monomer | $\Delta H_p^\circ$ (kJ mol$^{-1}$) | $\Delta S_p^\circ$ (J mol$^{-1}$ K$^{-1}$) | [a]State | References |
|---|---|---|---|---|
| | −74 | −51 | la | [49],[27] |
| | −75 | −55 | [b]lg | [50],[49] |
| | −83 | −75 | lc | [49] |
| | 5.1 | −29 | la | [50],[51] |
| | −5.4 | −40 | [c]ss | [32] |
| | −8.4 | −14.7 | [a]ss | [30] |
| | −10.5 | −15 | lg | [52], [50],[30] |
| | −27.4 | −65 | lc | [52],[51] |
| | −17.0 | −4 | lg | [50],[30] |
| | −14.0 | −6 | [e]ss | [30] |
| | −13.9 | -10.4 | la | [27] |
| | −14.1 | −26.1 | la | [53] |
| | −15 to −17 | −10 to −13 | la | [54] |
| | −13.8 ± 0.9 | −45 ± 3 | la | [55],[27] |
| | −12.1 ±0.5 | −42 ± 2 | [f]ss | [56] |
| | −9.9 | −39.2 | la | [57] |

| | | | | |
|---|---|---|---|---|
|  | −11.6 | −52 | la | [58] |
|  | −13.0 ± 0.4 | −34 ±1 | la | This work |
|  | −13.8 ± 0.3 | −46 ±1 | la | [14] |
|  | −15.8 ± 0.6 | −45 ± 2 | la | This work |
|  | −13.8 | −41.2 | [g]ss | [30] |
| | −19.3 ± 0.5 | −62 ± 2 | la | This work |
|  | −16.4 ± 0.9 | −55 ± 3 | la | This work |
|  | −18.5 ± 0.4 | −60 ± 1 | la | This work |
|  | −17.0 ± 0.5 | −55 ± 1 | la | This work |

| | | | | |
|---|---|---|---|---|
| | –17.1 ± 0.6 | –54 ± 2 | l a | 33 |
| | –18.0 ± 0.3 | –57± 1 | l a | This work |
| | –18.4 ± 0.5 | –58 ±2 | l a | This work |
| | –18.7 ± 0.4 | –59 ± 1 | l a | This work |
| | –16.8 ± 0.5 | –55 ± 2 | l a | This work |
| | –16.8 | –27.4 | [h]s s | 59 |
| | –22.9 | –25.0 | [i]s s | 60 |
| | –29.1 | –40.7 | l a | 60 |
| | –23.9 | –43.8 | [j]s s | 61 |

[a]State refers to state of monomer and polymer, respectively:  a = amorphous state (bulk polymer melt); g = glass,  l = liquid monomer, s = solution, c = semicrystalline. [b]This sample, reported as highly elastic, is assumed to be amorphous. [c]$CD_2Cl_2$, $[M]_0 = 10$ M, these estimates are likely impacted by the formation of a significant proportion of cyclic species. [d]Toluene/DCM (70:30 v/v), $0.2 < [M]_0 < 0.5$ M [e]Toluene/DCM (70:30 v/v), $[M]_0 = 2.0$ M [f]Tolune, $[M]_0 = 3.0$ M [g]Toluene/DCM (70:30 v/v), $1.8 < [M]0 < 2.0$ M [h]Toluene $[M]_0 = 0.2$ M [i]1,4 dioxane, $[M]_0 = 1.0$ M [j]Toluene, $[M]_0 = 1.0$ M

### 4.2.4 Impact of Polyester Structure on Entanglement Molar Mass

In Chapter 3, the entanglement molar mass of PMVL (refered to in this Chapter as Pβ1) was estimated from the plateau modulus of a high molar mass (~100 kg mol$^{-1}$) sample. The same stradegy was used to estimate the entanglement molar mass of a number of represenative poly($n$-alkyl-δ-valerolactones), as shown below for Pδ5. Whereas estimates of the entanglement molar mass ($M_e$) of Pα1 (7.7 kg mol$^{-1}$) was significantly higher that of PCL (3.0 kg mol$^{-1}$), the other poly(methyl–valerolactones) were all relatively low (4.3, 2.2, and 3.4 kg mol$^{-1}$, for Pβ1, Pγ1, and Pδ1, respectively). When the substituent position is fixed the entanglement molar mass of the polymer increases with substituent length. Pδ5, for example, has an entanglement molar mass (13.5 kg mol$^{-1}$) that is about four times larger than Pδ1.

### 4.2.5 Impact of Polyester Structure on Thermal Properties

Despite the differences in entanglement molar masses, there were negligible differences in the thermal properties of the $n$-alkyl substituted poly(δ-valerolactones) studied. Whereas unubstituted poly(δ-valerolactone) (Pδ0) is semicrystalline ($T_m$ = 55 °C), addition of a methyl substituent is sufficient to disrupt crystallinity in these atactic polymers. Notably, all lactones used in this work are racemic and the DPP catalyst used is not enantioselective. Addition of the methyl group also increases the glass transition temperature ($T_g$) slightly (from –60 °C to –52 °C) as compared to the parent poly(valerolactone). However, as shown in Table 5.2, there is no significant change in the glass transition temperature when the methyl is replaced with longer $n$-alkyl chains. All of the polymers explored in this work have side chains that are incapable of crystallization at temperatures above the $T_g$. These data are summarized in Table 4.2.

**Table 4.2**

Monomer and polymer physical properties.

| Monomer | $^a M_w$ | $[M]_0$ | $^b \rho_{mon.}$ | $^c \rho_{pol.}$ | $^d T_c$ | $^e T_g$ | $^f M_e$ |
|---|---|---|---|---|---|---|---|
| | $(g\ mol^{-1})$ | | $(g\ cm^{-3})$ | $(g\ cm^{-3})$ | (°C) | (°C) | $(kg\ mol^{-1})$ |
| δ0 | 100.1 | 10.79 | 1.08 | 1.10 | | −60 | - |
| α1 | 114.1 | 9.11 | 1.04 | 1.10 | 560 | −51 | 7.7 |
| β1 | 114.1 | 9.11 | 1.04 | 1.10 | 230 | −52 | 4.3 |
| γ1 | 114.1 | 9.11 | 1.04 | 1.10 | 320 | −51 | 2.1 |
| δ1 | 114.1 | 9.11 | 1.04 | 1.10 | 170 | −51 | 3.4 |
| δ2 | 128.2 | 8.03 | 1.03 | 1.05 | 162 | −51 | - |
| δ3 | 142.2 | 6.75 | 0.96 | 1.02 | 150 | −48 | - |
| δ4 | 156.2 | 5.69 | 0.89 | 1.01 | 140 | −50 | - |
| δ5 | 170.2 | 5.58 | 0.95 | 0.97 | 150 | −51 | 13.5 |
| δ6 | 184.3 | 5.26 | 0.97 | 1.02 | 140 | −53 | - |
| δ7 | 198.3 | 4.74 | 0.94 | 0.95 | 130 | −53 | - |
| δ9 | 226.4 | 4.15 | 0.94 | 0.96 | 120 | −54 | - |

[a] Monomer molar mass. [b]Monomer density at room temperature (20 °C). [c]Polymer density at room temperature (20 °C) determined using a density gradient collumn [d]Ceiling temperature for polymerization of bulk monomer. [e]Glass transition temperature determined using Differential Scanning Calorimetry. Data were taken on the second heating ramp at a rate of 5 °C min^{-1}. [f]Entanglement molar mass calculated from plateau modulus determined using dynamic mechanical analysis.

### 4.2.6 Impact of Polyester Structure on Solubility Parameter

Block polymer phase behavior is influenced by a number of factors including the connectivity and volume fractions (*f*) of the constituent blocks, and the segregation strength of the disparate components ($\chi N$). Among these parameters the segment-segment interaction parameter, $\chi$, is a property inherent to a given pair of polymers. The interaction parameter is a measure of chemical incompatablity and generally increases with difference in solubility parameters between the two segments. This can be expressed by Equation 4.2:

$$\chi_{A-B} = \frac{V_{ref}\,(\delta_A - \delta_B)^2}{RT} \tag{4.2}$$

Here we use estimates of $\chi$ and the Hansen solubility parameter of PLA, (19.8 $J^{1/2}$ cm$^{-3/2}$) to calculate the solubility parameters of two different polyester midblocks.[62] Because the solubility parameter is independent of a reference volume, it is a convenient metric for comparing structurally dissimilar polymers. In this work we used the assumption that segregation strength at the lamellar to disorder phase boundary is constant (($\chi N$)$_{ODT}$ = 17.996 for ABA triblocks) to estimate $\chi$ for several compositionally symmetric ABA triblock polymers of different molar masses at the order to disorder transition. N was calculated from the triblock molar mass using a reference volume of 118 Å.[63] The temperature dependence of the segment-segment interaction parameter was fit to Equation 4.3.

$$\chi(T) = \frac{a}{T} + \beta \qquad\qquad\qquad\qquad (4.3)$$

This is shown below for PLA-Pδ5-PLA and PLA-Pβ1-PLA in Figure 4.5. From these estimates of $\chi(T)$ we approximate solubility parameters of $18.4\,J^{1/2}cm^{-3/2}$ and $16.8\,J^{1/2}cm^{-3/2}$ for poly(β1) and poly(δ5), respectively.
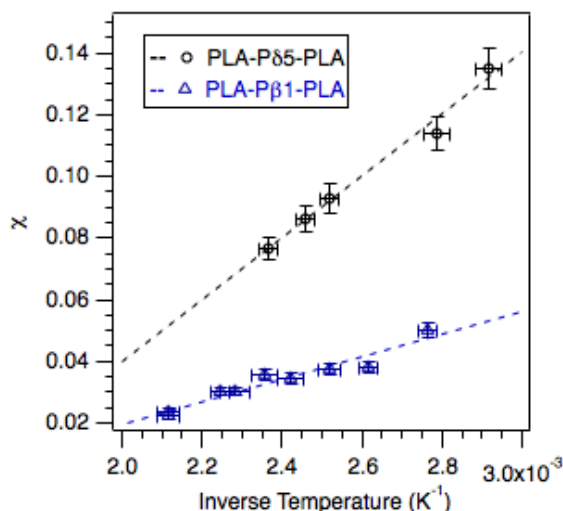


**Figure 4.5.**

Inverse temperature dependence of $\chi_{PLA-P\beta1}$ and $\chi_{PLA-P\delta5}$ fit to Equation 4.3. Molecular characterizations of these samples are given in Section 4.5 of this chapter. N was calculated from the number average molar mass determined by $^1$H NMR spectroscopy using a reference volume of 118 Å$^3$ and room temperature densities of 1.248 g cm$^{-3}$, 1.10 g cm$^{-3}$, and 0.97 g cm$^{-3}$ for PLA, Pβ1, and Pδ5, respectively. The error in $\chi$ is shown as 5% (estimated from the experimental uncertainty in $M_n$). The $T_{ODT}$ values shown are those determined using dynamic mechanical analysis; error was estimated using the range in the $T_{ODT}$ values measured for the same sample using multiple characterization methods (e.g., SAXS, DMA, and DSC).

In Chapter 2 a similar method was used to estimate the solubility paramter of poly(ε-caparolactone) and of poly(ε-cparolactone-co-ε-decalactone). It is gratifying to note here

that the constitutional isomers poly($\beta$1) and poly($\varepsilon$-caprolactone) are characterized by the same solubility parameter ($18.4\,J^{1/2}cm^{-3/2}$).[64] Poly($\delta$5) has more aliphatic content than poly($\beta$1); the solubity parameter of this polymer ($16.8\,J^{1/2}cm^{-3/2}$) is actaully close to that of polyisoprene.[65] On the basis of group contribution estimates, the solubility parameter is expected to continue to decrease as the length of the side chain increases. However, previous work with styrenic block polymers containing poly($n$–alkyl methacrylate) midblocks suggests that the value of the solubility parameter may plateau for longer (n > 10) side chains.[66,67,68]

## 4.3 Discussion

### 4.3.1 Kinetic Considerations

To maximize monomer conversion in the polymerization of low ceiling temperature monomers, it is necessary to conduct the polymerization at the lowest temperature and highest monomer concentration possible. Therefore it is important to select a catalyst robust and fast enough at low temperature to catalyze the polymerization without loss of control. In the bulk at room temperature, the DPP catalyst provides excellent control over polymer molar mass and functionality and typically yields polymers with low dispersity values ($Đ \leq 1.20$). Though the DPP catalyzed polymerization is first order in monomer when conducted in dilute conditions, it is pseudo-zero order when conducted the bulk.[42,69,70] Our results are consistent with an activated monomer mechanism where the rate limiting step is scission of the internal C-O bond of the activated monomer

130

species, as shown below in Figure 4.6. Because the monomer is more basic than the polymer, this mechanism favors polymerization over transesterification.[46]
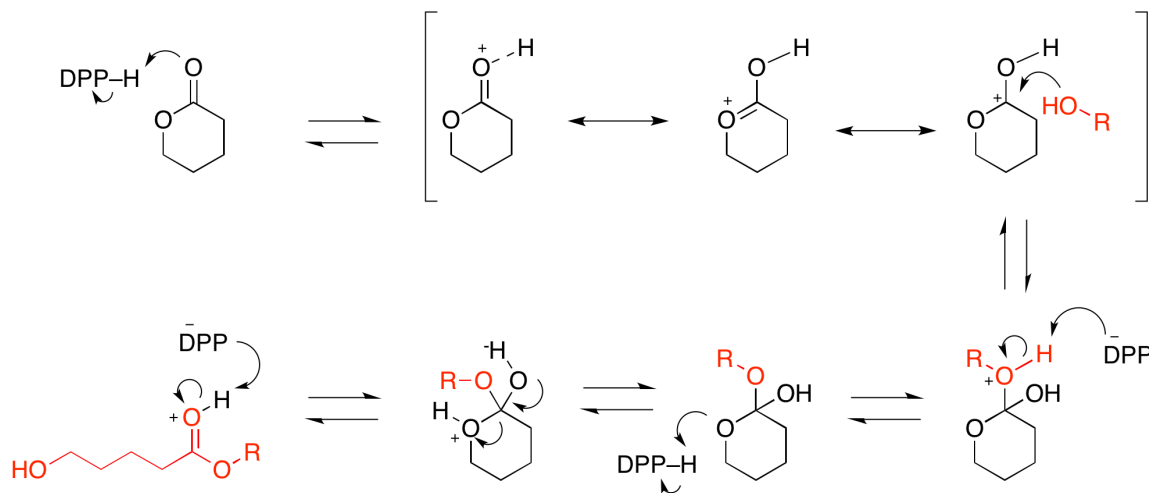


**Figure 4.6.**

Activated monomer mechanism for the acid catalyzed polymerization of diphenyl phosphate. ROH (shown above in red) represents the growing polymer chain.

DPP enables the synthesis of polymers with high control over molar mass and functionality regardless of lactone structure, this is demonstrated in Section 4.5 of this chapter. This high degree of synthetic control is particularly important in the context of block polymers where molecular architecture, composition, and overall molar mass are all intimately linked to the physical properties of the material.[20,63] We found that when the *n*-alkyl substituent is fixed at the δ position, the polymerization rate decreases only slightly as the chain length increases. These results suggest that kinetic considerations do not preclude the polymerization of lactone monomers with arbitrarily long side chains.

### 4.3.2 Thermodynamic Considerations

All of the substituted monomers we analyzed exhibit $\Delta H_p^{\circ}$ values that are significantly more negative than the value reported for of $\delta$–valerolactone ($\delta 0$). Indeed, for several of the $\delta$-substituted monomers the enthalpic drive to polymerize is greater than for the 7-memberd ring monomer $\varepsilon$-caprolactone.[50] We expect that minor structural changes (e.g., addition of an alkyl substituent) have a larger influence on the enthalpy of the lactone than on the corresponding polymer. Because ROTEP is an isodesmic reaction, differences in $\Delta H_p^{\circ}$ generally mirror difference in lactone ring strain. It is likely that the higher ring strain of the *n*-alkly substituted monomers compared to $\delta 0$ is largely due to unfavorable interactions between the alkyl substituents and hydrogen atoms across the ring (transannular strain). In this context it is unsurprising that within the $\delta$-substituted monomer series, $\Delta H_p^{\circ}$ is essentially constant. Owing to the high conformational freedom of *n*–alkanes, transannular ring strain should remain mostly constant as the substituent length increases. Despite possessing lower ring strain, $\delta$-valerolactone actually has a *higher* ceiling temperature than the substituted lactones because its polymerization is less entropically disfavored.

For the substituted monomers studied in this work, polymerization is two to three times more than entropically disfavored the polymerization of $\delta$-valerolactone. For electronic ground state systems, the change in entropy upon polymerization is the sum of translational, rotational, and vibrational components:

$$\Delta S_p^{\circ} = \Delta S_{p\,Trans.}^{\circ} + \Delta S_{p\,Rot.}^{\circ} + \Delta S_{p\,Vib.}^{\circ} \tag{4.4}$$

Gains in rotational and vibrational degrees of freedom can lead to positive changes in $\Delta S^{\circ}_p$ but are only rarely large enough to fully offset the large decrease in translational entropy that usually accompanies polymerization.[71,72] We assume that for $\delta$-lactones addition of an alkyl substituent will have a much smaller impact on $\Delta S^{\circ}_{p\ Vib.}$ and $\Delta S^{\circ}_{p\ Trans.}$ than on $\Delta S^{\circ}_{p\ Rot}$. The addition of a substituent likely decreases the internal rotational freedom a polymer chain relative to its unsubstituted parent. The rotational freedom of a $\delta$-lactone is less influenced by addition of a substituent because, for $\delta$-valerolactone the small cyclic structure largely prohibits internal bond rotation anyway. At fixed ring size therefore, addition of a substituent tends to decrease $\Delta S^{\circ}_{p\ Rot}$ and thus $\Delta S^{\circ}_p$ relative to an unsubstituted monomer of the same ring size because of restricted rotation in the monomer. The end result is that the addition of substituents to $\delta$-valerolactone render the polymerization less thermodynamically favorable.

For the specific case of *n*-alkyl $\delta$–lactones entropy and enthalpy of polymerization are loosely correlated as shown in Figure 4. This enthalply–entropy compensation behavior, while not unprecedented, presents an interesing dichotomy.[73] To maximize thermodynamic polymerizability the substituent should be placed in the position that *minimizes* ring strain (an enthalpic phenomena), in this case the α position. This is because the alpha substituent has the least entropically unfavorable impact on the polymerization. The problem of low ceiling temperature could also be avoided by using a substituted seven-membered lactone (e.g., menthone) because polymerization is less entropically disfavored for monomers with larger ring size.[12,59] We note, however, that

133

in the palette of natural lactones, five and six membered rings are much more prevalent.[74]
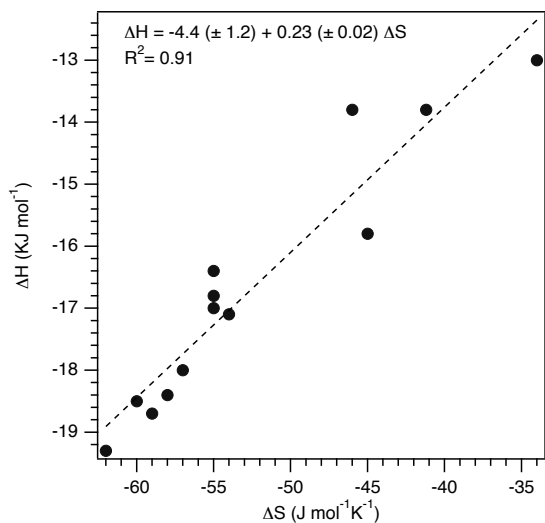


**Figure 4.7**

Apparent correlation between $\Delta H_p^0$ and $\Delta S_p^0$ for *n*-alkyl $\delta$–lactones studied in this work. Unsubstituted VL is not included in this analysis.

### 4.3.3 Polymer Structure-Property Relationships

We have previously demonstrated using block polymers comprised of aliphatic polyesters, e.g. poly(menthide), poly($\varepsilon$-decalactone), and poly(6-methyl-$\varepsilon$-caprolactone), that the addition of bulky substituents can be used to modify the rheological and mechanical properties of the block polymer.[11,13,59] This tuneability is at least partially due to differences in the chain cross-section and entanglement molar mass of the soft segment.[22,75,76] The presence of bulky substituents, however, can also lead to an elevation of the glass transition temperature and a concomitant reduction of the service

temperature of the elastomer.[77] We have shown in this work that by introducing *n*-alkyl substituents of different sizes it is possible to tune entanglement molar mass without significantly elevating the glass transition temperature.[78]

Modulatuion of aliphatic polyester structure can potentially be used as a tool to design degradable block polymer for a range of specific applications. The methyl–substituted polyesters P$\delta$1 and P$\beta$1 for example, are appealing soft blocks for the synthesis of tough plastics and elastomers due to their low entanglement molar masses.[79] The lower modulus of the high entanglement molar mass polymers (e.g., P$\delta$5, poly(menthide), and poly($\varepsilon$-decalactone) makes them attractive for use in pressure sensitive adhesives.[9,80,81,82,83] One can easily draw an analogy between these aliphatic polyesters and the low glass transition temperature polydienes currently used in the manufacture of styrenic thermoplastic elastomers. P$\delta$1, for instance has an entanglement molar mass close to 1,4–poly(isoprene), whereas P$\delta$5 is more similar to that of poly(ethylethylene) or 1,4-*co*-1,2-polybutadiene.[84] The ability to design polymers with tunable entanglement molar masses also has important implications for processing.

As with entanglement molar mass, the solubility parameters of the aliphatic polyester is also inherent to the structure of the lactone monomer. Although the location of the alkyl substituent has very little effect on polymer polarity, increasing alkyl substituent size causes the polymer to become more hydrophobic. This has important implications for the design of polyester block polymers. For example, while the polarity of the midblock segment can obviously determine solvent resistance, it also directly impacts its compatability with formulation additives. The latter can indirectly influence

characteristics like stability, transparency, and optical clarity. A more subtle consideration is the interaction between the two blocks. In general, the larger the difference between the solubility parameters of the hard and soft blocks, the larger the magnitude of the Flory–Huggins interaction parameter, $\chi$. Since in this work the hard block is poly(lactide), at a fixed molar mass, decreasing the polarity of the midblock segment effectively increases the segregation strength of the two blocks.[11,13,64,85,86,87,88,89] This is an important characteristic to consider because it dictates the minimum molar mass required for microphase separation to occur, required for desirable mechanical properties, and it also influences practical processing temperatures.

Our studies on $\delta$-lactone polymerizability suggest to to maximize polymerization rate and improve conversion, it is ideal to select a $\gamma$-substituted monomers. Although a modest ceiling temperature (315 °C in bulk monomer) may, in general, be considered a synthetic inconvenience, it is possible to leverage this characteristic to facilitate recycling.[32] With regards to polymer design, we note that there is no single perfect polymer; instead one focus on matching a material with a specific property profile to the application for which it is best suited. For example, while P$\gamma$1 may be ideal for the synthesis of tough plastics and elastomers, P$\delta$9 may be more suitable for use in pressure sensitive adhesives.

## 4.4 Conclusions

Our results demostrate that it is both thermodynamically and kinetically feasible to polymerize substituted δ-valactones with arbitrarily long *n*-alkyl substituents. We have shown that, by changing the length of the substituent, the entanglement molar mass and solubility parameter can be modulated without impacting the glass transtion temperature. By understanding synthetic limitations and block polymer structure property relationships; we show that aliphatic polyesters block polymers can be designed to mirror the properties of commercially relevant styrenic block polymers. These degradable block polymers, sophisticated materials custom-tailored to meet a specific use, are the environmentally friendly plastics of tomorrow.

## 4.5 Experimental Section

### 4.5.1 Materials

δ-Valerolactone (δ0) (Acros), δ-hexalactone (δ1) (Aldrich), δ-octalactone (δ3) (ACS International), δ-nonalactone (δ4) (Aldrich), δ-decalactone (δ5) (Aldrich), δ-undecalactone (δ6) (Aldrich), δ-dodecalactone (δ7) (Aldrich), and δ-tetradecalactone (δ9) (Aldrich), were purchased, distilled under reduced pressure over calcium hydride, and passed through a column of dry activated alumina without exposing to air. δ-Heptalactone (δ2) (a gift from Vigon International) was also distilled under reduced pressure over calcium hydride. Toluene (Fisher), used for block polymer syntheses was distilled to remove the azeotrope, stirred over calcium hydride for at least 24 hours, then distilled a second time under argon. Monomers and solvents used in polymerizations were degassed using three freeze pump thaw cycles and stored under nitrogen until use. Methyl Iodide (Fisher) and Ti(OiPr)$_4$ (Aldrich) were purchased and used as received.

Tin(II) 2-ethylhexanoate (Aldrich) was distilled (3x) under reduced pressure. 1,4-Benzenedimethanol (Aldrich) and diphenyl phosphate (Acros) were dried under reduced pressure at room temperature for 96 hours. (±)-Lactide, a kind gift from Ortec Inc (Easely, SC), was used as received. Benzyl alcohol (99%, Sigma- Aldrich) was purchased and used without additional purification. 1,5,7-Triazabicyclo[4.4.0]dec-5-ene (Aldrich) was sublimed twice prior to use. All monomers, catalysts, and reagents mentioned previously were stored and handled in a nitrogen-atmosphere glove box.

Solvents, including acetonitrile, chloroform, diethyl ether, dichloromethane, ethyl acetate, hexanes, and methanol were purchased used as received unless otherwise noted. When specified as dry, THF was distilled over sodium/benzophenone. Chloroform noted as dry was washed with water to remove trace ethanol, dried over calcium chloride, and distilled. Dichloromethane specified as dry was stirred over 3 Å molecular sieves, distilled, and sparged with argon.

*n*-Butyl lithium (2.5 M in hexanes, Aldrich) was concentrated under vacuum then used to prepare a 1.1 M solution in dry THF. Diisopropyl amine (Aldrich) was dried over KOH and distilled prior to use. Methyl Iodide (Fisher) 3-methyl-1,5-pentane diol (TCI America), copper chromite (Aldrich), 2-methyl-2-propen-1-ol (Aldrich), but-3-enoic acid (Aldrich), p-toluene sulfonic acid (Aldrich), titatnium (IV) isopropoxide (Aldrich), Grubbs $2^{nd}$ Generation catalyst (Aldrich), palladium on activated carbon (10%, unreduced, Acros), potassium carbonate (Aldrich), piperidine (Aldrich), propionaldehyde (Aldrich), methyl acrylate (Aldrich), glacial acetic acid (Aldrich), sodium borohydride (Fisher), and trifluoroacetic acid (Aldrich) were purchased and used as received.

Glass vials, ampules, pipets, pressure vessels, Teflon caps, and Teflon-coated magnetic stir bars were dried in a 110 °C oven for a minimum of 6 hours prior to use. Pressure vessels, used for polymer and block polymer syntheses, were charged and sealed in a glovebox under nitrogen then quickly removed and placed in a heating bath. Ampules were charged in a glovebox, capped with a septum, removed, and flame sealed under vacuum.

**4.5.2 Synthetic Methods**

All of the monomers and synthetic intermediates synthesized in this work have previously been reported. In each case, the ^{1}H NMR spectrum and GC/MS data of the samples we produced agreed published data. For conveinience each compound is indicated with a reference number, in bold, following its name.

*Synthesis of 3-methyltetrahydro-2H-pyran-2-one* (α1) **1**: 3-methyltetrahydro-2H-pyran-2-one (α-methyl-δ-valerolactone) was synthesized using the method reported by Hoffman *et al.*[90] Freshly distilled diisopropyl amine (122 g, 1.2 mol) was dissolved in dry THF (500 ml) and transferred under via cannula to a 5-necked kettle reactor equipped with gas inlet, mechanical stirrer, thermometer, and rubber septum, an argon atmosphere was maintained in the reactor by means of a bubbler. This solution was cooled to −78 °C, then a cold (−78 °C) solution of *n*-butyl lithium (500 ml, 1.1 mol in THF) was added by cannula. δ-Valerolactone (δ0) (100g, 1.0 mol) was then added slowly by cannula so that the internal temperature of the reactor did not exceed −60 °C. Following complete addition the reactor was stirred at −78 °C for one hour. The reactor was then warmed to −40 °C and MeI (213 g, 1.5 mol) was injected slowly so that the internal temperature did not exceed −30 °C. The reaction was stirred for three hours then warmed to 0 °C and quenched by drop wise addition of saturated aqueous ammonium chloride. The quenched reaction was extracted with diethyl ether, washed sequentially with water, aqueous hydrochloric acid, aqueous sodium thiosulfate, and brine, then dried over magnesium sulfate, filtered, and evaporated to provide viscous orange oil. Distillation of the oil was yielded α-methyl-δ-valerolactone (79 grams, 70% yield). Residual traces of δ-valerolactone and α,α-dimethyl-δ-valerolactone were removed by column

chromatography (silica gel, 2:1 hexanes:ethyl acetate). The α-methyl-δ-valerolactone thus obtained was dried over calcium hydride and distilled over reduced pressure prior to use.

*Synthesis of 4-methyltetrahydro-2H-pyran-2-one* (β1) **2**: 4-methyltetrahydro-2H-pyran-2-one (β1) was synthesized using the method of Longley *et al.*[91] In a 3L round bottomed flask fitted with a thermometer, reflux condenser, and bubbler 3-methyl-1,5-pentanediol (2L, 16.9 moles) and copper chromite (100 grams) were stirred and heated to 200 °C until hydrogen evolution slowed (~12 hours). The reaction was then cooled and β1 (1700 grams, 85% yield) was removed by reduced pressure distillation directly from the reaction flask. The crude product was further purified by repeated distillation from calcium hydride.

*Synthesis of 5-methyltetrahydro-2H-pyran-2-one* (γ1) **5**: Initial attempts to reproduce the purportedly regioselective Baeyer Villiger oxidation of 3-methylcyclopentanone[92] were unsuccessful. Multiple replicates yielded a nearly 1:1 mixture of lactones **2** and **5**. Because we were unable to separate these products by distillation or column chromatography we used two different alternative methods to prepare **5**.

*Synthesis of but-3-enoic acid 2-methyl-allyl ester **3***: But-3-enoic acid 2-methyl-allyl ester was synthesized using the method of Andreana *et al.*[93] A 500 ml round bottomed flask was charged with but-3-enoic acid (24.4 grams, 0.28 mol), 2-methyl-2-propen-1-ol (20.4 grams, 0.28 mol), dry chloroform (0.3 L), and p-toluene sulfonic acid (0.5683 grams, 0.0029 moles). The reaction vessel, equipped an inverse Dean Stark trap and

condenser was heated to reflux and stirred for 24 hours. The product was concentrated under reduced pressure. Column chromatography (silica gel, 70:30 hexanes:ethyl acetate) was used to isolate but-3-enoic acid 2-methyl-allyl ester (37.2 g, 95%).

*Synthesis of 5-methyl-3,6-dihydro-pyran-2-one* **4:** The unsaturated lactone 4 was synthesized using ring closing metathesis of **3**.[93] A 3 L, 3-necked round bottom flask equipped with thermometer, reflux condenser, and gas inlet was charged with dry chloroform (2L), ester 3 (2.00 grams, 0.014 moles), Ti(OiPr)$_4$, (1.06 grams, 0.0043 moles) and refluxed under constant argon flow for 1.5 hours. Grubbs second generation catalyst (0.11 grams, 0.00012 moles) was added and the reaction refluxed for 6 hours. The solution was concentrated under reduced pressure and passed through a thin pad of silica gel to remove residual catalyst. Column chromatography (silica gel, 2:1 hexanes:ethyl acetate) was used to obtain the unsaturated lactone **4** (0.5 grams, 31% yield).

*Synthesis of 5-Methyltetrahydro-2H-pyran-2-one (γ-methyl-δ-valerolactone) (γ1)* **5** *(Method 1):* The unsaturated lactone 4 (3.0 grams, 0.027 mol) was dissolved in dry THF (30 ml). The solution was sparged with argon for 20 minutes, then transferred under argon to a stainless steel reactor containing 0.3 grams dried palladium on charcoal (10 wt% loading). The argon was vented and the vessel charged with 500 psig hydrogen. The reaction was stirred overnight at room temperature then flushed with argon. The solution was filtered and concentrated to obtain crude γ-methyl-δ-valerolactone. The crude product was subjected to column chromatography (silica gel, 4:1 hexanes:ethyl acetate) to yield lactone **5** (2.8 grams, 90% yield). The γ1 thus obtained was dried over calcium hydride and distilled under reduced pressure prior to use.

*Synthesis of methyl 4-formylpentanoate (methyl 4-methyl-5-oxopentanoate)* **6**: Methyl 4-Formylpentanoate was synthesized using the general method of Oikawa *et al.*[94] To a 3L round bottom flask potassium carbonate (100 grams, 0.724 moles) and piperidine (400 ml, 4.05 mol) were added and stirred vigorously. The mixture was cooled to 0 °C and propionaldehyde (145 ml, 2.02 mol) was added dropwise using an addition funnel. The solution was stirred 24 hours then filtered through celite to remove solids, washing with diethyl ether. Residual ether was removed from the filtrate by rotary evaporation and the crude enamine was dissolved in acetonitrile (1 L) the mixture was stirred vigorously at room temperature and methyl acrylate (345 ml, 4.00 mol) was added dropwise. Following addition the reaction was stirred at room temperature 12 hours then refluxed an additional 24 hours. Acetic acid (230 ml, 4.00 mol) and water (1 L) were then added and the solution was refluxed an additional 2 days. The solution was cooled, saturated with sodium chloride, extracted with ether (3 x 1L), washed with aqueous sodium bicarbonate, dried over magnesium sulfate, and concentrated. Column chromatography (silica gel, 3:1 hexanes:ethyl acetate) gave methyl ester **6** in (213 grams, 73 % yield).

*Synthesis of methyl 5-Hydroxy-4-methylpentanoate* **7**: Methyl-5-hydroxy-4-methylpentanoate was synthesized using the method reported by Archibald *et al.*[95] In a typical procedure, methyl 4-formylpentanoate (20.0 grams, 0.138 mol) was dissolved in methanol (100 ml) and cooled to 0 °C. Sodium borohydride (2.5 grams, 0.066 mol) was added slowly over the course of ½ hour. The mixture was stirred at 0 °C and monitored by TLC (3:1 hexanes:ethyl acetate) until the reaction was complete (~1h). The solution was warmed

to room temperature and the solvent was evaporated off under reduced pressure. Water (60 ml) was added to the resulting semisolid residue. The solution was extracted with diethyl ether (3x50 ml), dried with magnesium sulfate, and concentrated to give the crude product (19.2 grams), by ^{1}H NMR an 8:2 mixture of alcohol **7** and lactone **5**. The crude product used without further purification.

*Synthesis of 5-methyltetrahydro-2H-pyran-2-one (γ1)* **5** *Method 2:* The crude alcohol **7** (19.2 g) was dissolved in dichloromethane (500 ml) and trifluoroacetic acid (1 ml, 6 mmol) was added. The resulting solution was stirred for two days at room temperature then 200 ml of saturate aqueous sodium bicarbonate was added and the aqueous layer separated. The aqueous layer was extracted with dichloromethane (2x 150 ml) and the combined organic layers dried over sodium sulfate and concentrated under deduced pressure. Column chromatography (silica gel, 4:1 hexanes:ethyl acetate) was used to isolate the lactone **5** (12.6 g, 0.11 mol, 70% yield from **6**). The γ1 thus obtained was dried over calcium hydride and distilled under reduced pressure prior to use.

*General procedure for the kinetics experiments with δ-valerolactone (VL), a-methyl-δ-valerolactone (a1), β-methyl-δ-valerolactone (β1), γ-methyl-δ-valerolactone (γ1), δ-methyl-δ-valerolactone (δ1), δ-ethyl-δ-valerolactone (δ2), δ-propyl-δ-valerolactone (δ3), δ-butyl-δ-valerolactone (δ4), δ-pentyl-δ-valerolactone (δ5), δ-hexyl-δ-valerolactone (δ6), δ-heptly-δ-valerolactone (δ7), or δ-nonyl-δ-valerolactone (δ9):* Unless otherwise noted room temperature kinetics experiments were carried out in triplicate in a nitrogen atmosphere glove box with a temperature of 27 ± 2 °C. Kinetic experiments were conducted using either benzyl alcohol or 1,4 benzene dimethanol as an initiator and either diphenyl phosphate or 1,5,7-tiazabicyclo[4.4.0]dec-5-ene as a catalyst. The

initiator was first weighed in a tared vial containing a magnetic stir bar then monomer was added and the contents stirred. When the initiator was fully dissolved the solution was transferred to a second massed vial containing catalyst and stirred to initiate the polymerization. Aliquots were removed periodically to monitor reaction progress; monomer and initiator conversion were determined using $^1$H NMR. The TBD and DPP catalyzed reactions were quenched by dissolving the samples in deuterated chloroform containing ~0.5 mg/ml benzoic acid and triethylamine, respectively. The time course of the experiment was largely dependent on the lactone structure. Whereas experiments with α1, β1, γ1, and δ0 monomers were typically compleate within 10 hours, experiments with δ-alkyl substituted monomers approached equilibrium after about 2 to 12 days at room temperature.

*General procedure for the thermodynamics experiments with a-methyl-δ-valerolactone (a1), β-methyl-δ-valerolactone (β1), γ-methyl-δ-valerolactone (γ1), δ-methyl-δ-valerolactone (δ1), δ-ethyl-δ-valerolactone (δ2), δ-propyl-δ-valerolactone (δ3), δ-butyl-δ-valerolactone (δ4), δ-pentyl-δ-valerolactone (δ5), δ-hexyl-δ-valerolactone (δ6), δ-heptly-δ-valerolactone (δ7), or δ-nonyl-δ-valerolactone (δ9):* Unless otherwise noted thermodynamic experiments were conducted in triplicate in vacuum sealed glass ampules. In standard procedure 1,4 benzene dimethanol and diphenyl phosphate were added to a vial under nitrogen and dissolved in lactone monomer (typically ~2 grams). For each experiment the molar ratio of monomer:catalyst:initiator ratio was about 100:1:0.5 The reaction was stirred until both catalyst and initiator were dissolved, then the reaction was divided into 8 to 10 1-ml glass ampules. These ampules were sealed under vacuum and each one was stirred in an oil bath of a different temperature (in the range of 30 °C to 130 °C). An additional vial from each triplicate set was incubated

145

in a refrigerator at -4.5 °C without stirring. These ampules were maintained at their assigned temperatures for a minimum 72 hours (more typically 1-2 weeks for δ-substituted monomers), after this time one ampule the set of triplicates was removed from each temperature, quenched with triethylamine in chloroform, and an aliquot removed for $^1$H NMR analysis. To ensure the polymerizations were at equilibrium the remaining two sets of the triplicate were quenched at later times. Reactions for which the conversion remained constant over the three times tested were taken to be at equilibrium.

*General procedure for the synthesis of difunctional poly(β-methyl-δ-valerolactone) (Pβ1) and poly(δ-pentyl-δ-valerolactone) (Pδ5):* To synthesize a difunctional polyester 1,4 benzene dimethanol was added to the monomer (either β1 or δ5) in a pressure vessel equipped with a magnetic stir bar and stirred until completely dissolved. The ratio of monomer to alcohol was varied to target polymers of different molecular weights. When the initiator was dissolved, diphenyl phosphate (~0.2-2 mol% relative to monomer) or triazabicyclo[4.4.0]dec-5-ene (~0.1 to 1.0 mol% relative to monomer) was added to initiate the polymerization. The reaction was stirred at room temperature until the monomer conversion, determined by $^1$H NMR analysis of a quenched aliquot, approached equilibrium. The reaction time was dependent upon the monomer used, the molar mass targeted, and the catalyst loading. The reaction was quenched by the addition of 5 equivalents, relative to catalyst, of triethylamine. The quenched polymer was diluted with chloroform, precipitated in cold methanol and dried for a minimum of 24 hours at room temperature in a vacuum oven.

*General procedure for the synthesis of triblock polymers:* A difunctional telechelic macroinitiator (either P(β1) or P(δ5)) and (±)-lactide were dissolved in toluene (100 ml) in a pressure vessel. The contents were stirred until fully dissolved then Sn(Oct)$_2$ (~0.1 mol%) was added. The pressure vessel was capped and the pressure vessel stirred in a 110 °C oil bath for 1-2 hours. After this time the reaction was removed to cool to room temperature. The block polymer was diluted with chloroform, precipitated in cold methanol and dried for a minimum of 24 hours at room temperature in a vacuum oven.

*Example Synthesis of poly(δ-decalactone), Pδ1 (4.7):* In a nitrogen atmosphere glove box 1,4 benzene dimethanol (1.3957 grams, 0.0101mol) and δ-decalactone (δ5) (50.0 ml, 0.280 mol) were added to a 150 ml pressure vessel. The contents were stirred until the initator was fully dissolved then triazabicyclo[4.4.0]dec-5-ene (0.2678, 0.00192 mol) was added. The solution was stirred for 20 hours then quenched with benzoic acid, diluted in chloroform, and precipitated in methanol. ^{1}H NMR (500 MHz, CHLOROFORM-*d*) δ(ppm): 0.91-0.80 (m, 88 H, -CH$_3$) 1.20 – 1.34 (m, 172 H) 1.47-1.67 (m, 171) 2.24-2.39 (m, 56 H, C=O-**CH$_2$**CH$_2$CH$_2$CH(CH$_2$CH$_2$CH$_2$CH$_2$CH$_3$)O-), 3.63-3.54 (m, 2H, -**CH$_2$**OH), 4.80-4.93 (m, 1H, 26 H, C=O-CH$_2$CH$_2$CH$_2$C**H**(CH$_2$CH$_2$CH$_2$CH$_2$CH$_3$)O-), 5.15-5.06 (s, 4H, Ar-CH$_2$-OR), 7.32-7.36 (s, 4H, Ar-H)

*Example Synthesis of poly(lactide)-poly(δ-decalactone)-poly(lactide), Pδ5 (10.5, 0.51):* In a nitrogen atmosphere glove box, Pδ5 (4.7) (10.0 grams, 0.952 mmol) and (±)-lactide (0.09119 grams, 0.0912 mol) were dissolved in toluene (100 ml) in a 150 ml pressure vessel. The contents were stirred until fully dissolved then Sn(Oct)$_2$ (26.8 mg, 0.066 mmol) was

added. The solution was stirred for 2 hours then cooled, diluted in chloroform, and precipitated in methanol. $^1$H NMR (500 MHz, CHLOROFORM-$d$) $\delta$(ppm): 0.80-.091 (m, 85 H, -CH$_3$) 1.16 – 1.33 (m, 176) 1.42-1.68 (m, 462 H) 2.22-2.37 (m, 56 H), 4.44-3.28 (m, 2H, C**H**CH$_3$OH), 4.80-4.92 (m, 27 H, C=O CH$_2$CH$_2$CH$_2$C**H**(CH$_2$CH$_2$CH$_2$CH$_2$CH$_3$)O-) 5.11-5.09 (s, 4H, Ar-**CH$_2$**-OR) 5.25-5.11 (m, 83H, -OC=O-C**H**(CH$_3$)-O-) 7.32-7.36 (s, 4H, Ar-**H**)

### 4.5.3 Characterization Methods

General characterization and instrumental methods used for this work are provided in Appendix A. The molecular characteristics of polymer samples described in this chapter are given in the tables below.

*Determination of T$_{ODT}$ values from Differential Scanning Calorimetry*

The T$_{ODT}$ values for the three lowest mass samples L$\delta$5L samples were observed as exotherms in the first heating ramp (Figure 4.13). Data shown are from the first heating ramp (10 °C min$^{-1}$). The T$_{ODT}$ of the PLA-P$\beta$1 -PLA samples and of the two highest molar mass PLA-P$\delta$1-PLA samples and could not be reliably identified using this method.

### 4.5.4 Summary of Polymer Samples Discussed

**Table 4.3.**

**Telechelic Pδ5 diol macroinitiatiors**

| Sample | [a]$M_{N\ (NMR)}$ (kg mol$^{-1}$) | [b]Đ | [c]$T_g$ (°C) |
|---|---|---|---|
| Pδ5 (4.7) | 4.7 | 1.03 | −56 |
| Pδ5 (5.4) | 5.4 | 1.03 | −56 |
| Pδ5 (6.8) | 6.8 | 1.05 | −55 |
| Pδ5 (7.3) | 7.3 | 1.03 | −55 |
| Pδ5 (8.1) | 8.1 | 1.06 | −54 |

[a]Molar mass determined by $^1$H NMR spectroscopy using benzylic methylene protons a an internal standard. [b]Dispersity determined by MALLS-SEC. [c]Determined by Differential Scanning Calorimetry of δ5 midblock.

**Table 4.4.**

**PLA-δ5-PLA Triblocks**

| Sample | $^a M_N$ (kg mol$^{-1}$) | $^b Đ$ | $^c T_g$ (°C) | $^c T_g$ (°C) | $^d T_{ODT}$ (°C) | $^e T_{ODT}$ (°C) | $^f T_{ODT}$ (°C) | $^g d$ (nm) | $^g$Morp. |
|---|---|---|---|---|---|---|---|---|---|
| PLA-δ5- PLA (10.5, 0.51) | 10.5 | 1.04 | −44 | 28 | 70 | 77 | 72 | 11.7 | Lam. |
| PLA-δ5- PLA (12.4, 0.50) | 12.4 | 1.04 | −45 | 30 | 86 | 92 | 84 | 13.3 | Lam. |
| PLA-δ5- PLA (15.2, 0.51) | 15.2 | 1.05 | −46 | 33 | 123 | 129 | 124 | 13.8 | Lam. |
| PLA-δ5- PLA (16.3, 0.51) | 16.3 | 1.18 | −46 | 35 | 134 | - | 132 | 14.6 | Lam. |
| PLA-δ5- PLA (18.5, 0.50) | 18.5 | 1.03 | −45 | 40 | 150 | - | 150 | 15.1 | Lam. |

[a]Molar mass determined by $^1$H NMR spectroscopy using benzene dimethanol aromatic protons as an internal standard. [b]Dispersity determined by MALLS-SEC. [c]Determined by Differential Scanning Calorimetry. Data were taken on the second heating ramp at a rate of 5 °C min$^{-1}$. [d]Determined using dynamic mechanical analysis. The $T_{ODT}$ is defined as the onset of the precipitous drop in G' on heating at a rate of 1 °C min$^{-1}$. Experiments were conducted at 2% strain with a frequency of 1 rad s$^{-1}$. [e]Determined using Differential Scanning Calorimetry. [f]Determined using variable temperature SAXS, $T_{ODT}$ is defined as the onset of the precipitous drop in intensity of $q^*$ upon heating. [g]Primary domain spacing and morphology was determined using room temperature SAXS.

**Table 4.5.**

**Telechelic Pβ1 diol macroinitiatiors**

| Sample | $^a M_N$ (NMR) (kg mol$^{-1}$) | $^b M_w$ (SEC) (kg mol$^{-1}$) | $^b Đ$ | $^c T_g$ (°C) |
|---|---|---|---|---|
| Pβ1 (14.1) | 18.9 (*11.1) | 14.1 | 1.04 | −52 |
| Pβ1 (18.5) | 18.5 | 18.5 | 1.05 | −51 |
| Pβ1 (19.9) | 18.7 | 19.9 | 1.06 | −53 |
| Pβ1 (22.2) | 21.1 | 22.2 | 1.06 | −52 |
| Pβ1 (24.7) | 22.3 | 24.7 | 1.07 | −53 |
| Pβ1 (29.8) | 28.0 | 29.8 | 1.06 | −56 |

[a]Molar mass determined by $^1$H NMR spectroscopy using benzylic methylene protons a an internal standard (*determined using end group methylene protons as the internal standard). [b]Determined by MALLS-SEC with a dn/dc = 0.0625 ml g$^{-1}$. [c]Determined by Differential Scanning Calorimetry of midblock. Data were taken on the second heating ramp at a rate of 5 °C min$^{-1}$.

**Table 4.6**

**PLA-β1-PLA Triblocks**

| [a]Sample | [b]Đ | [c]$T_g$ (°C) | [c]$T_g$ (°C) | [c]$T_m$ (°C) | [d]$T_{ODT}$ (°C) | [e]d (nm) | [e]Morp. |
|---|---|---|---|---|---|---|---|
| PLA-β1-PLA (32.5, 0.53) | 1.14 | −47 | 30 | - | 89 | 26 | [f]Dis. |
| PLA-β1-PLA (38.7, 0.49) | 1.18 | −47 | 28 | - | 109 | 21 | Lam. |
| PLA-β1-PLA (39.9, 0.47) | 1.10 | −46 | 44 | - | 124 | 31 | Cyl. |
| PLA-β1-PLA (43.6, 0.46) | 1.18 | −47 | 38 | - | 140 | 34 | Cyl. |
| PLA-β1-PLA (50.5, 0.48) | 1.10 | −47 | 46 | - | 172 | 32 | Cyl. |
| PLA-β1-PLA (67.9, 0.53) | 1.09 | −48 | 48 | - | 200 | 29 | Lam. |
| PLLA-β1-PLLA (41.9, 0.44) | 1.09 | −47 | - | 146 | 151 | 29 | [g]Dis. Cyl. |
| PLLA-β1-PLLA (50.5, 0.48) | 1.11 | −44 | 50 | [i]129 | 170 | 32 | [g]Dis. Lam. |
| PLLA-β1-PLLA (64.4, 0.51) | 1.10 | −49 | 49 | 160 | 200 | 29 31 | [g]Dis. Lam. |

[a]Molar mass was calculated from the midblock molar mass, determined using MALLS-SEC and the triblock composition, determined by ^{1}H NMR spectroscopy. [b]Determined by MALLS-SEC of triblock. [c]Determined by Differential Scanning Calorimetry. Data were taken on the second cycle at a heating rate of 5 °C min^{-1}. [d]Determined using dynamic mechanical analysis. The $T_{ODT}$ is defined as the onset of the precipitous drop in G' on heating at a rate of 1 °C min^{-1}. Experiments were conducted at 2% strain with a frequency of 1 rad s[-1]. [e]Primary domain spacing and morphology was determined using room temperature SAXS. Samples were annealed at 100 °C for at least 12 hours prior to cooling to room temperature. [f]The sample was annealed above its $T_{ODT}$ and appears to be microphase separated but not well ordered. [g]Annealed samples are disordered in the semicrystalline state. When melted and annealed below the $T_{ODT}$ (at 120 °C) the samples adopt the indicated morphology prior to crystallization.
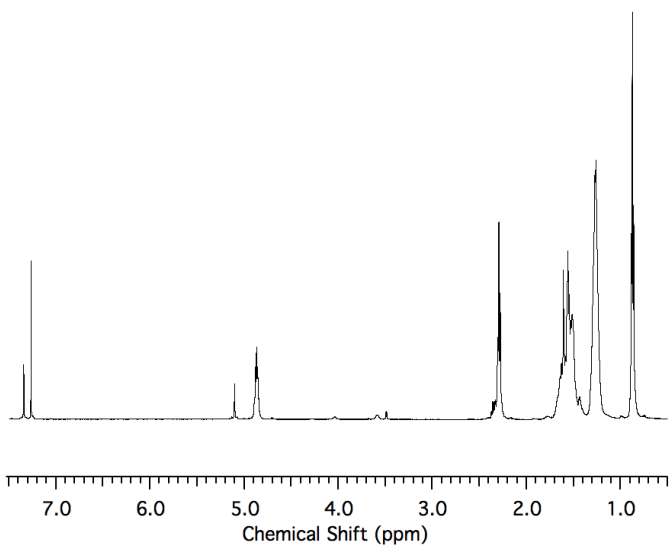
**Figure 4.8**

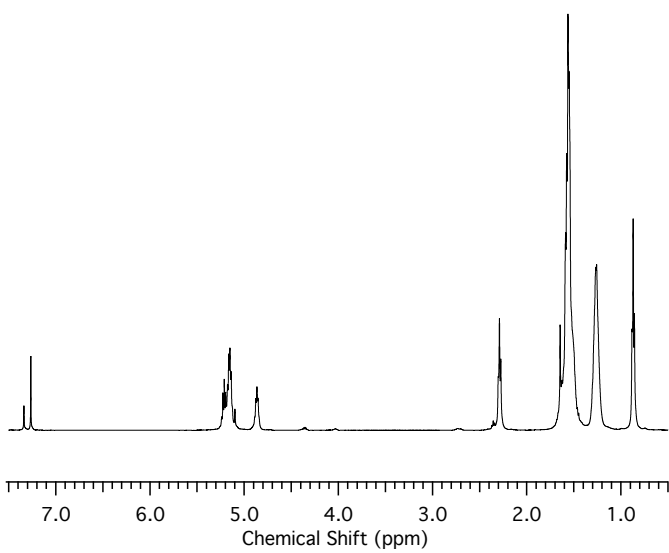$^{1}$H NMR spectrum of representative of P85 (4.7 kg mol$^{-1}$) in CDCl$_3$.



**Figure 4.9**

$^{1}$H NMR spectrum of representative PLA-85-PLA triblock, L85L (10.5, 0.51) in CDCl$_3$.
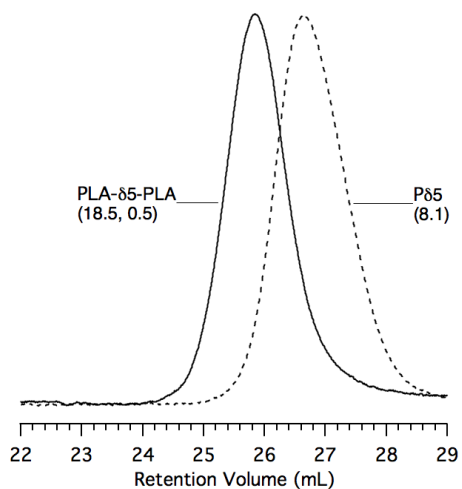
**Figure 4.10**

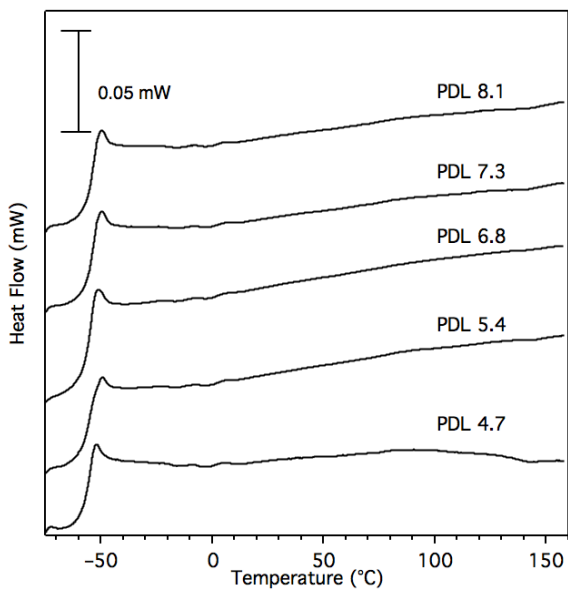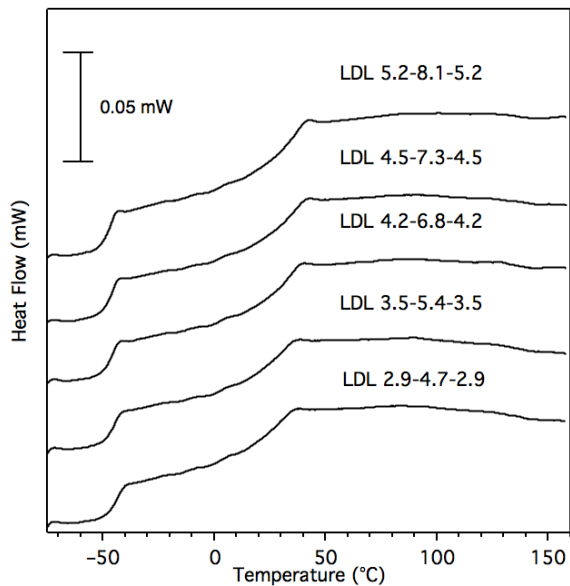SEC overlay of Pδ5 (8.1), and PLA-δ5-PLA (18.5, 0.5).



**Figure 4.11**

Thermograms of Pδ5 midblocks. To ensure consistent thermal history the samples was first heated to 100 °C (rate of 5 °C min$^{-1}$) and cooled at the same rate. Data shown are from the second heating ramp (5 °C min$^{-1}$).
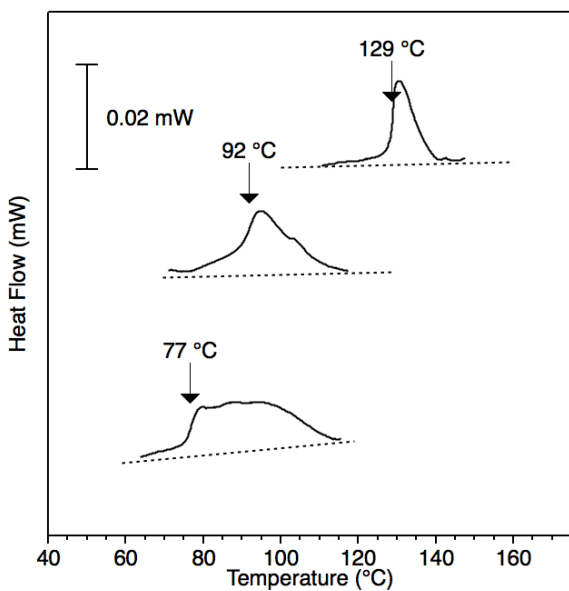
153

**Figure 4.12**

Thermograms of L-δ5-L triblocks. To ensure consistent thermal history the samples was first heated to 100 °C (rate of 5 °C min$^{-1}$) and cooled at the same rate. Data shown are from the second heating ramp (5 °C min$^{-1}$).



**Figure 4.13**

Differential thermograms of L-δ5-L triblocks showing $T_{ODT}$ values of select Lδ5L triblocks. Data shown are from the first heating ramp (10 °C min$^{-1}$). The $T_{ODT}$ is defined as the inflection point found by taking the maximum of the derivative of heat flow with respect to temperature.
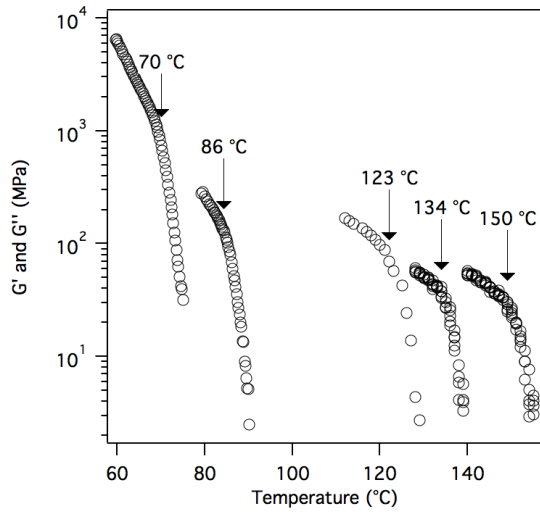
154

**Figure 4.14**

Dynamic mechanical analysis of PLA-**δ5**-PLA triblocks. The $T_{ODT}$ is defined as the onset of the precipitous drop in G' upon heating at a rate of 1 °C min$^{-1}$. Experiments were conducted at 2% strain with a frequency of 1 rad s$^{-1}$.
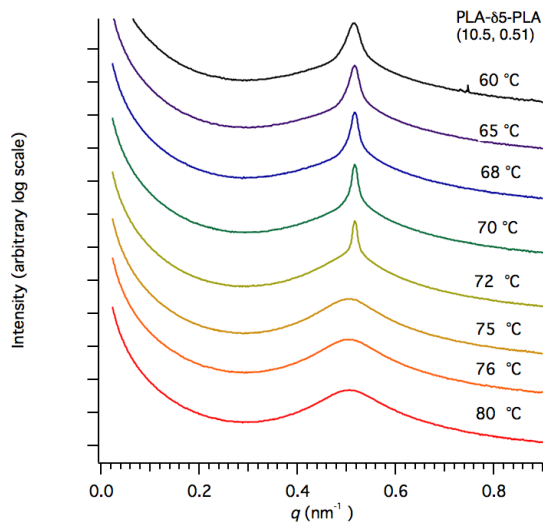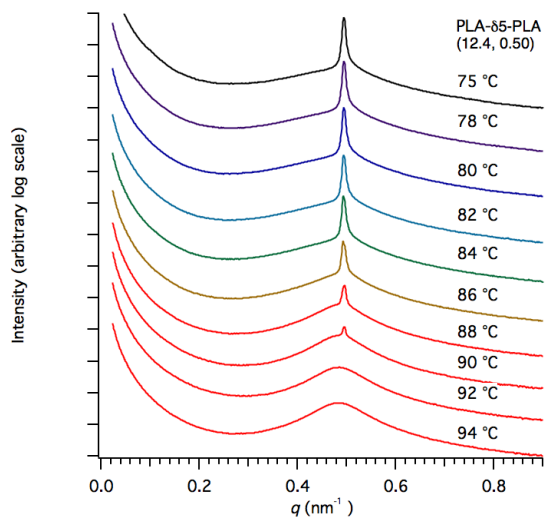


**Figure 4.15**

Variable temperature 1D SAXS of PLA-δ5-PLA (10.5, 0.51) upon heating through the $T_{ODT}$. Samples were heated above the $T_{ODT}$, and annealed for 12 hours at 65 °C prior to analysis. The sample was heated to the indicated temperature and annealed 2 minutes prior to data collection.

**Figure 4.16**

Variable temperature 1D SAXS of PLA-δ5-PLA (12.4, 0.50) upon heating through the $T_{ODT}$. Samples were heated above the $T_{ODT}$, and annealed for 12 hours at 65 °C prior to analysis. The sample was heated to the indicated temperature and annealed 2 minutes prior to data collection.
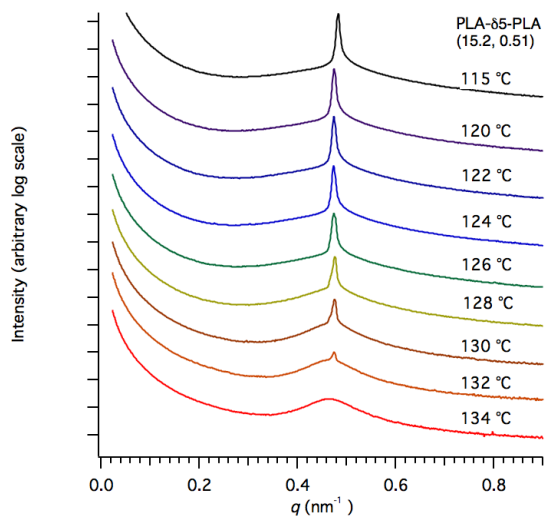


**Figure 4.17**

Variable temperature 1D SAXS of PLA-δ5-PLA (15.2, 0.51) upon heating through the $T_{ODT}$. Samples were heated above the $T_{ODT}$, and annealed for 12 hours at 65 °C prior to analysis. The sample was heated to the indicated temperature and annealed 2 minutes prior to data collection.

**Figure 4.18**

Variable temperature 1D SAXS of PLA-δ5-PLA (16.3, 0.51) upon heating through the $T_{ODT}$. Samples were heated above the $T_{ODT}$, and annealed for 12 hours at 65 °C prior to analysis. The sample was heated to the indicated temperature and annealed 2 minutes prior to data collection.
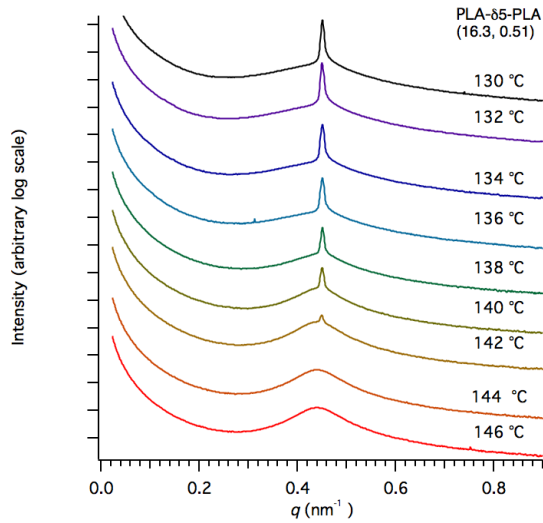


**Figure 4.19**

Variable temperature 1D SAXS of PLA-δ5-PLA. Sample Lδ5L (18.5, 0.50) upon heating through the $T_{ODT}$. Samples were heated above the $T_{ODT}$, and annealed for 12 hours at 65 °C prior to analysis. The sample was heated to the indicated temperature and annealed 2 minutes prior to data collection.
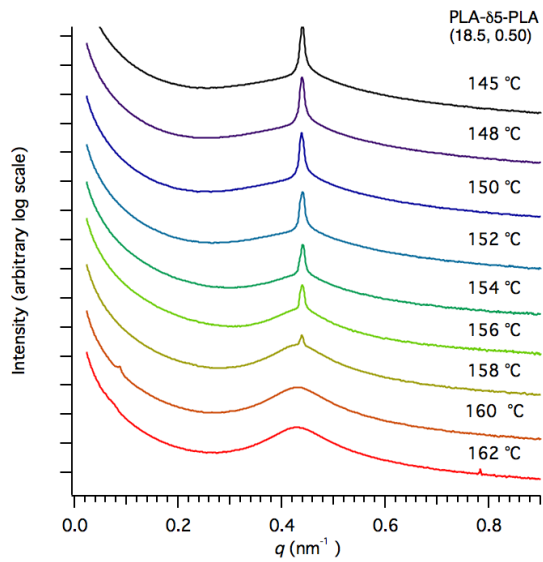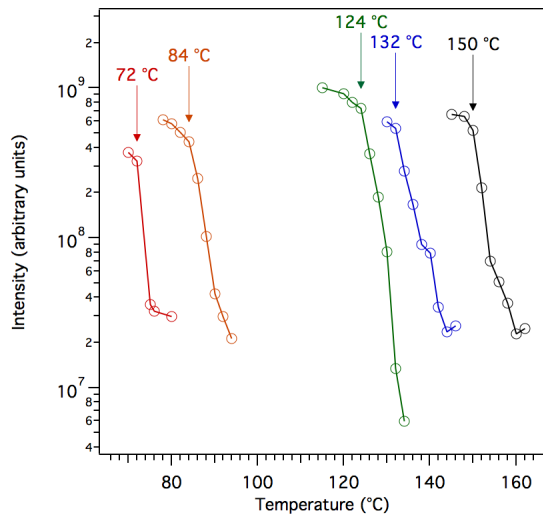
**Figure 4.20**

Temperature dependence of scattering intensity of $q^*$ for the PLA-P85-PLA triblocks shown in Figures S41-S35. For each sample the $T_{ODT}$ (marked with arrow) was taken as the onset of the precipitous drop in intensity.
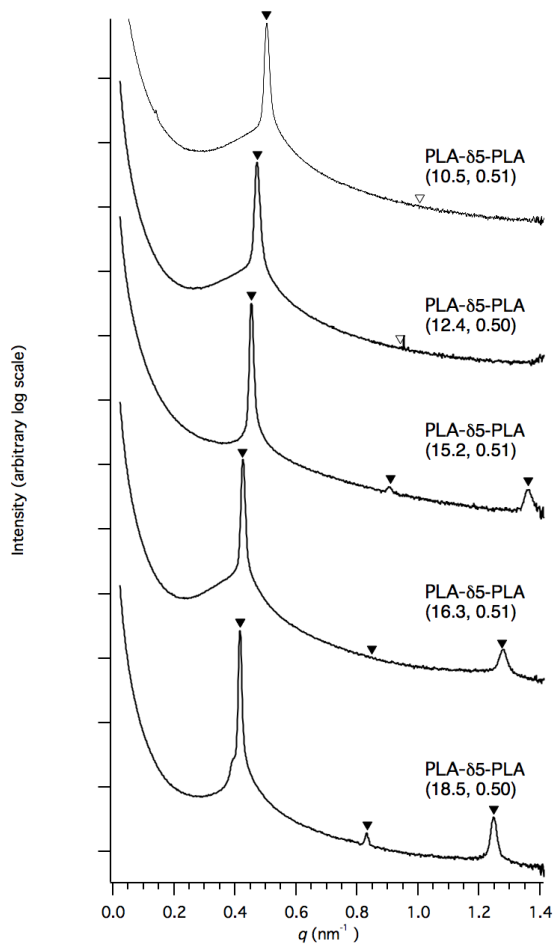
**Figure 4.21**

Room temperature SAXS spectra of PLA-PδS-PLA triblocks. Samples were heated above the $T_{ODT}$, cooled, and annealed for 2 days at 65 °C prior to analysis. The principle peaks are marked with (▼). Calculated reflections for anticipated lamellar morphologies are also marked with (▼) and (▽) denoting reflections that are present, and absent respectively.

159
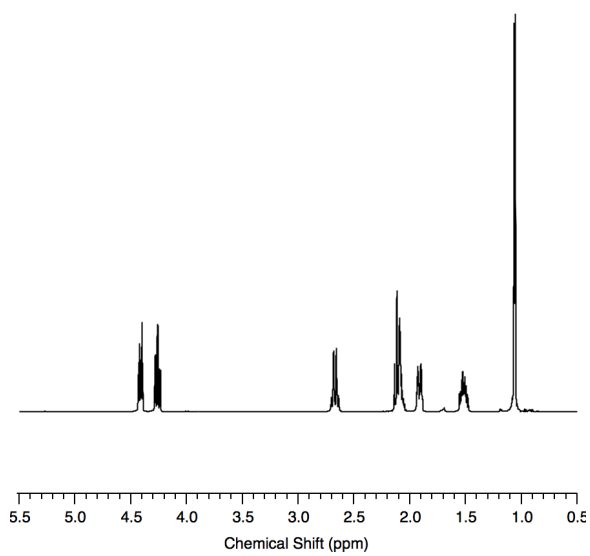
**Figure 4.22**

$^1$H NMR spectrum of β1 in CDCl$_3$.
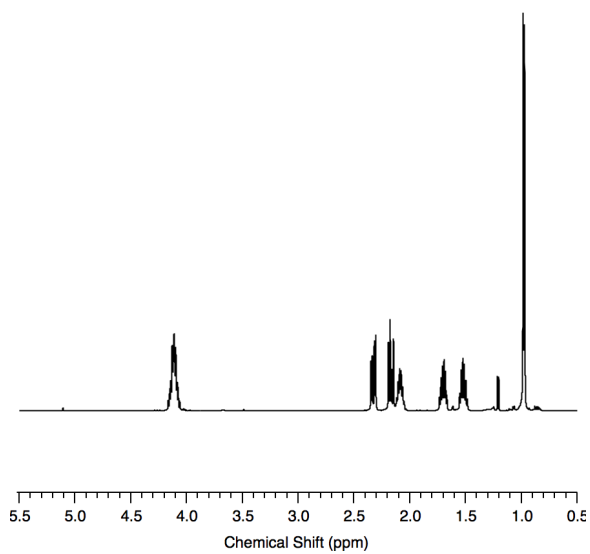


**Figure 4.23**

$^1$H NMR spectrum of Pβ1 (29.8) diol in CDCl$_3$.

160
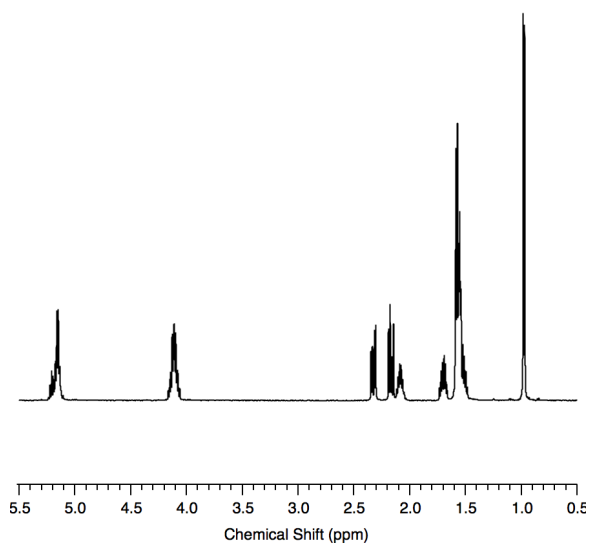
**Figure 4.24**

$^1$H NMR spectrum of PLA-β1-PLA (67.9, 0.53) triblock in CDCl$_3$.
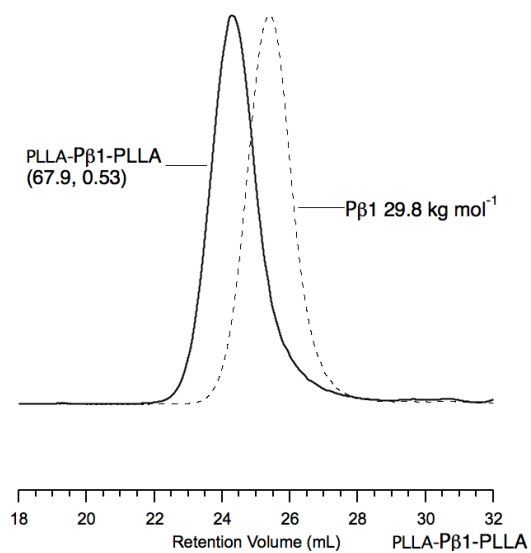


**Figure 4.25**

SEC overlay of Pβ1 (29.8) telechelic prepolymer and and PLA- Pβ1-PLA triblock (67.9, 0.51).
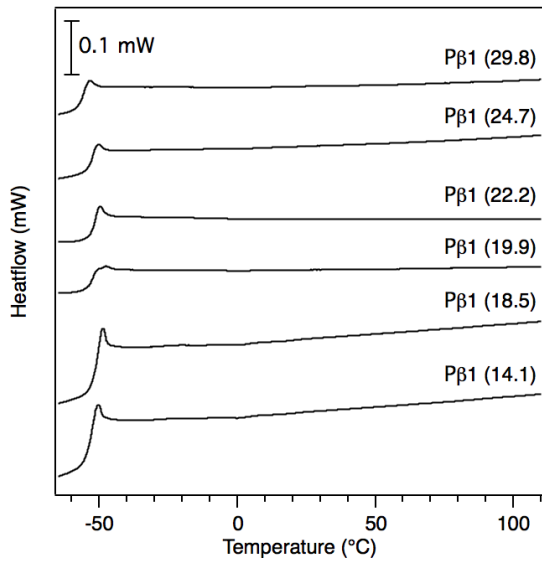
**Figure 4.26**

Differential thermograms of Pβ1 midblocks. To ensure consistent thermal history the samples was first heated to 100 °C (rate of 5 °C min$^{-1}$) and cooled at the same rate. Data shown are from the second heating ramp (5 °C min$^{-1}$).
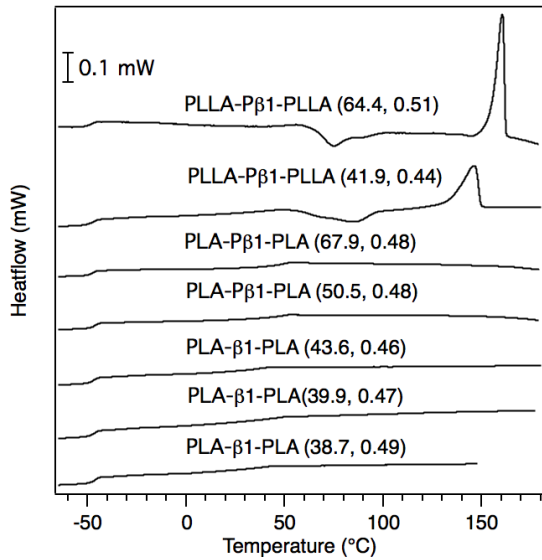


**Figure 4.27**

Differential thermograms of L-β1-L triblocks. To ensure consistent thermal history the samples was first heated to 100 °C (rate of 5 °C min$^{-1}$) and cooled at the same rate. Data shown are from the second heating ramp (5 °C min$^{-1}$).

162
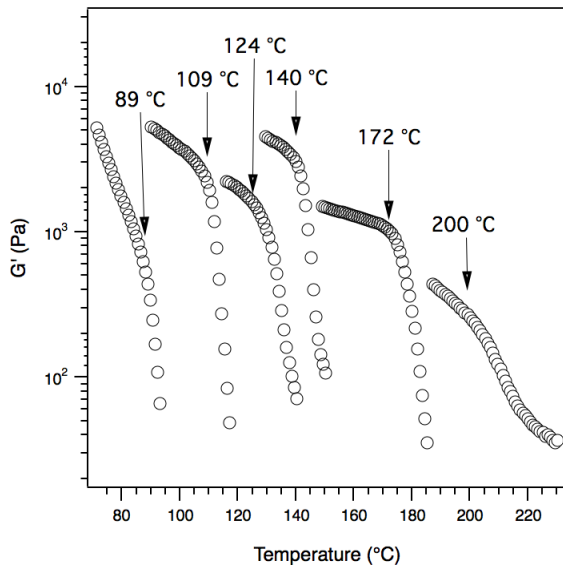
**Figure 4.28**

Dynamic mechanical analysis of PLA-**β1**-PLA triblocks. The $T_{ODT}$ values were defined as the onset of the precipitous drop in G' on heating at a rate of 1 °C min$^{-1}$. Experiments were conducted at 2% strain with a frequency of 1 rad s$^{-1}$.
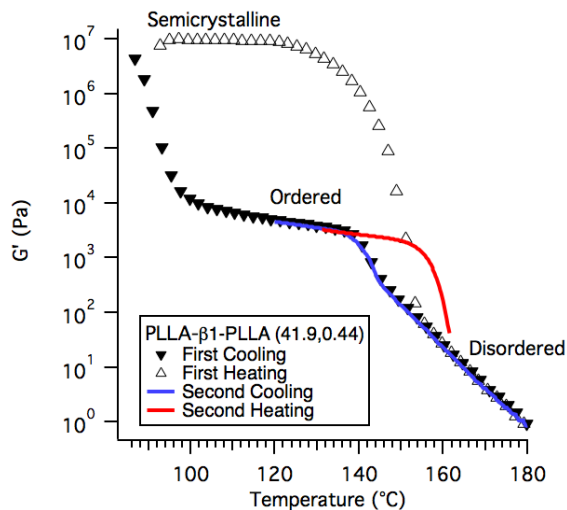


**Figure 4.29**

Dynamic mechanical analysis of semicrystalline triblock PLLA-**β1**-PLLA (41.9, 0.44). In the first cycle the sample was cooled from the melt (180 °C) at a rate of 1 °C min$^{-1}$ through ordering and crystallization transitions, the sample was then heated to 180 °C to a disordered melt. On the second cycle the polymer was cooled to reorder then reheated without allowing the polymer to crystallize. A similar method was used to estimate the $T_{ODT}$ values of other semicrytalline polymers.

163
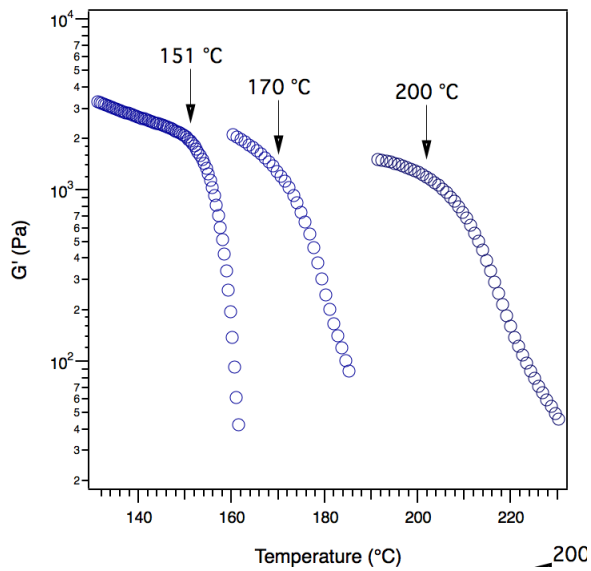
**Figure 4.30**

Dynamic mechanical analysis of PLLA-**β1**-PLLA triblocks. The $T_{ODT}$ values were defined as the onset of the precipitous drop in G' on second heating cycle at a rate of 1 °C min$^{-1}$. Experiments were conducted at 2% strain with a frequency of 1 rad s$^{-1}$.
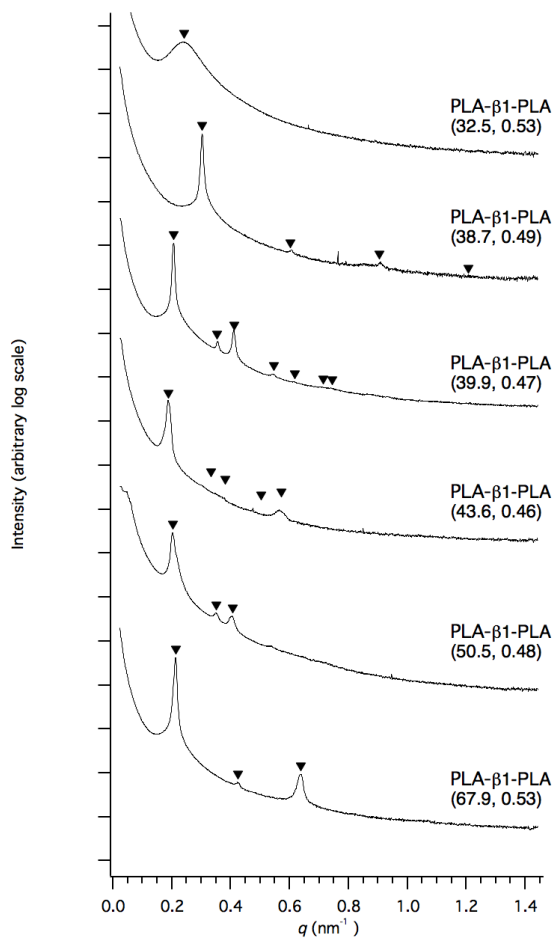
**Figure 4.31**

Room temperature SAXS of PLA-β1-PLA triblocks. Samples were heated above the $T_{ODT}$, cooled, and annealed for 2 days at 100 °C prior to analysis. The principle peaks are marked with (▼). Calculated reflections for anticipated lamellar or hexagonally close packed cylindrical morphologies are also marked with (▼).
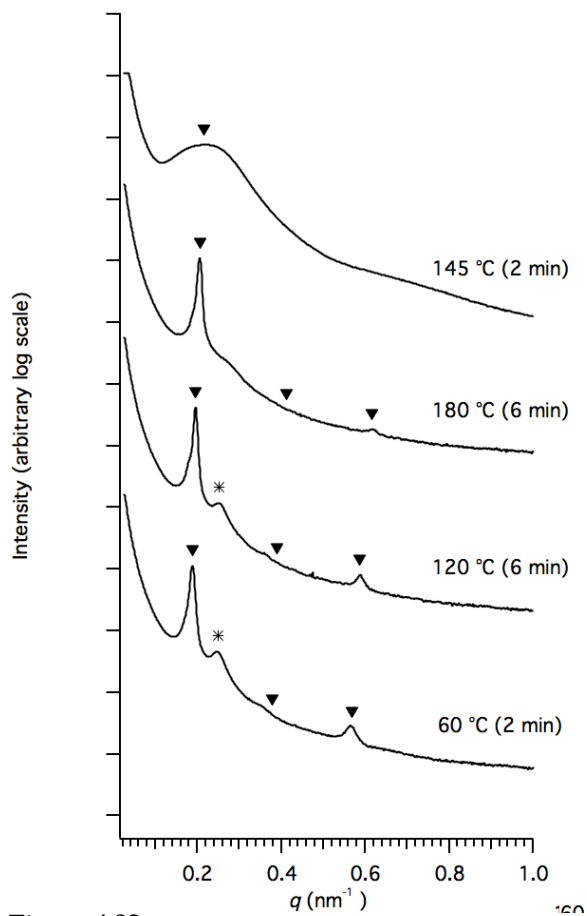
**Figure 4.32**

Variable temperature SAXS of PLLA-β1-PLLA (64.4, 0.51). The sample, disordered and semicrystalline at 145 °C, was melted by heating to 180 °C. When annealed above the crystallization temperature at the annealing times and temperatures indicated this sample adopted an ordered lamellar morphology. Calculated reflections for anticipated lamellar morphologies are marked with (▼). Upon cooling a broad peak (marked with *) emerges near the primary peak, perhaps due to incipient crystallization of the PLLA domains.

## 4.6 References

(1) Andrady, A. L.; Neal, M. A., Applications and societal benefits of plastics. *Philosophical Transactions B* **2009**, *364,* (1977-1984)

(2) PlasticsEurope Plastics–the Facts 2014-2015 **http://www.plasticseurope.org/** (Accessed December 21, 2015)

(3) Thompson, R. C.; Swan, S. H.; Moore, C. J.; vom Sall, F. S. Our plastic age *Phil. Trans. R. Soc. B* **2009**, *364,* (1973-1976)

(4) Corcoran, P. L., Moore, C. J., Jazvac, K. *GSA Today* An anthropogenic marker horizon in the future rock record. **2014**, *24,* (4-8)

(5) Romer, J.R., Tamminen, L. M. Plastic Bag Reduction Ordinances: New York City's Proposed Charge on All Carryout Bags as a Model for U.S. Cities *Tulane Environmental Law Journal* **2014**, *27,* (237-275)

(6) Romer, J.R. The Evolution of SF's Plastic Bag Ban *Golden Gate University Environmental Law Journal* **2007**, *439,* (439-465)

(7) Tsui, A.; Wright, Z. C.; Frank, C. W. Biodegradable Polyesters from Renewable Resources *Annu. Rev. Chem. Biomol. Eng.* **2013**, *4,* (143-170)

(8) Dijkstra, P. J.; Zhong, Z.; Wim, M.; Feijen, S.; Feijen, J. Chapter 16 Controlled Synthesis of Biodegradable Poly(ester)s in *Biorelated Polymers: Sustainable Polymer Science and Technology Springer Science,* Chiellini, E.; Gil, H.; Brauneeg, G., Buchert, J.; Gatenholm, P., van der Zee, Maarten; Ed. New York, **2001**, (179-194)

(9) Wanamaker, C. L.; Tolman, W. B.; Hillmyer, M. A. Hydrolytic Degradation Behavior of a Renewable Thermoplastic Elastomer *Biomacromolecules* **2009**, *10,* (443-448)

(10) Wanamaker, C. L.; O'Leary, L. E.; Lynd, N. A.; Hillmyer, M. A.; Tolman, W. B. Renewable-Resource Thermoplastic Elastomers Based on Polylactide and Polymenthide *Biomacromolecules* **2007**, *8,* (3634-3640)

(11) Martello, M. T.; Hillmyer, M. A. Polylactide-Poly(6-methyl-ε-caprolactone)-Polylactide Thermoplastic Elastomers *Macromolecules* **2011**, *44,* (8537-8545)

(12) Lin, J. O.; Chen, W.; Shen, Z.; Ling, J. Homo- and Block Copolymerizations of ε-Decalactone with L-Lactide Catalyzed by Lanthanum Compounds. *Macromolecules* **2013**, *46,* (7769–7776)

(13) Martello, M. T.; Hillmyer, M. A.; Schneiderman, D. K. Synthesis and Melt Processing of Sustainable Poly(ε-decalactone)-block-Poly(lactide) Multiblock Thermoplastic Elastomers *ACS Sustainable Chemistry and Engineering* **2014**, *2,* (2519-2526)

(14) Xiong, M.; Schneiderman, D. K.; Bates, F. S.; Hillmyer, M. A.; Zhang, K. The production of mechanically tunable block polymers from sugar *PNAS* **2014**, *23,* (8357-8362)

(15) MacDonald, J. P.; Parker, M. P.; Greenland, B. W.; Hermida–Merino, D.; Hamley, I. W.; Schaver, M. P. Tuning thermal properties and microphase separation in aliphatic polyester ABA copolyesters *Polymer Chemistry* **2015**, *6,* (1445-1453)

(16) Olsén, P., Borke, T.; Odelius, K., and Albertsson, A.-C. ε-Decalactone: A Thermoresilient and Toughening Comonomer to Poly(L-lactide) *Biomacromolecules* **2013**, *14,* (2883-2890)

(17) Ryner, M.; Albertsson, A.-C. Resorbable and Highly Elastic Block Copolymers from 1,5-Dioxepan-2-one and L-Lactide with Controlled Tensile Properties and Hydrophilicity *Biomacromolecules* **2002,** *3,* (601-608)

(18) Schneiderman, D. K.; Hill, E. M.; Martello, M. T.; Hillmyer, M. A. Poly(lactide)-*block*-poly(ε-caprolactone-*co*-ε-decalactone)-block-poly(lactide) copolymer elastomers *Polym. Chem.* **2015,** *6,* (3641-3651)

(19) Andronova, N.; Albertsson, A.-C. Resilient Bioresorbable Copolymers Based on Trimethylene Carbonate L-Lactide, and 1,5-Dioxepan-2-one *Biomacromolecules* **2006,** *7,* (1489-1495)

(20) Hillmyer, M.A.; Tolman, W.B. Aliphatic polyester block polymers: renewable, degradable, and sustainable *Accounts of Chemical Research* **2014,** *47,* (2390-2396)

(21) Pitt, C. G.; Gratzl, M. M.; Kimmel, G. L.; Surles, J.; Schindler, A. Aliphatic Polyesters II. The Degradation of Poly (D,L-lactide), Poly (ε-caprolactone), and Their Copolymers in Vivo *Biomaterials* **1981,** 2, (215-220)

(22) Tong, J.-D.; Jerôme, R. Dependence of the Ultimate Tensile Strength of Thermoplastic Elastomers of the Triblock Type on the Molecular Weight between Chain Entanglements of the Central Block. *Macromolecules* **2000,** *33,* (1479–1481)

(23) Yao, K.; Tang, C. Controlled Polymerization of Next-Generation Renewable Monomers and Beyond *Macromolecules* **2013,** *46,* (1689-1712)

(24) Lu, W.; Ness, J. E.; Xie, W.; Zhang, X.; Minshull, J.; Gross, R. A. Biosynthesis of Monomers for Plastics from Renwable Oils *JACS* **2010,** *132,* (15451-15455)

(25) Beller, H. R.; Lee, T. S.; Katz, L. Natural products as biofuels and bio–based chemicals: fatty acids and isopreneoids *Natural Product Reports* **2015,** *32,* (1508–1526)

(26) Jambunathan, P.; Zhang, K. Combining biological and chemical approaches for green synthesis of chemicals *Current Opinion in Chemical Engineering* **2015,** *10,* (35-41)

(27) Duda, A.; Kowalski, A.; Libiszowski, J.; Penczek, S. Thermodynamic and Kinetic Polymerizability of Cyclic Esters *Macromol. Symp.* **2005,** *224,* (71-83)

(28) Leitão, M. L.; Pilcher, G.; Meng-Yan, Y., Brown, J. M.; Conn, A. D. Enthalpies of combustion of γ-butyrolactone γ-valerolactone, and δ-valerolactone *J. Chem. Thermodynamics* **1990,** *22,* (885-891)

(29) Alemán, C.; Betran, O.; Casanovas, J.; Houk, K.N., Hall, H. K. Jr. Thermodynamic Control of the Polymerizability of Five-, Six, and Seven-Membered Lactones *Journal of Organic Chemistry* **2009,** *74,* (6237-6244)

(30) Save, M.; Schappacher, M.; Soum, A. Controlled Ring–Opening Polymerization of Lactones and Lactides Initiated by Lanthanum Isopropoxide, 1 General Aspects and Kinetics *Macromol. Chem. Phys.* **2002,** *203,* (889-899)

(31) Houk, K.N.; Jabbari, A.; Hall, H. K., Jr.; Alemán, C. Why δ-Valerolactone and γ-Butyrolactone Does Not *Journal of Organic Chemistry* **2008,** *73,* (2674-2678)

(32) Hong, M.; Chen, E. Completely recyclable biopolymers with linear and cyclic topologies via ring-opening polymerization of γ-butyrolactone *Nature Chemistry* **2015,** *8,* (42-49)

168

(33) Martello, M. T.; Burns, A.; Hillmyer, M. Bulk Ring-Opening Transesterification Polymerization of the Renewable δ-Decalactone Using an Organocatalyst *ACS Macro. Lett.* **2012**, *1,* (131-135)

(34) Olsén, P.; Odelius, K.; Albertsson, A.-C. Thermodynamic Presynthetic Considerations for Ring-Opening Polymerization *Biomacromolecules* Article ASAP **2016**, *17,* (699-709)

(35) Duda, A.; Kowalski, A.; Penczek, S. Uyama, H; Kobayashi, S. Kinetics of the Ring-Opening Polymerization of 6-, 7-, 9-, 12-, 13-, 16-, and 17-Membered Lactones. Comparison of Chemical and Enzymatic Polymerizations *Macromolecules* **2002**, *35,* (4266-4270)

(36) van der Mee, L; Helmich, F.; de Bruijn, R.; Vekemans, J. A. J. M.; Palamans, A. R. A.; Meijer, E. W. Investigation of Lipase-Catalyzed Ring-Opening Polymerizations of Lactones with Various Ring Sizes: Kinetic Evaluation *Macromolecules* **2006**, *39,* (5021-5027)

(37) Labet, M.; Thielemans, W. Synthesis of polycaprolactone: a review. *Chem. Soc. Rev.* **2009**, *38,* (3484-38504)

(38) Albertsson, A.-C.; Srivastava, R. K. Recent developments in enzyme-catalyzed ring-opening polymerization *Advanced Drug Delivery Reviews* **2008**, *60,* (1077-1093)

(39) Kamber, N. E.; Jeong, W.; Waymouth, R. M.; Pratt, R. C.; Lohmeijer, B. G. G.; Hedrick, J. L. Organocatalytic Ring-Opening Polymerization *Chem. Rev.* **2007**, *107,* (5813-5840)

(40) Lohmeijer, B. G. G.; Pratt, R. C.; Leibfarth, F.; Logan, J. W.; Long, D. A.; Dove, A. P.; Nederberg, F.; Choi, J.; Wade, C.; Waymonth, R. M.; Hedrick, J. L. Guanidine and Amidine Organocatalysts for Ring-Opening Polymerization of Cyclic Esters *Macromolecules* **2006**, *39,* (8574-8583)

(41) Kiesewetter, M. K.; Shin, E. J.; Hedrick, J. L.; Waymonth, R. M. Organocatalysis: Opportunities and Challenges for Polymer Synthesis *Macromolecules* **2010**, *43,* (2093-2107)

(42) Zhao, J.; Hadjichristidis, N. Polymerization of 5-alkyl-δ-Lactones catalyzed by diphenyl phosphate and their sequential organocatalytic polymerization with monosubstituted epoxides *Polymer. Chem.* **2015**, *6,* (2659-2668)

(43) Makiguchi, K.; Kikuchi, S.; Yanai, K.; Ogasawara, Y.; Sato, S.; Satoh, T.; Kakuchi, T. Diphenyl Phosphate/4– Dimethylaminopyridine as an Efficient Binary Organocatalyst System for Controlled/Living Ring–Opening Polymerization of L–Lactide Leading to Diblock and End–Functionalized Poly(L–Lactide)s *Journal of Polymer Science A: Polymer Chemistry* **2014**, *52,* (1047-1054)

(44) Miranda, M. O.; DePorre, Y.; Vasquez-Lima, H.; Johnson, M. A.; Marell, D. J.; Cramer, C. J.; Tolman, W. B.; Understanding the Mechanism of Polymerization of ε-Caprolactone Catalyzed by Aluminum Salen Complexes *Inorganic Chemistry* **2013**, *52,* (13692-13701)

(45) Marlier, E. E.; Macaranas, J. A.; Marell, D. J.; Dunbar, C. R.; Johnson, M. A>; DePorre, Y.' Miranda, M. O.; Neisen, B. D.; Cramer, C. J.; Hillmyer, M. A.; Tolman, W. B. *ACS Catalysis* **2016**, *6,* (1215-1224)

(46) Baśko, M; and Kubisa, P. Cationic Copolymerization of ε–Caprolactone and L,L–Lactide by an Activated Monomer Mechanism *Journal of Polymer Science: Part A: Polymer Chemistry* **2006**, *44,* (7071-7081)

(47) Küllmer, K.; Kikuchi, H.; Uyama, H.; Kobayashi, S. Lipase-catalyzed ring-opening polymerization of α-methyl-δ-valerolactone and α-methyl-ε-caprolactone *Macromol. Rapid Commun.* **1998**, *19,* (127-130)

(48) Kikuchi, H.; Uyama, H.; Kobayashi, S. Lipase-Catalyzed Ring-Opening Polymerization of Substituted Lactones *Polymer Journal* **2002**, *11,* (835-840)

(49) Yevstroprov, A. A. Lebedev, B.V.; Kulagina, T.G.; Lyudvig, Ye. B.; Belenkaya, B.G., The thermodynamic properties of β-propiolactone, its polymer, and its polymerization in the 0-400 K range *Polym. Sci.* USSR, **1979**, *21,* (2249-2256)

(50) Lebedev, B.V. Estropov, A.A. Thermodynamics of the Polymerization of Lactones *Dokl. Phys. Chem.* **1982**, *264,* (334)

(51) Duda, A.; Kowalski, A. Thermodynamica and Kinetics of Ring-Opening Polymerization in *Handbook of Ring-Opening Polymerization* Dubois, P.; Coulembier, O.; Raquez, J.-M. Wiley, Eds.; WILEY-VCH Verlag GmbH & Co. KGaA, Weinheim, **2009**; (6-7)

(52) Yevstropov, A.A.; Lebedev, B.V.; Kulagina, T. G.; Calorimetric study of δ-Valerolactone, poly-δ-valerolactone and of the process of polymerization of δ-valerolactone in the 13.8 to 340 K temperature range *Vysokomolekuliarnye soedineniia. Seriia A* **1982**, *24,* (568-574)

(53) Nishida, H.; Yamashita, M.; Endo, T.; Tokiwa, Y. Equilibrium Polymerization Behavior of 1,4-Dioxan-2-one in Bulk *Macromolecules* **2000**, *33,* (6982-6986)

(54) Lebedev, B.V.; Bykova, T.A.; Kiparisova, E.G.; Belen'kaya, B. G.; Filatova, V. N. Thermodynamics of p-dioxanone, of its polymerization and of poly(p-dioxanone) at 0-450 K *Vysokomolekuliarnye soedineniia. Seriia A & Seriia B* **1995**, *37,* (187-196)

(55) Libiszowski, J.; Kowalski, A.; Szymanski, R.; Duda, A.; Taquez, J. M.; Degée, P.; Dubois, P. Monomer-Linear Macromolecules-Cyclic Oligomers Equilibria in the Polymerization of 1,4-Dioxan-2-one *Macromolecules* **2004**, *37,* (52-59)

(56) Bechtold, K.; Hillmyer, M. A.; Tolman, W. B. Perfectly Alternating Copolymers of Lactic Acid and Ethylene Oxide as a Plasticizing Agent for Polylactide *Macromolecules* **2001**, *34,* (8641-8648)

(57) Lochee, Y.; Jhurry, D.; Bhaw-Luximon, A.; Kalangos, A. Biodegradable Poly(ester-ether)s: ring-opening polymerization of D,L-3-methyl-1,4-dioxan-2-ones using various initiator systems *Polym. Int.* **2010**, *59,* (1310-1318)

(58) Neitzel, A. E.; Petersen, M. A.; Kokkoli, E.; Hillmyer, M. A. Divergent Mechanistic Avenues to an Aliphatic Polyesteracetal or Polyester from a Single Cyclic Esteracetal *ACS Macro Lett.* **2014**, *3,* (1156-1160)

(59) Zhang, D. Hillmyer, M. A.; Tolman, W. B. Catalytic Polymerization of a Cyclic Ester Derived from a "Cool" Natural Precursor *Biomacromolecules* **2005**, *6,* (2091-2095)

(60) Duda, A.; Penczek, S. Thermodynamics of L-Lactide Polymerization. Equilibrium Monomer Concentration *Macromolecules* **1990**, *23,* (1636-1639)

(61) Wang, Y.; Hillmyer, M. A. Synthesis of Polybutadiene-Polylactide Diblock Copolymers Using Aluminum Alkoxide Macroinitiatiors. Kinetics and Mechanism *Macromolecules,* **2000,** *33,* (7395-7403)

(62) Schively, M. L.; Coonts, B. A.; Renner, W. D.; Southard, J. L., and Bennet, A. T. Physico-chemical characterization of a polymeric injectable implant delivery system *Journal of Controlled Release* **1995**, *33,* (237-243)

(63) Matsen, M.W. Effect of Architecture on the Phase Behavior of AB-Type Block Copolymer Melts *Macromolecules* **2012**, *45,* (2161-2165)

(64) Schneiderman, D.K.; Hill, E. M.; Martello, M.T.; Hillmyer, M.A. Poly(lactide)-block-poly(ε-caprolactone-co-ε-decalactone)-block-poly(lactide) copolymer elastomers *Polymer Chemistry* **2015**, *6,* (3641-3651)

(65) Grulke, E. A. in Brandrup, J.; Immergut, E. H., and Grulke, E. A. Polymer Handbook 4th Ed. John Wiley & Sons Inc. **1999**

(66) Wang, S.; Robertson, M. L. Thermodynamic Interactions between Polystyrene and Long–Chain Poly(n-Alkyl Acrylates) Derived from Plant Oils *ACS Applied Materials and Interfaces* **2015,** *1,* (12109-12118)

(67) Lewin, J. L.; Maerzke, K. A.; Schulz, N. E.; Ross, R. B.; Sipmann, J. I. Prediction of Hildebrand solubility parameters of acrylate and methacrylate monomers and their mixtures by molecular simulation *J. App. Sci.* **2010**, *116,* (1-9)

(68) Wang, S.; Kesava, S. V.; Gomez, E. D.; Robertson, M. L. Sustainable Thermoplastic Elastomers Derived from Fatty Acid *Macromolecu*les **2013**, *46,* (7202-7212)

(69) Makiguchi, K.; Satoh, T.; Kakuchi, T. Diphenyl Phosphate as an Efficient Cationic Organocatalyst for Controlled/Living Ring-Opening Polymerization of δ-Valerolactone and ε-Caprolactone *Macromolecules* **2011,** *44,* (1999-2005)

(70) Makiguchi, K.; Ogasawara, Y.; Kikuchi, S.; Satoh, R.; Kakuchi, T. Diphenyl Phosphate as an Efficient Acidic Organocatalyst for Controlled/Living Ring–Opening Polymerization of Trimethylene Carbonates Leading to Block, End–Functionalized, and Macrocyclic Polycarbonates *Macromolecules* **2013,** *46,* (1772-1782)

(71) Manzini, B.; Hodge, P.; Ben–Haida, A. Entropically–driven ring–opening polymerization of macrocyclic esters with up to 84–membered rings catalyzed by polymer–supported Candida antarctica *Polymer. Chem.* **2010,** *1, (*339-346)

(72) Sawada, H. Thermodynamics of Polymerization. 1. *Journal of Macromolecular Science C: Polymer Reviews* **1969,** *3,* (313-396)

(73) Kałużyński, K.; Penczek, S. Anionic Polymerization of 2-Oxo-1,2,3 λ5-dioxaphosphorinane. Thermodynamics *Makromol. Chem.* **1979,** *180,* (2289-2293)

(74) Shilna, I. and Nakata, K.; Medium–Sized Lactones In *Natural Lactones and Lactams: Synthesis, Occurrence and Biological Activity, Janecki, T., Ed.; Wiley:* Weinheim, Germany **2014** (193-227)

(75) Vincent, P.I. A correlation between critical tensile strength and polymer cross-sectional area *Polymer* **1972,** *13,* (558-560)

(76) Dobkowski, Z. Determination of Critical molecular weight for entangled macromolecules using the tensile strength data *Rheol Acta* **1995,** *34,* (578-585)

(77) Yu, J. M.; Dubois, P.; Jerome, R. Synthesis and Properties of Poly(isobornyl methacrylate (IBMA)-*b*-butadiene (BD)-*b*-IMBA Copolymers: New Thermoplastic Elastomers of a Large Service Temperature Range *Macromolecules* **1996,** *29, (*7316-7322)

(78) Fetters, L. J.; Lohse, D. J.; Milner, S. T.; Graessley, W. W. Packing Length Influence in Linear Polymer Melts on the Entanglement, Critical, and Reptation Molecular Weights *Macromolecules* **1999,** *32,* (6847-6851)

(79) Kanai, H.; Sullivan, V.; Auerbach, A. Impact Modification of Engineering Thermoplastics *Journal of Applied Polymer Science* **1994,** *53,* (527-541)

(80) Daoulas, K. C.; Theodorou, D. N. Experimental and Self–Consistent–Field Theoretical Study of Styrene Block Copolymer Self–Adhesive Materials *Macromolecules* **2004,** *37,* (5093–5109)

(81) Shin, J.; Lee, Y.; Tolman, W.B.; Hillmyer, M. A. Pressure-Sensitive Adhesives from Renewable Triblock Copolymers *Macromolecules* **2011,** *4,* (87-94)

(82) Sangjun, L.; Lee, K.; Kim, Y.-W.; Shin, J. Preparation and Characterization of a Renewable Pressure–Sensitive Adhesive System Derived from ε-Decalactone, L-Lactide,

Epoxidized Soybean Oil, and Rosin Ester *ACS Sustainable Chemistry and Engineering* **2015,** *3,* **(**2309-2320)

83 Kraus, G.; Rollmann, K. W. The Entanglement Plateau in the Dynamic Modulus of Rubbery Styrene–Diene Block Copolymers. Significance to Pressure–Sensitive Adhesive Formulations *Journal of Applied Polymer Science* **1977,** *21,* (3311-3318)

(84) Fetters, L. J.; Lohse, D. J.; Richter, D.; Witten, T. A.; Zirkel, A. Connection between Polymer Molecular Weight, Density, Chain Dimensions, and Melt Viscoelastic Properties *Macromolecules* **1994,** *27,* (4639-4647)

(85) Lee, I.; Panthani, T. R.; Bates, F. S. Sustainable Poly(lactide-b-butadiene) Multiblock Copolymers with Enhanced Mechanical Properties. *Macromolecules* **2013,** *46,* (7387–7398)

(86) Wolf, J. H.; Hillmyer, M.A.; Ordered Nanoporous Polycyclohexylethylene *Langmuir* **2003,** *19* (6553-6560)

(87) Schmidt, S.C.; Hillmyer, M.A. Morphological Behavior of Model Poly(ethylene-alt-propylene)-b-Polylactide Block Polymers *J. Poly. Sci. Part B: Polym. Phys.* **2002,** *40,* (2364-2376)

(88) Lee, S.; Gillard, T. M.; Bates, F. S. Fluctuations, order, and disorder in short diblock copolymers *AIChE Journal,* **2013,** *59,* (3502-3513)

(89) Zalusky, A. S.; Olayo-Vales, R.; Wolf, J. H.; Hillmyer, M.A. Ordered Nanoporous Polymers from Polystyrene-Polylactide Block Copolymers *J. Am. Chem. Soc.* **2002,** *124,* (12761-12773)

(90) Hoffman, W. F. ; Scolnick, E.; Smith, R. L. HMG-COA Reductase Inhibitors US 4851436 1989

(91) Longley, R. I.; Emerson, W. S. β-Methyl-δ-Valerolactone *Organic Synthesis Coll.* **1963,** *4,* (677)

(92) Takahashi, K.; Komine, K.; Yokoi, Y.; Ishihara, J.; Hatakeyama, S. Stereocontrolled Total Synthesis of (–)-Englerin A *Journal of Organic Chemistry* **2012,** *77,* (7364)

(93) Andreana, P.R.; McLellan, J. S.; Chen, Y.; Wang, P. G. Synthesis of 2,6-Dideoxysugars via Ring-Closing Olefinic Metathesis *Organic Letters* **2002,** *4,* (3875)

(94) Oikawa, M.; Oikawa, H.; Ichihara, A. Reductive Opening of α-Methylspiroketals *Tetrahedron* **1995,** *51,* (6237)

(95) Archibald, S. C.; Barden, D. J, Bazin, J. F. Y.; Felming, I.; Foster, C. F.; Mandal, K. A.; Parker, D.; Takaki, K.; Ware, A. C.; Williams, A. R. B.; Zwicky, A. B. Stereocontrol in organic synthesis using silicon-containing compounds. Studies directed toward the synthesis of ebelactone A *Organic and Biomolecular Chemistry* **2004***, 2,* (1051)

# Chapter 5. Chemically Recyclable Biobased Polyurethanes[**]

Polyurethanes, in the form of coatings, adhesives, sealants, elastomers, and foams, play a vital role in the consumer goods, automotive, and construction industries. However, the inevitable disposal of non-degradable post-consumer polyurethane products constitutes a massive waste management problem that has yet to be solved. This chapter describes the synthesis of biobased and chemically recyclable polyurethanes. Poly(β-methyl-δ-valerolactone) (PMVL), which was in Chapter 3 and Chapter 4 explored as a soft block for the synthesis of block polymer thermoplastic elastomers, is here used to replace petroleum-derived polyols in the synthesis of thermoplastic polyurethanes and flexible foams. Notably, these materials can rival commercial PUs in performance. More excitingly, β-methyl-δ-valerolactone monomer can be recovered from the polyurethane in high purity and high yield using a pyrolytic recycling method. This recycling strategy bypasses many of the technical challenges that currently preclude the practical chemical recycling of PUs

---

## 5.1 Introduction

Millions of tons of polyurethanes (PUs) are produced annually for use in the consumer goods, automotive, and construction industries. The global market for PU materials, valued at \$47 billion in 2014, is expected to increase by 50% in the next decade.[1] The incredible commercial success of these materials is due to their low cost and high versatility. The same basic reaction — the condensation of polyols and isocyanates — can be optimized to generate elastic materials for footwear, soft and flexible foams for cushioning, and hard and rigid materials for construction. Because most commercial PUs are petroleum–derived and resistant to degradation, there are significant environmental challenges associated with the large-scale production and disposal of these materials.

A majority of polyurethanes on the market today are derived from petrochemicals; however in recent years, changing consumer preferences, and government policies, have increased the demand for bio-derived alternatives.[2,3,4] Owing to their wide availability and potential scalability, renewable polyols derived from low cost plant oils have attracted considerable attention.[5,6,7,8,9,10,11,12,13,14,15,16,17] When used in flexible foam formulations, natural oil polyols (NOPs) typically must be used in conjunction with petrochemical polyethers, such as ethylene oxide-terminated poly(propylene oxide).[18,9] Necessitated by the synthetic limitations inherent to most NOPs (i.e., lower end group reactivity and marginal control over functionality and total molar mass) this blending limits the total biobased content of the PU.[7] Synthetic strategies have been developed to

address some of these limitations.[19] However, these additional modifications increase the cost and the additional processing steps are undesirable from green chemistry and engineering perspectives.[2,20,21] Furthermore, the heterogeneous composition of NOPs can lead to inconsistent quality and properties of the final PU product.[22] Additionally, renewable polyurethanes derived from NOPs present similar disposal challenges as traditional, petroleum-derived polyurethanes.

While some PU products such as thermoplastic polyurethanes (TPUs) can be thermally reprocessed, the cross-linked chemical structure of thermoset polyurethane resins (including foams) prevents melt processing. Some reports related to the chemical recycling of polyurethanes exist in the patent literature and academic journals, but it is not widely practiced on an industrial scale.[23,24,25] One of the most researched methods of chemical recycling, glycolysis, uses the reaction of a glycol with a polyurethane at elevated temperatures to recover polyols suitable for use in the manufacture of new polyurethane materials.[23,26,27] A similar chemical recycling method, hydrolysis, uses water to the same effect.[28,29] The efficacy of these methods is somewhat limited since they naturally produce a mixture of recycled polyols if the foams to be recycled are chemically heterogeneous (i.e., prepared from different polyols). Moreover, the potential side byproducts can be somewhat complex as urethane, urea, biuret, and allophanate groups may all be present in polyurethanes.[23,30] Not surprisingly, one of the major disadvantages of these chemical recycling methods is the limited purity of the recovered polyol.[24]

In Chapter 3, we introduced an efficient semisynthetic route for the production of the cyclic lactone β--methyl-δ-valerolactone (MVL).[31,] Importantly, MVL monomer can be polymerized at room temperature without the use of solvent to obtain poly(β-methyl-δ-valerolactone) (PMVL), a rubbery polyester with a low glass transition temperature ($T_g$ = −51 °C). It was previously estimated that it is possible to produce MVL on a large scale at a cost of less than \$2 kg$^{-1}$, making PMVL a promising new biodegradable polymer for use in a variety of applications. In this Chapter, PMVL is utilized as a polyol for the synthesis of polyurethane foams and elastomers. PMVL derived PUs show similar thermal and mechanical properties to those currently on the market. Yet, unlike most commercial PUs, PMVL-based PUs can be easily chemically recycled via a pyrolytic depolymerization method (whereby valuable MVL monomer is recovered). This general strategy is summarized in Scheme 5.1.

**Scheme 5.1**

**Synthesis of TPUs and chemically recyclable foams from MVL**
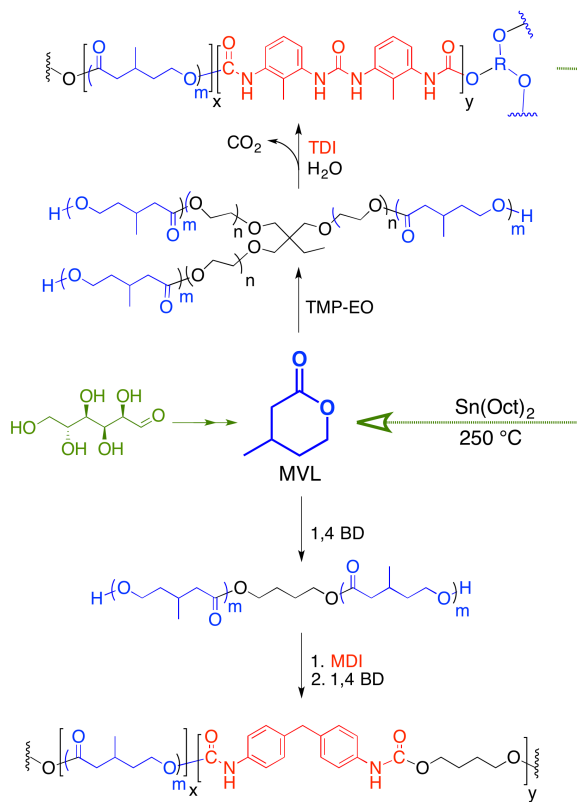


Here, $n \approx 1$ and $m = N_n/f$ where $N_n$ and $f$ are the degree of polymerization and functionality of the PMVL polyol, respectively. Both PUs can be approximated as segmented block polymers where x and y are proportional to the respective weight fractions of the soft and hard segments.

## 5.2 Results

### 5.2.1 Polyol Synthesis

As previously shown in Figure 3.5 a, by adjusting the ratio of MVL monomer to added alcohol initiator it is possible to access hydroxyl telechelic PMVL polyols with molar masses ranging from approximately 1 kg mol$^{-1}$ to nearly 100 kg mol$^{-1}$ (Figure 3.4). Whereas polyols used for the synthesis of polyurethane elastomers and foams are typically only low to moderate molar mass polymer; higher lower molar mass polymers are valuable for a number of other applications (e.g., the synthesis of block polymer adhesives and elastomers).[31] Practically, the molar mass range is limited on the lower end by initiator solubility and on the upper end by monomer purity. The functionality of the PMVL polyol can be controlled by using different alcohol initiators. While trimethylolpropane ethoxylate (TMP-EO) was used to prepare a trifunctional polyol for use in foam formulations, various diol initiators (e.g. 1,4 butane diol (BD), 1,3 propane diol (PD), and 1,4 benzene dimethanol (BDM)) were employed to synthesize linear polyols for the synthesis of TPUs. As demonstrated in Figure 5.1, matrix-assisted laser desorption/ionization (MALDI) was used to confirm molar mass control and to verify hydroxyl end group functionality.
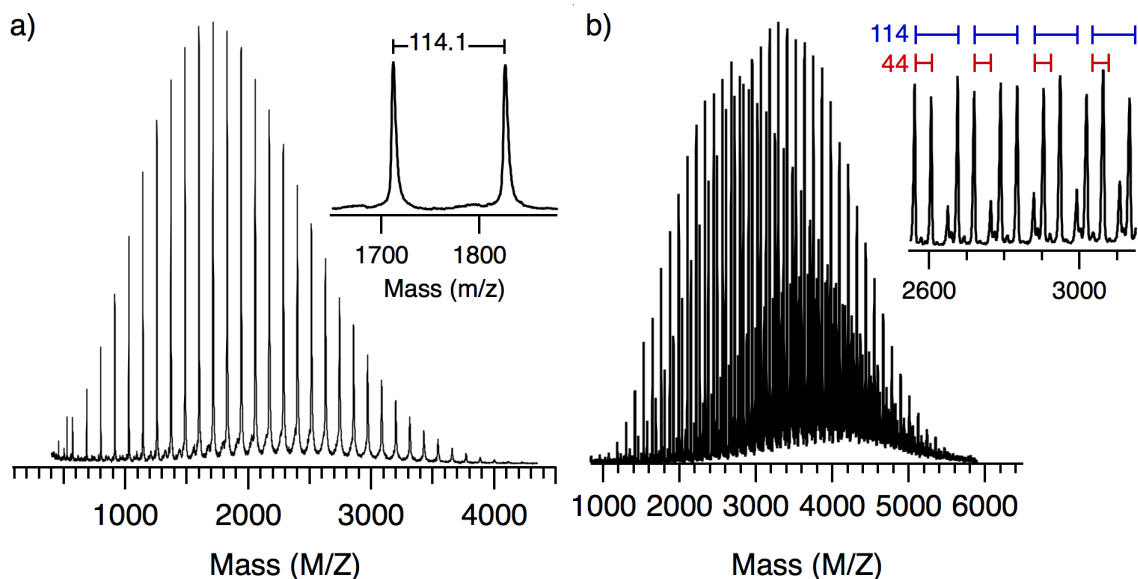
**Figure 5.1**

a) MALDI of a PMVL diol used in TPU syntheses. This polymer was synthesized using 1,4-benzenedimethanol as an initiator. b) MALDI of the PMVL2700 triol used for foam formulations. This polymer was synthesized using trimethylolpropane ethoxylate (with a distribution of EO lengths, nominal average molar mass of ~170 grams mol-1) as an initiator. Polymer chains initiated by four different species, specifically trimethylolpropane ethoxylate with 0, 1, 2, and 3 ethylene oxide repeats, are present. As shown in the inset, these different species are separated by the molar mass of ethylene oxide (44.05 grams mol-1). For chains with different degrees of polymerization initiated by the same alcohol, the difference in molar mass per repeat unit is the same as the molar mass of MVL monomer (114.15 grams mol-1).

The molecular characteristics of the PMVL polyols used in this work are summarized in Table 5.1. For all samples there was good agreement between the targeted molar mass, the molar mass estimated by proton nuclear magnetic resonance spectroscopy ($^1$H NMR) end group analysis, and the molar mass determined using MALDI. Moreover, the dispersity (Đ) values calculated from the MALDI data were similar to those determined using size exclusion chromatography with a multi-angle light scattering detector (MALLS-SEC). As expected, the glass transition temperature ($T_g$) values of the PMVL polyols, found using differential scanning calorimetry (DSC), were significantly

lower than the $T_g$ of high molar mass PMVL (about −60 °C and −50 °C, respectively). The zero-shear viscosities (η) of the PMVL polyol samples are slightly higher than amorphous polyether polyols of comparable molar mass but are similar to polyester polyols typically used in commercial foam formualtions.[17,32]

**Table 5.1**

**Molecular characteristics of PMVL polyols used for foam and TPU synthesis**

| Sample ID | [a]Initiator | [b]$M_{\text{n Theor.}}$ (kg mol⁻¹) | [c]$M_{\text{n, NMR}}$ (kg mol⁻¹) | [d]$M_{\text{n, MALDI}}$ (kg mol⁻¹) | [d]$Đ_{\text{MALDI}}$ | [e]$T_g$ (°C) | [g]η (cP) |
|---|---|---|---|---|---|---|---|
| M3000 diol | BDM | 2.6 | 3.0 | 2.4 | 1.19 | −63 | - |
| M2900 diol | PD | 3.1 | 2.9 | 4.1 | 1.09 | −62 | - |
| M5200 diol | BD | 5.6 | 5.2 | 5.0 | 1.54 | −60 | 4406 |
| M2700 triol | TMP-EO | 2.8 | 2.7 | 3.4 | 1.07 | −62 | 1643 |

[a]The indicated diol initiators are 1,4 benzene dimethanol, 1,3 propane diol, and 1,4 butane diol. The triol initiator was an ethylene oxide functionalized trimethylolpropane with a nominal molar mass of ~170 g/mol. Based on MALDI analysis of the PMVL 2700 triol (Figure 5.1.b), initiating species with 0, 1, 2, and 3 EO repeat units are all present. [b]The theoretical molar mass calculated from molar ratio of MVL:Initiator and monomer conversion as determined by ^{1}H NMR. [c]Molar mass estimated by 1H NMR end group analysis. [d]Molar mass and dispersity determined by MALDI; these values are compared to those found using SEC in the SI. [e]Gravimetric yield of recovered polyol based on observed monomer conversion. [e]$T_g$ values were determined using DSC and are reported on the second heating ramp (rate 10 °C min⁻¹) [g]Zero shear viscosity at 25 °C.

### 5.2.2 Synthesis and Characterization of PMVL TPUs

PMVL TPU samples were synthesized from PMVL diols in dimethylformamide using a sequential one-pot approach. Further details are given in the Section 5.5 of this chapter. The characteristics of representative PMVL TPU samples are summarized in Table 5.2. Using a standard definition of hard segment content, specifically the weight ratio of the

sum of the MDI and chain extender to the total mass of the polymer, hard segment contents ranging from 0.3 to 0.6 were targeted. For each sample, the composition determined using ^{1}H NMR spectroscopy ($d_7$-DMF) matched closely the theoretical composition. The molar mass and dispersity were determined using SEC (DMF mobile phase). Typical of step growth polymerization, a majority of the TPU samples were characterized by dispersity values close to 2.0. However, one sample, M3000B(0.44), exhibited a slightly higher dispersity (Đ = 2.64). This may indicate a small amount of chain coupling during the first step of the synthesis. Although all the TPU samples are ostensibly linear, it is possible that side reactions may cause the formation of lightly branched structures.[30]

**Table 5.2.**

**Characteristics of TPUs from PMVL**

| [a]Sample ID | [b]$M_n$ (kg mol$^{-1}$) | [b]Đ | [c]$T_g$ (°C) | [c]$T_m$ (°C) | [c]$\Delta H$ (J g$^{-1}$) | [e]$\sigma_b$ (MPa) | [e]$\varepsilon_b$ (%) | [e]$E_y$ (MPa) |
|---|---|---|---|---|---|---|---|---|
| M2900P(0.40) | 102.2 | 1.63 | −33 | 202 | 12.8 | 37±3 | 1000 ±20 | 7.2±0.2 |
| M2900P(0.41) | 31.8 | 1.98 | −33 | 162 | 7.03 | 6.4 ±0.2 | 290 ±30 | 4.3±0.2 |
| M3000B(0.44) | 49.9 | 2.64 | −35 | 192 | 13.5 | 6.4 ±0.2 | 250±50 | 2.6±0.1 |
| M3000B(0.53) | 30.5 | 1.46 | −35 | 196 | 19.2 | 9.3 ±0.2 | 70±7 | 46±2 |
| M3000B(0.60) | 40.3 | 2.02 | [d]na | 221 | 27.8 | 19.4 ±0.6 | 80±10 | 116±3 |

[a]The sample name is composed of three parts where (M####) indicates the molar mass of the PMVL diol precursor in g mol$^{-1}$, the letter P or B indicates the chain extender used (propane diol or butane diol, respectively), and the parenthetical numbers indicate the hard segment content (determined using ^{1}H NMR spectroscopy). More specifically, %HS=100*(MDI+CE)/(MDI+CE+PMVL) where MDI, CE, and PMVL are, respectively, the isocyanate, chain extender, and polyol components. [b]Relative molar mass and dispersity were determined by SEC (DMF, PS standards) [c]Determined using DSC, taken on the second heating ramp at a rate of 10 °C min$^{-1}$. [e]Ultimate tensile strength (σb) and maximum elongation (εb) are the stress and elongation at break. [d]Not observed by DSC on the second heating ramp; by DMA this sample has a Tg of −29 °C. Elastic modulus ($E_y$), σb, and εb, were determined using uniaxial extension tests at a constant crosshead velocity of 60 mm min$^{-1}$.

Generally, TPUs are segmented block polymers consisting of polyol soft segments connected by hard segments. Because they are prepared via random coupling, the hard segments (alternating copolymers of a diisocyante and diol chain extender) are of ill-defined length. Provided the molar masses of the individual segments are high enough, TPUs tend to phase separate to form a physically crosslinked material.[61] All of the PMVL TPU samples exhibited a soft segment glass transition temperature ($-50\ ^{\circ}\text{C} \leq T_g \leq -30\ ^{\circ}\text{C}$) slightly elevated relative to PMVL homopolymer. This suggests partial inclusion of hard segment copolymer in the soft domains. The $T_g$ values tend to decrease with hard segment content, indicating better phase separation at these compositions. As shown in Figure 5.2a, the PMVL TPUs displayed a broad endotherm near 200 °C ($160\ ^{\circ}\text{C} \leq T_m \leq 220\ ^{\circ}\text{C}$). This may be due to strong hydrogen bonding in these materials. Fourier transform infrared spectroscopy (ATR-FTIR) provided further evidence of microphase separation. In addition to the characteristic ester carbonyl stretch (C=O, 1727 cm$^{-1}$) of PMVL, hydrogen bonded urethane stretches (C=O 1702 cm$^{-1}$ and C-N 1614 cm$^{-1}$) were observed, this is shown in Figure 5.2 b. The position and intensity of the urethane N-H stretch (N-H 3324 cm$^{-1}$) is also a good indication of hydrogen bonding in these materials.[33,34,35]
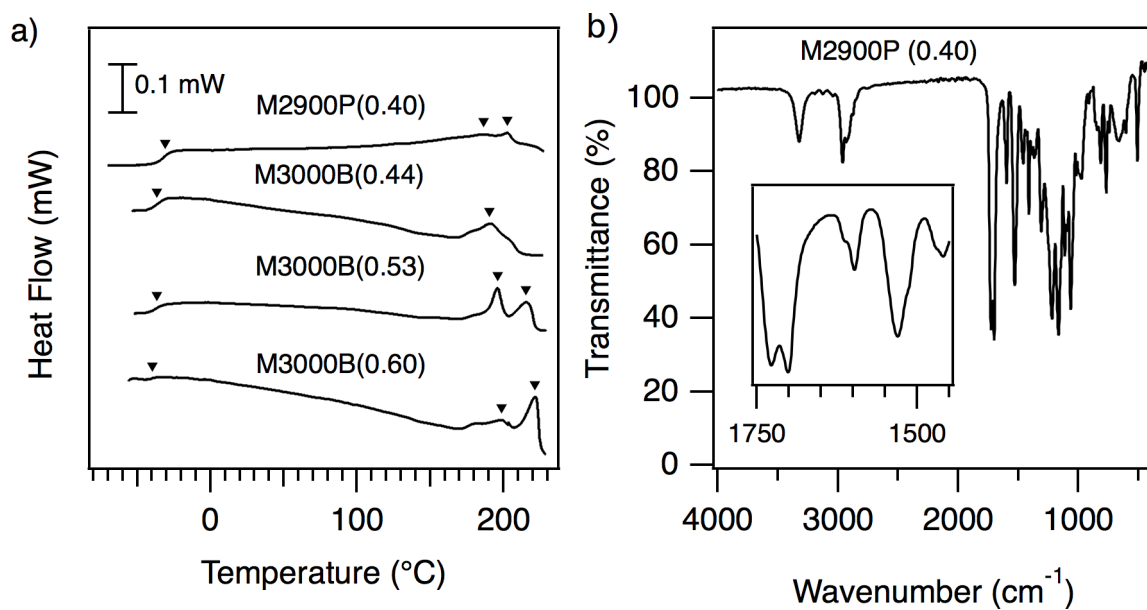
**Figure 5.2**

a) DSC thermogram of compression PMVL-TPU samples with increasing hard segment content. The (▼) markers indicate the Tg (taken as the inflection point) and local maxima of the endotherms (which may be due to melting of the hydrogen bonding domains). The data were taken on samples previously compression molded at 240 °C (~10 min) and are for the first heating ramp (heating rate of 10 °C min-1). b) ATR-FTIR of a compression molded specimen of the M2900P (0.4) sample described in Table 5.2.

Dynamic mechanical analysis (DMA) was used to corroborate these IR and DSC results. Compression molded rectangular strips were tested in tension mode. The samples were cooled through the glass transition, and then heated until the material began to flow ($T_{fl}$), as indicated by rapid decrease in modulus. This is shown with PMVL TPU M2900P as an example in Figure 5.3a. For each sample, the glass transition determined by DMA was close to values found using DSC (Figure 5.3b). The gently sloping plateau in E' and E" (for $T_g \leq T \leq T_{fl}$) is another good indication that the TPUs are microphase-separated. Although the softening of the material at high

temperatures could be interpreted as degradation, follow-up DMA experiments revealed that this transition was reversible on cooling.
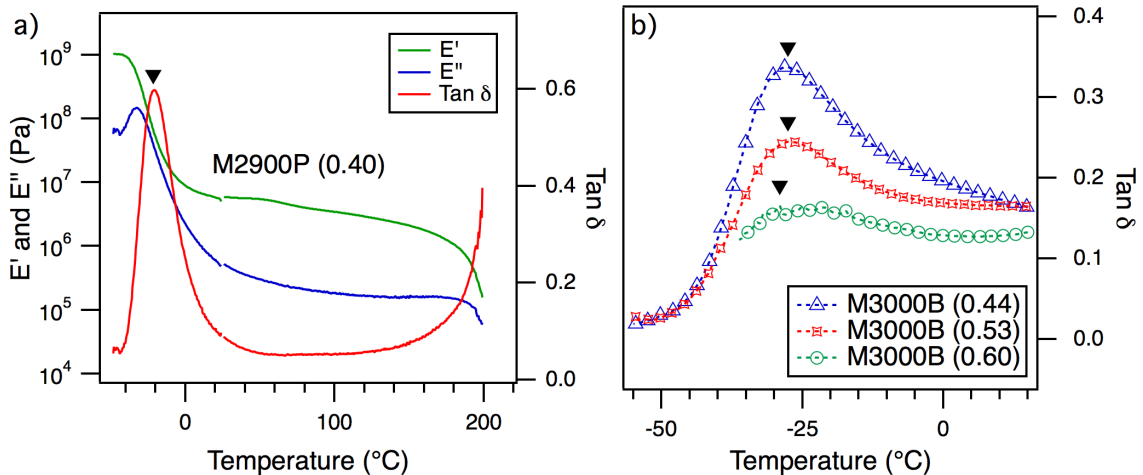


**Figure 5.3**

DMA of PMVL TPU M2900P(0.40). Data was taken on rectangular films under tension film mode at a cooling rate of 3 °C min^{-1} and a frequency of 1 rad s[-1]. The $T_g$ of this sample, taken as the peak in tan δ on cooling is −24 °C. b) DMA of PMVL TPUs of different hard segment content showing the glass transition temperature on cooling. Data was taken on rectangular films under tension film mode at a cooling rate of 3 °C min^{-1} and a frequency of 1 rad s[-1].

Mechanical properties of the TPUs, studied by uniaxial extension tests, were dependent on the molecular structure of the polymer. As expected, for a series of polymers with similar overall molar mass, i.e., M3000B (0.44), (0.53), and (0.60), the elastic modulus and stress at break both increased with hard segment content.[61,36,37] When the composition was fixed, tensile properties depend on the overall molar mass. Despite similar composition, sample M2900P(0.40), for example, had a stress at break that was nearly six times larger than M2900P(0.41), an analogous sample of lower overall molar mass. Due to their high hard segment content, the majority of the PMVL TPU samples

exhibited mechanical performance more typical of tough plastics than elastomers. However, as shown in Figure 5.4, M2900P (0.40) demonstrated excellent elasticity during hysteresis testing, with nearly complete recovery of applied strain over 20 cycles. This sample in particular is mechanically comparable to soft commercial thermoplastic polyurethanes.[59]
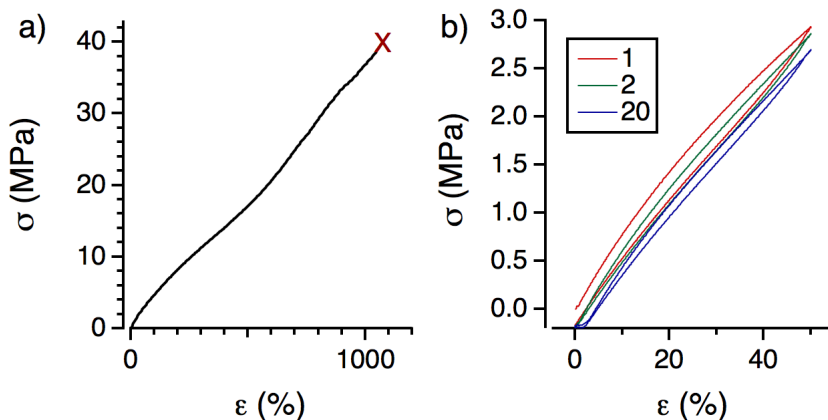


**Figure 5.4**

Representative tensile data obtained for uniaxial extension of PMVL TPU sample M2900P(0.40). Experiments were conducted with a constant crosshead velocity of 60 mm min$^{-1}$. b) Representative cyclic tensile experiment of M2900P(0.40) (1, 2, and 20 cycles, crosshead velocity of 60 mm min$^{-1}$, without rest between cycles) For the cycles shown the energy loss between the tension and relaxation steps is cycle1: 7.4%, cycle 2: 3.1%, and cycle 20: 1.2%.

## 5.2.3 Synthesis and Characterization of PMVL PU Foams

The formulations used to prepare the foam samples are given in Table 5.3. The characteristics of a few representative foams are summarized in Table 5.4. Similar to the TPUs described above, the foam samples can be idealized as segmented block polymers consisting of PMVL soft segments connected by hard segments rich in

185

urethane or urea linkages. These foam formulations, water reacts with the isocyanate groups of TDI to form an unstable carbamic acid that subsequently decomposes to generate $CO_2$ (blowing reaction) and a primary amine. The PMVL polyol and aromatic amines react simultaneously with TDI to create a crosslinked network (gelling reaction). The nanoscopic phase behavior of the resulting polyurethane is largely determined by the size and functionality of the polyol segment, the relative rates of the blowing and gelling reactions, and the ratio of TDI to polyol and water. The microscopic structure of the foam is influenced by both phase behavior of the polyurethane and the ability of the surfactant to stabilize the polymer foam as it rises.

**Table 5.3**

**PMVL Foam formulations (in parts by weight)**

| [a]Foam ID | Polycat 8 | Polycat 5 | $Sn(Oct)_2$ | Dabco 5164 | Dabco 5179 | Dabco 3043 | $H_2O$ | TDI 80:20 |
|---|---|---|---|---|---|---|---|---|
| M2700-A | 0.25 | 0.25 | - | 3 | - | - | 3 | 36.7 |
| M2700-B | 0.25 | 0.25 | - | 3 | - | - | 3 | 33.0 |
| M2700-C | 0.25 | 0.25 | - | 3 | - | - | 3 | 27.5 |
| M2700/5200-D | 0.25 | 0.25 | - | 1.4 | - | - | 2.9 | 17.8 |
| M2700-E | 0.25 | 0.25 | - | 2.9 | - | - | 2.9 | 26.8 |
| M2700-H | 0.23 | 0.22 | - | - | - | 1.4 | 1.5 | 35.7 |
| M2700-I | 0.62 | - | 0.46 | - | - | 4.3 | 4.4 | 35.7 |
| M2700-J | 0.25 | 0.12 | 0.18 | - | - | 2.9 | 2.9 | 26.8 |

[a] With the exception of M2700/5200-D, which is a blend of diol PMVL 5200, the  foams were prepared using only polyol PMVL 2700. The formulation is normalized to the total amount of PMVL (that is, in each PMVL is 100 parts by weight).

**Table 5.4**

**Characteristics of Representative PMVL Foams**

| [a]Sample ID | [b]$T_g$ (°C) | [b]$T_g$ (°C) | [c]$\rho$ (kg m$^{-3}$) | [d]$\sigma_T$ (kPa) | [e]$\varepsilon_b$ (%) | [f]$\sigma_{(C50)}$ (kPa) | [g]K (kPa) |
|---|---|---|---|---|---|---|---|
| M2700-A | −33 | 132 | 40±3 | 210±30 | 250±70 | 4.3±0.2 | 3.0±0.5 |
| M2700-B | −38 | 130 | 47±9 | 160±20 | 350±60 | 4.8±0.7 | 3.0±0.4 |
| M2700-C | −37 | 126 | 80±10 | 390±80 | 130±20 | 8.3±0.6 | 3.3±0.5 |
| M2700/5200-D | −39 | 128 | 47±5 | 130±30 | 570±140 | 3.3±0.3 | 1.0±0.1 |
| MCM00111 | | | | | 45±3 | 78±7 | 130 ±14 |
| MCM00131 | | | | | 40±1 | 110±20 | 170±30 |
| MCM00017 | | | | | 42±1 | 210 ±20 | 180 ±30 |

[a]Sample ID refers to the polyol used in the foam formulation. MCM foams are commercial foams with different firmness grades. [b]Glass transition temperatures were measured using DSC and were taken on the second heating at a ramp rate of 10 °C min$^{-1}$. [c]Density reported is the mass of a small cube cut from the core of a foam sample and divided by its measured volume. The top and bottom sections of the foam were not tested due to difference in appearance and density. Density is reported as the average and standard deviation of a minimum of five samples. Extension and compression tests were conducted parallel to the direction of the foam rise. [d]Ultimate tensile strength is defined as the stress at failure. All mechanical characteristics of foams are reported as the average and standard deviation of a minimum of five samples. [e]Maximum elongation is designated as strain at failure. [f]Compressive strength is defined as stress at 50% compression. [g]Compressive modulus ($\sigma/\varepsilon$) over the linear regime.

ATR-FTIR spectroscopy was used to provide insight on the molecular structure and composition of the crosslinked PMVL PU foams. As expected, all of the IR signals of PMVL homopolymer are preserved in the spectrum of the foam. As shown in Figure 5.5a, the characteristic PMVL ester carbonyl stretch (C=O, 1727 cm$^{-1}$) largely obscures the region where urethane or free urea cabonyl stretches are expected to occur. However, an additional signal, which likely corresponds to the stretch of hydrogen bonded urea carbonyls (C=O, 1640 cm$^{-1}$), is observed. This is shown, for example in Figure 5.5a. Broad signals, attributable to the N-H stretches of hydrogen bonding monodentate and bidentate ureas, are also present (at 3400-3245 cm$^{-1}$), as are

187

characteristic N-H bends (near 1540 cm$^{-1}$). Of these, the stretch at 1640 cm$^{-1}$ is a characteristic feature of organized hard domains, implying a microphase-separated structure.[38] Further evidence of a segregated structure was found using DSC (Figure 5.5b). Each of the PMVL foams exhibit two $T_g$ values, one near −35 °C, the other near 130 °C. The lower $T_g$ value is in every case higher than that of the polyol precursor (−60 °C), an observation that suggests partial mixing of the soft and hard regions of the foam. Within the temperature range of the DSC experiment (−80 °C < T < 180 °C) the sample was amorphous; however, bidentate urea hydrogen bonds are unlikely to melt below the degradation temperature of the material.



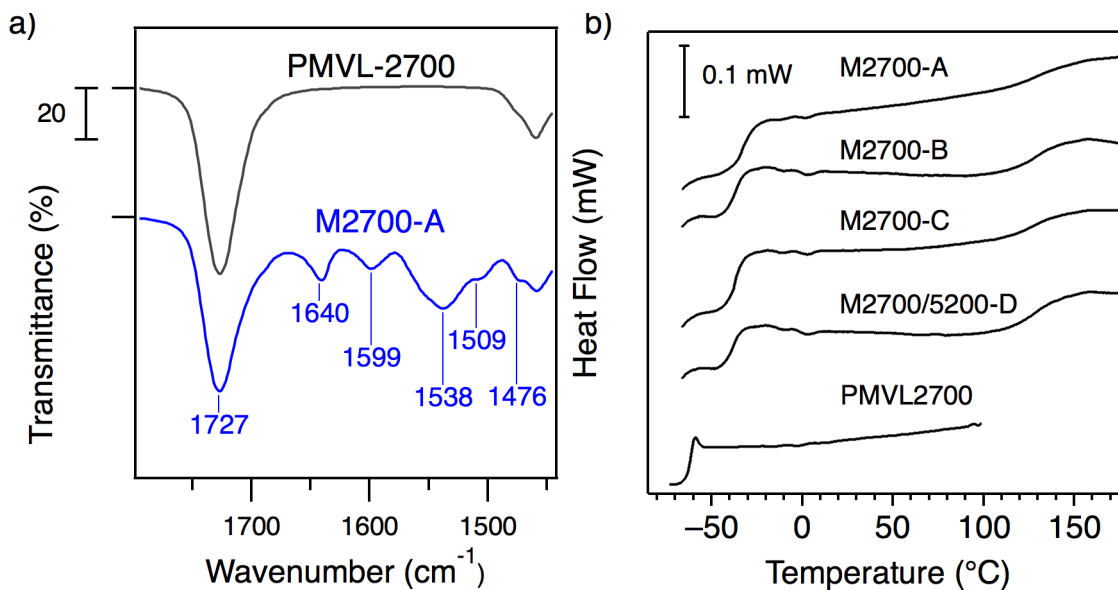**Figure 5.5**

 a) ATR-FTIR of PMVL2700 triol and PMVL PU Foam M2700-A. The spectra have been shifted vertically for clarity and ticks on the y-axis represent 100% transmittance for the respective samples. The full IR spectra for the foams in Table 3 are given if Figures S13-S16, b) DSC thermograms of PMVL triol and PMVL PU foams.  To avoid degradation, the PMVL triol was not heated above 100 °C.

Foam properties and cellular structure were tuned to some extent by changing both the TDI content in the formulation and the PMVL polyol. Samples M2700-A, M2700-B, and M2700-C in Table 5.4 were prepared using the same PMVL triol (2.7 kg mol$^{-1}$ with a nominal functionality of 3.0) but differ in the amount of TDI. Although the compressive modulus for A and B are similar, the compressive strength (defined in this work as the stress at 50% compression) is much higher for sample C. M2700/5200-D was prepared from a blend of PMVL2700 triol and PMVL5200 diol, and displayed the lowest compressive strength and modulus of the PMVL foams. For all four samples there is an inverse correlation between elongation at break and ultimate tensile strength. The lab scale tests used to characterize the mechanical properties of the foams were not ASTM standard (due to small sample size and equipment limitations). Because of this it may not be strictly valid to directly compare these mechanical results to the published mechanical data for soft flexible foams. However, the mechanical properties of a series of commercial flexible polyurethane foams of different firmness grades (McMaster-Carr Foams MCM00111, MCM00131, MCM00017) were also tested using the same tensile and compression testing procedures. The PMVL foams have similar compression modulus and compression strength to the commercial foams tested but exhibit improved tensile strength and elongation.

PMVL foam samples A, B, and D exhibit densities similar to commercial polyether based slabstock foams made using water and commercial grade TDI (most typically, 12–60 kg m$^{-3}$).[59] However, the density of foam sample C is nearly twice that of the other foams. The primary difference between these foams is their cell structures, Figure 5.6.

Foams samples A and B, prepared with similar TDI content, both exhibited large closed cells of irregular size. Samples C and D, prepared using less TDI, exhibited much smaller cell sizes. Sample C is primarily open cell with more geometric structures and relatively thick struts. In contrast, Sample D consisted of more rounded cells that were partially opened. An analogous foam with similar TDI content prepared using only PMVL2700 triol produced a fully open cell, suggesting that inclusion of the higher viscosity PMVL diol can also impact the cell structure significantly.[39]
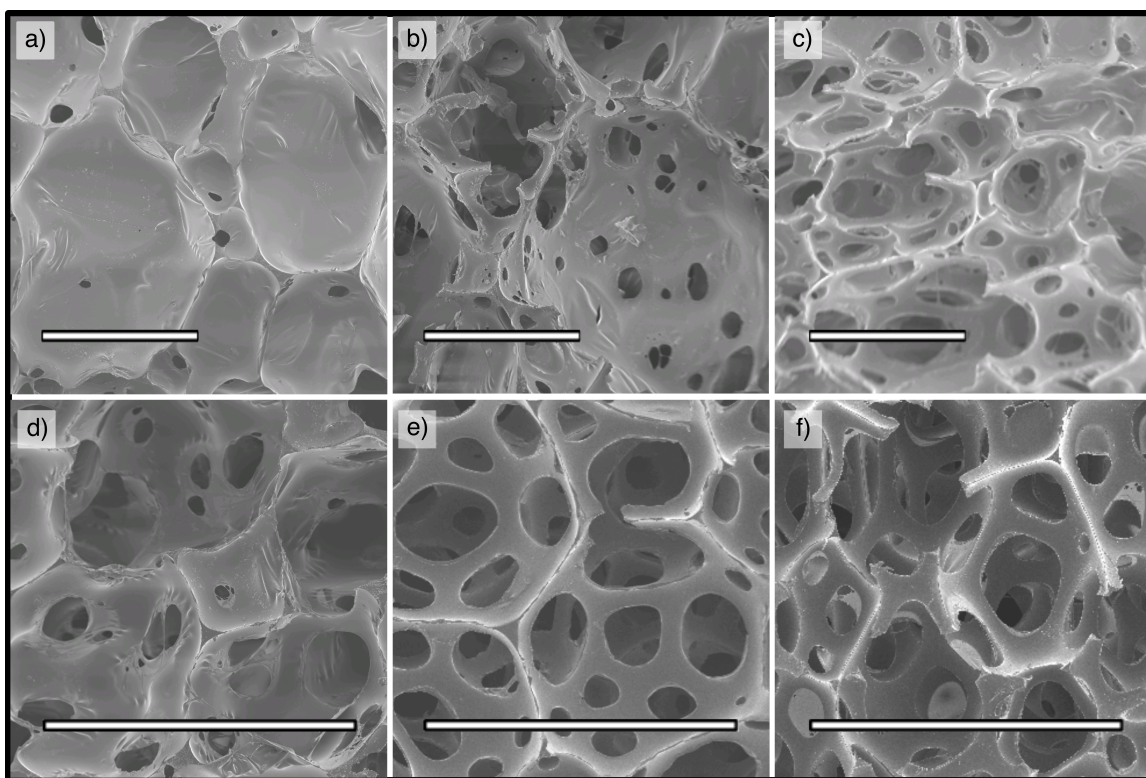


**Figure 5.6**

SEM images of PMVL PU Foams of different compositions. In all images the white bar represents 1 mm. a) Foam M2700-A b) Foam M2700-B c) Foam M2700-C d) Foam M2700/5200-D e) Foam M2700-E f) commercial foam (MCM00017)

## 5.2.4 Thermal Stability of PMVL Polyurethanes

The thermal stability of both foam and elastomer samples was analyzed using thermogravimetric analysis, shown below in Figure 5.7. In this work the degradation temperature ($T_d$) is defined as the temperature at which 5% mass loss is observed on heating under nitrogen at a ramp rate of 10 °C min$^{-1}$. Compared to PMVL Diol ($T_d$ = 150 °C) elastomers ($T_d$ = 225-291 °C) and foams ($T_d$ = 217-225 °C) both exhibit improved temperature stability compared to PMVL homopolymer. For both types of polyurethane, the degradation temperature was influenced by the isocyanate content, however the impact was more significant with the TPUs than the foam samples.
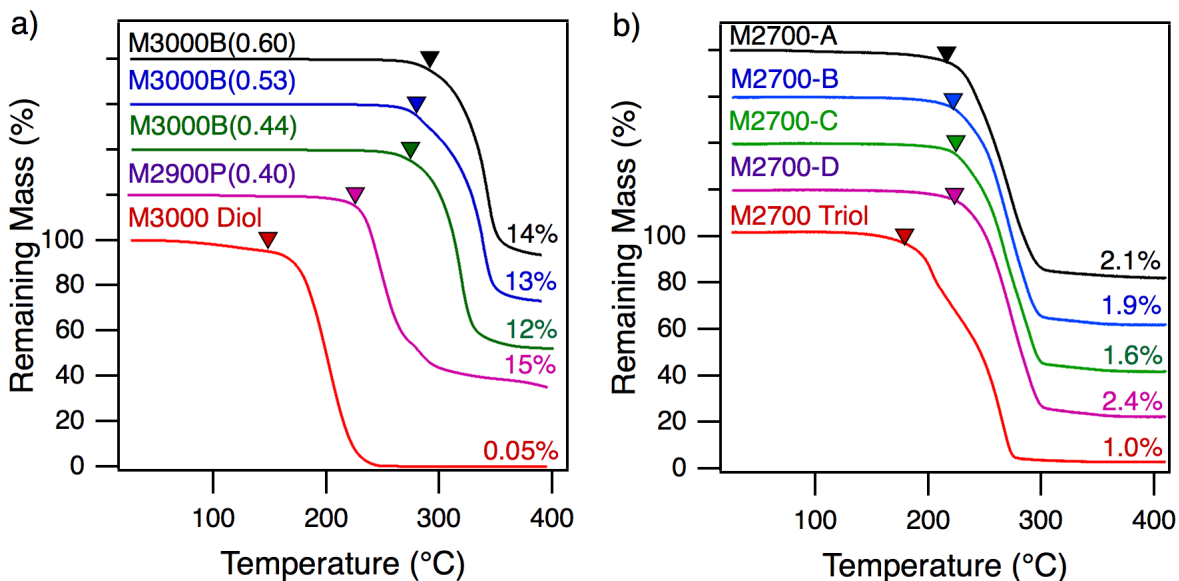


**Figure 5.7**

a) TGA of PMVL TPU samples of different compositions compared to PMVL homopolymer diol. Data taken while heating under nitrogen at a ramp of 10 °C min$^{-1}$. b) TGA of PMVL Foam samples of different compositions compared to PMVL homopolymer triol. Data taken while heating under nitrogen at a ramp of 10 °C min$^{-1}$.

Isothermal annealing experiments, shown in Figure 5.8, were conducted to examine the stability of PMVL polyurethanes over time. If no catalyst was present, both foam and elastomer samples were stable when annealed at temperatures below 180 °C; however mass loss was significantly accelerated at higher temperatures. As a specific example, PMVL foam sample M2700-A exhibits only 3% mass loss after 4 h at 180 °C but 15% mass loss after 4 h at 200 °C. PMVL TPU samples without residual catalyst (removed by precipitation) exhibit similar stability. However, degradation is significantly faster for samples prepared using a tin catalyst ($Sn(Oct)_2$). These results are rather dramatic but are in good agreement with previous studies regarding the impact of residual catalysts on the degradation of aliphatic polyesters.[40]



**Figure 5.8**

a) Overlay showing mass loss of M2700-A foam during isothermal annealing under nitrogen at indicated temperatures. The blowing and gelling catalysts were removed from this sample under reduced pressure at room temperature prior to analys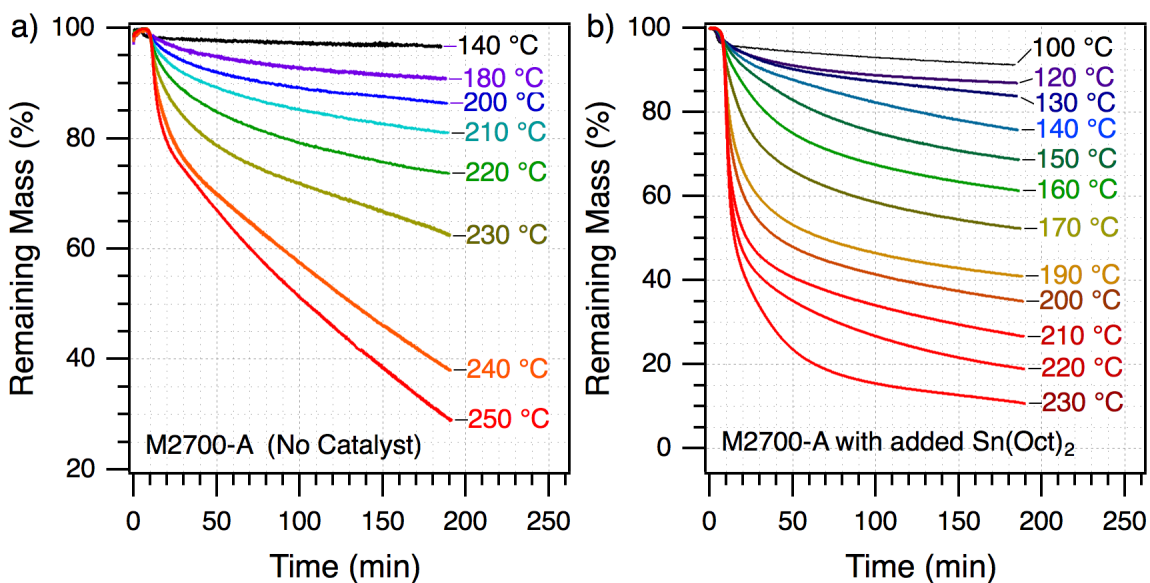is. b) Overlay showing mass loss of M2700-A foam during isothermal annealing under nitrogen at indicated temperatures. Prior to analysis the foam sample was submerged in a solution of hexanes containing $Sn(Oct)_2$ (0.1 wt% relative to the foam sample) for 5 days. The samples thus imbued were dried under vacuum at room temperature prior to TGA analysis.

### 5.2.5 Pyrolytic Recycling of PMVL Foams

These results are impressive but largely unsurprising as it is well known that $Sn(Oct)_2$ catalyzes polyester decomposition by transesterification and depolymerization.[40] To recycle PMVL foams back into MVL monomer, neat foam samples were heated in a short path distillation apparatus under dynamic vacuum (170-250 °C, ~100 mTorr).[31] Data from a number of distillation experiments are summarized below in Table 5.5. During the recycling process all volatile products were collected in a receiving flask cooled by liquid nitrogen. It is possible to recycle foams prepared using only amine catalysts; however, the recycling reaction was faster when $Sn(Oct)_2$ was present (either added during the foam formulation or to the foam immediately prior to recycling). Although the MVL yield (50 to 99%) was dependent on temperature, foam composition, and catalyst concentration, in all cases the monomer was isolated in high purity ($\geq$95% by ^{1}H NMR spectroscopy). Since MVL monomer can be continuously removed by distillation, it is also possible to recycle MVL foams mixed with foams derived from other polyols. To demonstrate this, PMVL foam was mixed with an equal mass of commercial polyurethane foam and subjected to a recycling experiment under the same conditions used to recycle pure PMVL foams (200-250 °C, ~100 mTorr). In this mixed recycling experiment no significant decrease in the recovery or purity of MVL was observed.

**Table 5.5**

**PMVL Foam Distillation Summary**

| Entry | Foam ID | Scale (g) | Temp. (°C) | Time (h) | Yield (%) | [Sn(Oct)$_2$] (wt%) |
|-------|---------|-----------|------------|----------|-----------|---------------------|
| 1 | [a]M2700- H | 5.9 | 170 | 4.0 | 46% | 0.10 |
| 2 | M2700- I | 1.2 | 230 | 6.0 | 54% | 0.31 |
| 3 | [b] M2700-J | 4.3 | 220 | 10.5 | 95% | 0.14 |
| 4 | [c] M2700-J | 2.9 | 220 | 10.0 | 97% | 0.14 |
| 5 | [d] M2700-J | 2.9 | 200 | 10.0 | - | 0.14 |

[a]Sn(Oct)$_2$ was added immediately prior to distillation. All other foams had this catalyst present in the original formulation (see Table 5.3 for full formulation). [b]Sample was a heterogeneous mixture of 01DB06A (2.2 g) and MCM 8643K511 (2.1 g). [c]Kinetics are shown in Figure 5.9a. [d]Yield is not calculated as samples of foam residue were removed from the experiment at 2, 5, and 10 hours for ATR-FTIR and elemental analysis; these data are shown in Figure 5.9.

The monomer recovery of MVL from PMVL foam over time was also measured. Figure 5.9a shows that 85% of MVL monomer was recovered within the first two hours of distillation at 225 °C. Longer reaction times resulted in slightly higher yields (a total yield of 97% after ten hours), but monomer recovery was slower during the final stages of the process. In a parallel experiment, samples of degraded foam and aliquots of recovered monomer were removed from the distillation after two, five, and ten hours. Over the course of the distillation there was no significant change in the purity of the recovered MVL; all of the samples analyzed were greater than 99% pure by gas chromatography (GC). The samples of foam residue were insoluble; however, elemental analysis revealed an increase in nitrogen content. The FTIRs of the degraded foam samples, shown in Figure 5.9b, displayed a concomitant decrease in the intensity of stretch corresponding to the PMVL ester (1729 cm$^{-1}$) carbonyl. Taken together, the IR

and elemental analysis results are consistent with removal of MVL and retention of crosslinked urea and high boiling amine products.
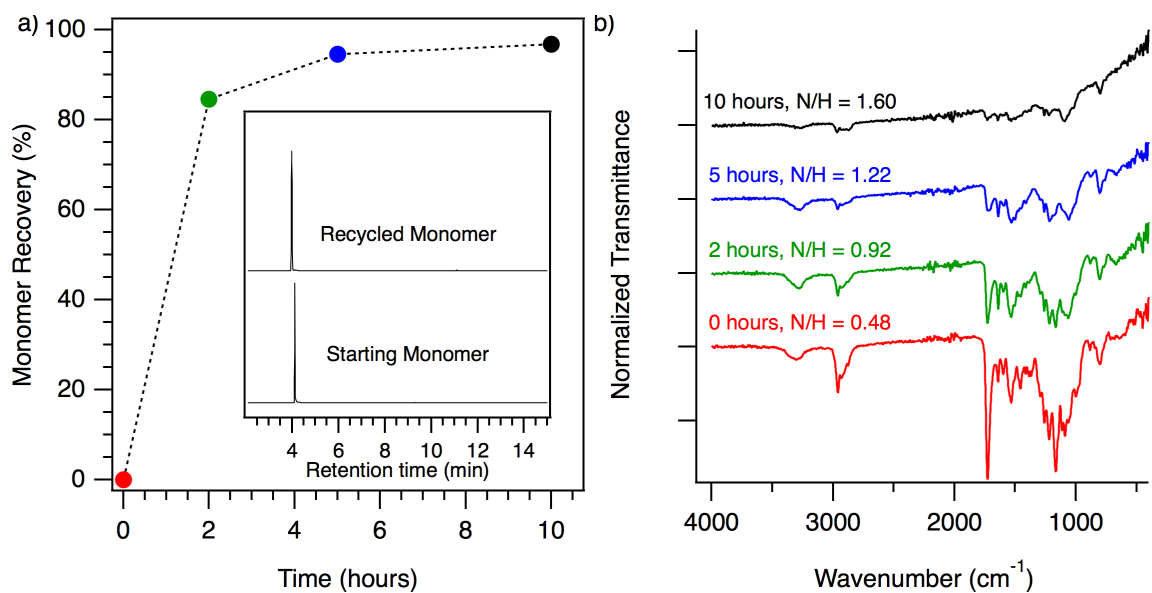


**Figure 5.9**

a) MVL recovery over time during a 10 hour distillation experiment conducted at 220 °C. (inset) Overlay showing GC chromatographs of recovered monomer (cumulative after 10 hours) compared to the pure MVL originally used to prepare the PMVL polyol contained in the foam. b) ATR-FTIR of foam residue from distillation flask at indicated time. The N/H mass ratio, determined by elemental analysis (average of two samples), is also indicated for each. These experiments are detailed in Table 5.5, entries 4 and 5, respectively.

a)

114

b)

$$N_N = [M_w - (22.99 + 90.12)]/114.1$$

4900    5000

4       8    $12 \times 10^3$
Mass (M/Z)

46      48      50      52      54
$N_N$

**Figure 5.10**

a) MALDI of a PMVL diol prepared using MVL monomer recycled from pyrolysis of a PMVL PU foam. b) Analysis of the MALDI data shows the peak spacings are consistent with charged PMVL polymer chains differing by MVL repeat units (114.1 g mol-1). It is assumed that individual chains are assumed to be associated with a sodium couterion (22.99 g mol-1) and were initiated by butanediol (90.12 grams mol-1). PMVL chains initiated by other species are not observed.

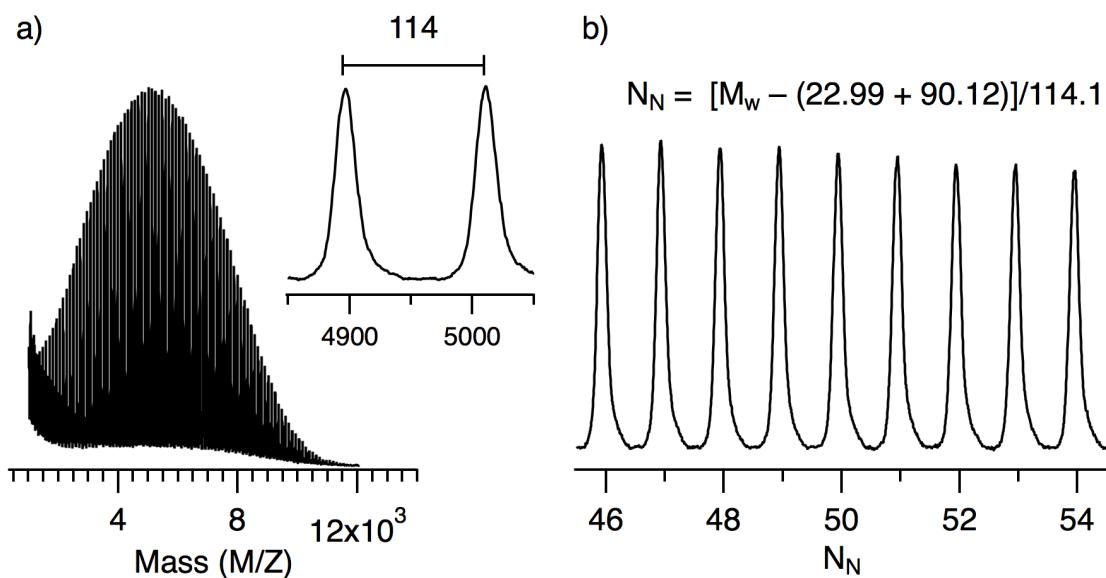To demonstrate the utility of this recycling approach, MVL recovered from the depolymerization of PMVL foam was used to prepare new PMVL polyols. An alcohol initiator (1,4 butane diol) and an acid catalyst (HCl in ether) were added directly to the receiving flask containing MVL from the distillation experiment. The flask was capped and the contents stirred until the reaction reached equilibrium, followed by removal of the catalyst under vacuum. The molar mass of the resulting PMVL ($M_{n, MALDI}$ = 2.08 kg mol$^{-1}$, Đ = 1.55) was close to the theoretical molar mass ($M_{n, theor.}$ = 2.28 kg mol$^{-1}$). In this sample, the majority of PMVL were initiated by 1,4 butane diol; however some chains were initiated by minor contaminants, e.g., the hydroxy acid of MVL. These

196

contaminants were higher boiling than MVL and could easily be removed by simple distillation. Recycled MVL purified in this manner was used to prepare a new polyol that is, by MALDI, indistinguishable from an analogous sample prepared from virgin monomer. This is demonstrated above in Figure 5.10).

## 5.3 Discussion

### 5.3.1 Comparison of PMVL to Other Renewable Polyols

The ease and versatility of synthesis makes PMVL polyols attractive alternatives to biobased polyols for a variety of applications. Because MVL is polymerized in the bulk at room temperature without the use high temperatures or solvents, the synthesis of PMVL polyols fully embodies the tenets of green chemistry. The use of HCl as a ROTEP catalyst is convenient for the synthesis of low molar mass polyols as it can be removed under reduced pressure, avoiding the precipitation step previously required to remove catalyst and unreacted monomer.[31] Precise control over the ring opening polymerization of MVL enables the synthesis of PMVL polyols with tailored functionality and molar masses. Whereas NOPs typically have complex molecular structures due to the heterogeneous triglyceride mixtures present in plant oil, PMVL polyols are well defined.[17] In this regard, biobased PMVL is more similar to petrochemical polyetherols than natural oil polyols.

In the past, a variety of other lactones have been explored as starting materials for the synthesis of polyesterol polyurethanes. Poly(ε-caprolactone) (PCL) derived TPUs, for example, have been explored for use in degradable medical devices.[35] Neat PCL,

however, is semicrystalline ($T_m$ = 60 °C) and is an unsuitable building block for applications where high elasticity is required.[41,42] Alkyl-substituted aliphatic polyesters, such as the renewable polymers poly(δ-decalactone) and poly(carvomenthide), are amorphous and can be used to prepare polyurethanes, but the precursor monomers are much more expensive than MVL.[58,43] Additionally, these telechelic polymers are secondary alcohols, making them less reactive than PMVL.

Because PMVL is easily synthesized, reactive, bioderived, and potentially low-cost, it is an appealing building block for the manufacture of sustainable commodity materials. PMVL can be successfully integrated into products that require distinct polyol characteristics, namely TPUs and PU foams. In general, TPUs prepared from natural oils can be somewhat soft, due to the presence of long dangling alkyl chains that can act as plasticizers.[16,17,44,45] Commercial polyurethanes, however, are most typically prepared from polyesters or polyethers without long dangling branches. The methyl-substituents of PMVL are sufficient to render the soft segments amorphous but do not inhibit hydrogen bonding between the ester and urethane segments. Consequently, use of PMVL as a soft segment enables the synthesis of TPUs with excellent mechanical properties, similar to soft commercial TPUs (the mechanical properties of these materials vary widely, however most typically exhibit a strain at break of 350 to 800% and a stress at break of 20 to 50 MPa.

Soft segment dangling ends can also contribute to inferior properties in PU foams.[46] To combat this problem, and to increase reactivity, vegetable oil polyols are typically mixed with petroleum-based polyols when used to prepare polyurethanes.[47] In foams, this blending strategy limits total bioderived content but generally results in better density

control, more homogeneous cell structures, and better mechanical performance.[46] Here, foams were made using PMVL as the sole polyol, leading to materials with high bioderived content. Using a two-component, one-pot procedure, foams with compression properties and densities similar to commercial soft foam were produced. It was also possible to adjust the properties of the foam by changing the ratio of isocyante:PMVL in the formulation. Although the biodegradability of the PMVL PUs has not yet been investigated, polyurethanes with structurally similar soft segments have previously been shown to be susceptible to hydrolysis by microbial esterase enzymes.[48,49,50,51] It is thus likely that these bioderived materials are also biodegradable, adding to their attractiveness as new sustainable materials.

### 5.3.2 Thermal Degradation Mechanism

As noted previously, the thermal stability of the PMVL materials studied in this work depend on a number of factors. PMVL polyol has low thermal stability due to its thermodynamic tendency to depolymerize when heated.[31] This presumably occurs via unzipping depolymerization off the end polymer and is faster for low molar mass polymers, due to a higher concentration of hydroxyl end groups.[52] The thermal stability of the PMVL TPUs (provided no residual catalyst is present) is improved because the hydroxyl end groups of the polymer have reacted with isocyanates and are no longer available to participate in depolymerization or transesterification reactions. Blocking the end group of the polymer with a urethane cannot fully prevent thermal degradation from occurring. Water molecules–either adsorbed on the surface of the polymer or generated by decarboxylation of other degradation products–can hydrolyze the PMVL backbone *in situ* leading to the formation of new alcohol endgroups.[52,53,54]

Additionally, the urethane bond is known to be reversible; in a pyrolytic environment it can reverse on heating to form isocyanates and alcohols (typically at 180 °C $\leq$ T$_d$ $\leq$ 250 °C).[55,56,57] This dissociation mechanism, and subsequent depolymerization of the resulting hydroxy-terminated PMVL is likely the major degradation pathway for PMVL PUs under pyrolysis conditions. Consistent with this interpretation, when no catalyst is present both types of PMVL PUs (foams and thermoplastics) are stable at temperatures below the expected reversion temperature of the urethane bond. Practically, information about PMVL TPU stability can be used in conjunction with DMTA data to help define the appropriate use and processing conditions for a given sample. Although the foams are chemically cross-linked and cannot be thermally processed, knowledge of the thermal stability can also be used to help design the optimal conditions for chemical recycling.

As discussed previously, one of the major factors that precludes chemical recycling of polyurethane foams is limited purity of the recovered polyol. Glycolysis and hydrolysis, two potential chemical PU recycling methods, suffer from heterogeneity in the recovered polyol itself (i.e., range of functionality and molar mass) and non-polyol contaminants from potential side reactions. This is further complicated in the presence of mixed waste streams when the recovered polyol may consist of a variety of polymer types (e.g., polyesters and polyethers). Ultimately, these recycled polyols cannot be incorporated into high-value products, as concerns over quality control arise due to batch-to-batch variation.

The recycling method described for PMVL-derived materials removes concerns over polyol heterogeneity because it directly regenerates the original MVL monomer,

bypassing recovery of the polyol entirely. This is summarized in Scheme 5.2. Because monomer is recovered in high yield and purity, it can be polymerized into PMVL with precisely targeted functionality and molar mass. This, in turn, can be used in a variety of PU applications, including new foams and elastomers, with the same integrity as the originally synthesized PVML polyol. This method truly embodies a cyclic lifecycle with little waste and low energy cost, resulting in an overall value-added approach.

**Scheme 5.2.**



MVL                      Crosslinked Foam Residue
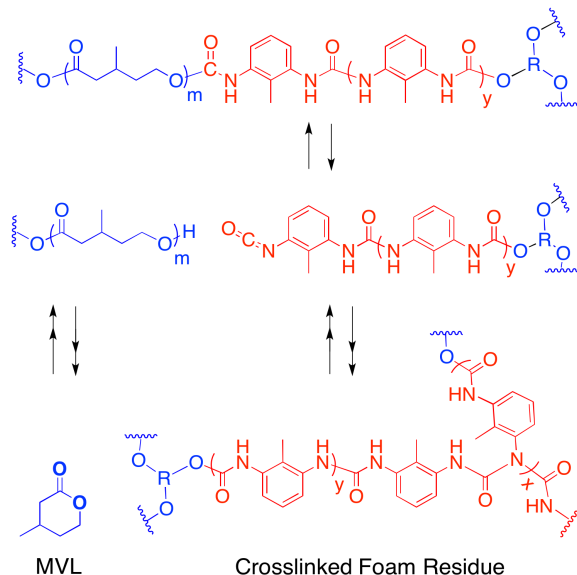
In the first step PMVL polyurethane foam degrades by reversion of the polyurethane bond to form PMVL-OH and a crosslinked isocyanate-terminated polymer. The PMVL quickly depolymerizes to yield MVL monomer, which is continuously removed by distillation. The isocyanate reacts with urethane or urea linkages in the remaining foam to for respectively, allophanate or biuret linkages.

This pyrolytic recycling method takes advantage of the polyurethane reversion and the thermodynamic tendency of PMVL to depolymerized at elevated temperatures,

demonstrated in Scheme 5.2.[31] Although it is possible to recycle foams using only amine catalysts as the blowing and gelling catalysts, the rate of PMVL depolymerization can be accelerated by the addition of $Sn(Oct)_2$, a well-known catalyst for polyester decomposition by transesterification.[40] This catalyst is often used as a gelling catalyst in industrial flexible PU foam formulations, so its incorporation into a PMVL-derived foam formulation would benefit both production and recycling. Running the distillation at 225 °C under vacuum with $Sn(Oct)_2$ present at 0.14%, over 85% MVL monomer is recovered after only 2 hours, and upwards of 96 % after ten hours.

The relatively low MVL boiling point (BP) enables us to recover monomer at high purity under the described conditions (BP ~ 35 °C at 0.1 Torr). Diaminotoluene isomers (BP~69 °C at 0.1 Torr), which could conceivably be formed from the degradation of urea bonds, do not accumulate in appreciable amounts (they are not observed in the GC chromatograph or the ^{1}H NMR spectrum of the recovered material). Likely, any isocyanate-terminated polymers formed *in situ* by reversion of the urethane bond quickly react with urea or urethane functionalities in the foam; forming a highly crosslinked material.[30,55] When considering the crosslinked foam residue that remains after the distillation, in theory, it should also be possible to recover additional foam reagents such as initiator polyols (e.g., trimethylolpropane) and amines using split phase glycolysis.[23] This would further increase the attractiveness of PMVL PU materials from a waste reduction standpoint.

## 5.4 Conclusions

In this chapter the renewable monomer MVL was used as a feedstock for the synthesis of functional polyurethane materials. Analogous to commercial polyether polyols, PMVL can be synthesized with a high degree of synthetic control. Unlike many bioderived polyols, the molecular weight and functionality of PMVL can be easily tuned to access polyols for a wide range of applications. This was demonstrated demonstrated this using a divergent approach. In one example, PMVL diols of various molar masses were reacted with MDI and an alcohol chain extender to prepare thermoplastic polyurethanes. In a second example, a PMVL triol was reacted with TDI and water to prepare flexible foams. In both cases, the properties of the resulting materials were tuned in a predictable manner by adjusting synthetic parameters (e.g. polyol molar mass and ratios of isocyanate:chain extender:polyol). Encouragingly, both the foam and TPU materials compared favorably to commercial analogs. Most excitingly, however, PMVL polyurethanes were recycled back to MVL monomer in high purity and yield using a simple pyrolysis approach. Because the moderate boiling point of the lactone facilitates its removal and separation from other degradation products, this strategy bypasses many of the technical challenges that currently preclude chemical recycling of polyurethanes on an industrial scale.

## 5.5 Experimental Details

General characterization methods are included in <u>Appendix A.</u>

### 5.5.1 Materials

Trimethylolpropane ethoxylate (4/15 EO/OH Mn ~170, Aldrich), was purchased and dried over 3A molecular sieves prior to use. MDI (Aldrich), and $Sn(Oct)_2$ (Aldrich), 1,4 -butanediol (Aldrich), 1,3-propanediol (Aldrich) and hydrogen chloride (2 M in diethyl ether, Aldrich) were used as received. Dimethylformamide (Fisher), used for PU elastomer syntheses, was distilled from BaO and passed through a column of dry activated basic alumina prior to use. Diphenyl phosphate (Acros) and 1,4 Benzene dimethanol (Aldrich) were dried under reduced pressure at room temperature for 96 h prior to use.

Solvents, including, chloroform, hexanes, tetrahydrofuran, and methanol were purchased and used as received unless otherwise noted. Round bottomed flasks and Teflon-coated magnetic stir bars used for polyol synthesis were dried in a 110 °C oven for a minimum of 6 hours prior to use. Molecular sieves (3Å, Aldrich) and basic alumina (Brockmann activity I, 50-200 um, ACROS) were dried under reduced pressure at 250 °C for 24 h and stored in an oven at 110 °C prior to use. MALDI sample preparation materials *trans*-2-[3-(4-*tert*-Butylphenyl)-2-methyl-2-propenylidene]malononitrile (DCTB, Aldrich) matrix and sodium trifluoroacetate (NaTFA, Aldrich) were purchased and used as received.

Foam reagents including, toluene diisocyanate (TDI, technical grade 80:20 mixture of 2,4 and 2,6 isomers, Aldrich); gelling and blowing catalysts *N,N*-dimethylcyclohexylamine (DMCHA, 99%, Aldrich), *N,N,N',N'',N''*-pentamethyldiethylenetriamine (PMDETA, 99%, Aldrich), and tin(II) 2-ethylhexanoate (tin octoate, 92.5-100%, Aldrich); and silicone surfactants Dabco® 5179 and 5164 (Air Products) were used as received. Ethylene oxide-capped poly(propylene oxide) polyols, Pluracol 4156 (a triol with a nominal OH number of 56), Pluracol 593 (a triol with a nominal OH number of 46), and Pluracol P1062 (a diol with a nominal OH number of 29) were a gift from BASF. Commercial foams of three different firmness ratings were purchased from McMaster Carr. The product numbers MCM00111, MCM00131, and MCM00017 correspond to firmness ratings of 1, 2, and 3, respectively.

### 5.5.2 Synthetic Details

*General Comments on PMVL Polyol Synthesis:* To prepare low molar mass PMVL polyols for use in PU materaials, an acid (either diphenyl phosphate [DPP] or HCl in diethyl ether) was used to catalyze the polymerization of MVL. Under typical conditions (bulk, 20 °C, $[MVL]_0/[Cat.] \approx 50$, $[10 < MVL]_0/[ROH] < 100$), the polymerization approached equilibrium within 3 hours. If HCl is used as the polymerization catalyst, both it and MVL monomer can be removed *in vacuo* without quenching. Because HCl is more volatile than the lactone, it can be removed rapidly from the polymer without significant PMVL depolymerization. It is important that this process is conducted at a room temperature or under mild heating because the polyol can depolymerize even

without catalyst present. The diphenyl phosphate catalyzed reactions were quenched by addition of triethylamine (TEA) in chloroform. In each case the resulting polymer solution was washed with cold aqueous sodium hydroxide (0.1 N solution, 0 °C) to remove MVL, DPP, and TEA. Under these conditions the aqueous washes hydrolyze MVL to the corresponding water-soluble hydroxy acid form but do not affect polymer structure.[58]

*Synthesis of PMVL 2700 triol:* In a 3 L round bottom flask, trimethylolpropane ethoxylate (118 grams) was dissolved in MVL (2.0 liters). Diphenyl phosphate (4.04 grams) was added and the flask capped with a septum. The solution was cooled to −5 °C using a salt bath, stirred for 4 hours, then transferred to a −20 °C freezer for an additional 8 hours. After this time triethylamine was added to quench the catalyst, then the polyol was warmed to room temperature, diluted with chloroform (4L), and then washed three times with 0.2 N NaOH and once with brine. The organic layer was dried over NaOH, filtered, then concentrated under reduced pressure to obtain PMVL (1.97 kg, 97% yield based on observed MVL conversion of 96%).

*PMVL TPU Synthesis:* Thermoplastic polyurethanes were prepared from PMVL using a two-step, one-pot procedure. (This general synthetic strategy is commonly used in the synthesis of TPUs from MDI.[59] An isocyanate-terminated prepolymer was first generated *in situ* by adding a DMF solution of $Sn(Oct)_2$ and hydroxyl terminated PMVL diol to methylene diphenyl diisocyante (MDI) at 70 °C. The ratio of PMVL to MDI was adjusted to target different compositions; however, in each case there was a large excess (>10 functional group equivalents) of isocyanate relative to alcohol. The solution was stirred for 0.5 h after the addition of PMVL to ensure the polymer was fully end

capped, then chain extender (either 1,3 propane diol or 1,4 butane diol) was added to prepare the TPU. The amount of chain extender added was adjusted to maintain a slight excess of isocyante (~1.1 eq) relative to total hydroxyl groups.

It has previously been demonstrated that this two-step strategy results in higher uniformity of the hard blocks, and consequently enhances thermal and mechanical properties, when compared to TPUs prepared using a one-pot, one-step process.[60,61] After stirring overnight at 70 °C, the reactions were cooled and the TPU samples were isolated by dropwise precipitation in methanol (this precipitation also removes $Sn(Oct)_2$ from the sample). The TPU samples thus obtained were dried in a vacuum oven prior to analysis.

*PMVL Foam Synthesis:* The procedure used to synthsize PMVL soft foams mimicked the two-component formulations commonly used industrially.[59] First, PMVL polyol, surfactant (Dabco 5164), blowing (Polycat5) and gelling (Polycat8) catalysts, and blowing agent (water) were mixed in a 10 ounce polypropylene cup (in some samples an additional catalyst, stannous octoate [$Sn(Oct)_2$], was also added). Then, toluene diisocyantate (TDI) (a 80:20 mixture of 2,4 and 2,6 isomers) was added and components were homogenized for ~10 seconds. Stirring was then stopped and the foam was allowed to rise freely. In some samples the rise profile was recorded and temperature was monitored using a thermocouple embedded in the center of the cup. Foams were allowed to cure at room temperature for at least 24 hours prior to characterization. The

top and bottom of the foams were trimmed off and samples were cut from the center of the core and used for mechanical characterization and density measurements.

*General procedure for foam synthesis:* Foams were made in clear ten ounce PETE cups. A polyol was weighed directly into the cup on an analytical balance. Catalysts, surfactants, and water were subsequently measured and added using volumetric syringes. A stand mixer with a ½" 3-blade propeller-shaped head was used to mix these components at 2,000 RPM for ~30 seconds. Once the mixture was homogenous, TDI was quickly transferred into the cup (while under continuous mixing) with a volumetric syringe. Mixing was continued for another 5-7 seconds. The foaming reaction and curing was allowed to occur at ambient room temperature inside the cup. The samples were allowed to age at room temperature for a minimum of 24 hours prior to testing.

### 5.5.3 Recycling Methods

*General Recycling Procedure*

Foam samples were cut into pieces and placed in a round bottom flask containing a stir bar (if $Sn(Oct)_2$ was not present in the original foam formulation, 0.3 % (w/w) was added to the still flask and mixed manually). Using a simple distillation setup with the receiving flask submerged in liquid $N_2$, the apparatus was placed under vacuum and the still flask was heated to 210 °C for 6 h. Material collected in the receiving flask was analyzed directly to determine percent MVL monomer recovery and purity.

*Kinetic analysis*

Using the same experimental setup as described previously, a simple distillation was run on the PMVL foams and foam samples were removed at time points 2, 5, and 10 h for subsequent infrared (IR) and elemental analysis (EA) to monitor the intensity of the PMVL ester stretch and nitrogen content, respectively. At the same time, a sample of the receiving flask material was taken for NMR and GC analysis to determine percent purity. An additional recycling progression experiment was run where the receiving flask was weighed at time points 0, 2, 5, and 10 h to monitor percent recovery throughout the depolymerization. The starting weight of the foam sample was 2.853 g with 71.2 % PMVL content (i.e., 2.031 g PMVL).

*Recycling from mixed foam sources*

In an additional control soft commercial foam [McMaster-Carr 8643K511 Firmness Rating 3, product MCM00017] was mixed with PMVL foam in a 1:1 ratio. Following a 10.5 h depolymerization experiment at 220 °C, MVL was recovered in 94.8% yield and $\geq$95% purity (determined by $^1$H NMR spectroscopy).

*Extraction experiment*

Foams were prepared using the procedure described previously and allowed to cure for 1 day at room temperature. The foam was then cut lengthwise and a sample taken from the center of the core for DSC, ATR-FTIR, and elemental analysis. The remainder of the foam was weighed and transferred to a jar where it was submerged in ~500 ml

ethyl acetate. The ethyl acetate was refreshed at 24, 48, and 96 hours. After 120 hours the foam was removed, filtered, and dried under air prior to more thorough drying in a vacuum oven. The combined ethyl acetate fractions for each sample and analyzed by GC/MS. The dried foam were each reweighed, and then characterized by IR and elemental analysis. These foams are assumed to have no residual catalyst present.

*Imbuing Foam with Sn(Oct)₂*

A PMVL foam sample from which the residual contaminants were previously removed by extraction was submerged in a solution of hexanes containing $Sn(Oct)_2$ (0.1 wt% relative to foam) for 5 days. The samples thus imbued were dried under vacuum at room temperature prior to TGA analysis.

### 5.5.4 Polyol Characterization Methods

*MALDI Analysis*

Matrix assisted laser desorption/ionization spectra were obtained using an AB Sciex 5800 MALDI TOFTOF system, equipped with two-stage time of flight (TOF) analysis and an Opti-Beam™ on-axis Nd:YAG laser. All spectra were collected in positive ion and linear operating modes. Sample spot preparation was as follows. A 20 mg/mL solution in THF of *trans*-2-[3-(4-*tert*-Butylphenyl)-2-methyl-2-propenylidene]malononitrile (DCTB) matrix and a 1 mg/mL solution in THF of sodium trifluoroacetate (NaTFA) positive ion salt were mixed 10:1, respectively, to prepare a stock matrix:salt solution. A 2 mg/mL polymer solution was prepared separately in THF. A 1 µL volume of the matrix:salt stock solution was pulled into a 10 µL syringe,

followed by 0.5 µL of the prepared polymer solution. The 1.5 µL matrix/salt/polymer solution was hand-spotted onto a MALDI sample plate and air dried before analysis.

*Viscosity measurements*

The zero-shear viscosities of the polymer samples were determined using an ARES-G2 rheometer with 25 mm parallel plates. The temperature was controlled using a nitrogen-purged oven.

## 5.5.4 TPU Characterization Methods

*Size exclusion chromatography (DMF)*

Relative molar mass and dispersity of PMVL-TPUs were determined using size exclusion chromatography with DMF containing 0.1 M LiBr as the mobile phase with a flow rate of 1 mL/min at 30 °C. Molar mass and dispersity are reported relative to poly(styrene) standards.

*In situ FT-IR*

The progress of selected PMVL TPU synthesis reactions were monitored *in situ* using a Mettler Toledo ReactIR 4000 equipped with a diamond AT-FTIR probe. These reactions were conducted under argon in a three-neck round bottom flask fit with an 24/40 IR probe adaptor but were otherwise similar to the standard TPU synthesis described previously.

*Mechanical Testing*

The TPU films for both DTMA and uniaxial extension tests were prepared by compression molding at 200 °C for 10 min to form a plaque of uniform thickness (approximately 0.5 mm). After cooling and ageing for a 24-hour period the films were cut with a dog-bone-shaped die to prepare test specimens with dimensions that were 3.0 mm (width) 10.0 mm (gauge length).

*Dynamic Mechanical Thermal Analysis*

The TPU glass transition ($T_g$) and flow temperature ($T_f$) values were identified using dynamic mechanical thermal analysis using an RSA- G2 rheometer with clamp fixtures. Dog-bone-shaped samples were cut from a compression-molded film of polymer with dimensions similar to those used for uniaxial extension and hysteresis tests. To confirm reversibility of the flow transition, additional experiments were run on an ARES-G2 rheometer with 25 mm parallel plates. The temperature was controlled using a nitrogen-purged oven. All temperature ramps were conducted at an angular frequency of 1 rad s$^{-1}$ and a strain of 1-2% unless otherwise noted. In these experiments the sample was heated through the flow temperature, cooled to 100 °C at a rate of 5 °C min$^{-1}$, then reheated at the same rate.

## 5.5.5 Foam Characterization Methods

*Density determination*

Cubes of foam were cut from the core of a foam cylinder and weighed. The dimensions of the cube then measured using a ruler and the volume calculated. The mass was

divided by the calculated volume to estimate the room temperature density. For each foam a minimum of five samples were analyzed.

*Mechanical testing*

Foam samples used for uniaxial extension tests were rectangular strips cut from the core of a cylindrical foam sample. The exact dimensions of each sample were determined using a caliper and were approximately 5.0 mm (width) 5.0 mm (thickness) and 20 mm (total sample length). Uniaxial extension measurements on foam samples were conducted using an RSA-G2 rheometer equipped with a clamp geometry suitable for a rectangular films. In the tensile test the sample was inserted in the geometry and clamped. Following this the gap was adjusted to zero the normal force. The value of this gap was taken as the gauge length of the sample (typically ~15 mm). The samples were extended at a constant crosshead velocity of 13 mm min$^{-1}$ to failure.

Foam compression measurements were conducted on foam samples of approximately 18 mm (width) by 18 mm (length) by 12 mm (height) using an RSA- G2 rheometer (TA instruments) equipped with 25 mm parallel plates. With a starting gap of approximately 12 mm, the samples were compressed to 50% strain at a constant crosshead velocity of 0.2 mm/s. The samples were immediately extended at this same velocity (0.2 mm/s) to the starting position to complete one compression cycle. To measure hysteresis, 20 such cycles were performed with no rest between cycles. The sample was then allowed to rest for 10 min, and one more cycle was performed.

In addition to the compression strengths and moduli reported in the main manuscript, the hysteresis characteristics of the foams were assessed. Qualitatively, all foams showed the same basic behavior. There was considerable hysteresis between the first and second compression steps, with only modest energy loss (area under the stress-strain curve) for subsequent cycles. After 10 min of rest, compression was comparable to the second compression step, showing good but incomplete recovery. Each compression step reached approximately the same stress at 50% strain, demonstrating similar compressive strength. The hysteresis data for a representative sample, M2700-A, are given in Figure 5.11, below.
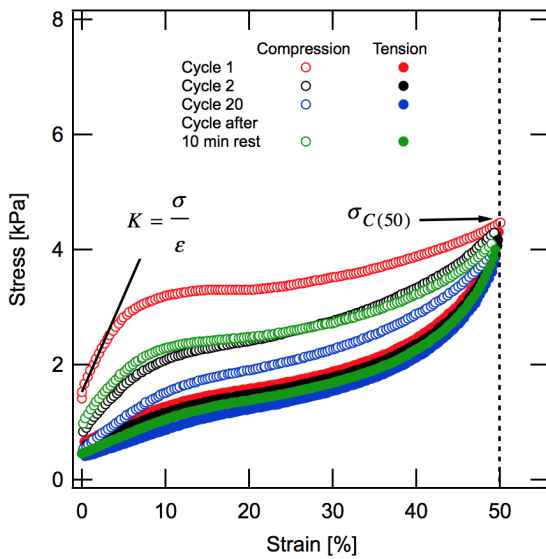


**Figure 5.11**

Representative compression data for Foam Sample M2700-A showing hysteresis during compression tests. The compression modulus was determined from the linear region of the stress-strain curve, while the compressive strength was assessed as the stress at 50 % strain. The slight starting stress is due to imperfect foam dimensions.

*Scanning Electron Microscopy*

Scanning electron microscopy (SEM) imaging was performed on a JEOL 6500 field emission gun scanning electron microscope to examine cell size and morphology. For best resolution and least sample charging, SEM analysis was performed at 5.0 kV on foam samples coated with 50 Å of platinum using a VCR high-resolution indirect ion-beam sputter coater.
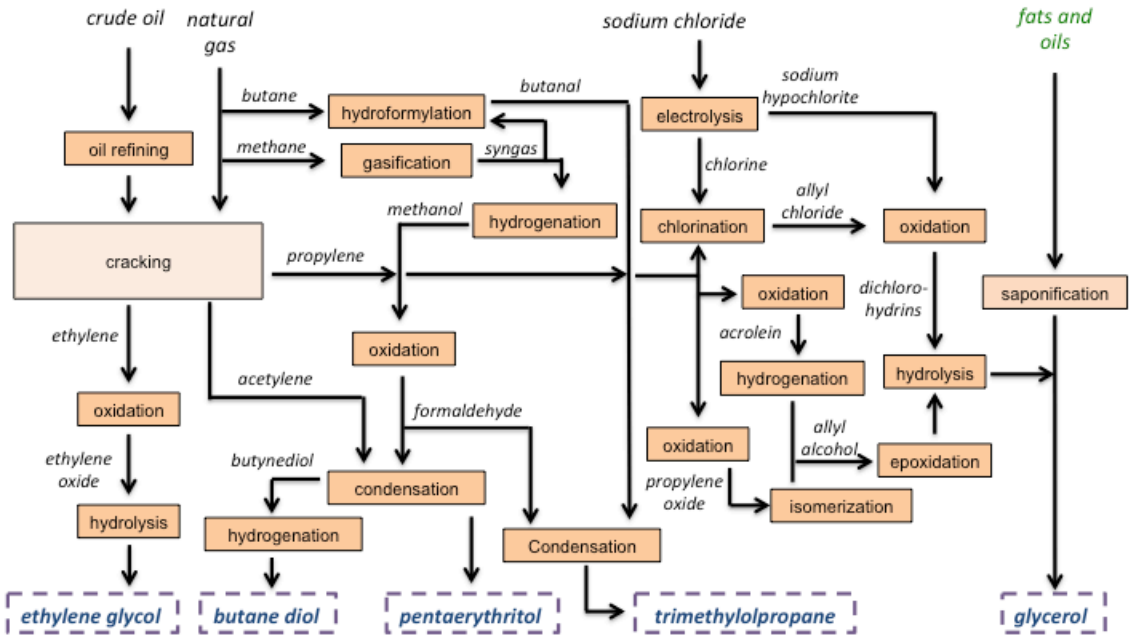
**Figure 5.12**

Major feedstocks and reactions used to produce common initiators used for industrial polyol synthesis.
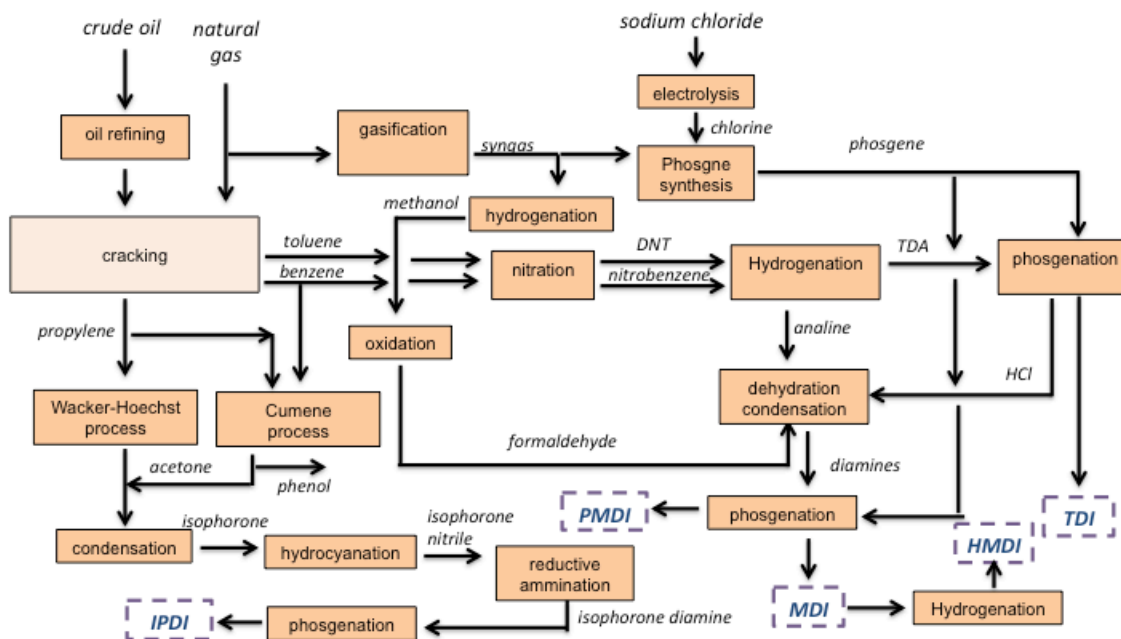
**Figure 5.13**

Major feedstocks and reactions used to produce common isocyanates used for industrial polyurethane synthesis.

**Figure 5.14**

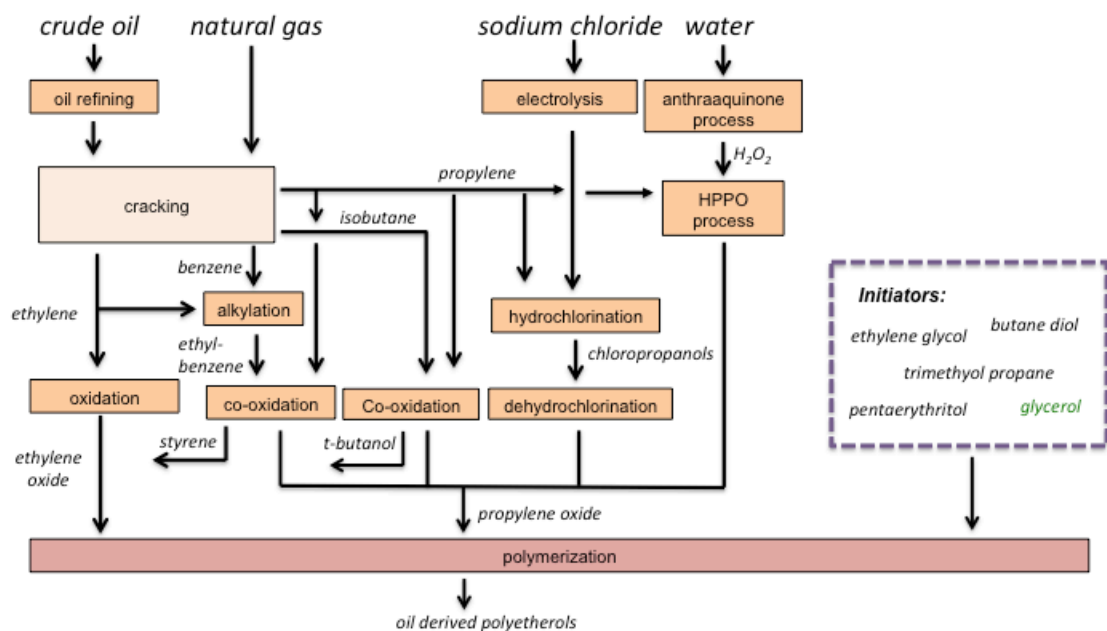Major feedstocks and reactions used to produce commercial polyetherols for polyurethane synthesis. The synthesis of the initiators is shown in Figure 5.12.

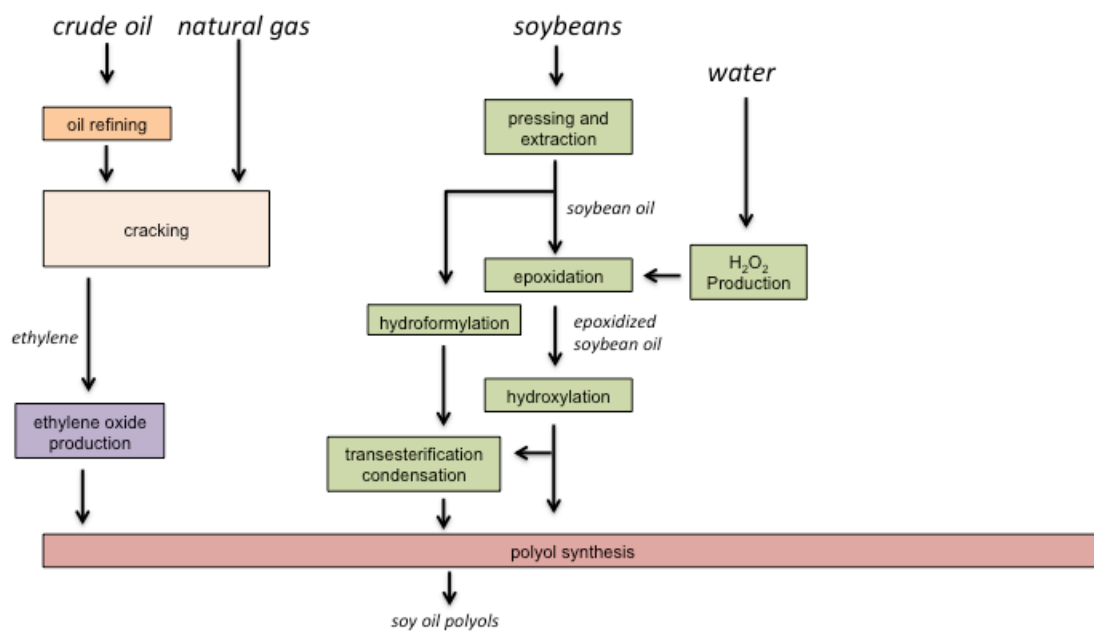**Figure 5.15**

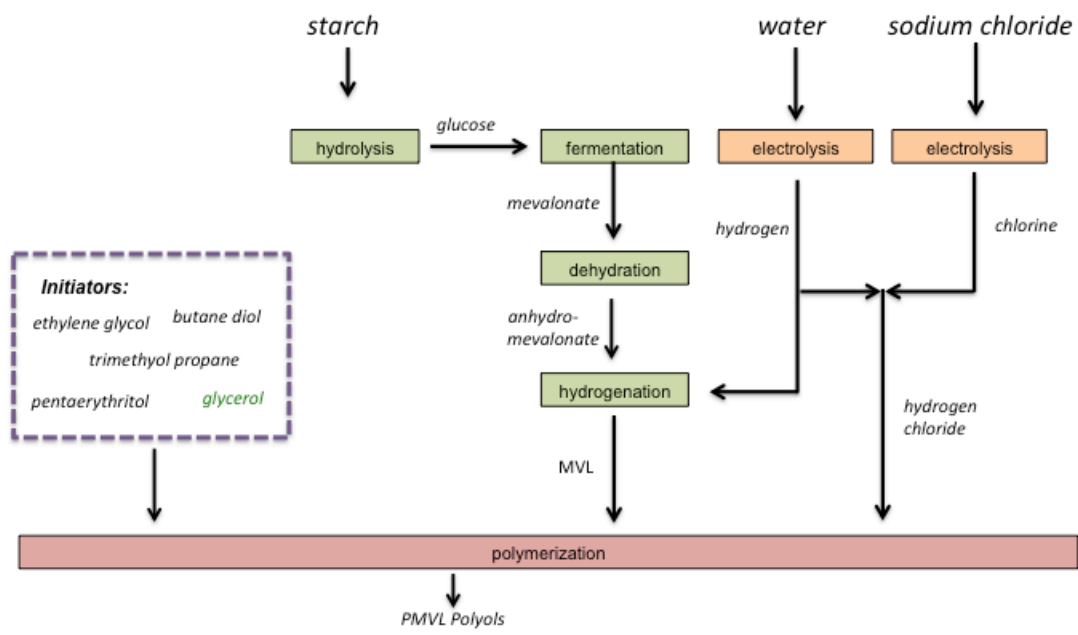Major feedstocks and reactions used to produce soy-derived polyols for polyurethane synthesis.

**Figure 5.16**

Major feedstocks and reactions used to produce PMVL polyols. The synthesis of the initiators is shown in Figure 5.12.

# 5.6 References

(1) American Chemistry Council, Economic and Satatistics Department The Economic Benefits of the U. S. Polyurethanes Industry, **2014**

(2) Helling, R. K.; Russel, D. A. Use of life cycle assessment to characterize the enviromental impacts of polyol production options *Green Chemistry* **2009**, *11,* (380-389)

(3) Hermann, B.; Carus, M.; Patel, M.; Blok, K. Currrent policies affecting the market penetration of biomaterials *Biofuels, Bioprod. Bioref.* **2011**, *5,* (708-719)

(4) Hojabri, Leila; Kong, X.; Narine, S. Fatty Acid-Derived Diisocyante and Biobased Polyurethane Produced from Vegetable Oil: Synthesis, Polymerization, and Characterization *Biomacromolecules* **2009**, *10,* (884-891)

(5) Ligadas, G.; Ronda, J. C.; Galia, M.; Cadiz, V. Plant Oils as Platform Chemicals for Polyurethane Synthesis: Current State of the Art *Biomacromolecules* **2010**, *11,* (2825-2835)

(6) de Espinosa, L. M.; Meier, M. A. R. Plant oils: The perfect renewable resource for polymer science?! *European Polymer Journal* **2011**, *47,* (837-852)

(7) Petrovic, Z. S.; Cvetkovic, I.; Hong, D.; Wan, X.; Zhang, W.; Abraham, T. W.; Malsam, J. Vegetable oil-based triols from hydrofomylated fatty acids and polyurethane elastomers *Eur. J. Lipid Sci. Technol.* **2010**, *112,* (97-102)

(8) Yeganeh, H.; Mehdizadeh, M. R. Synthesis and properties of isocyanate curable millable polyurethane elastomers based on castor oil as a renewable resource polyol *European Polymer Journal* **2004**, *40,* (1233-1238)

(9) Zhang, L.; Jeon, H.; Malsam, J.; Herrington, R.; Macosko, C. Substtuting soybean oil-based polyol into ployurethane flexible foams *Polymer,* **2007**, *48,* (6656-6667)

(10) Zhang, C.; Madbouly, S.; Kessler, M. Bio-Based Polyurethanes Prepared from Different Vegetable Oils *ACS Applied Materials and Interfaces* **2015**, *7,* (1226-1233)

(11) Tan, S.; Abraham, T.; Ference, D.; Macosko, C. W. Rigid polyurethane foams from a soybean oil-based Polyol *Polymer,* **2011**, *52,* (2840-2846)

(12) Alam, M.; Akram, D.; Sharmin, E.; Zafar, F.; Ahmad, S. Vegetable oil based eco-friendly coating materials: A review article *Arabian Journal of Chemistry* **2014**, *7,* (469-479)

(13) Beltran, A.A.; Boyaca, L.A. Preparation of Oleochemical Polyols Derived From Soybean Oil *Latin American Applied Research* **2011**, *41,* (69-74)

(14) Cinelli, P.; Anguillesi, I.; Lazzeri, A. Green synthesis of flexible polyurethane foams from liquefied lignin *European Polymer Journal* **2013**, *49,* (1174-1184)

(15) Pawlik, H.; Prociak, A.; Influence of Palm Oil-Based Polyol on the Properties of Flexible Polyurethane Foams *J. Polym. Environ* **2012**, *20,* (438-445)

(16) Zlatanic, A.; Lava, C.; Zhang, W.; Petrovic, Z. S. Effect of Structure on Properties of Polyols and Polyurethanes Based on Different Vegetable Oils *Journal of Polymer Science Part B: Polymer Physics* **2004**, *42,* (809-819)

(17) Petrovic, Z. S.; Polyurethanes from Vegetable Oils *Polymer Reviews* **2008**, *48,* (109-155)

(18) Fan, H.; Tekeei, A.; Suppes, G. J.; Hsieh F.-H. Rigid Polyurethane Foams made from High Viscosity Soy-Polyols *Journal of Applied Polymer Science* **2013**, (1623-1629)

(19) Palaskar, D.; Boyer, A.; Cloutet, E.; Alfos, C.; Cramail, H. Synthesis of Biobased Polyurethane form Oleic and Ricinoleic Acids as the Renewable Resources via the AB-Type Self-Condensation Approach *Biomacromolecules* **2010,** *11,* (1202-1211)

(20) Anastas, Paul; Eghbali, Nicolas. Green Chemistry: Principles and Practice *Chem. Soc. Rev.* **2010,** *39, (*301-312)

(21) McDonough, W.; Braungart, M.; Anastas, Paul T.; Zimmerman, J. B. Peer Reviewed: Applying the Principles of Green Engineering to Cradle-to-Cradle Design *Environmental Science & Technology* **2003,** *37,* (434A-441A)

(22) Li, Y.; Luo, X.; Hu, S. Bio-based polyols and polyurethanes Springer (Cham, Switerzerland), **2015.**

(23) Simon, D.; Borreguero, A. M.; de Lucas, A.; Molero, C.; Rodriguez, J. F. Novel polyol initiator from polyurethane recyling residue *J. Mater. Cycles Waste Manag.* **2014,** *16,* (525-532)

(24) Yang, W.; Dong, Q.; Liu, S.; Xie, H.; Liu, L.; Li, Jinhui Recycling and disposal methods for polyurethane foam wastes *Procedia Enviromental Sciences* **2012,** *16,* **(**167-175)

(25) Yanagishita, Y.; Kato, M.; Toshima, K.; Matsumura, S. Chemoenzymatic Synthesis and Chemical Recycling of Sustainable Polyurethanes *ChemSusChem* **2008**, *1,* (133-142)

(26) Simon, D.; Borreguro, A. M.; de Lucas, A.; Gutierrez, C.; Rodriquez, J.F. Sustainable Polyurethanes:Chemical Recycling to Get It E. Jimenz et al (eds.), *Enviroment and Climate Change 1.:Enviromental Chemistry of Pollutants and Wastes,* Hbd Env Chem **2015,** *32,* (229-260)

(27) Borda, J.; Pasztor, G.; Zsuga, M. Gylcolysis of polyurethane foams and elastomers *Polymer Degradation and Stability* **2000,** *68,* (419-422)

(28) Campbell, G.A.; Meluch, W.C. Polyurethane Foam Recycling. Superheated Steam Hydrolysis *Environmental Science Technology* **1976,** *10,* (182-185)

(29) Mahoney, L.R.; Weiner, S.A.; Ferris, F.C. Hydrolysis of Polyurethane Foam Waste *Environmental Science Technology* **1974,** *8,* (135-139)

(30) Dusek, K.; Spirkova, M.; Havlicek, I. Network Formation of Polyurethanes Due to Side reactions *Macromolecules* **1990**, *23,* (1774-1781)

(31) Xiong, M., Schneiderman, D.K., Bates, F.S.; Hillmyer, M. A.; Zhang, K. The production of mechanically tunable block polymers from sugar *PNAS* **2014,** *23,* (8357-8362)

(32) Sonnenschein, M. Polyurethanes: Science, Technology, Markets and Trends, John Wiley & Sons Inc. (Hoboken, NJ, US), **2015.**

(33) Tanaka, T.; Yokaoyama, T.; Yamaguchi, Y. Quantitative Study on Hydrogen Bonding between Urethane Compond and Ethers by Infrared Spectroscopy *Journal of Polymer Science A-1* **1968**, *6, (*2137-2152)

(34) Bandekar, J.; Klima, Suzzanne FTIR spectroscopic studies of polyurethanes Part 1. Bonding between urethane C-O-C groups and the NH groups *Journal of Molecular Structure* **1991,** *263,* (45-57)

(35) Sobczak, M. Synthesis and Characterization of Polyurethane Based on Oligo(ε-caprolactone) Prepared by Free-Metal  Method *Journal of Macromolecular Science, Part A: Pure and Applied Chemistry* **2011,** *48,* **(**373-380)

(36) Saralegi, A.; Rueda, L.; Fernandex-d'Arlas, B.; Mondragon, I.;Eceiza, A.; Corcuera, A., Thermoplastic polyurethanes from renewable resources: effect of soft segment chemical structure and molecular weight on morphology and final properties *Polymer International* **2013,** *62,* 1, (106-115)

(37) Bagdi, K.; Molnar, K.; Sajo, I.; Pukanszky, B., Specific interactions, structure, and properties in segmented polyurethane elastomers, *exPRESS Polymer Letters* **2011**, *5,* (417-427)

(38) Suen, W.; Paul, C. W. A Spectroscopic Analysis of the Phase Evolution in Polyurethane Foams *Macromolecules* **2005**, *38,* (9192-9199)

(39) Turner, R.B.; Nichols, J.B.; Kuklies, R.A. The Influence of Viscosity on Cell Opening of a Flexible Molded Foam *Journal of Cellular Plastics* **1989**, *25,* (117-124)

(40) Jamshidi, K.; Hyon, S.-H, and Ikada, Y. Thermal Characterization of polylactides *Polymer* **1988**, *29*, (2229-2234)

(41) Sonnenschein, M. F.; Lysenko, Z.; Brune, D. A.; Wendt, B. L.; Schrock, A. K. Enhancing polyurethane properties via soft segment crystallization *Polymer* **2005**, *46,* (10158-10166)

(42) Liow, S.W.; Lipik, V.T.; Widjaja, L.K.; Venkatraman, S. S.; Abadie, M. J.M. Enhancing mechanical properties of thermoplastic polyurethane elastomers with 1,4-trimethylene carbonate, epsilon-caprolactone, and L-lactide copolymers via soft segment crystallization *eXPRESS Polymer Letters* **2011**, *5,* (897-910)

(43) Gurusamy-Thangavelu, S. A.; Emond, S. J.; Kulshrestha, A.; Hillmyer, M. A.; Macosko, C. W.; Tolman, W. B.; Hoye, T. R. Polyurethanes based on renewable polyols from bioderived lactones *Polym. Chem.* **2012**, *3,* (2941)

(44) Petrovic, Z. S.; Cvetkovic, I.; Hong,D.; Wan, X.; Zhang, W.; Abraham, T.; Malsam, J. Polyester Polyols and Polyurethanes from Ricinoleic Acid *Journal of Applied Polymer Science* **2007**, *108,* (1184-1190)

(45) Xu, Y.; Petrovic, Z.; Das, S.; Wilkes, G. L. Morphology and properties of thermoplastic polyurethanes with dangling chains in ricinoleate-based soft segments *Polymer* **2008**, *49,* (4248-4258)

(46) Zhang, C.; Kessler, M. R. Bio-based Polyurethane Foam Made from Compatible Blends of Vegetable-Oil- Based Polyol and Petroleum-based Polyol *Sustainable Chemsitry and Engineering* **2015**, *3,* (743-749)

(47) Babb, D.A. Polyurethanes from Renewable Resources *in Synthetic Biodegradable Polymers* Springer (Berlin) **2012,** (315-360)

(48) Howard, G. T. *International Biodeterioration and Biodegradation* **2002,** *49,* (245-252)

(49) Darby, R.T.; Kaplan, Am. M. Fungal Susceptibility of Polyurethanes *Appl. Microbiol.* **1968**, *16,* (900-905)

(50) Nakajima-Kambe, T.; Shigeno-Akutsu, S.; Nomura, N.; Onuma, F.; Nakahara, T.; Microbial degradation of polyurethane, polyester polyurethanes, and polyether polyurethanes, *Appl. Microbiol. Bioechnol.* **1999**, *51,* (134-140)

(51) Dupret, I.; David, C.; Colpaert, M.; Loutz, J.-M.; Wauven, C. Biodegradation of poly(ester-urethane)s by a pure strain of micro-organisms *Macromol. Chem. Phys.* **1999**, *200*, (2508-2518)

(52) Persenaire, O.; Alexandre, M.; Degee, P.; Dubois, P. Mechanisms and Kinetics of Thermal Degredation of Poly($\varepsilon$-Caprolactone) *Biomacromolecules* **2001**, *1,* (288-294)

(53) Abe, H.; Takahashi, N.; Ju Kim, K.; Mochizuki, M.; Doi, Y. Degradation Processes of End-Capped Poly(L-Lactide)s in the Presence and Absence of Residual Zinc Catalyst *Biomacromolecules* **2004**, *5,* (1606-1614)

(54) McNeil, I.C.; Leiper, H. A. Degredation Studies of Some Polyesters and Polycarbonates–2. Polylactide: Degredation Under Isothermal Conditions, Thermal Degradation Mechanism and photolysis of the Polymer *Polymer Degradation and Stability* **1985**, *11,* (309-326)

(55) Yang, W.P.; Macosko, C. W.; Wellinghoff, S. T.; Thermal degredation of urethanes based on 4,4'-diphenylmethane diisocyanate and 1,4-butane diol (MDI/BDO) *Polymer* **1986,** *27,* (1235-1241)

(56) Lee, J. M.; Subramani, S.; Lee, Y. S.; Kim, J. H. Thermal Decomposition Behavior of Blocked Diisocyanates Derived from Mixture of Blocking Agents *Macromolecular Research* **2005,** *13,* (427-434)

(57) Delebecq. E.; Pascault, J.-P.; Boutevin, B.; Ganachaud, F. On the Versatility of Urethane/Urea Bonds: Reversibility, Blocked Isocyanate and Non-isocyanate Polyurethane *Chemical Reviews* **2013,** *113,* (60-118)

(58) Tang, D.; Macosko, C. W.; Hillmyer, M. A. Thermoplastic polyurethane elastomers from biobased poly($\delta$-decalactone) diols *Polym. Chem.* **2014,** *5,* **(**3231-3237)

(59) Woods, G. *The ICI Polyurethanes Book 2nd Ed.* **1990**

(60) Versteegen, R. M.; Kleppinger, R.; Sijbesma, R. P.; Meijer, E. W. Properties and Morphology of Segmented Copoly(ether urea)s with Uniform Hard Segments *Macromolecules* **2006,** *39,* **(**772-783)

(61) Yilgör, I.; Yilgor, E.; Wilkes, G. L. Critical parameters in designing segmented polyurethanes and their effect on morphology and properties: A comprehensive review *Polymer* **2015,** *58,* (A1-A36)

# Appendix A. General Characterization Methods

*$^1$H NMR spectroscopy*

Spectra were collected on a Varian INOVA-500 spectrometer. Chemical shifts were reported in the units of ppm and referenced to the protic impurities in the deuterated solvents (CDCl$_3$ unless noted and DMSO-d6 or DMF-d7 for PMVL TPU samples). $^1$H NMR spectra are reported as the average of at least 24 scans and were acquired using a 5 second acquisition time and a 10 second delay. $^{13}$C NMR spectra were collected on the same spectrometer operating at 126 MHz. Chemical shifts reported are referenced to middle solvent at 77.36 ppm.

*Size exclusion chromatography (THF mobile phase)*

Dispersity and mass-average molar mass were determined using a size exclusion chromatography instrument with THF as the mobile phase at 25 °C and a flow rate of 1 mL min$^{-1}$. Size exclusion was performed with three successive Phenomenex Phenogel-5 columns. The dn/dc of Pβ1 (PMVL) was determined directly using a refractometer with a 635 nm LED as the light source. Several THF solutions of a 28.0 kg mol$^{-1}$ Pβ1 diol were prepared in triplicate with known concentrations between 0.01 and 0.2 g ml$^{-1}$. The value of dn/dc, 0.0625 ml g$^{-1}$, was also used as the dn/dc for Pα1, Pγ1, and Pδ1. The dn/dc values of Pδ5 and other δ-n-alkly-substituted δ-valerolactones were estimated using size exclusion chromatography with samples of known concentration in THF. This indirect ("in-line") method uses the total area of the RI signal and the assumption of 100% of the sample mass is recovered to calculate d*n*/d*c*. We believe these

assumptions lead to negligible error in the estimated molar mass because the dn/dc values of Pβ1 samples determined using the indirect method (0.058-0.062) were similar to the value measured directly with a refractometer.

*Size exclusion chromatography (CHCl₃ mobile phase)*

The relative mass average molar mass ($M_{m-PS}$) of unpurified polymer samples was determined via size exclusion chromatography (SEC) on a liquid chromatograph (Agilent 1100 series) equipped with a HP 1047A RI detector. Polymer samples were prepared in chloroform and passed through three successive Varian PLgel Mixed-C columns with chloroform as the mobile phase at 35 °C with a flow rate of 1 mL/min. Molecular weight characteristics of the samples were referenced to polystyrene standards (Polymer Laboratories).

*Differential Scanning Calorimetry*

Differential scanning calorimetry was conducted on a TA Instruments Q-1000 DSC. Samples were analyzed in hermetically sealed aluminum pans. Typically, samples were equilibrated at −80 °C, heated to 100 °C (or in some cases 200 °C) at 10 °C min$^{-1}$, cooled to −80 at 5 °C min$^{-1}$, then reheated to 100 °C (or 200 °C) at the same rate. To ensure consistent thermal history, glass transitions and melting endotherms are reported upon the second heating cycle unless otherwise noted (e.g., foam samples). For this work we used $\Delta H_f^0$ = 139.5 J g$^{-1}$, the enthalpy of fusion for fully crystalline poly(ε-caprolactone), as a reference value to calculate copolymer crystallinity.[1]

*Small Angle X-ray Scattering*

SAXS analysis was performed at the Advanced Photon Source (APS) at Argonne National Laboratory in beamline Sector12-ID-B. Unless otherwise noted, samples were cut from plaques compression molded at temperatures above the poly(lactide) glass transition and were annealed at 120 °C for 12 hours and 60 °C for 8 hours prior to cooling to room temperature. Experiments were conducted using a sample to detector distance of 360 cm and energy of 13.9984 keV. Scattering intensities were monitored using a silicon pixel Pilatus detector.

Additional SAXS experiments were performed at the DuPont-Northewstern Dow Collaborative Access Team (DND-CAT) Synchrotron Research Center located at Sector 5 of the APS. For these experiments the energy was 16.4000 keV, and scattering intensities were monitored using a CCD area detector at a sample to detector distance of 850 cm. To obtain 1-D spectra the 2-D scattering patterns were azimuthally integrated to give the scattering intensity with respect to the scattering vector ($q$).

Still other SAXS experiments were performed at the University of Minnesota Characterization Facility on a home-built 6-meter instrument operating at a sample distance of 405 cm. The instrument was fitted with a Bruker Hi-Star multi-wire area detector, a Rigaku Ultrex 18kw generator with copper radiation x-rays of monochromatic wavelength = 1.54 Å, and a thermally controlled sample chamber capable of accessing temperatures between −20 and 200 °C.

*Dynamic Mechanical Analysis (shear, parallel plates)*

The order–disorder transition temperatures of block polymers were determined by dynamic mechanical analysis using a TAInstruments DHR-3 instrument equipped with electrically heated 25 mm plates and a nitrogen-purged sample chamber. Alternatively, the order–disorder transition temperatures were identified using dynamic mechanical analysis using an ARES-G2 rheometer with 25 mm parallel plates. For these experiments the temperature was controlled using a nitrogen-purged oven. All temperature ramps were conducted at an angular frequency of 1 rad $s^{-1}$ and a strain of 1-2% unless otherwise noted. Dynamic strain sweeps were conducted at temperatures near the $T_{ODT}$ to ensure the measurements were in the linear regime. Isothermal frequency sweeps were also conducted near the $T_{ODT}$ to corroborate the temperature ramp data. Dynamic mechanical analysis experiments on homopolymer and statistical copolymer samplers were conducted on a TA Instruments ARES-G2 rheometer using 8 mm plates. The sample temperature was controlled using an oven cooled with liquid nitrogen.

*Compression Molding*

Specimens for mechanical tests were prepared by compression molding the triblock or multiblock polymer between two Teflon sheets at an elevated temperature (usually 120 °C for samples containing atactic PLA blocks and 190 °C for samples containing isotactic PLLA blocks) to form a plaque of uniform thickness (~0.5 mm). After cooling and ageing for a 24-hour period the plaques were cut with a dog-bone-shaped die to prepare test specimens with dimensions that were 3.0 mm (width) 10.0 mm (gauge length).

*Uniaxial Extension Tests*

Tensile measurements were performed on a Shimadzu Autograph AGS-X Series tensile tester (Columbia, MD). All samples were elongated at constant crosshead velocity (either 50, 60 or 110 mm min$^{-1}$ as noted) until failure.

*Hysteresis testing of TPE and TPU samples*

Hysteresis tests were conducted in triplicate using a Shimadzu Autograph AGS-X Series tensile tester. Samples were elongated at a constant crosshead velocity (typically 110 mm min$^{-1}$ or 60 mm min$^{-1}$) to an applied strain (typically 67%) and relaxed at the same rate. For a few samples, tensile hysteresis experiments were conducted on a RSA-G2 rheometer (TA Instruments).

*Density Determination*

For most samples densities were measured using a temperature regulated density gradient column prepared from isopropanol and diethylene glycol and were taken as the average of a minimum of 6 trials. The column was calibrated using floats of known density and the temperature was regulated at 23 °C using a water bath. Small, bubble-free spheres of polymer were introduced to the column and allowed to equilibrate for 1 h. The height of each sample was recorded and the density was calculated based on calibration standards.

Using this method, the density of P6MCL was determined to be 0.97 g cm$^{-3}$. The densitity value of semicrystalline poly(ε-caprolactone) was taken as the value previously measured by otheres (1.15 g cm$^{-3}$ for PCL).[2,3] The amorphous density of PCL was taken

as the theoretical value, 1.02 g cm$^{-3}$.[4]   Because poly($\varepsilon$-caprolactone) and poly($\varepsilon$-decalactone) have only negligable differences in density for the block statistical copolymers discussed in Chapter 2 and in , we used a constant value (1.02 g cm$^{-3}$) to calculate midblock volume fraction regardless of compostion.[5] Based on the thermal expansion coeffecients for PLA and PCL, we  estimate that for symetric ($f_{LA} \approx$ 0.5) block polymers the use of these room temperature density values leads to errors of $\leq 5\%$  in volume fraction at higher temperatures; this error is predicted to be more significant in samples containing a majority PLA.[6,7]

*Thermogravimetric analysis*

Thermogravimetric analysis (TGA) was performed on a Perkin Elmer Diamond TGA/DTA or on a TA Instruments Q500 with typical sample size of 10–15 mg.  In dynamic heating experiments samples were heated in aluminum pans under nitrogen or air (as indicated) at a rate of 10 °C min$^{-1}$ to a final temperature of 450 °C. In isothermal experiments samples were heated to the annealing temperature a rate of 20 °C min$^{-1}$, then annealed for the at least four hours.

*Elemental Analysis*

All elemental analyses (HCN test) were performed in duplicate by Midwest Microlab, LLC (Indianapolis, IN).

*AT-FTIR*

 Fourier transform infrared (FTIR) spectra were obtained using a Bruker Alpha Platinum ATR-FTIR instrument with a diamond single bounce crystal. The data

reported are the average of at least 16 scans and were acquired using a 4 s acquisition time.

*GC/MS analysis*

Tandem gas chromatography/low resolution mass spectrometry (GC/MS) was performed on a mass selective detector that used electron impact (EI) ionization. Samples were prepared in ethyl acetate with a concentration close to ~0.1 mg/ml.

# References

(1) Guo Q. and Groeninckx G., Crystallization Kinetics Poly(e-caprolactone) in Miscible Thermosetting Polymer Blends of Epoxy Resin and Poly (e-caprolactone), *Polymer*, **2001,** *42,* (8647-8655)

(2) Bittiger, H.; Marchessault, R. H. Crystal Structure of Poly($\varepsilon$-Caprolactone) *Acta Cryst.* **1970**, *B26,* (1923-1927)

(3) Furuhashi, Y.; Sikorski, P.; Atkins, E.; Iwata, T.; Doi, Y.  Structure and Morphology of the Aliphatic Polyester Poly($\delta$-valerolactone) in Solution-Grown Chain-Folded Lamellar Crystals *Journal of Polymer Science B Polymer Physics* **2001**, *39,* (2622-2634)

(4) Lovinger, A. J.; Hadden, B. J.; Padden, F. J.; Mirau, P. A. Morphology and Properties of Polycaprolactone-Poly(dimethyl siloxane)-Polycaprolactone Triblock copolymers  *Journal of Polymer Science Part B Polymer Physics* **1993**, *31,* **(**115-123)

(5) Martello, M. T.; Burns, A.; Hillmyer, M. Bulk Ring-Opening Transesterification Polymerization of the Renewable $\delta$-Decalactone Using an Organocatalyst. *ACS Macro Lett.*, **2012,** *1,* (131–135)

(6) Henton, D. E.; Gruber, P.; Lunt, J.; Randall, J. Polylactic Acid Technology in *Natural Fibers, Biopolymers, and Biocomposites* Mohanty, A. K.; Misra, M.; Drzal, L. T.,  Ed.;  CRC: Boca Raton, Fl **2005, (**527-528)

(7) Crescenzi, V.; Manzini, G.; Calzolari, G.; Borri, C. Thermodynamics of Fusion of Poly-$\beta$-Propiolactone and Poly-$\varepsilon$-Caprolactone Comparative analysis of the Melting of Aliphatic Polylactone and Polyester Chains *European Polymer Journal* **1972**, *8,* (449-463)

# Appendix B. Statistical Copolymers

For the simple case of the polymerization of two monomers that conform to a terminal reactivity model, the relationship between the feed ratio and the mole fraction of a given component in the polymer can be described using by the copolymer composition equation[2]:

$$F_1 = \frac{r_1 f_1^2 + f_1 f_2}{r_1 f_1^2 + 2 f_1 f_2 + r_2 f_2^2} \tag{B1}$$

In this equation $F_1$ and $f_1$ are the mole ratio of monomer 1 in the polymer and feed, respectively. The variables $r_1$ and $r_2$ are ratios of the rate constants of self-propagation to cross propagation ($k_{p1,1}$ / $k_{p1,2}$ and $k_{p2,2}$ / $k_{p2,1}$) for monomer 1 and monomer 2, respectively. Linear forms of this equation can be used to determine reactivity ratios provided the relationship between $F_1$ and $f_1$ are known for a wide range of monomer feed ratios. Two of the most common methods for determining reactivity ratios for two component systems, the Fineman-Ross (F-R) method and the Kelen-T*üdös* (K-T) method follow this general strategy; while both methods generally require that the polymer composition be determined at low conversion (<5%), a modified from of the K-T method has been developed for higher conversion cases.[66] The analogous model for terpolymers was developed by Alfrey and Goldfinger (AG) and later modified by

others.[67,68] To predict the composition of a terpolymer using the (AG) model the feed composition and six reactivity ratios, two for each pair of monomers, are required.

In addition to the copolymers of ε-caprolactone and ε-decalactone, described in Chapter 2, a number of other copolymer sets were investigated. These include: the statistical copolymers of δ-valerolactone and ε-decalactone, the statistical copolymers of δ-valerolactone and ε-caprolactone, and the statistical terpolymers of ε-caprolactone, ε-decalactone, and δ-valerolactone. These studies are described in this Appendix.

## B.1 Copolymers of ε-Caprolactone and ε-Decalactone

In chapter 2 we showed the reacticity ratios for the copolymerization of ε-caprolactone and ε-decalactone favor the addition of ε-caprolactone regardless of the chain end structure ($r_{CL} = 5.9 \pm 0.7$ and $r_{DL} = 0.03 \pm 0.01$). These reactivity ratios favor the formation of a gradient microstructures. To explore this we looked at the sequence length distributions of poly(ε-caprolactone-*co*-ε-decalactone) statistical copolymers using ^{13}C NMR spectroscopy. Samples were prepared by dissolving ≈ 100 mg of copolymer in a 1-2 ml of $CDCl_3$. Once samples had been inserted into NMR tubes, they were injected with 100 μL of a 3.7 mM Chromium(III) acetylacetonate solution and mixed. Integral identities were determined by adding 10 weight % homopolymer to a 50 mol % copolymer.[1] In samples where homopolymer had been added, peaks with obvious increases in intensity were assigned as having resulted from caprolactone-caprolactone (CC) or decalactone-decalactone (DD) sequences. Caprolactone-decalactone (CD) and decalactone-caprolactone (DC) peaks were determined on the basis of proximity to the
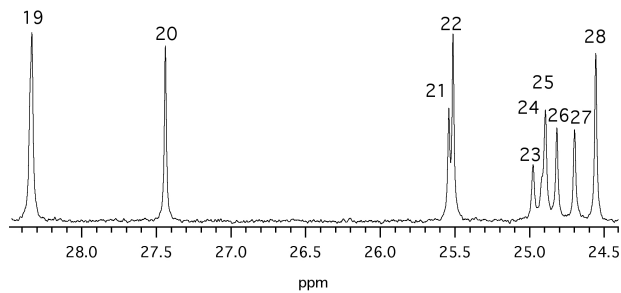
respective homopolymer peaks. Relevant regions of a ^{13}C spectrum of a representative PCD copolymer are shown below in Figure B.1 a-f, and corresponding peak assignments are given in Table B.1. Microstructures were analyzed using the method outlined by Qiu *et al.*[2]

**(a)**
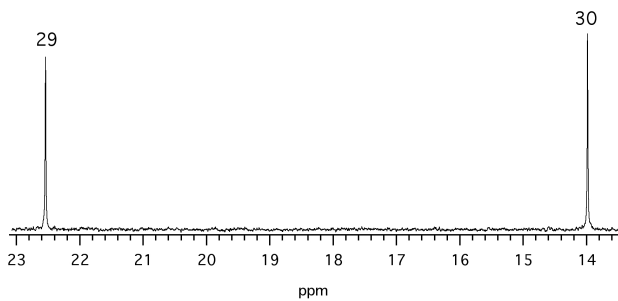


**(b)**



**(c)**
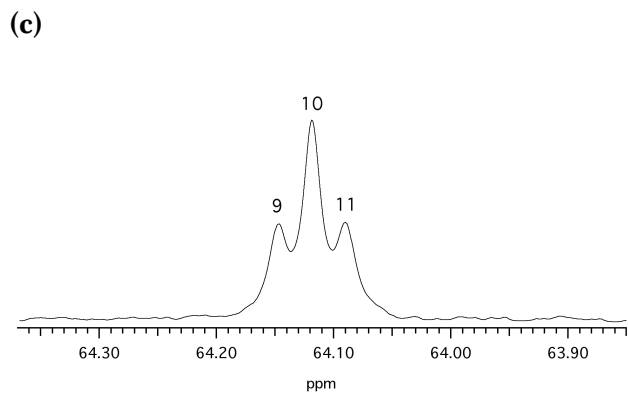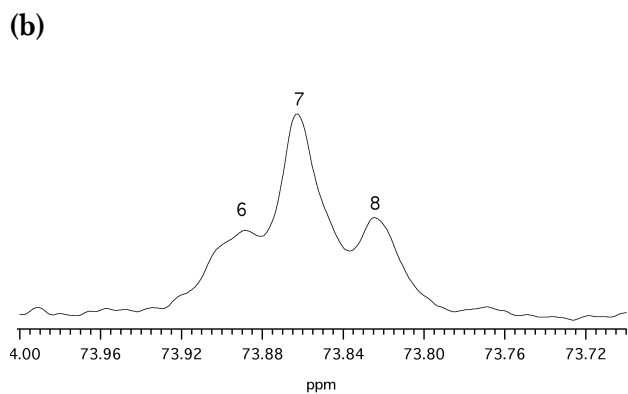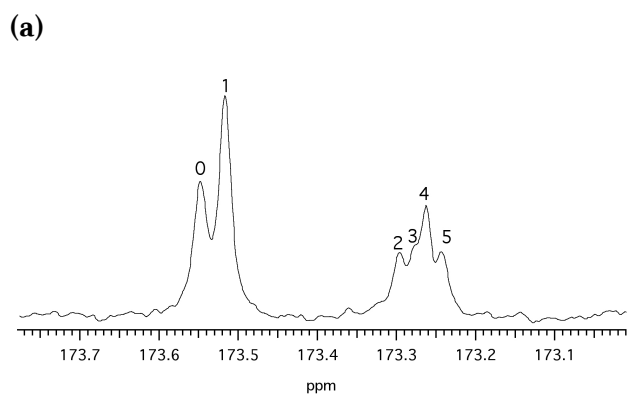
**(d)**
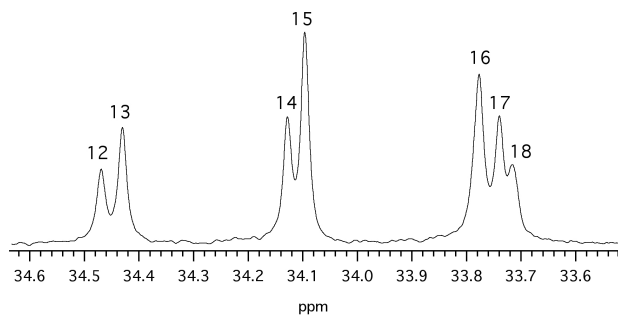


**(e)**



**(f)**



**Figure B.1**

a-f. Relevant regions of a 13C NMR spectrum of a representative a poly(ε-caprolactone-co-ε-decalactone) copolymer showing CC, DD, DC, and CD resonances. Assignments are given in Table B.1.

**Table B.1**

$^{13}$C Peak assignments for PCD copolymers

| Peak Number(s) | Sequence Assignment |
|:---:|:---:|
| 0 | DC |
| 1 | CC |
| 2+4+5 | DC |
| 3 | DD |
| 6+8 | CD |
| 7 | DD |
| 9+11 | DC |
| 10 | CC |
| 12 | DD |
| 13 | CD |
| 14 | DC |
| 15 | CC |
| 16 | CD+DD |
| 17 | CD |
| 18 | DD |
| 19 | CD+CC |
| 20 | DC+DD |
| 21 | DC |
| 22 | CC |
| 23+24+25+26 | 2DD +2DC |
| 27 | DC |
| 28 | CC |
| 29 | DD+DC |
| 30 | DD+DC |

Using this method the probability of addition values was determined for several different compositions of copolymers.

$$P_{CC} = \frac{[CC]}{[CC]+[CD]} \tag{B2}$$

$$P_{CD} = \frac{[CD]}{[CC]+[CD]} \tag{B3}$$

$$P_{DC} = \frac{[DC]}{[DC]+[DD]} \tag{B4}$$

$$P_{DD} = \frac{[DD]}{[DC]+[DD]} \tag{B5}$$

From these results the average sequence lengths were estimated:

$$\bar{v} = \frac{1}{P_{CD}} \tag{B6}$$

$$\bar{\mu} = \frac{1}{P_{DC}} \tag{B7}$$

Here $\bar{v}$ and $\bar{\mu}$ represent the average PCL and PDL sequence lengths, respectively, in a poly($\varepsilon$-caprolactone-*co*-$\varepsilon$-decalactone) copolymer.

These results were compared to those predicted using the known composition and experimentally determined reactivity ratios ($r_C$ and $r_D$) reported in Chapter 2.

$$\bar{v} = 1 + r_C \frac{[C]}{[D]} \tag{B8}$$

$$\bar{\mu} = 1 + r_D \frac{[C]}{[D]} \tag{B9}$$

The probability of addition values were also calculated:

$$P_{CC} = \frac{[C]\, r_C}{[C]\, r_C + [D]} \tag{B10}$$

$$P_{CD} = \frac{[D]}{[C]\, r_C + [D]} \tag{B11}$$

$$P_{DD} = \frac{[D]\, r_D}{[D]\, r_D + [C]} \tag{B12}$$

$$P_{DC} = \frac{[C]}{[D]\,r_D + [C]} \tag{B13}$$

The calculated probability and sequence lengths are compared to the experimentally

observed values for a number of compositions in Table B2.

**Table B.2**

**Sequence length analyses for representative poly(ε-caprolactone-*co*- ε-decalactone) statistical copolymers**

| [a]$F_C$ | [b]$P_{CC}$ | [b]$P_{CD}$ | [b]$P_{DC}$ | [b]$P_{DD}$ | [c]$\bar{\nu}$ | [d]$\bar{\mu}$ |
|---|---|---|---|---|---|---|
| 0.592 | 0.643 | 0.357 | 0.576 | 0.424 | 2.80 | 1.74 |
| | (0.895) | (0.105) | (0.980) | (0.020) | (9.52) | (1.02) |
| 0.785 | 0.807 | 0.193 | 0.843 | 0.157 | 5.18 | 1.19 |
| | (0.956) | (0.044) | (0.992) | (0.008) | (22.70) | (1.01) |
| 0.874 | 0.887 | 0.112 | 0.927 | 0.072 | 8.93 | 1.08 |
| | (0.975) | (0.024) | (0.996) | (0.004) | (41.40) | (1.00) |

[a]Compositions were determined using ^{13}C NMR spectroscopy. Values indicated in parentheses are theoretical compositions used to calculate sequence lengths and probability of addition. [b]Probability of addition values determined using ^{13}C NMR spectroscopy. Values indicated in parentheses were calculated from composition and experimentally determined reactivity ratios. [c]Average CL sequence length calculated from probability of addition determined using ^{13}C NMR spectroscopy. Values indicated in parentheses were calculated from composition and experimentally determined reactivity ratios. [d]Average DL sequence length calculated from probability of addition determined using ^{13}C NMR spectroscopy. Values indicated in parentheses were calculated from the feed composition using experimentally determined reactivity ratios.

Although the calculated average CL sequence length, $\bar{\nu}$, is correctly anticipated to

increase as $f_C$ approaches 1.0, the reactivity ratios consistently overestimate this value

compared to the results observed using ^{13}C NMR spectroscopy. Although more work is

necessary to explain this difference, the moderately high disparities of the polymers

used for sequence length analysis could indicate some randomization of the polymer microstructure by intermolecular transesterification. Additionally, as shown in Table B.3, there are slight differences in the compositions determined using $^{13}$C NMR spectroscopy and the compositions determined using $^1$H NMR spectroscopy, this may indicate some error in the model we used to analyze polymer microstructure.

**Table B.3**

**Molecular characteristics of poly(ε-caprolactone-*co*- ε-decalactone) statistical copolymers detailed in Table B.2**

| Sample ID | [a]Target $M_n$ (kg mol$^{-1}$) | [b]$F_C$ | [c]$F_C$ | [d]Reaction Time (min) | [e]$M_n$ (kg mol$^{-1}$) | [e]Đ |
|---|---|---|---|---|---|---|
| 1 | 16 | 0.711 | 0.592 | 40 | 25.5 | 1.89 |
| 2 | 16 | 0.809 | 0.785 | 40 | 33.8 | 1.66 |
| 3 | 15.5 | 0.894 | 0.874 | 40 | 35.1 | 1.68 |

[a]Target molar mass calculated from mole ratio of monomer to initiator. [b]Mole percent calculated by 1H NMR spectroscopy. [c]Mole fraction ε-caprolactone in polymer determined using 13C NMR spectroscopy. [d]Reactions carried out in 180˚C oil baths. [e]Measured via SEC with poly(styrene) standards. The molar mass using this method is about double the expected molar mass due to the difference in hydrodynamic volume of PDL and PS.

**Table B.4**

**Thermal Characteristics of representative poly(ε-caprolactone-*co*- ε-decalactone) statistical copolymers**

| [a]$F_{CL}$ | [a]$M_N$ | [b]$T_M$ (°C) | [b]$T_g$ (°C) | [c]X (%) |
|---|---|---|---|---|
| 1.00 | 22.1 | 56.8 | −62 | 49 |
| 0.96 | 21.6 | 48.5 | −62 | 39 |
| 0.94 | 24.8 | 52.5 | −61 | 45 |
| 0.92 | 22.3 | 49.9 | −62 | 39 |
| 0.91 | 21.5 | 44.8 | −62 | 39 |
| 0.89 | 15.5 | 44.6 | −62 | 34 |
| 0.88 | 20.2 | 39.2 | −63 | 29 |
| 0.85 | 21.2 | 40.8 | −61 | 27 |
| 0.77 | 20.5 | 18.2 | −64 | 16 |
| 0.74 | 16.1 | 21.3 | −64 | 19 |
| 0.73 | 17.9 | 19.5 | −63 | 1.2 |
| 0.71 | 16.0 | 18.7 | −62 | 5.5 |
| 0.69 | 19.4 | - | −62 | - |
| 0.63 | 18.3 | - | −62 | - |
| 0.60 | 17.7 | - | −60 | - |

[a]Copolymer compositions and number average molar masses were determined using ^{1}H NMR spectroscopy. [b]Thermal characteristics were determined using DSC and are reported for the second heating (5 °C min^{-1}). [c]X was found using the reference heat of fusion (139.5 J g^{-1}) for fully crystalline poly(caprolactone).
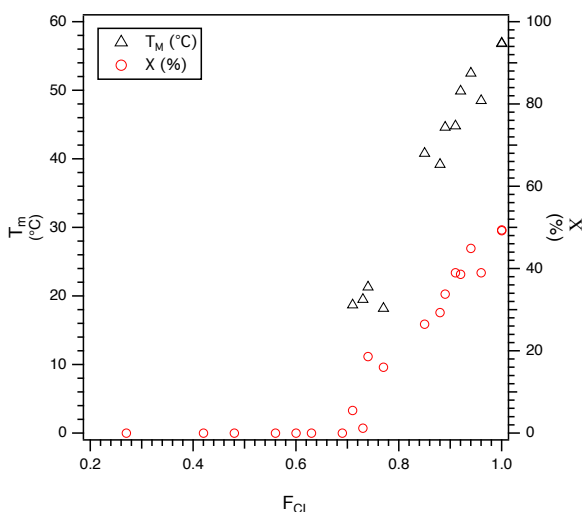
**Figure B.2**

Dependence of $T_m$ and X on composition for PCD copolymers. Melting point are the values of the exotherm peak maximum. $T_m$ values were determined by DSC on the second heating ramp with a rate of 5 °C min-1. Crystallinity was estimated using a reference enthalpy of fusion of 139.5 J g$^{-1}$.

## B.2 Copolymers of δ-Valerolactone and ε-Decalactone

The difference in ring size of δ-valerolactone and ε-caprolactone can result in a catalyst-dependent change in the homopolymerization rates of these monomers, however, the nucleophilicity of the poly(δ-valerolactone) and poly(ε-caprolactone) primary alcohol end groups are nearly identical.[3,4,5] The copolymerization of δ-valerolactone with ε-decalactone should thus be qualitatively similar to the copolymerization of ε-caprolactone with ε-decalactone. Unlike ε-caprolactone and ε-decalactone, the equilibrium monomer concentration for the homopolymerization δ-valerolactone is appreciable at relevant reaction temperatures.[3,6,7] Because of this, the polymer composition at equilibrium can noticeably diverge from feed composition under

conditions that favor depolymerization. Provided the copolymerization is conducted in the bulk at 120 °C, this effect is minimized.

Whereas poly(ε-decalactone) is fully amorphous poly(δ-valerolactone) and poly(ε-caprolactone) are both semicrystalline with melting temperatures near 60 °C. For both poly(ε-decalactone-co-ε-caprolactone) (PCD) (discussed in Chapter 2) and poly(ε-decalactone-co-δ-valerolactone) (PVD) (detailed below), the percent crystallinity and melting point decrease with the addition of ε-decalactone; at a critical composition, 35% and 40% for PCD and PVD, the polymers are amorphous. This behavior is similar to the behavior of other poly(ε-caprolactone) copolymers that containing similar noncrystallizable comonomers.[8,9,10]

## B.3 Copolymers of δ-Valerolactone and ε-Caprolactone

In the case of poly(δ-valerolactone-co-ε-caprolactone) (PCV) all compositions are semicrystalline; however, a significant depression of melting temperature is observed at nearly equimolar composition. This is consistent with previous reports.[11,12,7]

**Table B.5**

Thermal Characteristics of representative poly(δ-valerolactone-*co*-ε-decalactone) statistical copolymers

| [a]$F_{DL}$ | [a]$F_{VL}$ | [b]$T_M$ (°C) | $\Delta H$ (J g$^{-1}$) | $T_g$ (°C) | [c]$X$ (%) |
|---|---|---|---|---|---|
| 0.17 | 0.84 | 53.4 | 51.4 | −62 | 37 |
| 0.22 | 0.78 | 38.0 | 46.3 | −59 | 33 |
| 0.32 | 0.69 | 23.1 | 30.0 | −58 | 22 |
| 0.55 | 0.45 | | | −59 | |
| 0.68 | 0.32 | | | −57 | |
| 0.62 | 0.38 | | | −59 | |
| 0.67 | 0.34 | | | −58 | |
| 0.60 | 0.40 | | | −60 | |
| 0.72 | 0.28 | | | −56 | |
| 0.78 | 0.22 | | | −54 | |
| 0.84 | 0.16 | | | −55 | |
| 0.92 | 0.08 | | | −55 | |
| 1.00 | | | | −55 | |

[a]Copolymer compositions and number average molar masses were determined using $^1$H NMR. All polymer samples had similar number average molar masses, approximately 15-20 kg mol$^{-1}$.
[b]Thermal characteristics were determined using DSC and are reported for the second heating (5 °C min$^{-1}$). [c]$X$ was estimated using the reference heat of fusion (139.5 J g$^{-1}$) for fully crystalline poly(caprolactone).

**Table B.6**

**Thermal Characteristics of representative poly(δ-valerolactone-*co*- ε-caprolactone) statistical copolymers**

| [a]$F_{CL}$ | $F_{VL}$ | [b]$T_M$ (°C) | [b]$\Delta H$ (J g$^{-1}$) | [b]$T_g$ (°C) | [c]$X$ (%) |
|------|------|------|------|------|------|
| 1.00 | 0.00 | 57 | 68.7 | −62 | 49.2 |
| 0.90 | 0.11 | 46 | 59.9 | −62 | 42.9 |
| 0.82 | 0.18 | 35 | 60.2 | −64 | 43.1 |
| 0.80 | 0.20 | 27 | 60.0 | −64 | 43.0 |
| 0.79 | 0.21 | 38 | 49.4 | −65 | 35.4 |
| 0.79 | 0.21 | 31 | 64.2 | −61 | 46.0 |
| 0.66 | 0.34 | 27 | 56.8 | −64 | 40.7 |
| 0.60 | 0.40 | 20 | 59.8 | −60 | 42.9 |
| 0.59 | 0.41 | 20 | 60.0 | −60 | 43.0 |
| 0.54 | 0.46 | 22 | 50.4 | −64 | 36.1 |
| 0.48 | 0.52 | 21 | 56.5 | −64 | 40.5 |
| 0.46 | 0.54 | 21 | 51.2 | −64 | 36.7 |
| 0.35 | 0.65 | 24 | 49.8 | −63 | 35.7 |
| 0.34 | 0.66 | 23 | 46.8 | −64 | 33.5 |
| 0.31 | 0.69 | 27 | 62.7 | −63 | 44.9 |
| 0.19 | 0.81 | 36 | 51.3 | −62 | 36.8 |
| 0.11 | 0.89 | 43 | 67.5 | −61 | 48.4 |
| 0.08 | 0.92 | 48 | 65.9 | −60 | 47.2 |
| 0.00 | 1.00 | 55 | 67.8 | −60 | 48.6 |
| 0.00 | 1.00 | 54 | 69.5 | −56 | 49.8 |

[a]Copolymer compositions and number average molar masses were determined using ^{1}H NMR. All polymer samples had similar number average molar masses, approximately 15-20 kg mol$^{-1}$. [b]Thermal characteristics were determined using DSC and are reported for the second heating (5 °C min$^{-1}$). [c]$X$ was found using the reference heat of fusion (139.5 J g$^{-1}$) for fully crystalline poly(caprolactone).
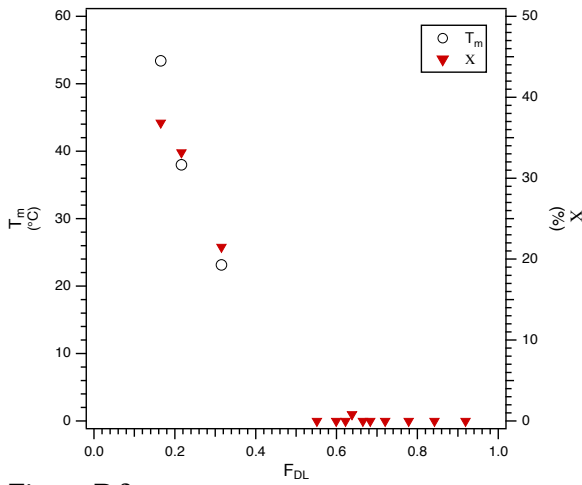
**Figure B.3**

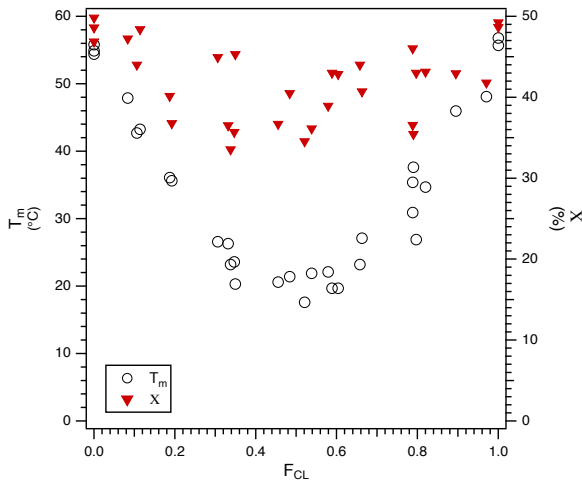Dependence of crystallinity and melting point on poly(ε-decalactone)-co–poly(δ-valerolactone) composition



**Figure B.4**

Dependence of crystallinity and melting point on poly(ε-caprolactone)-co–poly(δ-valerolactone) composition

## B.4 Terpolymers of δ-Valerolactone, ε-Decalactone, and ε-Caprolactone

The crystallinity and maximum peak melting temperature of a number of copolymers and terpolymers are plotted in the ternary diagrams in Figures B.5. Although we acknowledge there is no fundamental significance to peak melting temperature[13] [Crist 2003] we have chosen to use these data for Figure B.5 as the final melting temperature is not easily identified for samples with low crystallinity or broad melting transitions. In both ternary diagrams the contour lines connect samples with similar thermal properties. At fixed ε-decalactone content the terpolymers behave similarly to the CV copolymers, that is, the melting temperature is minimized as the polymers approach an equimolar ratio of δ-valerolactone to ε-caprolactone.
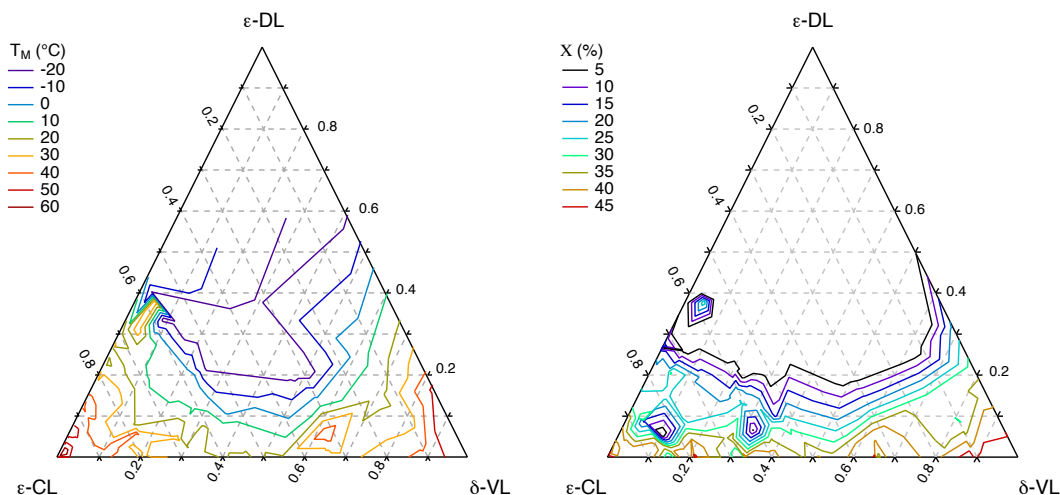


**Figure B.5**

(left) Ternary diagram showing the melting points of poly(ε-caprolactone-*co*-δ-valerolactone-*co*-ε-decalactone) terpolymers over a range of compositions. The contour lines connect polymer samples with similar melting points. (right) Ternary digramn for the same samples showing crystallinity over a wide range of compositions. The bottom edge is representative of poly(ε-caprolactone-*co*-δ-valerolactone) while the left and right sides represent poly(ε-caprolactone-*co*-ε-decalactone) and poly(δ-valerolactone-*co*-ε-decalactone), respectively. The melting point and melting enthalpy of each sample was determined by DSC on the second heating ramp at a rate

of 5 °C min$^{-1}$ and is taken as the peak maximum. The apex of the plot contains amorphous polymers comprised of a majority ε-decalactone.
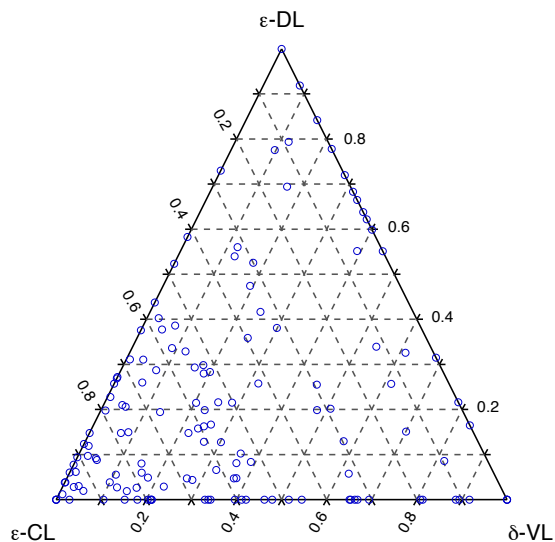


**Figure B.6**

Terpolymer compositions used for construction of ternary diagrams (Figures B.5) The bottom edge of the triangle is representative of poly(ε-caprolactone-*co*-δ-valerolactone) while the left and right sides represent poly(ε-caprolactone-*co*-ε-decalactone) and poly(δ-valerolactone-*co*-ε-decalactone), respectively.

# B.5 References

(1) Gross, R. A.; Kumar, A; Kalra, B.; Dekhterman, A. Efficient Ring-Opening Polymerization and Copolymerization of ε-caprolactone and ω-pentadecalactone catalyzed by *Candida Antarctica* Lipase B. *Macromolecules.* **2000,** *33, (*6303-6309)

(2) Qiu, X.; Zhou, Z.; Gobbi, G.; Redwine, O. Error Analysis for NMR Polymer Microstructure Measurement without Calibration Standards. *Anal. Chem.* **2009,** *81,* (8585-8589)

(3) Save, M.; Schappacher, M.; Soum, A. Controlled Ring-Opening Polymerization of Lactones and Lactides Initiated by Lanthanum Isopropoxide, 1 General Aspects and Kinetics *Macromol. Chem. Phys.* **2002,** *203,(*889-899)

(4) Duda, A.; Kowalski, A.; Penczek, S.; Uyama, H.; Kobayashi, S. Kinetics of the Ring-Opening Polymerization of 6-, 7-, 9-, 12-, 13-, 16-, and 17-Membered Lactones. Comparision of Chemical and Enzymatic Polymerizations *Macromolecules* **2002,** 35, (4266-4270)

(5) Pratt, R. C.; Lohmeijer, B. G. G.; Long, D. A.; Waymouth, R. M.; Hedrick, J. L. Triazabicyclodecene: A Simple Bifunctional Organocatalyst for Acyl Transfer and Ring-Opening Polymerization of Cyclic Esters *JACS,* **2006,** *128, (*4556-4557)

(6) Yevstropov, A. A.; Lebedev, B. V.; Kulagina, T. G. Calorimetric study of δ-valerolactone, poly-δ-Valerolactone and of the process of polymerization of of δ-valerolactone in the 13.8 to 340 K temperature range *Vysokomolekuliarnye soedineniia Seriia A* 24 **1982, (**568-574)

(7) Storey, R. F.; Hoffman, D.C. Copolymerization of ε-caprolactone and δ-valerolactone *Mackromol. Chem. Marcomol. Symp.* **1991,** *42/43,* (185-193)

(8) Albertsson, A.-C; Gruvegard, M. Degradable high-molecular-weight random copolymers, based on ε-caprolactone and 1,5-dioxepan-2-one, with non-crystallizable units inserted in the crystalline structure *Polymer* **1995,** *36,* (1009-1016)

(9) Vion, J-M; Jerome, R.; Teyssie, P.; Aubin, M.; Prud'homme, R. E. Synthesis, Characterization, and Miscibility of Caprolactone Random Copolymers
*Macromolecules* **1986,** *19,* (1828-1838)

(10) Goulet, L.; Prud'homme, R. E. Crystallization Kinetics and Melting of Caprolactone Random Copolymers *Journal of Polymer Science: Part B: Polymer Physics* **1990,** *28, (*2329-2352)

(11) Faÿ, F.; Renard, E.; Langlois, V.; Linossier, I.; Vallée-Rehel, K. Development of poly(ε-caprolactone-co-δ-valerolactone) as new degradable binder used for antifouling paint *European Polymer Journal* **2007,** *43, (*4800-4813)

(12) Fernàndez, J.; Etxeberria, A.; Sarasua, J. Synthesis, structure, and properties of poly(L-lactide-co-ε-caprolactone) statistical copolymers *Journal of the Mechanical Behavior of Biomedical Materials* **2012,** *9,* (100-112)

(13) Crist, B. Thermodynamics of statistical copolymer melting *Polymer* **2003,** *44, (*4563-4572)

# Appendix C. Kinetics of DPP-Catalyzed Lactone Polymerizations

In Chapter 3, the results of kinetics of polymerization of β1 (or MVL) with the basic organocatalyst TBD were reported (Figure 3.4). With that particular catalyst, a semilogarithmic anamorphosis of monomer consumption verses time was linear. This suggests that the polymerization is first order in monomer, similar the behavior reported for δ5 (or δ-decalactone) with the same catalyst.[1] Interestingly, the DPP catalyzed polymerization of β1 exhibits different behavior. In the bulk with this catalyst the polymerization rate appeared constant until the reaction reaches equilibrium (Figure 4.2 c). Because of this, if the kinetic equations are written to include residual monomer a semilogarithmic anamorphosis appears concave up (Figure 4.2 e). This peculiar behavior for DPP catalyzed polymerization was also observed for each of the monomers studied in this work.

Generally, assuming the rate of polymerization is dependent on monomer, initiator, and catalyst concentration a differential rate law can be written as:

$$-\frac{d[M]}{dt} = [M]^x [DPP]^y [ROH]^z \tag{C1}$$

While the polymerization of β1 did not appear to be first order in monomer, a semi-logarithmic plot of initiator conversion over time (Figure 4.2 d) was linear, suggesting

initiator consumption was first order in hydroxyl concentration. To determine whether polymerization is also first order in hydroxyl concentration we varied the target molar mass from ~3 kg mol$^{-1}$ to 40 kg mol$^{-1}$ while maintaining fixed initial concentrations of β1 monomer and DPP. Under these conditions the observed rate constant ($k_{obs}$) decreases with target molar mass. This is true at two different catalyst loadings, 500:1 or 1000:1. Moreover, at a fixed monomer to initiator ratio (180:1) the rate increases with catalyst concentration. These results are summarized in Table C.1, below.

**Table C.1.**

**Effect of initiator and catalyst concentration of polymerization of β1**

|  | [a]$k_{obs}$ (M$^{-1}$ min) | [b]$[M]_0$ (M) | [c]$[DPP]_0$ (M) | [d]$[BnOH]_0$ (M) | $[M]_0/[I]_0$ | $[M]_0/[DPP]_0$ | [e]$M_N$ (kg mol$^{-1}$) |
|---|---|---|---|---|---|---|---|
| β1 | 0.039 | 9.11 | 0.018 | 0.070 | 131 | 502 | 13.5 |
| β1 | 0.031 | 9.11 | 0.018 | 0.048 | 188 | 493 | 19.3 |
| β1 | 0.093 | 9.11 | 0.019 | 0.17 | 54 | 488 | 5.5 |
| β1 | 0.070 | 9.11 | 0.020 | 0.082 | 111 | 448 | 11.4 |
| β1 | 0.15 | 9.11 | 0.018 | 0.33 | 25 | 473 | 2.6 |
| β1 | 0.023 | 9.11 | 0.018 | 0.022 | 406 | 496 | 41.7 |
| β1 | 0.017 | 9.11 | 0.0087 | 0.050 | 182 | 972 | 17.3 |
| β1 | 0.011 | 9.11 | 0.0091 | 0.033 | 274 | 1005 | 28.1 |
| β1 | 0.082 | 9.11 | 0.0087 | 0.67 | 13 | 964 | 1.3 |
| β1 | 0.030 | 9.11 | 0.0091 | 0.099 | 92 | 924 | 8.8 |

[a]Observed psuedo zero–order rate constant. [b]Inital monomer concentration calculated from monomer density and monomer molar mass (Table 4.2). [c]Inital catalyst concentration calculated from added amounts of catalyst and monomer. [d]Initiator concentration calculated from added amounts of benzyl alcohol and monomer. [e]Theoretical molar mass calculated from observed equilibrium conversion and initial concentrations of monomer and initator.

From these points, the experimentally observed rate law is:

$$-\frac{d[M]}{dt} = [M]^0[DPP]^{0.7}[ROH]^{0.7}k_p \qquad\qquad (C2)$$

If the catalyst and initiator concentrations are fixed then the monomer concentration can be described as:

$$[M]_t = [M]_0 - k_{obs}t \qquad\qquad (C3)$$

In this expression the observed rate constant ($k_{obs}$) is related to the polymerization rate constant:

$$k_{obs} = k_p[DPP]^{0.7}[ROH]^{0.7} \qquad\qquad (C4)$$

To study the impact of monomer structure on polymization rate a number of kinetics experiments were conducted where fixed the ratios of [M]:[ROH] and of [M]:[DPP] were fixed. These bulk polymerization experiments are summarized in Table C2, below. Although the polymerizations were all run in bulk monomer, the starting monomer concentration was different for each of the alkyl–substituted lactones studied. Therefore [BnOH] and [DPP] were also different for each monomer in the δ-substituted series.

**Table C.2**

**Effect of substituent position on kinetics of polymerization**

| | $^a k_{obs}$ (M$^{-1}$ min) | $^b$[M]$_0$ (M) | $^c$[DPP] (M) | $^d$[BnOH] (M) | [M]/[I] | [M]/[DPP] | $^e$M$_N$ (kg mol$^{-1}$) | $^f$t$_{1/2}$ (min) |
|---|---|---|---|---|---|---|---|---|
| δ0 | 0.047 | 10.8 | 0.043 | 0.045 | 238 | 231 | 23.8 | 115 |
| δ0 | 0.054 | 10.8 | 0.043 | 0.045 | 238 | 248 | 23.8 | 100 |
| δ0 | 0.043 | 10.8 | 0.043 | 0.045 | 238 | 253 | 23.8 | 126 |
| α1 | 0.015 | 9.11 | 0.044 | 0.054 | 169 | 209 | 18.5 | 304 |
| α1 | 0.019 | 9.11 | 0.045 | 0.054 | 169 | 203 | 18.5 | 240 |
| α1 | 0.012 | 9.11 | 0.043 | 0.054 | 169 | 214 | 18.5 | 380 |
| β1 | 0.042 | 9.11 | 0.045 | 0.055 | 165 | 202 | 16.9 | 108 |
| β1 | *0.044* | *9.11* | *0.047* | 0.055 | *165* | *195* | 16.9 | 104 |
| β1 | *0.037* | *9.11* | *0.042* | 0.055 | *165* | *214* | 16.9 | 123 |
| *γ1* | *0.096* | *9.11* | *0.043* | *0.045* | *202* | *211* | *22.6* | 47 |
| *γ1* | *0.094* | *9.11* | *0.042* | *0.045* | *202* | *216* | *22.6* | 48 |
| *γ1* | *0.093* | *9.11* | *0.039* | *0.045* | *202* | *233* | *22.5* | 49 |
| δ1 | 0.0045 | 9.11 | 0.044 | 0.054 | 205 | 167 | 20.8 | 1012 |
| δ1 | 0.0059 | *9.11* | *0.045* | *0.044* | *209* | *201* | *21.2* | 772 |
| δ1 | *0.0057* | *9.11* | *0.044* | *0.044* | *209* | *208* | *21.2* | 800 |
| δ1 | 0.0046 | *9.11* | *0.044* | *0.044* | *209* | *209* | *21.2* | 990 |

$^a$Observed psuedo zero–order rate constant. $^b$Initial monomer concentration calculated from monomer density and monomer molar mass (Table 4.2). $^c$Inital catalyst concentration calculated from added amounts of catalyst and monomer. $^d$Initiator concentration calculated from added amounts of benzyl alcohol and monomer. $^e$Theoretical molar mass calculated from observed equilibrium conversion and initial concentrations of monomer and initator. $^f$Time required to reach 50% conversion.

**(continued). Effect of n-alkyl length on kinetics of polymerization**

| | [a]$k_{obs}$ (M$^{-1}$ min) | [b][M]$_0$ (M) | [c][DPP] (M) | [d][BnOH] (M) | [M]/[I] | [M]/[DPP] | [e]$M_N$ (kg mol$^{-1}$) | [f]$t_{1/2}$ (days) |
|---|---|---|---|---|---|---|---|---|
| δ2 | 0.0021 | 8.04 | 0.039 | 0.090 | 89 | 209 | 10.3 | 1.3 |
| δ2 | 0.0023 | 8.04 | 0.040 | 0.090 | 89 | 222 | 10.3 | 1.2 |
| δ2 | 0.0019 | 8.04 | 0.035 | 0.090 | 89 | 203 | 10.3 | 1.5 |
| δ3 | 0.00041 | 7.02 | 0.035 | 0.036 | 211 | 202 | 27.0 | 5.9 |
| δ3 | 0.00044 | 7.02 | 0.036 | 0.036 | 211 | 196 | 27.0 | 5.5 |
| δ3 | 0.00054 | 7.02 | 0.035 | 0.036 | 211 | 202 | 27.0 | 4.5 |
| δ4 | 0.00039 | 5.72 | 0.028 | 0.029 | 197 | 202 | 30.0 | 5.1 |
| δ4 | 0.00043 | 5.72 | 0.027 | 0.029 | 197 | 209 | 30.0 | 4.6 |
| δ4 | 0.00038 | 5.72 | 0.036 | 0.029 | 197 | 198 | 30.0 | 5.2 |
| δ5 | 0.00027 | 5.61 | 0.028 | 0.28 | 203 | 201 | 30.8 | 7.2 |
| δ5 | 0.00027 | 5.61 | 0.028 | 0.028 | 203 | 201 | 30.8 | 7.2 |
| δ5 | 0.00028 | 5.61 | 0.032 | 0.028 | 203 | 177 | 30.8 | 7.0 |
| δ6 | 0.00031 | 5.26 | 0.026 | 0.025 | 208 | 204 | 34.1 | 5.9 |
| δ6 | 0.00030 | 5.26 | 0.025 | 0.025 | 209 | 0.99 | 34.1 | 6.1 |
| δ6 | 0.00033 | 5.26 | 0.027 | 0.025 | 208 | 196 | 34.1 | 5.5 |
| δ7 | 0.00032 | 4.75 | 0.036 | 0.023 | 212 | 166 | 37.8 | 5.2 |
| δ7 | 0.00026 | 4.75 | 0.029 | 0.023 | 212 | 210 | 37.8 | 6.3 |
| δ7 | 0.00028 | 4.75 | 0.030 | 0.023 | 212 | 201 | 37.8 | 5.9 |
| δ9 | 0.00027 | 4.13 | 0.023 | 0.019 | 215 | 176 | 43.3 | 5.3 |
| δ9 | 0.00027 | 4.13 | 0.021 | 0.019 | 215 | 194 | 43.3 | 5.3 |
| δ9 | 0.00026 | 4.13 | 0.021 | 0.019 | 215 | 192 | 43.3 | 5.5 |

[a]Observed psuedo zero–order rate constant. [b]Initial monomer concentration calculated from monomer density and monomer molar mass (Table 4.2). [c]Inital catalyst concentration calculated from added amounts of catalyst and monomer. [d]Initiator concentration calculated from added amounts of benzyl alcohol and monomer. [e]Theoretical molar mass calculated from observed equilibrium conversion and initial concentrations of monomer and initator. [f]Time required to reach 50% conversion (calculated from the observed rate constant).

Calculation of polymerization rate constant ($k_p$) allows direct comparison of monomers with different starting conditions. The calculated rate constants for the monomers studied in this work are shown in Table C3.

**Table C.3.**

**Rate constant for DPP catalyzed bulk polymerization**

|  | $^a k_p$ (M$^{-1}$ min) | $^b k_p$ (M$^{-1}$ min) |
|---|---|---|
| γ1 | 7.7 ± 0.2 | 51 ± 2 |
| δ0 | 3.8 ± 0.4 | 25 ± 3 |
| β1 | 2.8 ± 0.1 | 17 ± 0.6 |
| α1 | 1.1 ± 0.2 | 6.4 ± 1.3 |
| δ1 | 0.40 ± 0.07 | 2.6 ± 0.5 |
| δ2 | 0.11 ± 0.006 | 0.61 ± 0.02 |
| δ3 | 0.049 ± 0.008 | 0.36 ± 0.06 |
| δ4 | 0.056 ± 0.009 | 0.46 ± 0.09 |
| δ5 | 0.029 ± 0.02 | 0.23 ± 0.01 |
| δ6 | 0.052 ± 0.0005 | 0.47 ± 0.02 |
| δ7 | 0.036 ± 0.002 | 0.29 ± 0.04 |
| δ9 | 0.057 ± 0.004 | 0.57 ± 0.05 |

[a]Calculated from the observed rate constants in Table C2 and the observed rate law for the polymerization of β1 (Equation C2). [b]Calculated from the observed rate constants in Table C2 and the assumption that the rate is first order in catalyst and initiator. Data shown are the average and standard deviation of the replicates shown for each monomer.

The unusual rate behavior probably due to the activated monomer mechanism (Figure 4.6). The monomer concentration doesn't directly influence the rate of polymerization because the rate-limiting step is likely scission of the internal C-O bond of the activated lactone, (H-M$^+$). Baśko and Kubisa previously investigated the cationic copolymerization of ε-CL and L-Lactide using triflic acid.[2]   They also observed a complex kinetics scheme that they attribute to an activated monomer mechanism. Although the rate law (Equation C2) is an empirical description of the kinetic behavior, it is likely an oversimplification.

It is possible that the fractional orders are due to the fact that the DPP catalyst does not just activate the monomer but can also protonate the monomer, polymer ester, and polymer hydroxy end groups. The activated monomer concentration is related to the monomer concentration and the equilibrium constants for the protonation of the monomer ($K_m$), polymer ($K_p$), and hydroxy ($K_{OH}$) groups.

$$[H - M^+] = \frac{[H^+]}{1 + \frac{[P]K_P}{[M]K_M} + \frac{[ROH]\,K_{OH}}{[M]K_M}} \tag{C5}$$

In this expression [H$^+$] is the acid concentration, [P] is the concentration of polymer units, and [ROH] is the concentration of alcohol groups.

This can be rearranged to:

$$[H - M^+] = \frac{[H^+][M]}{[M]+[P]\frac{K_P}{K_M}+[ROH]\frac{K_{OH}}{K_M}}$$  (C6)

If the pKa of the lactone is similar to the pKa of the esters in the linear polymer then $K_P/K_M$ is about 1. Since the alcohol concentration and total number of ester units ([M]+[P]) are both constant, the denominator is constant and Equation C6 can be simplified to the following form:

$$[H - M^+] = [H^+][M][A]$$  (C7)

Where A is a constant:

$$A = \frac{1}{[M]+[P]\frac{K_P}{K_M}+[ROH]\frac{K_{OH}}{K_M}}$$  (C8

Equivalently:

$$[H - M^+] = [M][B]$$  (C9)

Where B is a constant:

$$B = \frac{[H^+]}{[M]+[P]\frac{K_P}{K_M}+[ROH]\frac{K_{OH}}{K_M}}$$  (C10)

Even though the monomer is not part of the rate-limiting step, an integrated rate law can be written which includes monomer concentration:

$$\frac{-d[M]}{dt} = -k[\text{H} - \text{M}^+][ROH] = k[M][B][ROH] \tag{C11}$$

The integrated rate law is thus:

$$ln\left[\frac{[M]_0}{[M]_{[t}}\right] = k[B][ROH]t \tag{C12}$$

Therefore, even for the activated monomer mechanism a first order plot *should* be linear with a slope that is equal to the rate coefficient ($k$). In this case $k$ is not the propagation rate constant $k_p$. The fact that the rate seems to accelerate on a semi-logarithmic first-order suggests that $K_P/K_M$ is not equal to 1 (and B is not constant). If the lactone is more basic than the ester groups in the polymer then the rate will accelerate because the concentration of the activated monomer, $[\text{H}-\text{M}^+]$, should increase as the reaction proceeds. For reversible reactions near equilibrium the rate law should also include the depolymerization rate constant. However, for this work we take the rate over the linear regime and neglect to include depolymerization effects.
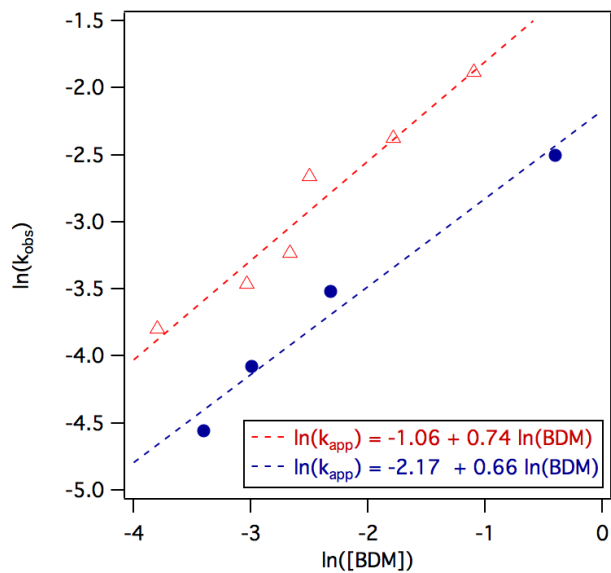
**Figure C.1**

Impact of initiator concentration on apparent pseudo-zero-order rate constant for the room temperature polymerization of β1 conducted at catalyst loadings of (△)$[M]_0$:$[DPP]_0 \approx 500$:1 and (●) $[M]_0$:$[DPP]_0 \approx 1000$:1. Polymerizations were conducted in the bulk at temperatures of $27 \pm 2$ °C. The data represented here are provided in Table C1.
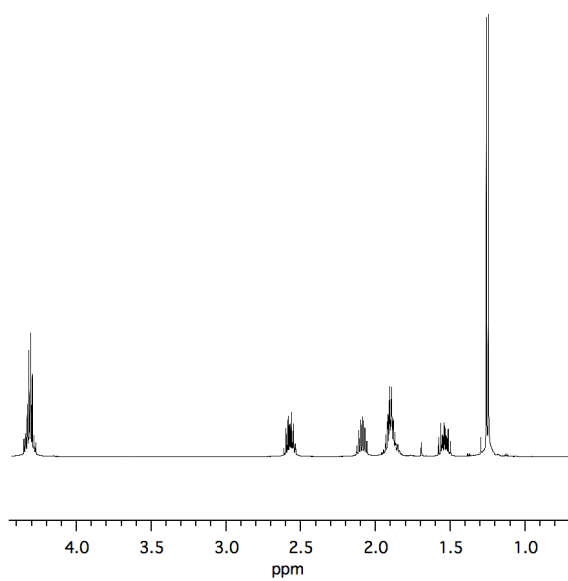
**Figure C.2**

$^1$H NMR spectrum of α1 in CDCl$_3$.
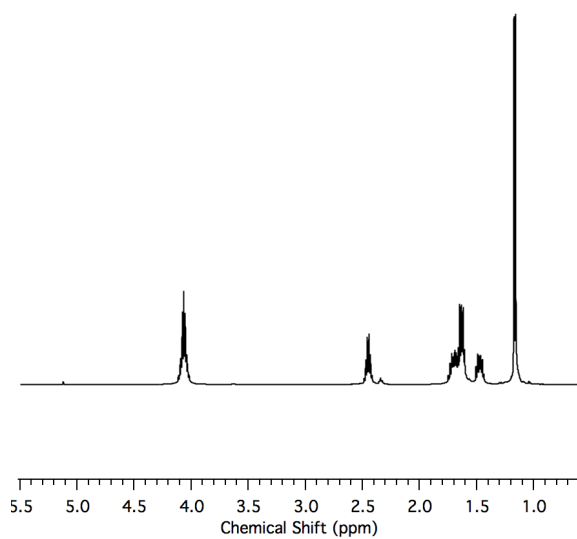


**Figure C.3**

$^1$H NMR spectrum of Pα1 in CDCl$_3$.
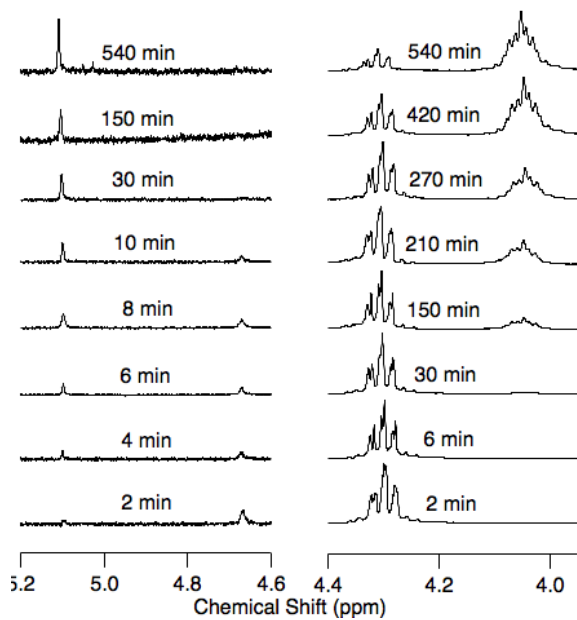
**Figure C.4**

^{1}H NMR spectra overlay of aliquots from the bulk polymerization, room temperature (~27 °C) of α1 quenched at the indicated times. Initial conditions were $[DPP]_0$ = *0.044* M  $[BnOH]_0$ = *0.054* M, and $[α1]_0$ = 9.11 M.  Above left: The Benzyl methylene protons shift from 4.65 ppm in the free alcohol to 5.10 ppm in the ester. Above right: The δ methylene protons, present at 4.25 ppm in the lactone, shift to 4.05 ppm in the polyester.
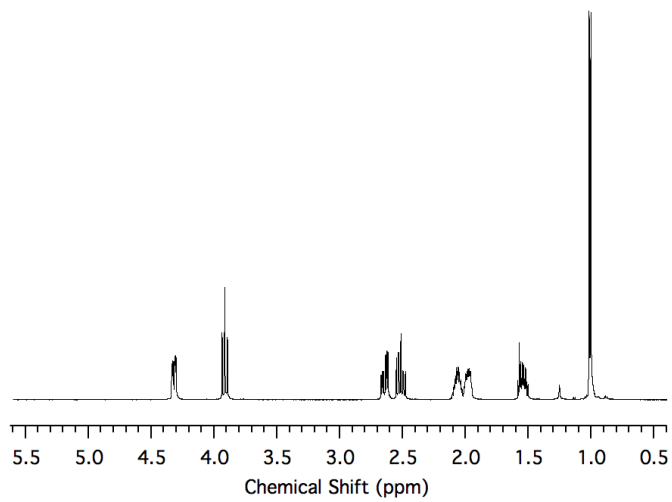
**Figure C.5.**
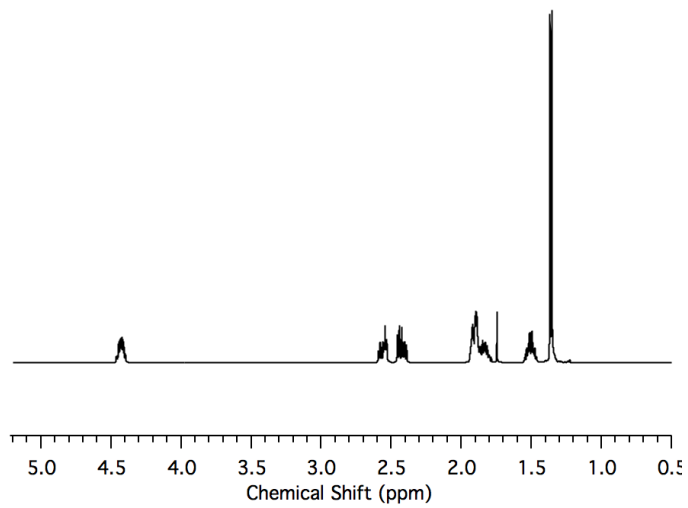
$^1$H NMR spectrum of γ1 in CDCl$_3$.
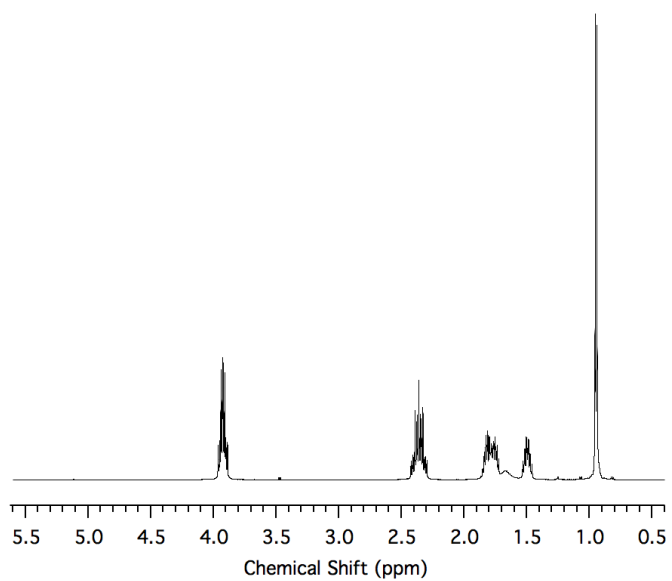


**Figure C.6**

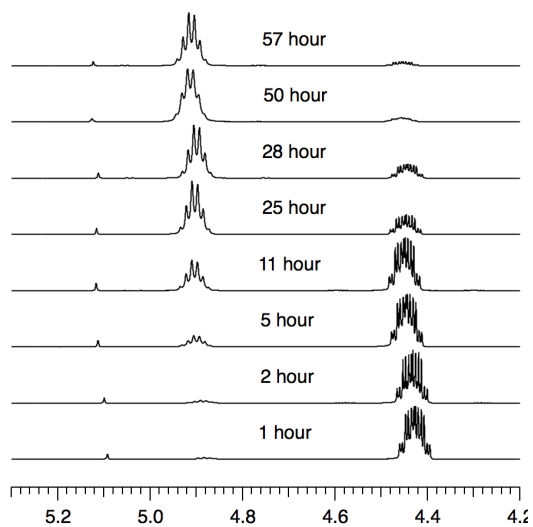$^1$H NMR spectrum of representative Pγ1 in in CDCl$_3$.
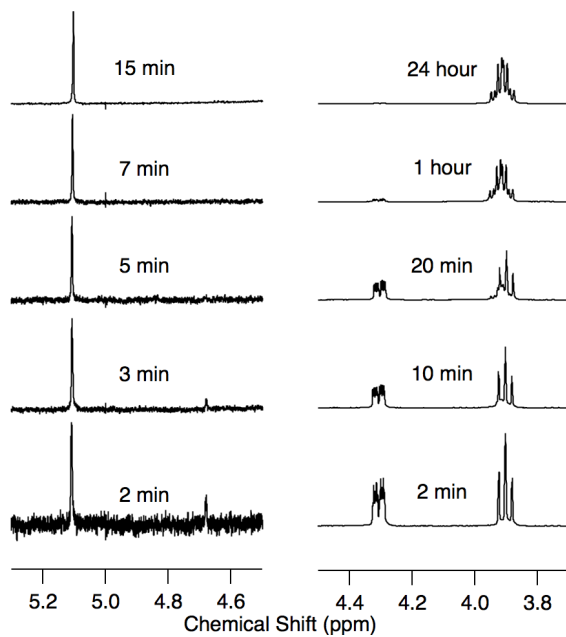
**Figure C.7**

^{1}H NMR spectra (CDCl$_3$.) overlay of aliquots from the bulk polymerization, room temperature (~27 °C) of γ1 quenched at the indicated times. Initial conditions were [DPP]$_0$ = *0.043* M [BnOH]$_0$ = *0.045* M, and [γ1]$_0$ = 9.11 M. Above left: The benzyl methylene protons shift from 4.65 ppm in the free alcohol to 5.10 ppm in the ester. Above right: The δ methylene protons, present at 4.25 ppm and 3.9 ppm in the lactone, coalesce at 3.90 ppm in the polyester.

**Figure C.8**

$^1$H NMR spectrum of δ1 in CDCl$_3$.
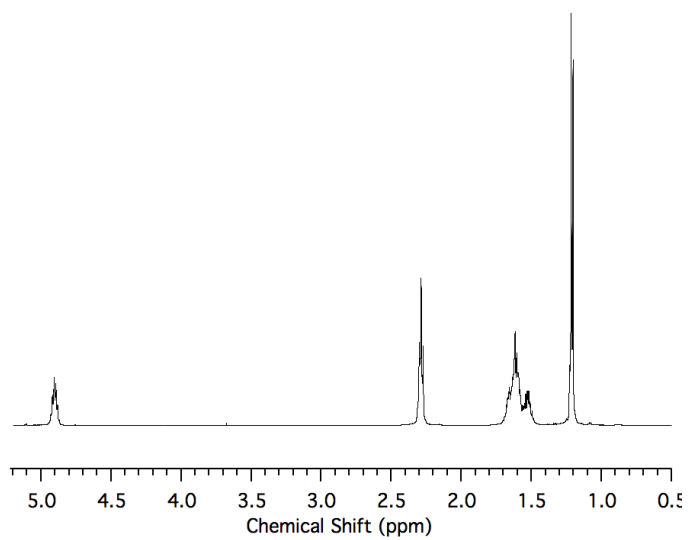


**Figure C.9**

$^1$H NMR spectrum of representative Pδ1 in CDCl$_3$.

263

**Figure C.10**

$^1$H NMR spectra (CDCl$_3$.) overlay of aliquots from the bulk polymerization, room temperature (~27 °C) of δ1 quenched at the indicated times. Initial conditions were [DPP]$_0$ = *0.044* M [BnOH]$_0$ = *0.054* M, and [δ1]$_0$ = 9.11 M. The δ methine proton, present at 4.4 in the lactone, shifts to 4.9 ppm in the polyester.
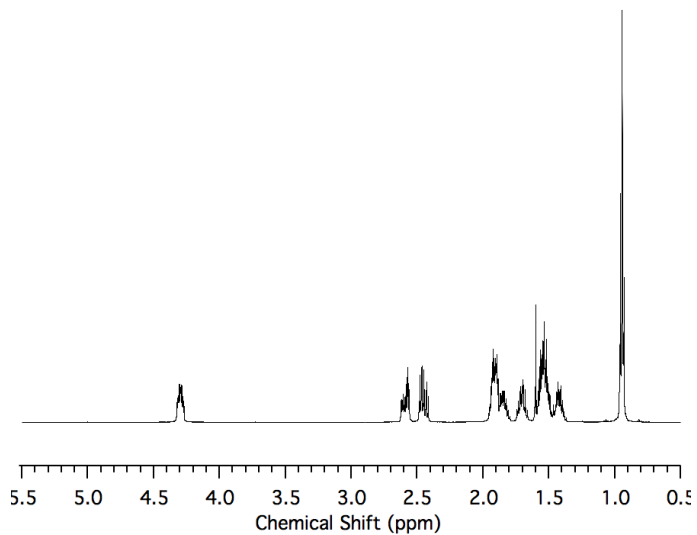
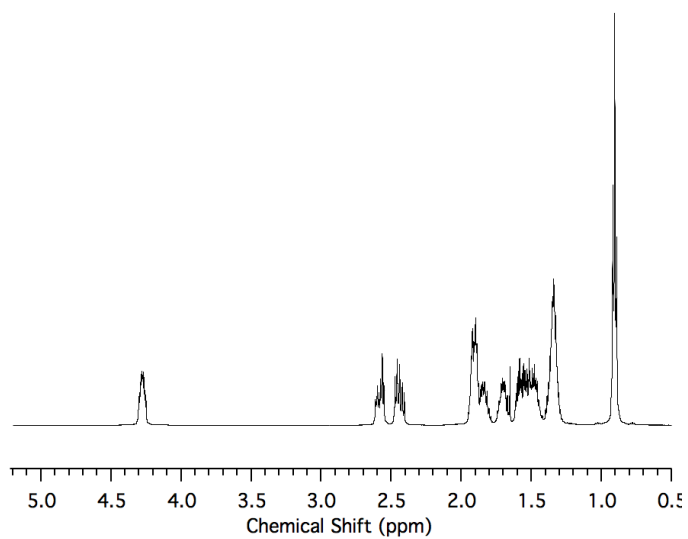**Figure C.11**

$^1$H NMR spectrum of **83** in CDCl$_3$.



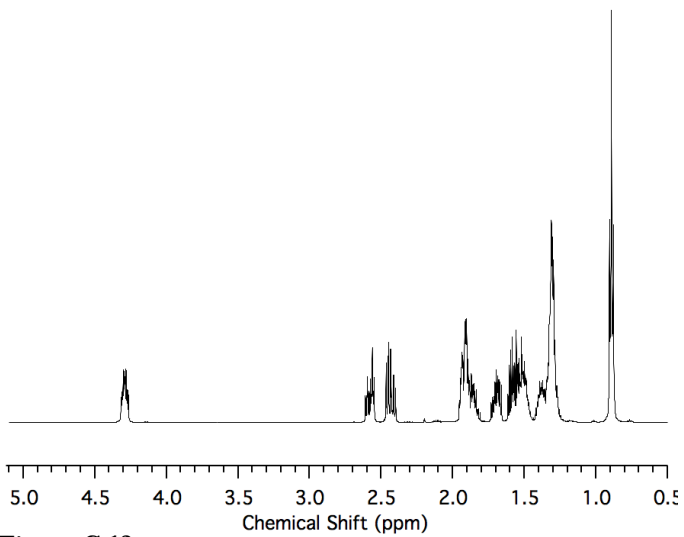**Figure C.12**

$^1$H NMR spectrum of **84** in CDCl$_3$.

265

**Figure C.13**

$^1$H NMR spectrum of **85** in CDCl$_3$.

**Figure C.14**

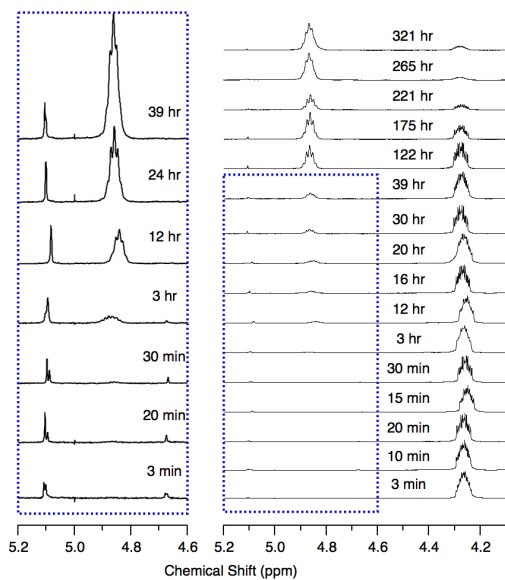$^1$H NMR spectra (CDCl$_3$) overlay of aliquots from the bulk polymerization of δ5 quenched at the indicated times. Initial conditions were [DPP]$_0$ = 0.028 M [BnOH]$_0$ = 0.028, and [δ5]$_0$ = 5.61 M. Above left: The Benzyl methylene protons shift from 4.65 ppm in the free alcohol to 5.10 ppm in the initiated polyester. Above right: The δ methine proton, present at 4.25 ppm in the lactone, shifts to 4.85 ppm in the polyester. Similar sifts were observed for the other n-alkyl δ-valerolactone monomers.
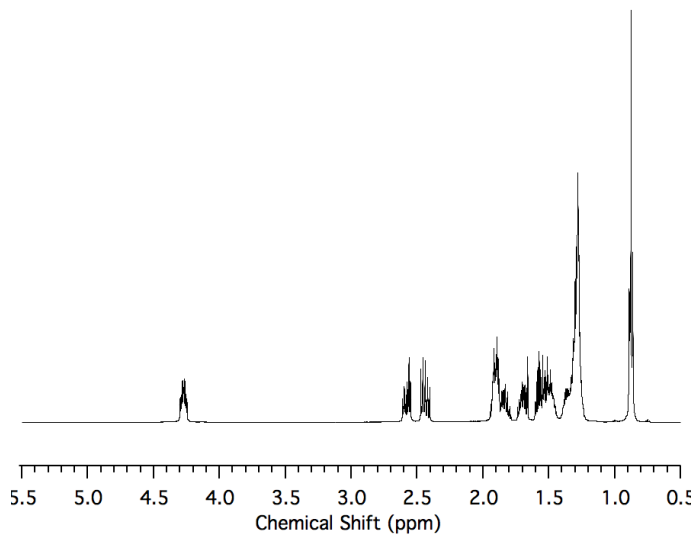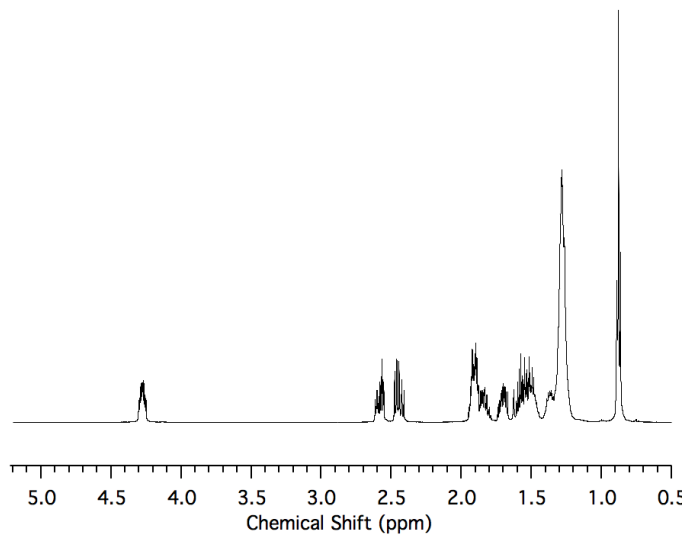
**Figure C.15**

$^1$H NMR spectrum of **86** in CDCl$_3$.



**Figure C.16**

$^1$H NMR spectrum of **87** in CDCl$_3$.

268

**Figure C.17**

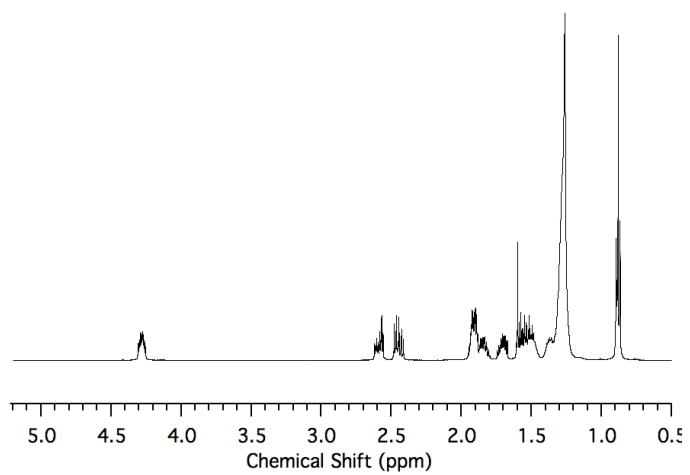$^1$H NMR spectrum of **89** in CDCl$_3$.

# References

(1) Martello MT, Burns A, Hillmyer M Bulk Ring-Opening Transesterification Polymerization of the Renewable δ-Decalactone Using an Organocatalyst. *ACS Macro Lett* **2012,** *1,* (131-135)
(2) Baśko, M.; Kubisa, P. Cationic Copolymerization of ε-Caprolactone and L-Lactide by an Activated Monomer Mechanism *Journal of Polymer Science A*: *Polymer Chemistry* **2006,** *44,* (7071)

# Appendix D. Thermodynamics of Lactone Polymerizations

Reaction conditons affect not only the kinetics of polymerization but also the thermodynamics. In Chapter 4 we assume ΔH and ΔS are independent of thermperature over the ranges studied. To learn how monomer structure impacts polymerization thermodynamics, we used the temperature dependence of the equilibrium monomer concentration to estimate $\Delta H_p^\circ$ and $\Delta S_p^\circ$. This is shown in Figure 2 and Figures S62-71, where the residual monomer concentration is fit to Equation D1:

$$ln\left(\frac{[\text{M}]_{eq}}{[M]_{ss}}\right) = \frac{\Delta H_p^\circ}{RT} - \frac{\Delta S_p^\circ}{R} \qquad \text{(D1)}$$

In this expression T is the temperature at which the polymerization is conducted and $[M]_{ss}$ is a standard state monomer concentration. Although we define $[\text{M}]_{ss}$ as 1.0 for convenience,[1] the polymerizations were conducted in the bulk ( 4.1 < $[\text{M}]_0$ < 10.8 M). There is a significant difference in the ceiling temperature depending on the concentration.

For example with β1, $[\text{M}]_{eq}$ =1.0 results in a calculated ceiling temperature of 27 °C:

$$T_c = \frac{-13800}{-46} = 300 \text{ K}$$

However, in the bulk ($[\text{M}]_{eq}$ =9.1 M), $T_c$ is 226 °C:

271

$$T_c = \frac{-13800}{8.314\, ln(9.1) - 46} = 500 \text{ K}$$

Although it is convenient to assume $[M]_{ss} = 1$ M, this assumption can lead to inaccurate comparison of monomers with differ bulk concentrations. Notably, it is not strictly true that the ring strain is independent of the concentration and solvent. However, is possible to recalculate $\Delta S$ and $\Delta H$ for the actual bulk concentration as discussed in detail by Olsén et. al.[2] The figures below show the Van't Hoff plots for the following monomers: α1, β1, γ1, δ1, δ2, δ3, δ4, δ5, δ6, δ7, and δ9. Notably, the bulk polymerizations of the monomers studied in this work in this work can be compared directly because the monomer and polymer states are the same; for each reaction the liquid monomer (l) is transformed to an amorphous polymer (a). These data are summarized in Chapter 4 (Table 4.1).

**Figure D.1**

Van't Hoff plot showing inverse temperature dependence of α1 polymerization.



**Figure D.2**

Van't Hoff plot showing inverse temperature dependence of β1 polymerization.

273

**Figure D.3**

Van't Hoff plot showing inverse temperature dependence of γ1 polymerization.



**Figure D.4**

Van't Hoff plot showing inverse temperature dependence of δ1 polymerization.

274
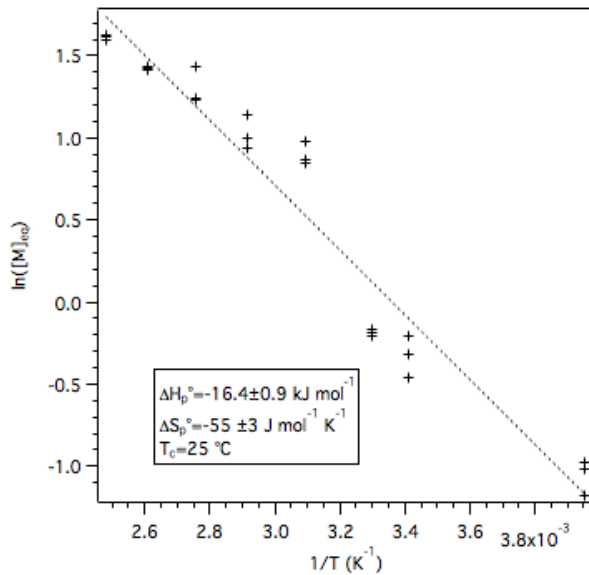
**Figure D.5.**

Van't Hoff plot showing inverse temperature dependence of δ2 polymerization.
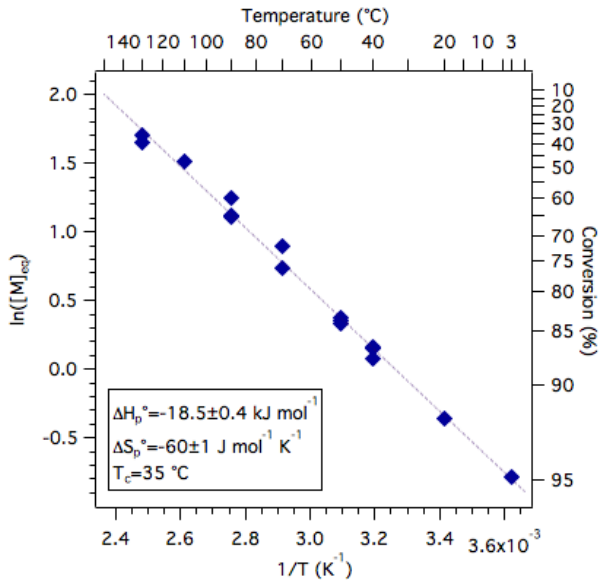


**Figure D.6**

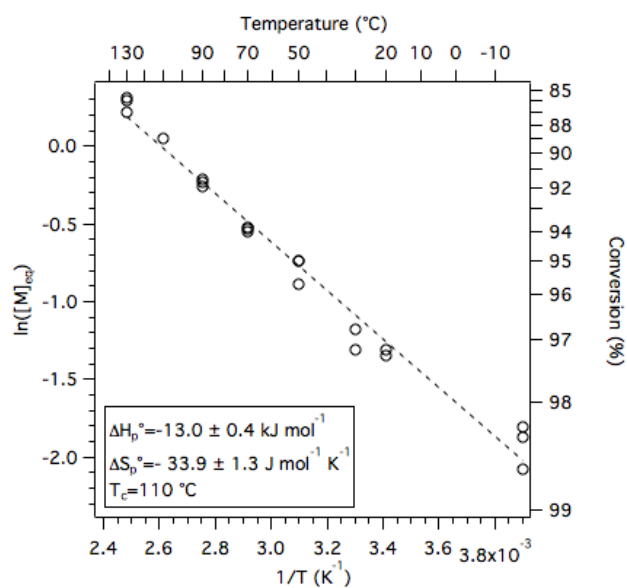Van't Hoff plot showing inverse temperature dependence of δ3 polymerization.

275
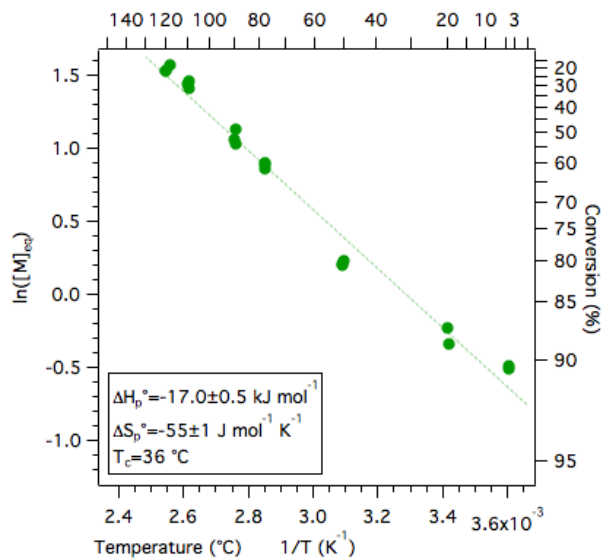
**Figure D.7**

Van't Hoff plot showing inverse temperature dependence of δ4 polymerization.
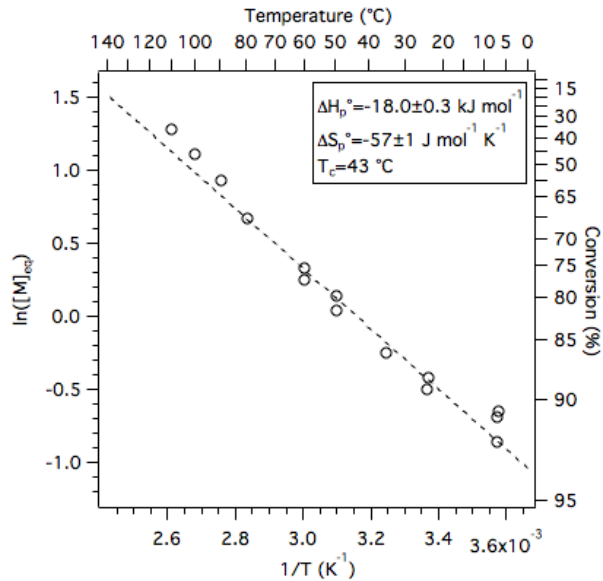


**Figure D.8**

Van't Hoff plot showing inverse temperature dependence of δ5 polymerization.
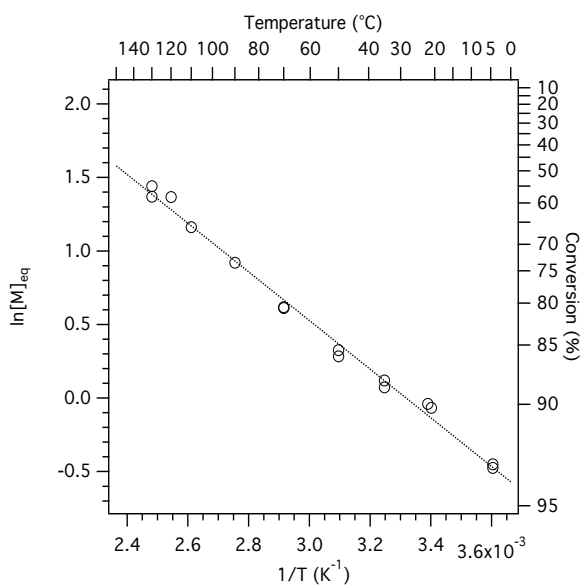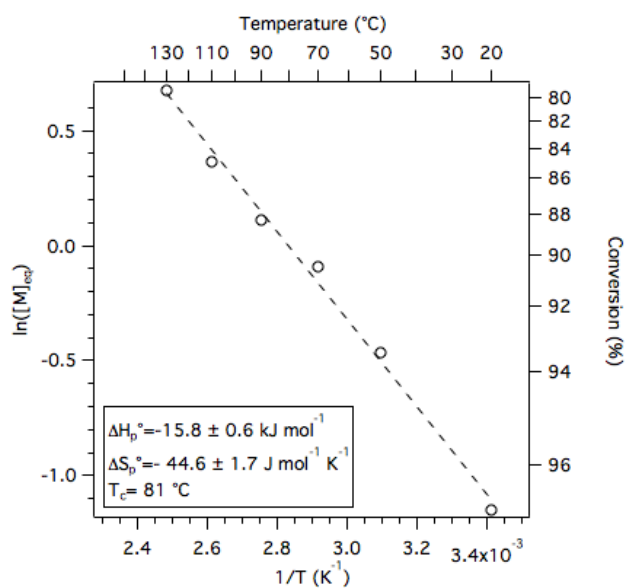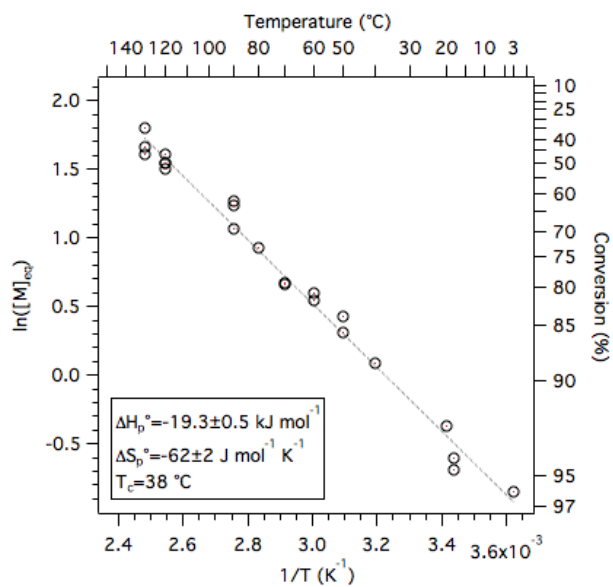
276
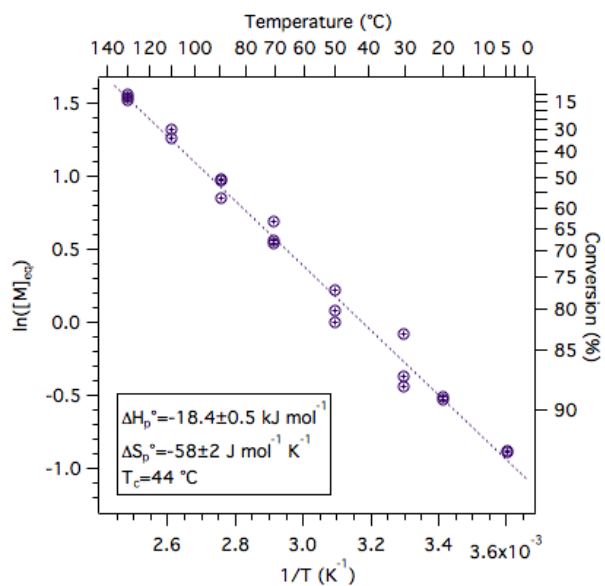
**Figure D.9**

Van't Hoff plot showing inverse temperature dependence of δ6 polymerization.
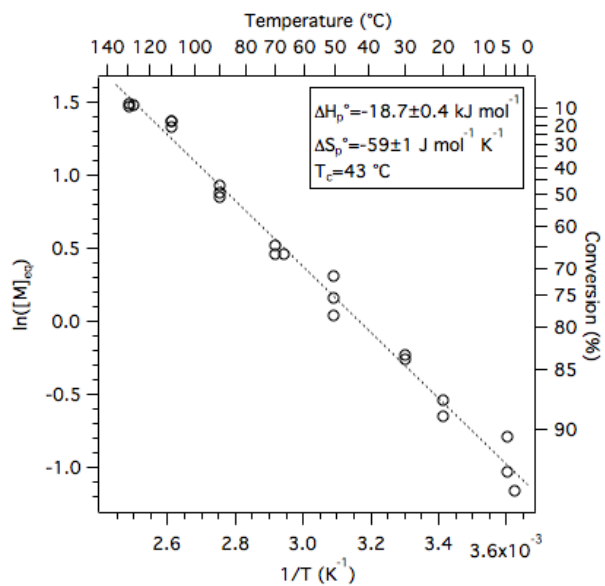


**Figure D.10.**

Van't Hoff plot showing inverse temperature dependence of δ7 polymerization.

277
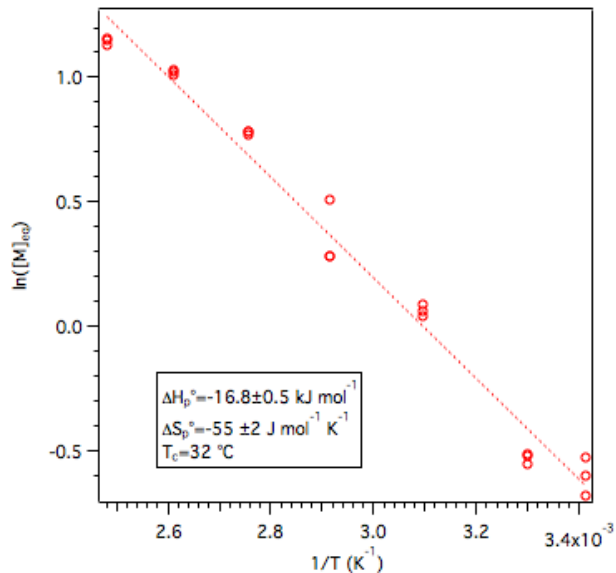
**Figure D.11**

Van't Hoff plot showing inverse temperature dependence of δ9 polymerization.

# References

(1) Dainton, F. S.; Irving, K. J. Some Thermodynamic and Kinetic Aspects of Addition Polymerisation *Q. Rev.* **1958,** 12, **(**61)

(2) Olsén, P.; Odelius, K.; Albertsson, A.-C. Thermodynamic Presynthetic Considerations for Ring-Opening Polymerization *Biomacromolecules,* **2016,** *17,* (699-709)

# Appendix E. Block Polymer Thermodynamics

As disscused in Chapter 2 and in Chapter 4, in this work we assume the temperature dependance of $\chi$ is inverse and follows the emperical relationship:

$$\chi(T) = \frac{\alpha}{T} + \beta \tag{E1}$$

In those chapters we reported the enthaplic ($\alpha$) and entropic ($\beta$) contributions to $\chi(T)$ for poly(lactide) with each of a number of different aliphatic polyesters. Specifically, for each polymer pair of interest we prepared a number of compositionally symmetric (volume fraction of PLA approximately 0.5) triblock samples of different molar masses. For each sample a reference volume-normalized degree of polymerization, N, was calculated from the molar mass of the triblock ($M_n$). The order to disorder transition temperature ($T_{ODT}$) of each sample was found using dynamic mechanical analysis. We used the mean field assumption ($\chi$ N=17.996 at the lamellar to disorder phase boundary) to estimate $\chi$ at the $T_{ODT}$ for each sample. Supplemental SAXS and DMA data not included in Chapter 2 and Chapter 4 are provided in this Appendix.

For PCL-PLA:

$$\chi(T) = \frac{28.7 \pm 2}{T} - 0.03 \pm 0.005 \tag{E2}$$

For Pβ1-PLA:

$$\chi(T) = \frac{37 \pm 4}{T} - 0.054 \pm 0.009 \tag{E3}$$

For PCD77-PLA:

$$\chi(T) = \frac{45.8 \pm 12.5}{T} - 0.07 \pm 0.03 \tag{E4}$$

For PCD66-PLA:

$$\chi(T) = \frac{56.3 \pm 9.6}{T} - 0.09 \pm 0.03 \tag{E5}$$

And for Pδ5-PLA:

$$\chi(T) = \frac{100 \pm 7}{T} - 0.16 \pm 0.02 \tag{E6}$$

Using these relationships it is possible to estimate the interaction parameter at various temperatures. For example, at 25 °C, we estimate that $\chi_{\beta1\text{-PLA}} = 0.074$ and $\chi_{85\text{-PLA}} = 0.18$.

These results with the block statistical copolymers (e.g. LCD77L and LCD66L) suggest that the block miscibility varies predictably with composition, as $F_{CL}$ increases midblock becomes less aliphatic and the segment–segement interaction parameter decrease; however within error both of the α and β terms are the same for two polymer systems. More accurate estimatations of the temperature dependent interaction parmeters are required to determine wether or not this trend is statistically significant.

For block–statistical copolymers, if regular mixing is obeyed and if the solubility parameter of the statistical copolymer midblock varies linearly with the volume fractions of the components then it should be possible to estimate the interaction parameter from the composition. Others have shown that this is applies in the case of polystyrene-poly(ethylene-alt-propylene) block–random copolymers[1] but fails for unknown reasons in ternary systems containing a poly(ethylene) block.[2] With the assumption that regular mixing will be obeyed in the case of fully polyester poly(lactide)-block-statistical copolymer systems, at a given temperature, the segement–segment interaction parameter of a PLA–*block*-PCD block polymer can be estimated from the compositon and the known interaction parameters of PLA–*block*-PDL and PLA–*block*-PCL. At 140 °C this method predicts interaction parameters, $\chi_{\text{L-CD77}} = 0.05$ and $\chi_{\text{L-CD66}} = 0.06$, that are slightly different than those calculated from the

temperature dependant expresions above. More accurate estimatations of the temperature dependent interaction parmeters is required to determine wether or not this deviation is significant.

*ε-Caprolactone-co-δ-Valerolactone Copolymers*

Of the compositionally symmetic LCV50L triblocks investigated in this work three polymers had displayed clear order to disorder transitions as determined by dynamic mechanical analysis. From these polymers the interaction parameter of PLA and PCV50 is estimated to be:

$$\chi_{PLA-PCV50} = \frac{(7.9 \pm 3.6)}{T} + (0.003 \pm 0.009) \tag{12}$$

This crude estimate suggests that the PCV50 copolymer is even more miscible with PLA than PCL and PMVL.

*Solubility Parameter Estimates*

The $\chi$ parameter values are unitless but have an embedded reference volume because for each triblock N (from which $\chi$ at the $T_{ODT}$ was estimated) was calculated from molecular weight using a reference volume, in this work 118 $\text{Å}^3$ (or equivalently 71.1 $\text{cm}^3 \text{ mol}^{-1}$). Using the $\chi$ values at a specific temperature it is possible to estimate the solubility parameters a given polymer using the relationship expressed in equation E7.

$$\chi_{A-B} = \frac{V_{ref}(\delta_A - \delta_B)^2}{RT} \qquad \text{(E7)}$$

In this expression R is the gas constant (8.314 J K$^{-1}$ Mol$^{-1}$) and T is the temperature (in K). For this work we employed the same reference volume used to estimate of $\chi$ ($V_{ref}$ = 71.1 cm$^3$ mol$^{-1}$), and the solubility parameter of PLA ($\delta_A$ = 19.8 J$^{1/2}$ cm$^{-3/2}$).[3]

$$\delta_A - \sqrt{\frac{(\chi_{A-B})RT}{V_{ref}}} = \delta_B \qquad \text{(E8)}$$

Notably, the arbitrary reference volume used to estimate $\chi$ essentially cancels out in this equation.
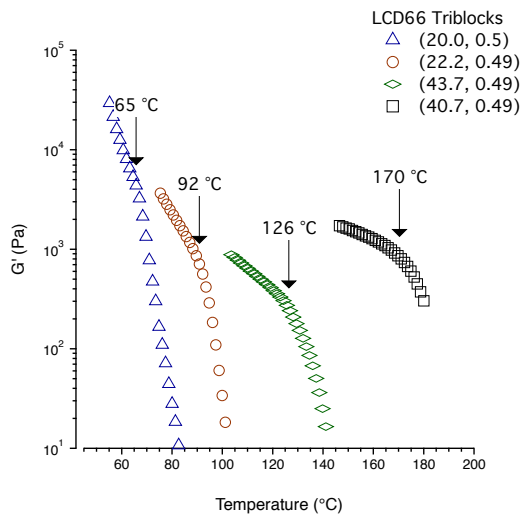
**Figure E.1**

Isochronal temperature ramp data on heating (1 rad s-1, 1°C min-1, 1% strain) or LCDL triblock copolymers LCD65L (20.0, 0.50), LCD66L (22.2, 0.5), LCD67L (43.7, 0.49), LCD63L (40.7, 0.49).
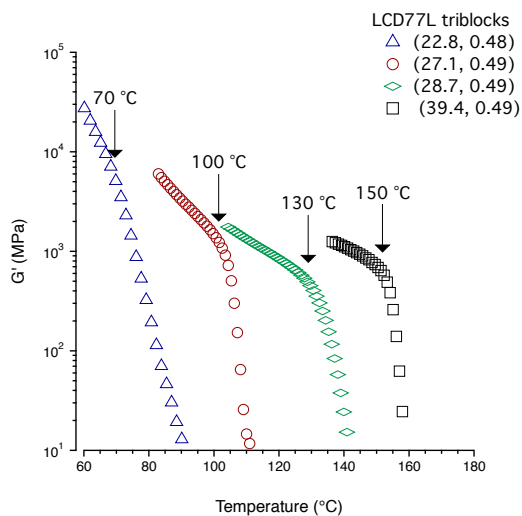


**Figure E.2**

Isochronal temperature ramp data on heating (1 rad s$^{-1}$, 1°C min$^{-1}$, 1% strain) for LCDL triblock copolymers LCD78L (22.8, 0.48), LCD77L (27.1, 0.49), LCV76L (28.7, 0.49), LCV76L (39.4, 0.49).
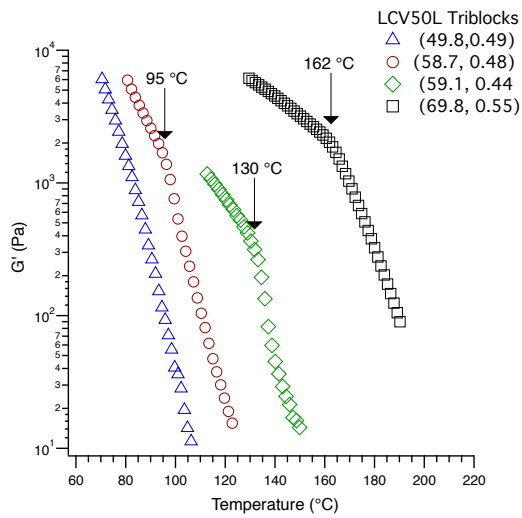
**Figure E.3**

Isochronal temperature ramp data on heating for LCV50L triblock copolymers LCV50L (49.8, 0.50), LCVL (58.7, 0.48), LCVL (59.1, 0.44), LCVL (69.8, 0.55).
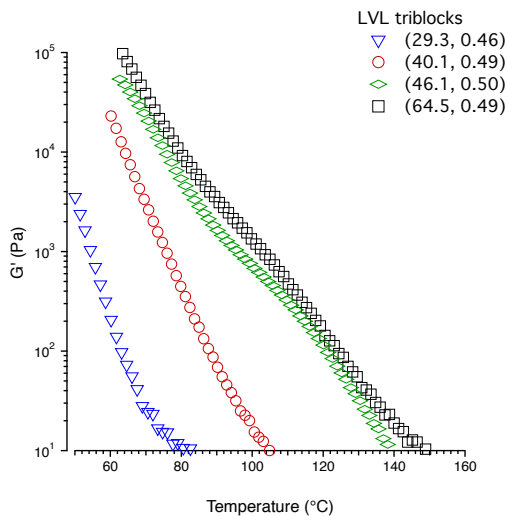


**Figure E.4**

Isochronal temperature ramp data on heating for LVL triblock copolymers LVL (29.3, 0.46), LCD77L (40.1, 0.49), LCV76L (46.1, 0.50), LCV76L (64.5, 0.49). From the corresponding room temperature SAXS spectra we believe samples LCD77L (40.1, 0.49), LCV76L (46.1, 0.50), and LCV76L (64.5, 0.49) are ordered; however, the $T_{ODT}$ values of these samples could not be identified using DMA.

285
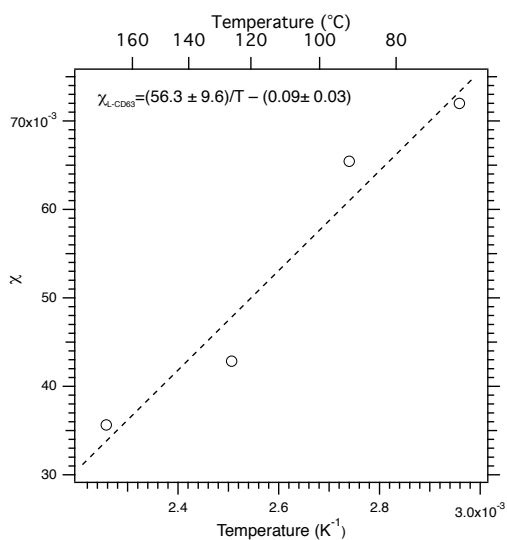
**Figure E.5**

($\chi$) temperature dependence for Lactide with CD66 copolymer. Points shown correspond to TODT values determined using DMA. These DMA data are provided in Figure E.1.
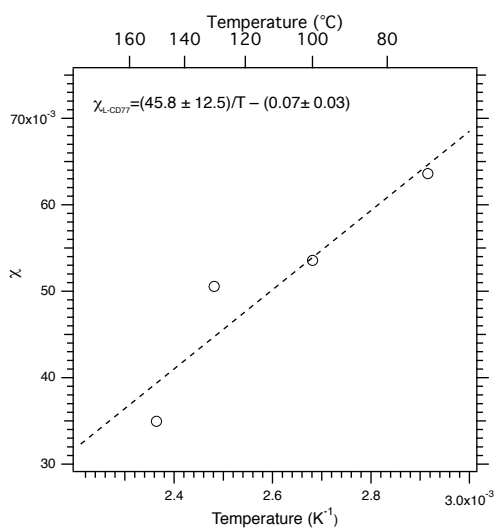


**Figure E.6**

($\chi$) temperature dependence for Lactide with CD77 copolymer. Points shown correspond to TODT values determined using DMA. These DMA data are provided in Figure E.2.

286
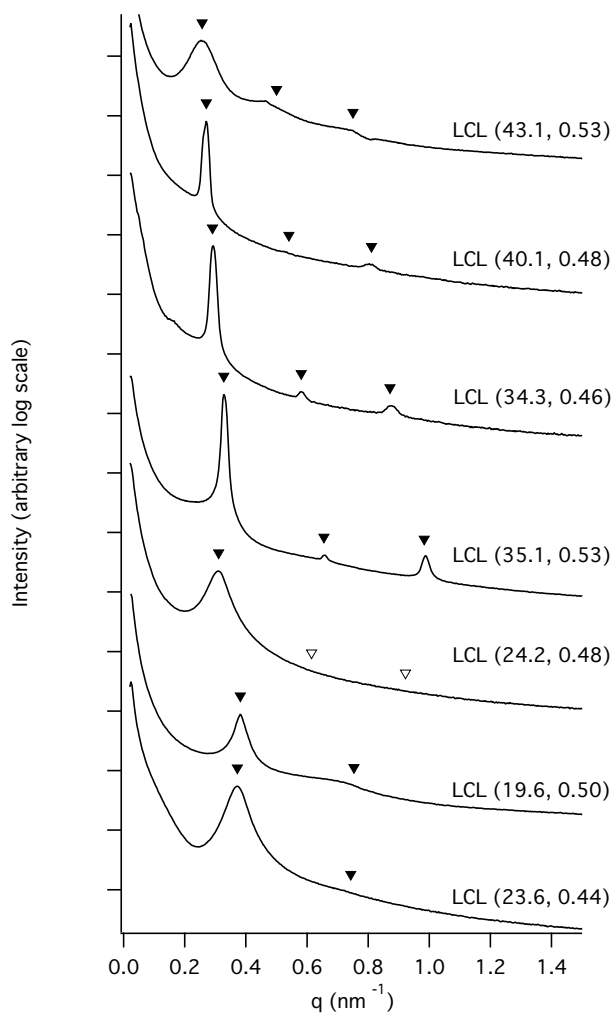
**Figure E.7**

Room temperature SAXS data for compositionally symmetric LCL triblock samples. The principle peaks are marked with (▼). Calculated reflections for anticipated lamellar morphologies are marked with (▼) and (▽) denoting reflections that are present, and absent respectively.
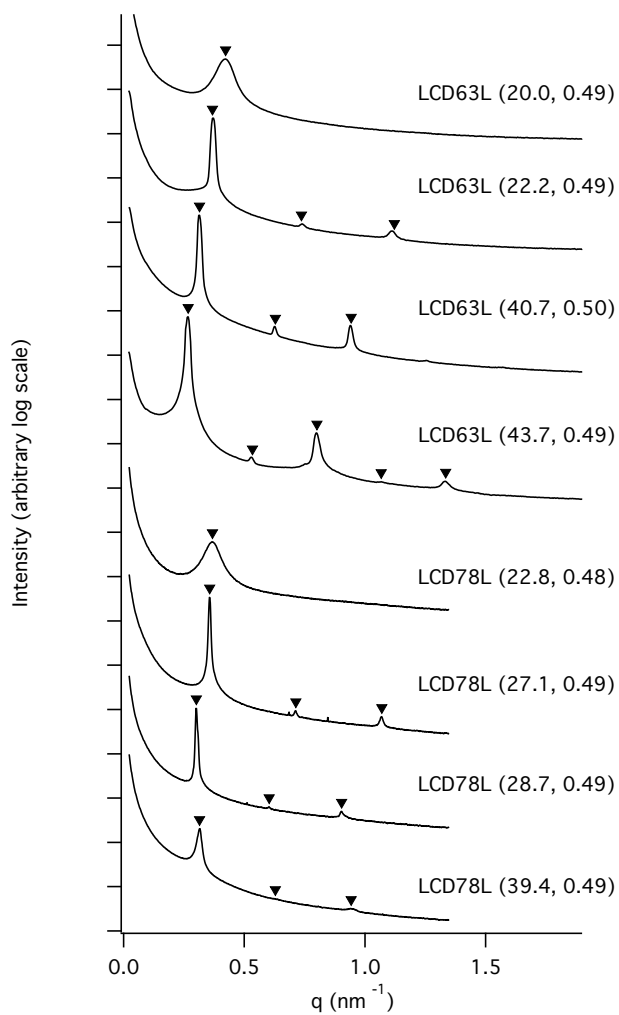
**Figure E.8**

Room temperature SAXS data for compositionally symmetric LCDL triblock samples. The principle peaks are marked with (▼). Calculated reflections for anticipated lamellar morphologies are marked with (▼) and (▽) denoting reflections that are present, and absent respectively.
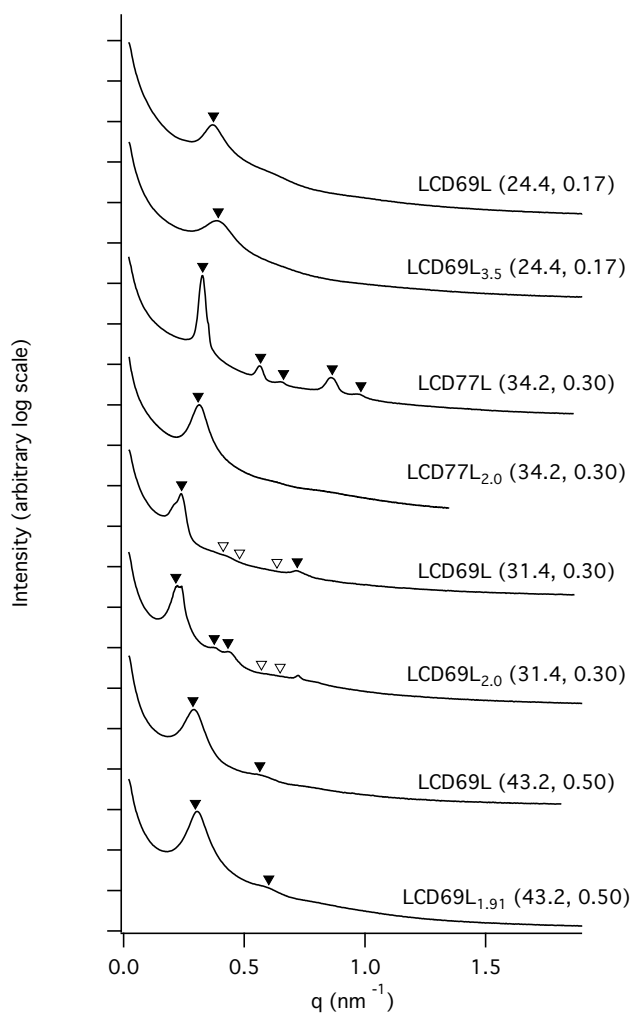
**Figure E.9.**

SAXS Data for LCDL triblocks and (LCDL)$_n$ multiblocks. The principle peaks are marked with (▼). For $f_{LA}$ = 0.33 and $f_{LA}$ = 0.30 the calculated reflections for anticipated cylindrical morphologies are marked with (▼) and (▽) denoting reflections that are present, and absent respectively.
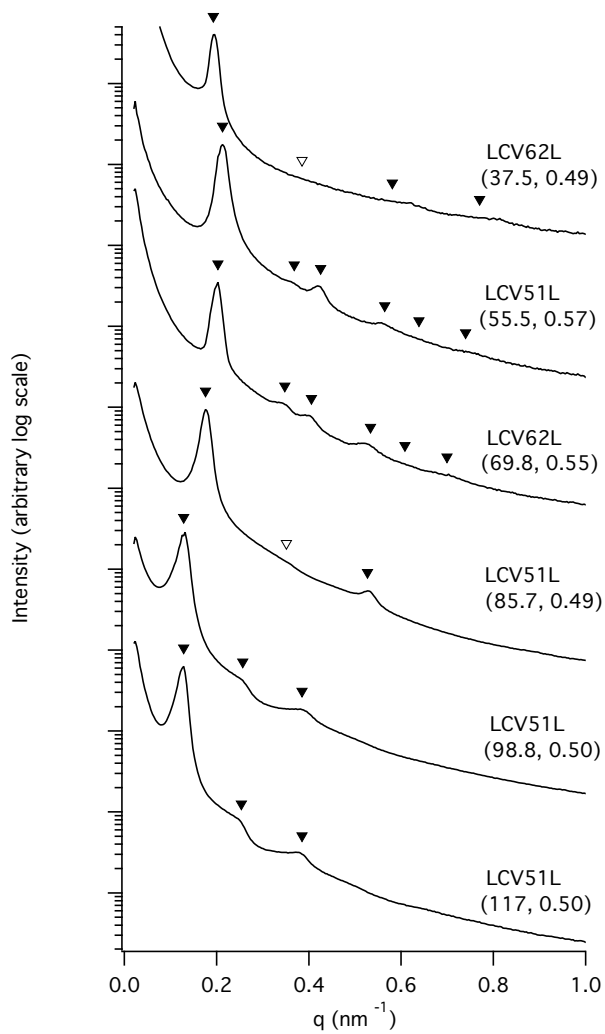
**Figure E.10**

Room temperature SAXS spectra of LCVL triblock polymers. The principle peaks are marked with (▼). The calculated reflections for anticipated cylindrical morphologies are marked with (▼) and (▽) denoting reflections that are present, and absent respectively.

290

# References

(1) Beckingham, B. S.; Register, R. A. Regular Mixing Thermodynamics of Hydrogenated Styrene–Isoprene Block–Random Copolymers *Macromolecules* **2013,** *46,* (3084-3091)

(2) Beckingham, B. S.; Burns, A. B., and Register, R. A. Mixing Thermodynamics of Ternary Block–Random Copolymers Containing a Polyethylene block *Macromolecules* **2013,** *46,* **(**2760-2766)

(3) Schively, M. L.; Coonts, B. A.; Renner, W. D.; Southard,  J. L., and Bennet, A. T.  Physico-chemical characterization of a polymeric injectable implant delivery system *Journal of Controlled Release* **1995**, 33, (237-243)

# Appendix F. Polymer Master Curves

In Chapters 2, 3, and 4, we reported the entanglement molar mass for a number of homopolymer and statistical copolymer samples. The molar mass between entanglements was estimated using dynamic mechanical analysis of a high molar mass sample (~100 kg mol$^{-1}$). Isothermal small amplitude oscillatory shear frequency sweeps were conducted for several temperatures ranging from −40 °C to 150 °C. A master curve was generated with reference temperature of 25 °C using horizontal shifts to tan δ. The shift facters thus obtained were applied to G' and G" to create a master curve. The plateau modulus ($G_N°$) was used to calculate the molar mass between entanglements, $M_e$.

$$M_e = \frac{\rho RT}{G_N^\circ} \tag{F1}$$

In this equation ρ, R, and T are the density, gas constant, and temperature, respectively. $G_N°$ was taken at frequency corresponding to the minimum in tan δ.

The master curves for the homopolymer and copolymer samples expored in this work are provided in this Appendix.
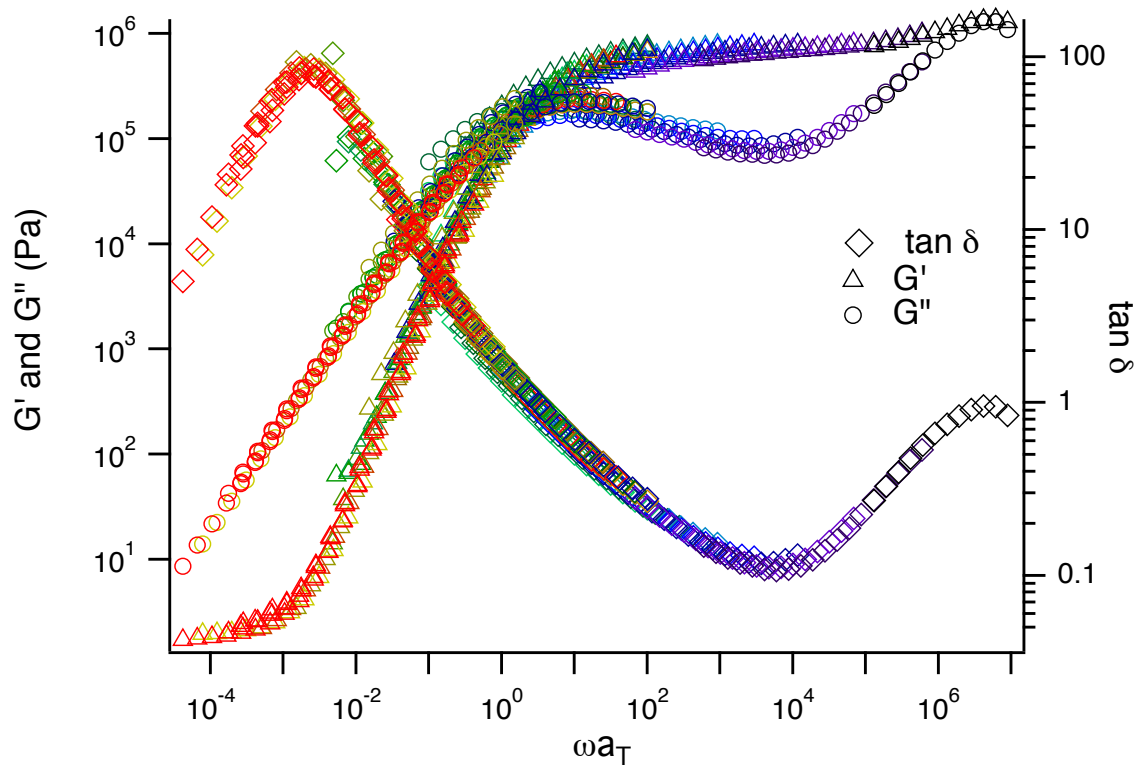
**Figure F.1**

Poly($\varepsilon$-Caprolactone-co-$\varepsilon$-Declactone) (PCD63) ($F_{CL}$=0.63) Master curve created using isothermal frequency sweeps (100 to 0.1 rad sec$^{-1}$) data were acquired from 180 °C to −30 °C. The reference temperature used is 25 °C.  The shift factors were obtained by shifting tan $\delta$ and applied to G' and G". No vertical shifts were applied.
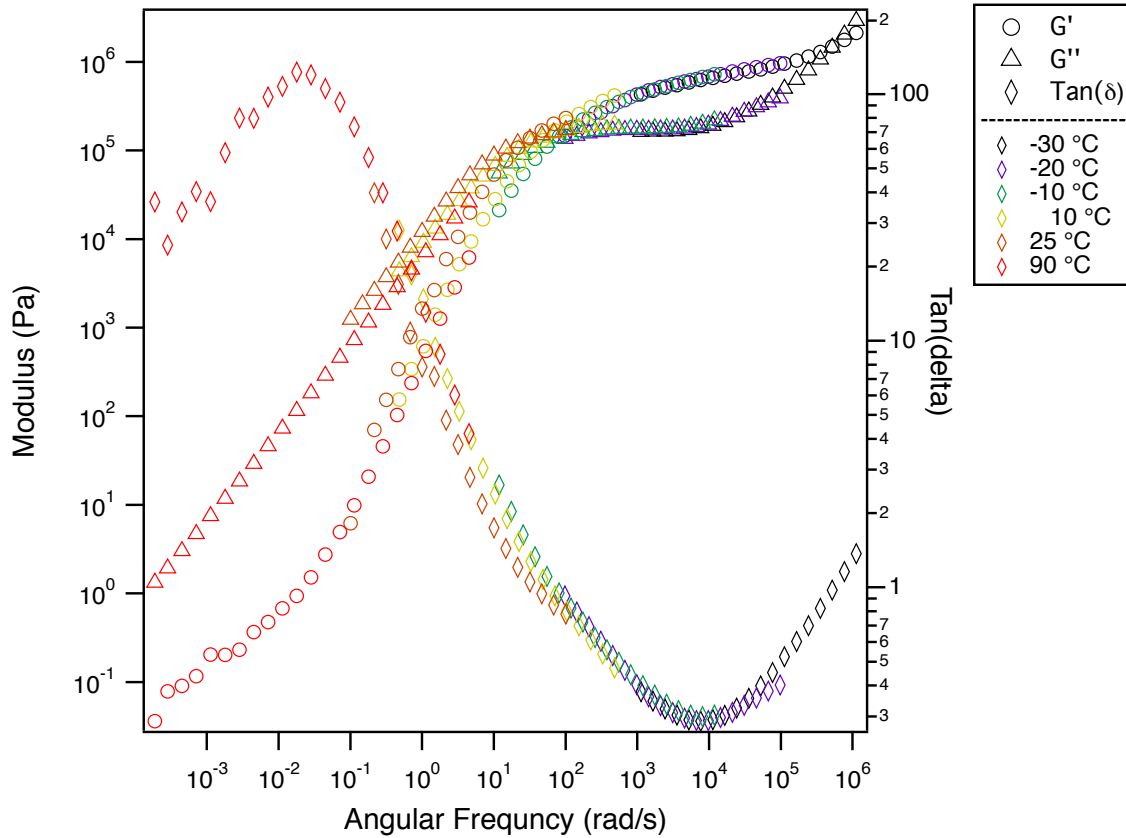
**Figure F.2**

Poly(6-Methyl-ε-Caprolactone) Master curve created using isothermal frequency sweeps (100 to 0.1 rad sec-1) data were acquired in 10 °C increments from 180 °C to -30 °C. The reference temperature used is 25 °C. The shift factors were obtained by shifting tan δ and applied to G' and G". No vertical shifts were applied.
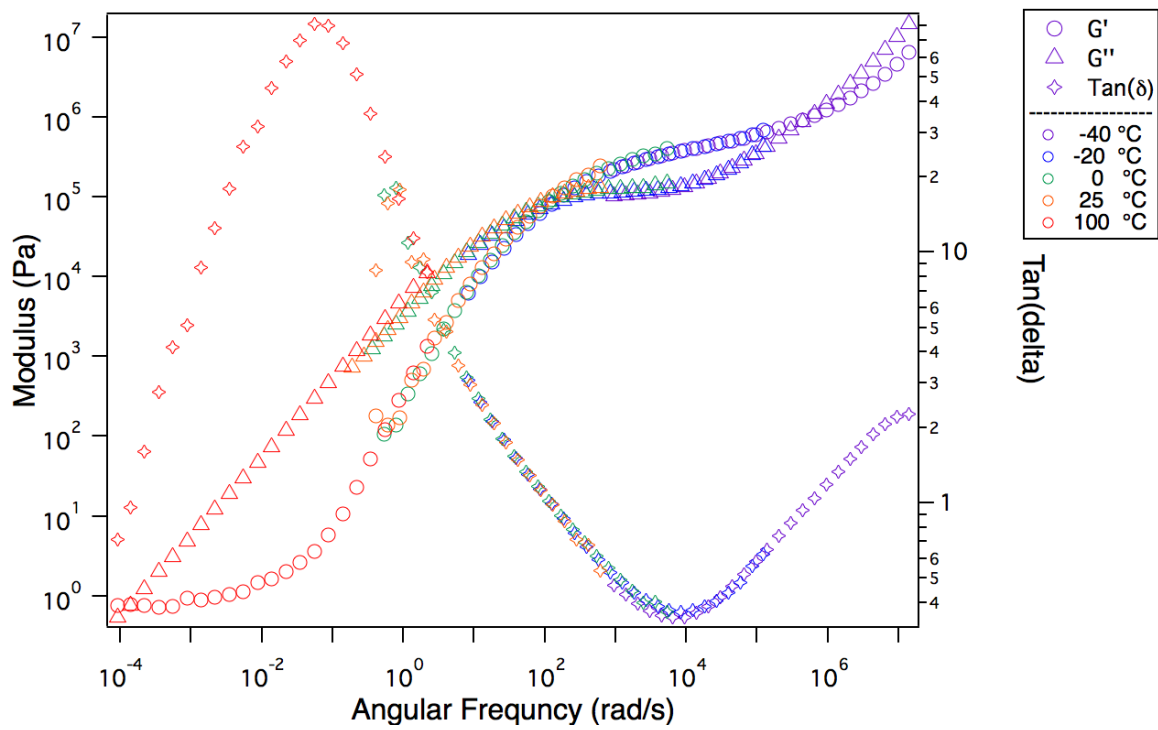
**Figure F.3**

Poly(α-Methyl-δ-valerolactone) (Pα1) Master curve created using isothermal frequency sweeps (100 to 0.1 rad sec$^{-1}$). The reference temperature used is 25 °C. The shift factors were obtained by shifting tan δ and applied to G' and G". No vertical shifts were applied.

**Figure F.4**

Poly(γ-Methyl-δ-valerolactone) (Pγ1) Master curve created using isothermal frequency sweeps (100 to 0.1 rad sec$^{-1}$ . The reference temperature used is 25 °C. The shift factors were obtained by shifting tan δ and applied to G' and G". No vertical shifts were applied.

**Figure F.5**

Poly(δ-Methyl-δ-valerolactone) (Pδl) Master curve created using isothermal frequency sweeps (100 to 0.1 rad sec$^{-1}$). The reference temperature used is 25 °C. The shift factors were obtained by shifting tan δ and applied to G' and G". No vertical shifts were applied.

**Figure F.6**

Poly(δ-pentyl-δ-valerolactone) or (Pδ5) Master curve created using isothermal frequency sweeps (100 to 0.1 rad sec$^{-1}$). The reference temperature used is 25 °C. The shift factors were obtained by shifting tan δ and applied to G' and G". No vertical shifts were applied.

**Figure F.7**

Poly(ε-Caprolactone-co-δ-valerolactone) ($F_{CL}$= 0.5) Master curve created using isothermal frequency sweeps (100 to 0.1 rad sec$^{-1}$) data were acquired in 10 °C increments from 180 °C to -10 °C. The reference temperature used is 25 °C. The shift factors were obtained by shifting tan δ and applied to G' and G". No vertical shifts were applied.

## Appendix G.  Notes on the Evolving Meaning of 'Plastic'

The purpose of this appendix is to provide some historical context for this work. This is done through the use of ten quotes about polymers from a diverse collection of sources published between 1852 and 2016. *The Graduate* is not among them.

> "His soul, constantly excited and unappeased goes about the world, the busy, toiling world like a prostitute crying: Plastic! Plastic! The plastic–that frightful word gives me gooseflesh–the plastic has poisoned him, and yet he can only live by this poison."
>
> —Charles Baudelaire, *The Pagan School,* (1852)

Charles Baudelaire, a mid 19th century French poet and art critic, wrote *The Pagan School,* as a rejection of Parnassian values and theories.[12] These poets believed in the pursuit of art for art's sake and preached withdrawal from modern life to focus disciplined writing, specifically, rigidity of form and faultless style. In their eyes, the convergence the two were both necessary and essential to the creation of beauty. Indeed the quintessence of poetry, the creation of transient and successive impressions of sound, demands that poetic beauty will be both dynamic and ephemeral. The Parnassians would have idealized this *plastic beauty* and pursued it as their ultimate goal. In this context, the word *plastic* (or *plastique* to Baudelaire) still retained its original meaning, the Greek word *plastikos* meant moldable.

Baudelaire argued that the formalist obsession with plastic beauty was perverse. Importantly, in the passage above he was not condemning plastics as a material. They did not yet exist–vulcanized rubber had been patented only eight years prior and the introduction of synthetic polymers was still over half a century away. In 1852, the year *The Pagan School* was written, the world was on the cusp of modernity. Following the Napoleonic wars, Europe was in a period of relative calm as the British Empire enjoyed a brief hegemony. The dominance of Britain during the Victorian era was due to superior manufacturing and shipping capability; indeed it was their desire to produce

high value textiles from cheap Indian cotton, which drove the early innovations of the first industrial revolution. As the effects this revolution rippled across the world, the global consumption of coal increased exponentially; however, the petroleum industry was only just beginning to develop.

In 1856, while attempting to synthesize quinine from coal tar, William Henry Perkin accidently manufactured the organic dye mauveine.[3] Perkin's eventual success in commercializing this discovery led to the development a synthetic dye industry and generated significant interest in the field of organic chemistry. In subsequent decades, German dye manufactures, including BASF (Badische Anilin und Soda Fabrik), Bayer (Farbenfabrikem vorm. Friedr. Bayer & Co.), and Hoechst (Teerfarbenfabrik Meister, Lucius & Co.) perfected the purification of individual organic compounds (e.g., phenol) from coal tar and also discovered many of the synthetic techniques widely used by organic chemists today.[456] The emerging pharmaceutical industry made use of these techniques developed by the dye manufactures to synthesize of antibiotics and analgesics; because both industries also employed the same phenolic coal-derived chemicals, there was little demarcation between the two.

Although inventors were experimenting with polymeric materials long before the turn of the century, the concept of macromolecular structure was not yet understood. The word *polymer* had been coined decades before by the Swedish chemist Berzelius, but his usage differed dramatically from the modern definition. At this time, research in the still nascent field of polymer science consisted mainly of the development of semisynthetic materials from cellulose.[7] However, these materials were initially

302

commercialized with mixed success. Patented by Alexander Parkes in 1862, nitrocellulose was briefly marked as synthetic ivory before the company went bankrupt only six years later due to scale-up costs. Not long after, the American inventor John Wesley Hyatt, simplified the nitrocellulose production process and began manufacturing Celluloid (meaning cellulose-like) for use in high-end consumer products like billiard balls.[7,8]

"Too tough a morsel for time to swallow; when pure, it rusts not, nor does it decay, and it can endure throughout all generations....What cellulose is, molecularly, is equally wholly beyond the comprehension of present-day man"

—Robert Kennedy Duncan, *The Wonders of Cellulose*, (1906)

At the time nobody knew quite what these new materials actually were. In his 1906 essay *The Wonders of Cellulose* Robert Kennedy Duncan, a professor of industrial chemistry at the University of Kansas, eloquently extoled the many virtues and uses of cellulose. At the same time he acknowledged that the actual chemical structure of cellulose was very much an unsolved mystery to contemporary chemists.[9] Duncan published several shorter magazine articles and books with the principle goal of explaining contemporary challenges of chemistry to a general audience.[10] A recurring theme in his writing is the belief that the persistent tendency of American academic scientists to devalue applied research in favor of the pursuit of pure science was inhibiting the development of domestic chemical and manufacturing industries.[11,12]

To help foster collaboration between academia and industry, Duncan established the first industrial research fellowship at the University of Kansas; he later went on to also

become director of the Mellon Institute for industrial research at the University of Pittsburg. Important innovations made at the institute, described in a 1914 Popular Mechanics article, included: the development of a method for the reliable industrial manufacture of bread, the discovery of a cheap and practical process to extract high-grade gasoline from petroleum waste, and the invention of a new material, *Amberoid*, that was said to be "odorless, insoluble in acids or alkalis, and non-explosive."[13] The adjective "non-explosive" was certainly not used by accident; celluloid (chemically, cellulose nitrate) is highly flammable and tends to explode under pressure or on high impact. [14,15]

> "If the new substance 'Bakelite' can fulfill the claims of its inventor and revolutionize the development of long distance high-speed electric railways, then it may take its place beside the electric current and the steam engine as one of the miracle workers of the modern world."
>
> —Washington Post, (1909)[16]

By the turn of the century the concept of chemical structure and functionality was well developed for small molecules however no one had yet rigorously applied this concept to the study of polymers. Two simultaneous lines of development were about to converge, creating for the first time an environment in which fully synthetic polymers could be invented. First, the commercial success of vulcanized rubber and cellulosic polymers had generated a demand for synthetic plastics, which these early semisynthetic materials alone simply could not meet. Second, the maturation of the field of organic chemistry–specifically, the development of more refined synthetic

techniques and a better understanding of the concepts of molecular structure–enabled for the first time a systematic investigation, guided by rational design.

In the summer of 1907, while attempting to produce lacquer for bowling alley floors, an inventor named Leo Baekeland invented the world's first fully synthetic polymer; a thermoset phenolic resin (later called Bakelite). Like Parkes and Hyatt before him, Baekeland was attempting to capitalize on a shortage of a naturally occurring material, shellac. This resin was an excellent insulator in high demand due to the development of consumer electronics but was produced in limited quantities by the lac bug (it took 15,000 beetles six months to produce a pound).[1718] Although the invention of Bakelite is frequently described as accidental or serendipitous, this is very much an over simplification. Baekeland, an organic chemist by training, certainly understood the potential of the underlying chemistry.

> "It will not burn. It will not melt. It is used in pipe stems, fountain pens, billiard balls, telephone fixtures, castanets, radiator caps, etc. In liquid form, it is a varnish. Jellied, it is a glue. Those familiar with its possibilities claim that in a few years it will be embodied in every mechanical facility of modern civilization."
>
> —Time Magazine, (1924)[19]

It had known for several decades that phenol would condense with aldehydes; however, the reaction was largely unexploited because its resultant crosslinked products were insoluble and tended to ruin laboratory equipment. In fact, in the time since Aldof von Baeyer had conducted the earliest work in this area over three decades earlier, another

German chemist, Adolf Luft, had obtained a patent for the "Process for Producing Plastic Compounds" from phenol, formaldehyde and sulfuric acid.[20] Luft and many others had experimented with these resins but had been unable to create a useful product. Baekeland's major contribution was not the discovery of phenolic resins, but rather the invention of an improved molding process to manufacture useful products from these resins.

Baekeland publicized his discovery in 1909, and in all was awarded over 400 patents related to production of Bakelite products.[17] By 1910 he had formed a company, the Bakelite Corporation, to market and manufacture his new material. Within a few years Bakelite replaced Celluloid in a number of applications, including billiard balls. It was cheaper to produce, easier to mold, and did not have the same tendency to ignite or explode. Moreover, Bakelite was versatile, subtle variations to the original formula (e.g., the dyes and fillers) could be used tailor its appearance and performance.[21] Following WWI, a number of synthetic polymers including, polyvinylchloride (1926), polystyrene (1930), polyethylene (1933), polymethylmethacrylate (or Plexiglas) (1933), and polyethylene terephalate (1941) were commercialized in short succession.[22] The close timing is not coincidental; rather, these discoveries were facilitated by a better understanding of polymer structure.

> "Dear colleague, leave the concept of large molecules well alone: organic molecules with a molecular weight above 5,000 do not exist. Purify your products, such as rubber, then they will crystallise and prove to be lower molecular substances."
>
> —Heinrich Wieland, *Letter to Staudinger*, (circa 1928)[23]

As early as 1920, Hermann Staudinger, then a professor of organic chemistry at Eidgenössische Technische Hochschule (ETH) in Zurich proposed that polymer materials were comprised of high molecular weight molecules or macromolecules (*makromoleküles* to Staudinger). In his seminal work, *Über Polymerisation,* Staudinger introduced the now familiar chain structures for polystyrene, polyisoprene, polyoxymethylene, among others. [24] His view was in contrast to the prevailing view at the time, that polymers were colloidal aggregates of small molecules held together by noncovalent interactions. Although the macromolecular hypothesis was initially met with strong opposition by most leading organic chemists, including Heinrich Wieland, Staudinger was not alone in his belief. A number of scientists had previously published experimental results that were in clear opposition to the colloidal explanation of polymers structure, however these were largely ignored. [25]

It was a stormy decade for the field. Despite a growing body of experimental evidence in support of the macromolecular hypothesis the prejudice against the notion of high molar mass molecules persisted. During this time, Michael Polanyi, a physical chemist and X-ray crystallographer suggested the diffraction pattern of cellulose was consistent with either an aggregate of dimer rings or a long molecule comprised of chemically linked hexoses units. [25] Although he argued either interpretation could be valid organic chemists believed the former was far more likely. The later idea was also rejected by most X-ray crystallographers, who at the time, believed that a molecule could not be larger than the unit cell of its crystal (by this argument the molar mass of a molecule had to be less than 1000 g mol$^{-1}$). [26] However, in 1928 K.H. Meyer and Herman Mark,

published a revised description of the structure cellulose–a long chain of glucose rings joined by covalent bonds.[25]

The Meyer-Mark model employed both primary (covalent linkages between individual sugar moieties within the polymer chain) and secondary bonding (e.g., hydrogen bonding between chains) to explain the observation of both crystalline and amorphous regions in cellulose. Meyer reiterated these views and suggested the possibility of a distribution of polymer molecular weights in a follow-up work. Staudinger disagreed with Meyer about the importance of secondary bonding on polymer properties. What was initially a minor dispute eventually led to a number of contentious exchanges in the literature halted only when a journal editor refused to print any more of their papers on the subject.[25] Notably, Meyer, Mark, and Staudinger all believed that polymers were long chain molecules rather than colloidal aggregates, contrary to the view of most other established chemists at the time.

Also among the apostates was Wallace Carothers, who in 1928 was just beginning his career at DuPont.[27] He and his team made a number of lucrative synthetic discoveries including invention of neoprene (1930) and nylon (1935). This synthetic work also had important theoretical ramifications. In particular, Carothers's work with the step growth synthesis of polyesters and polyamides established that polymers could be prepared using well-understood condensation reactions, which lent credence to Staudinger's theory. Additionally, as part of Carothers's attempts to prepare high molar mass polymers, he worked out a theory of step growth polymerization and derived the now-eponymous equation relating monomer conversion to degree of polymerization. As

a result of these well-documented and careful studies, there was little question about the existence of macromolecules by the mid 1930s.[28]

> "It is a world free from moth and rust and full of color…. a world in which man, like a magician, makes what he wants for almost every need, out of what is beneath him and around him, coal, water, and air."
>
> —Yarsley & Couzens, *Plastics,* (1941)

Victor Yarsley and Edward Couzens, coauthors of *Plastics,* watched this revolution in the field of polymer science firsthand. Yarsley, an industrial consultant and consultant, had studied chemistry at ETH Zürich and had spent much of the late 1920s and early 1930s conducting extensive research on cellulose acetate in a small independent research lab.[29] Couzens, then head of research at BX Plastics (a company that manufactured a variety of thermoplastics), was also a chemist by training.[30] The pair of scientists wrote *Plastics* to explain to the general public both the immediate importance of synthetic polymers to the war effort and to describe the great potential of these materials for use in commercial applications. However, they also hoped to educate others about the chemical structure of polymers. Perhaps owing to the fact that all types of synthetic polymers were generally called plastics, the layperson was somewhat confused about what these materials actually were.

The introduction of Bakelite had whet consumer's appetite for synthetic materials. However, by the onset of the Second World War, the public was a bit jaded.[22] On one hand, newspaper and magazine articles had glamorized plastics for decades, touting them as mysterious and magical inventions, which would soon supplant conventional

materials such as metal, ivory, and wood. However, the wide variety of polymers developed during interbellum period had been commercialized with mixed success. In general, plastics were also viewed as trivial and inferior substitutes; plastic was the stuff used to make gadgets and gaudy jewelry but was not strong enough or durable enough to be a manufacturing material. WWII had many effects on the plastics industry.

By necessity, new uses for synthetic polymers were explored and new methods were developed to improve the durability and performance of synthetic polymers. As blockades led to shortages of silk and rubber, the production of plastics accelerated–in 1941 production in the United States doubled.[22] Whereas Nylon was used to replace silk in parachutes, rope, and armor, Plexiglas became an important material for use in aircraft windshields. Moreover, the war also greatly accelerated the development of synthetic rubber (a discovery which directly led to the development of block polymers). Importantly, the war demonstrated to consumers that plastics could be both tough and superior to wood and metal in many applications. In the US in particular, the war drove a rapid increase manufacturing capability in all industries (not just plastics).

The mass production methods previously developed by Henry Ford for the auto industry were applied in earnest to the manufacture of airplanes, tanks, armored cars, and ships. Simultaneously, chemical companies increased production of petrochemicals used to manufacture explosives. A knock-on effect of increased manufacturing activity during WWII was that real wages in America rose dramatically during the war; additionally, wealth became more evenly distributed as many women and minorities held jobs for the first time. After the war ended and rations were no longer in effect,

there was a tremendous market for manufactured goods. Americans wanted to buy cars, washing machines, radios, and other consumer products. Manufactures saw a great opportunity in cheap lightweight, petroleum-derived plastics. The invention of the last major commodity plastic, polypropylene (1954), marked a transition in the plastics industry from an era of discovery and development to one of diversification. It was at this time that synthetic polymers really began to proliferate. The "Plastic Age" prophesied by Yarsley and Couzens had arrived.

> "But until now imitation materials have always indicated pretension, they belonged to the world of appearances, not to that of actual use; they aimed at reproducing cheaply the rarest of substances, diamonds, silk, feathers, furs, silver, all the luxurious brilliance of the world. Plastic has climbed down, it is a household material. It is the first magical substance which consents to be prosaic."
>
> —Roland Barthes, *Plastics*, in *Mythologies*, (1957)

A few years later, in 1947, a special issue of *House Beautiful* included an extensive insert devoted to plastics, including articles with such titles as *"Fine Art for 39¢", "All Plastics are Not Alike", and "So You Never Thought Plastics Could Be SO Elegant!".*[31] The writers enthusiastically endorsed plastics for many uses in the home, lauding their beauty, comfort, and utility. A lone cautionary article *"What's wrong with plastics?"* warned against using plastics without discretion. However, the objections purely aesthetic; the author advised against purchasing tacky or ugly plastic objects designed to look like familiar old materials. [32] The potential of plastics was nearly limitless, provided the right type of plastic was selected for the right application. This idea was carried to its natural

conclusion in 1957, when a futuristic all-plastic house was included in Disney's *Tommorwland* exhibit.[33]

The same year, Roland Bathes, a French philosopher and semiotician published a collection of essays, *Mythologies.* In it he attempted to deconstruct several myths of popular culture. Reflective of the universality of synthetic polymers had achieved by this time, he included an essay in which he considered the importance of plastic–and its meaning as both a substance and a symbol. He wrote that, because *plastic materials* could be used for almost any application, they effectively epitomized transmutability. However, at the same time, Barthes noted the success of plastics in becoming everyday materials had already begun to change the very meaning of the word *plastic.* Whereas plastic *as an adjective* had formerly meant moldable, plastic *as noun* had come to imply cheap and commonplace.[34]

> "Take out plastic from a modern city––what do you get—complete breakdown. We're totally dependent on it."
> —Kit Pedler and Gerry Davis, *Mutant 59: The Plastic Eaters*, (1973)

Although all-plastic houses never really became a reality (the *Tommorowland* house was torn down, with considerable difficulty, a decade after it was built), the production of plastics accelerated exponentially in subsequent decades.[33] Initially, most people were blithely unaware of the potential negative impacts of plastics on human health and the environment. However, the late 1960s and early 1970s were characterized by an increased environmentalism worldwide. In the US, a number of conservation bills, including the clean Air Act (1970), the National Environmental Policy Act (1970), and

the Water Pollution Control Act (1972), were passed in rapid succession.[35] At the same time there was a push at the community level for recycling programs. For example, the first bottle bill, which instituted refundable deposits on plastic beverage bottles, was instituted 1971. Additionally, the first post consumer plastic waste-recycling mill was opened in Pennsylvania in 1972.[36]

These community-driven recycling initiatives are reflective of both the proliferation of disposable plastic products and of a growing awareness of the prevalence of plastic litter in the environment. Essentially, this is the paradox of plastics: because they are inert they have potential to cause harm if disposed of improperly. However, in many applications, plastics also pose a threat *when* they break down. The 1969 Michael Crichton novel *The Andromeda Strain* (two years later a film adaptation with the same name) touches on this idea. In it an extraterrestrial microorganism mutates from a deadly pathogen to a "benign" form that degrades plastic and rubber. It escapes its containment to migrate to the upper atmosphere where it wrecks havoc on spacecraft.

Kit Pedler and Gerry Davis' *Mutant 59: The Plastic Eaters*, published a few years later also explores this theme. In this work, scientists invent a polymer, Degron that breaks up under the influence of light and oxygen. Extensive use of this degradable plastic in packaging applications results in its introduction into sewer systems where is serves as food for bacteria. Chaos ensues when a bacterial strain evolves that consumes all types of plastic, not just the ones intended to degrade. Outside science fiction, plastics designed for degradation were not seriously researched until the oil crisis of the late 1970s and were not commercialized until nearly a decade later.[37]

313

"They sped across the sand, the only people for miles and miles. There was plastic everywhere. 'You will see a lot of plastic," the man who rented the Jeep said, "but it is plastic from all over the world"

—Joy Williams, *Health*, (1985)

Early on, concerns over plastic pollution were mainly aesthetic; litter was seen as an eyesore and blight on the landscape. However, as more and more plastic accumulated in the environment it soon became   apparent that its presence constituted a serious public health issue. Plastic was first discovered in the guts of sea birds in 1960 and as early as 1970 scientists speculated that the ingestion of plastic debris could introduce toxic chemicals to the food chain.[38,39] The International Convention for the Prevention of Pollution From Ships was signed in 1973 (though a complete ban on the intentional disposal of plastics at sea was not fully enacted until fifteen years later).[40]

Despite this legislation, nearly 9 million tons of plastic leak into the ocean annually.[4142] The vast majority comes from land-based sources, however almost 20% comes from ships, either lost accidentally or waste intentionally dumped. Although much of this trash sinks or gets caught up in oceanic gyres, some eventually floats to shore. Oceanographers have even used found flotsam from cargo ships (e.g, Nike cross-trainers from *Hansa Carrier* (1990), Friendly Floaties bath toy spoils *Ever Laurel*, and Legos from *Tokio Express* (1997) to map ocean currents.[43,44,45]

In Joy Williams' short story *Health*, a young girl on vacation recalls that she has been told that the plastic strewn over the beach is from all over the world. This sentiment; that plastic pollution is simultaneously ubiquitous (trash is everywhere) and somehow exotic (this particular trash has travel across oceans) again captures a strange duality similar to that described by Barthes. In demonstrating its utility, plastic had previously fallen in status from mystical to commonplace; in demonstrating its durability, it has now become dangerous.

> "They choke sewer drains and waterways, or they just roll around on the streets: tumbleweeds from some petroleum-based hellscape."
>
> —New York Times, (2016)[46]

Most people alive today have never known a world without plastics. There is little question that as the global population grows and become more urbanized the demand for synthetic polymers will continue to increase. Yet our relationship with these materials continues to evolve. For many people the word plastic carries with it now, new (largely negative) connotations. Successful commercialization of new sustainable polymers today may help to influence humanity's future relationship with synthetic materials. If history has taught us anything, it is that it is a relationship that is, in fact, very plastic.

# References

(1) Grünberg, L. *The Mystery of Values, Studies in Axiology,* Grünberg, C. and Grünberg, L. Eds. **2000**, Rodophi B.V. Amsterdam, Netherlands

(2) Derrida, J. *The Gift of Death 2nd Edition,* David Willis Trans. **1999,** University of Chicago Press, Chicago, Illinois, USA

(3) Hager, R. *The Demon Under the Microscope* Random House, Inc. New York, USA, **2006**

(4) Bayer AG, April 6th 2016, History [Online] http://www.bayer.com/en/1881-1914.aspx Accessed April 20th, 2016

(5) BASF, 2016, About Us 1865-1901 The Birth of the Chemical Industry and The Era of Dyes [Online] https://www.basf.com/en/company/about-us/history/1865-1901.html Accessed April 19th, 2016

(6) Advameg, Inc. 2016 History of Hoechst, A.G. [Online] http://www.referenceforbusiness.com/history2/22/Hoechst-A-G.html Accessed April 12th, 2016

(7) Reilly, J. A. Celluloid Objects: Their Chemistry and Preservation *Journal of the American Institute for Conservation,* **1991,** *30 (2),* (145)

(8) Our State Institutions XVII-The Manufactures of Albany, *New York Times,* January 19, **1872**

(9) Duncan, R. K. The Wonders of Cellulose *Harpers Monthly Magazine,* September, **1906,** (573)

(10) Bacon, Raymond, F. Obituaries: Robert Kennedy Duncan, *The Journal of Industrial and Engineering Chemistry* **1914,** *6 (4)*

(11) Duncan, R.K. The Chemistry of Commerce: A Simple Interpretation of Some New Chemistry In Its Relation to Modern Industry. **1907**, Harper and Brothers Publishers, New York and London

(12) Duncan, R.K. Some Chemical Problems of Today. **1911**, Harper and Brothers Publishers New York and London

(13) Stockbridge, F. P. Harnessing Science to The Factory. *Popular Mechanics Magazine* **1914**, *21 (April)*, (474)

(14) Chinese Investigators Identify Cause of Tianjin Explosion *Chemical Engineering News* **2016**, (February 8th)

(15) Hyatt, J. W. Address of Acceptance, *Journal of Industrial and Engineering Chemistry* **1914,** *6(2),* (158-161)

(16) Some Modern Inventions *The Washington Post,* **1909**, February 7th, (E4)

(17) American Chemical Society National Historic Chemical Landmarks. Bakelite: The World's First Synthetic Plastic. [Online] http://www.acs.org/content/acs/en/education/whatischemistry/landmarks/bakelite.html Acessed April 29th, 2016

(18) Freinkel, S. A Breif History of Plastic's Conquest of the World *Scientific American,* **2011**, (May 29th)

(19) Science: At Ithaca *Time Magazine,* **1924**, 4(12) September 22nd , (20)

(20) Bijker, W. E. Of Bicycles, Bakelites, and Bulbs Toward a Theory of Sociotechnical Change, **1995**, MIT Press, Cambridge Massachusetts, USA

(21) Keasbey, W.P. Did You Ever Wonder: What Bakelite Is and How It Got Its Name? *The Christian Science Monitor,* **1940**, Nov. 5th, (17)

(22) Nicholson, J. L.; Leighton, G. R., Plastics come of Age *Harpers Weekly,* **1942**, August, (300-307)

(23) Klug, Jörg; Commentary on Gáspár Jékly's article in EMBO reports, *EMBO reports* **2002**, *3,* (1004)

(24) Staudinger, H. Über Polymerisation Berichte der deutschen chemischen Gesellschaft (A and B Serieze) **1920**, *12* (*6),* (1073-1085)

(25) Stahl, A. G.; Development of a Modern Polymer Theory in *Pioneers in Polymer Science* Seymour, R.B. Ed. **1989**, Kluwer Academic Publishers, Dordrecht, The Netherlands

(26) Jékely, G. The human genome sequence: a triumph of chemistry *EMBO reports* **2002***, 3,* (594-595)

(27) Serpe, M. J.; Craig, S. L. Physical Organic Chemistry of Supramolecular Polymers *Langmuir,* **2007,** *23,* (1626-1634)

(28) Mark, H.F..; Remembering the Early Days of Polymer Science *Pioneers in Polymer Science* Seymour, R.B. Ed. **1989**, Kluwer Academic Publishers, Dordrecht, The Netherlands

(29) Plastics and a man named Yarsley. Epson and Ewell History Explorer [Online] http://www.epsomandewellhistoryexplorer.org.uk/Yarsley.html Accessed May 3rd, 2016

(30) Yarsley, V.E.; Couzens, E.G. *Plastics,* **1941**, Pelican Books, New York, USA

(31) The truth about plastics Gordon, E. (ed.) *House Beautiful,* **1947,** October, 89 *(10) 120-296*

(32) Gordon, E. What's wrong with plastics *House Beautiful,* **1947,** October, 89 (10) p166

(33) Monsanto House of the Future. Yesterland [Online] http://www.yesterland.com/futurehouse.html Accessed May 12th, 2017

(34) Barthes, R., *Mythologies* Translated by Lavers, A. Hall and Wang Publishers, New York, **1956**

(35) Shellenberger, M.; Nordhaus, T. The Death of Environmentalism: Global Warming Politics in a Post-Environmental World *Geopolitics, History and International Relations,* **2004**,

(36) Bottle Bill Resource Guide, What is a Bottle Bill? [Online] http://www.bottlebill.org/about/whatis.htm Accessed May 30th, 2016

(37) Ecomall. Degradable Plastics for Composting [Online] http://www.ecomall.com/greenshopping/biocycle.htm Acessed May 31st, 2016

(38) Thompson, R. C.; Swan, S. H.; Moore, C. J.; vom Saal, F. S Out Plastic Age *Phil. Trans. R. Soc. B.* **2009**, *364,* (1973-1976)

(39) Teuten, E. L.; Saquing, J. M.; Knappe, D. R. U.; Barlaz, M. A.; Jonsson, S.; Björn, A.; Rowland, S. J.; Thompson, R. C.; Galloway, T. S.; Yamashita, R.; Ochi, D.; Watanuki, Y.; Moore, C.; Viet, P. H.; Tana, T. S.; Prudente, M.; Boonyatumanond, R.; Zakaria, M. P.; Akkhavong, K.; Ogata, Y.; Hirai, H.; Iwasa, S.; Mizukawa, K.; Hagino, Y.; Imamura, A.; Saha, M.; Takada, H. Transport and release of chemicals from plastics to the environment and to wildlife *Phil. Trans. Royal Soc. B.* **2009,** *364,* (2027-2045)

(40) Rochman, C. M.; Browne, M. A.; Halpern, B. S.; Hentschel, B. T.; Hoh, E.; Karapanagioti, H. K.; Rios-Mendoza, L. M.; Takada, H.; Teh, S.; Thompson, R. C. Classify Plastics as Hazardous Waste Nature, **2013**, 494 (169-171)

(41) World Economic Forum, Ellen MacArthur Foundation and McKinsey and Company, The New Plastics Economy Rethinking the Future of Plastics, **2016**, http://www.ellenmacarthurfoundation.org/publications).

(42) Ocean Conservancy Stemming the Tide: Land-based strategies for a plastic-free ocean [Online] http://www.oceanconservancy.org/our-work/marine-debris/mckinsey-report-files/full-report-stemming-the.pdf Accessed January 15th, 2016

(43) Ebbesmeyer, C. C.; Ingraham, W. J., Jr., Pacific Toy Spill Fuels Ocean Current Pathways Research *EOS, Transactions of the American Geophysical Union* **1994**, (37) 425-432

(44) Ebbesmeyer, C. G.; Ingraham, Shoe Spill in the North Pacific *EOS, Transactions of the American Geophysical Union* **1992**, *73 (34)*, 361-365

(45) Ebbesmyer, C. C.; Ingraham, W. J. Jr.; Royer, T. C.; Grosch, C. E., Tub Toys Orbit the Pacific Subartic Gyre *EOS, Transactions of the American Geophysical Union* **2007**, *88, 1-4*

(46) New York Times Editorial Board, How New York Can Put an End to The Plastic Bag 2016 [Online] http://www.nytimes.com/2016/05/05/opinion/how-new-york-can-put-an-end-to-the-plastic-bag.html?_r=0 Accessed May 31st, 2016

# Bibliography

Abe, H.; Takahashi, N.; Ju Kim, K.; Mochizuki, M.; Doi, Y. Degradation Processes of End-Capped Poly(L-Lactide)s in the Presence and Absence of Residual Zinc Catalyst *Biomacromolecules* **2004**, *5,* (1606-1614)

Achkar, J.; Xian, M.; Zhao, H.; Frost, J. W. Biosynthesis of phloroglucinol. *J Am Chem Soc* **2005**, *127*, (5332-5333)

Advameg, Inc. 2016 History of Hoechst, A.G. [Online] http://www.referenceforbusiness.com/history2/22/Hoechst-A-G.html Accessed April 12th, 2016

Ajikumar P.K.; Xaio, W.-H.; Tyo, K. E. J.; Yong, W.; Simeon, F.; Leonard, E.; Mucha, O.; Phon, T. H.; Pfeifer, B.; Stephanopoulos, G. Isoprenoid pathway optimization for Taxol precursor overproduction in *Escherichia coli. Science* **2010**, *33*0, (70-74)

Albertsson, A.-C; Gruvegard, M. Degradable high-molecular-weight random copolymers, based on ε-caprolactone and 1,5-dioxepan-2-one, with non-crystallizable units inserted in the crystalline structure *Polymer* **1995,** *36,* (1009-1016)

Albertsson, A.-C.; Srivastava, R. K. Recent developments in enzyme-catalyzed ring-opening polymerization *Advanced Drug Delivery Reviews* **2008**, *60,* (1077-1093)

Alam, M.; Akram, D.; Sharmin, E.; Zafar, F.; Ahmad, S. Vegetable oil based eco-friendly coating materials: A review article *Arabian Journal of Chemistry* **2014,** *7,* (469-479)

Alemán, C.; Betran, O.; Casanovas, J.; Houk, K.N., Hall, H. K. Jr. Thermodynamic Control of the Polymerizability of Five-, Six, and Seven-Membered Lactones *Journal of Organic Chemistry* **2009,** *74,* (6237-6244)

Allsopp, M.; Walters, A.; Santillo, D.; Johnston, P. Plastic Debris in the World's Oceans **2006,** [report] Green Peace International

American Chemistry Council, Economic and Satatistics Department The Economic Benefits of the U. S. Polyurethanes Industry, **2014**

Anastas, Paul; Eghbali, Nicolas. Green Chemistry: Principles and Practice *Chem. Soc. Rev.* **2010,** *39, (*301-312)

Anderson, K. S.; Schreck, K. M.; Hillmyer, M. A. Toughening polylactide *Polymer Reviews* **2008,** *48, (1),* (85-108)

Andrady, A. L.; Neal, M. A., Applications and societal benefits of plastics. *Philosophical Transactions B* **2009,** *364,* (1977-1984)

Andreana, P.R.; McLellan, J. S.; Chen, Y.; Wang, P. G. Synthesis of 2,6-Dideoxysugars via Ring-Closing Olefinic Metathesis *Organic Letters* **2002***, 4,* (3875)

Andronova, N., and Albertsson, A.-C. Resilient Bioresorbable Copolymers Based on Trimethylene Carbonate, L-Lactide, and 1,5-Dioxepan-2-one *Biomacromolecules* **2006,** *7,* (1489-1495)

American Chemical Society National Historic Chemical Landmarks. Bakelite: The World's First Synthetic Plastic. [Online] http://www.acs.org/content/acs/en/education/whatischemistry/landmarks/bakelite.html Acessed April 29th, 2016

Archibald, S. C.; Barden, D. J, Bazin, J. F. Y.; Felming, I.; Foster, C. F.; Mandal, K. A.; Parker, D.; Takaki, K.; Ware, A. C.; Williams, A. R. B.; Zwicky, A. B. Stereocontrol in organic synthesis using silicon-containing compounds. Studies directed toward the synthesis of ebelactone A *Organic and Biomolecular Chemistry* **2004***, 2,* (1051)

Atsumi S.; Hanai T.; Liao J. C. Non-fermentative pathways for synthesis of branched-chain higher alcohols as biofuels. *Nature* **2008,** *451,* (86-89)

Babb, D.A. Polyurethanes from Renewable Resources *in Synthetic Biodegradable Polymers* Springer (Berlin) **2012, (**315-360)

Bacon, Raymond, F. Obituaries: Robert Kennedy Duncan, *The Journal of Industrial and Engineering Chemistry* **1914,** *6 (4)*

Bandekar, J.; Klima, Suzzanne FTIR spectroscopic studies of polyurethanes Part 1. Bonding between urethane C-O-C groups and the NH groups *Journal of Molecular Structure* **1991***, 263,* (45-57)

Bagdi, K.; Molnar, K.; Sajo, I.; Pukanszky, B., Specific interactions, structure, and properties in segmented polyurethane elastomers, *exPRESS Polymer Letters* **2011**, *5,* (417-427)

Bayer AG, April 6th 2016, History [Online] http://www.bayer.com/en/1881-1914.aspx Accessed April 20th, 2016

Barthes, R., *Mythologies* Translated by Lavers, A. Hall and Wang Publishers, New York, **1956**

BASF, 2016, About Us 1865-1901 The Birth of the Chemical Industry and The Era of Dyes [Online] https://www.basf.com/en/company/about-us/history/1865-1901.html Accessed April 19th, 2016

Baśko, M; and Kubisa, P. Cationic Copolymerization of ε–Caprolactone and L,L–Lactide by an Activated Monomer Mechanism *Journal of Polymer Science: Part A: Polymer Chemistry* **2006**, *44,* (7071-7081)

Bastian, S.; Liu, X.; Meyerowitz, J. T.; Snow, C. D.; Chen, M.M.; Arnold, F. H. Engineered ketol-acid reductoisomerase and alcohol dehydrogenase enable anaerobic 2-methylpropan-1-ol production at theoretical yield in *Escherichia coli. Metab Eng* **2011,** *13,* (345-352)

Bates, F.S.; Hillmyer, M. A.; Lodge, T. P.; Bates, C. M.; Delaney, K. M.; Fredrickson, G. H., Multiblock polymers: panacea or Pandora's box? *Science* **2012,** *336,* (434-440)

Bates, F. S., and Fredrickson, G. H.  Block Copolymers—Designer Soft Materials *Physics Today* **1999,** *52,* (32-38)

Bechtold, K.; Hillmyer, M. A.; Tolman, W. B.  Perfectly Alternating Copolymers of Lactic Acid and Ethylene Oxide as a Plasticizing Agent for Polylactide *Macromolecules* **2001,** *34,* (8641-8648)

Beckingham, B. S.; Burns, A. B., and Register, R. A. Mixing Thermodynamics of Ternary Block–Random Copolymers Containing a Polyethylene block *Macromolecules* **2013,** *46,* (2760-2766)

Beckingham, B. S.; Register, R. A. Regular Mixing Thermodynamics of Hydrogenated Styrene–Isoprene Block–Random Copolymers *Macromolecules* **2013,** *46,* (3084-3091)

Beller, H. R.; Lee, T. S.; Katz, L. Natural products as biofuels and bio–based chemicals: fatty acids and isopreneoids *Natural Product Reports* **2015,** *32,* (1508–1526)

Beltran, A.A.; Boyaca, L.A. Preparation of Oleochemical Polyols Derived From Soybean Oil *Latin American Applied Research* **2011,** *41,* (69-74)

Bijker, W. E. Of Bicycles, Bakelites, and Bulbs Toward a Theory of Sociotechnical Change, **1995,** MIT Press, Cambridge Massachusetts, USA

Bittiger, H.; Marchessault, R. H. Crystal Structure of Poly($\varepsilon$-Caprolactone) *Acta Cryst.* **1970,** *B26,* (1923-1927)

Boesel, L.F.; De Geus, M.; Thöny-Meyer, L. Effect of PLA crystallization on the structure of biomimetic composites of PLA and clay *J. Appl. Polym. Sci.* **2013,** *129,* 1109-1116

Borda, J.; Pasztor, G.; Zsuga, M. Gylcolysis of polyurethane foams and elastomers *Polymer Degradation and Stability* **2000,** *68,* (419-422)

Bottle Bill Resource Guide, What is a Bottle Bill? [Online] http://www.bottlebill.org/about/whatis.htm Accessed May 30th, 2016

Bougioukou, D.J.; Kille, S.; Taglieber, A.; Reetz, M.T. Directed Evolution of an Enantioselective Enoate-Reductase: Testing the Utility of Iterative Saturation Mutagenesis. *Adv Synth Catal* **2009,** *351,* 3287-3305

Broz, M. E.; VanderHart, D.L.; Washburn, N. R. Structure and mechanical properties of poly(D,L-lactic acid)/poly($\varepsilon$-caprolactone) blends *Biomaterials* **2003,** *24,* (4181-4190)

Campbell, G.A.; Meluch, W.C. Polyurethane Foam Recycling. Superheated Steam Hydrolysis *Environmental Science Technology* **1976,** *10,* (182-185)

Castillo, R. V.; Müller, A. J.; Raquez, J.-M.; Dubois, P. Crystallization Kinetics and Morphology of Biodegradable Double Crystalline PLLA-*b*-PCL Diblock Copolymers *Macromolecules* **2010,** *43,* (4149-4160)

Causey, T.B.; Zhou, S.; Shanmugam, K.T.; Ingram, L.O. Engineering the metabolism of *Escherichia coli* W3110 for the conversion of sugar to redox-neutral and oxidized products: homoacetate production. *Proc Natl Acad Sci USA* **2003,** *100,* (825-832)

Chinese Investigators Identify Cause of Tianjin Explosion *Chemical Engineering News* **2016**, (February 8th)

Cinelli, P.; Anguillesi, I.; Lazzeri, A. Green synthesis of flexible polyurethane foams from liquefied lignin *European Polymer Journal* **2013**, *49,* (1174-1184)

Cohn, D.; Salomon, A. H. Designing biodegradable multiblock PCL/PLA thermoplastic elastomers *Biomaterials* **2005**, *26,* (2297-2305)

Cok, B.; Tsiropoulous, I.; Roes, A. L.; Patel, M. K. Succinic acid production derived from carobhydrates: An energy and greenhouse gas assessment of a platform chemical toward a bio-based economy *Biofuels, Bioproducts, and Biorefining* **2014**, *8,* (16-29)

Corcoran, P. L.; Moore, C. J.; Jazvac, K. An Anthropogenic marker in the future rock record *GSA Today* **2013**, *24,* 4-8

Crescenzi, V.; Manzini, G.; Calzolari, G.; Borri, C. Thermodynamics of Fusion of Poly-β-Propiolactone and Poly-ε-Caprolactone Comparative analysis of the Melting of Aliphatic Polylactone and Polyester Chains  *European Polymer Journal* **1972**, *8,* (449-463)

Crist, B. Thermodynamics of statistical copolymer melting *Polymer* **2003**, *44, (*4563-4572)

Dainton, F. S.; Irving, K. J. Some Thermodynamic and Kinetic Aspects of Addition Polymerisation *Q. Rev.* **1958**, 12, (61)

Daoulas, K. C.; Theodorou, D. N.  Experimental and Self–Consistent–Field Theoretical Study of Styrene Block Copolymer Self–Adhesive Materials *Macromolecules* **2004**, *37,* (5093–5109)

Darby, R.T.; Kaplan, Am. M. Fungal Susceptibility of Polyurethanes  *Appl. Microbiol.* **1968**, *16,* (900-905)

Darensbourg, D. J., and Karroonnirun, O. Ring-Opening Polymerization of ʟ-Lactide and ε-Caprolactone of Utilizing Biocompatible Zinc Catalysts. Random Copolymerization of ʟ-Lactide and ε-Caprolactone  *Macromolecules* **2010**, *43,* (8880-8886)

de Espinosa, L. M.; Meier, M. A. R. Plant oils: The perfect renewable resource for polymer science?! *European Polymer Journal* **2011**, *47,* (837-852)

Delebecq. E.; Pascault, J.-P.; Boutevin, B.; Ganachaud, F. On the Versatility of Urethane/Urea Bonds: Reversibility, Blocked Isocyanate and Non-isocyanate Polyurethane *Chemical Reviews* **2013**, *113,* (60-118)

Dellomonaco, C.; Clomburg, J.M.; Miller, E.N.; Gonzalez R. Engineered reversal of the beta-oxidation cycle for the synthesis of fuels and chemicals. *Nature* **2011**, *476,* (355-359)

Derrida, J. *The Gift of Death 2nd Edition*, David Willis Trans. **1999**, University of Chicago Press, Chicago, Illinois, USA

Dijkstra, P. J.; Zhong, Z.; Wim, M.; Feijen, S.; Feijen, J.  Chapter 16 Controlled Synthesis of Biodegradable Poly(ester)s in *Biorelated Polymers: Sustainable Polymer Science and Technology  Springer*

*Science,* Chiellini, E.; Gil, H.; Braunegg, G., Buchert, J.; Gatenholm, P., van der Zee, Maarten; Ed. New York, **2001,** (179-194)

Dobkowski, Z. Determination of Critical molecular weight for entangled macromolecules using the tensile strength data *Rheol Acta* **1995,** *34,* (578-585)

Duda, A.; Penczek, S. Thermodynamics of L-Lactide Polymerization. Equilibrium Monomer Concentration *Macromolecules* **1990,** *23,* (1636-1639)

Duda, A.; Biela, T.; Libiszowski, J.; Penczek, S.; Dubois, P.; Mecerreyes, D.; Jérôme, R. Block and random copolymers of ε-caprolactone *Polymer Degradation and Stability* **1998,** *59,* (215-222)

Duda, A.; Kowalski, A.; Libiszowski, J.; Penczek, S. Thermodynamic and Kinetic Polymerizability of Cyclic Esters *Macromol. Symp.* **2005,** *224,* (71-83)

Duda, A.; Kowalski, A.; Penczek, S. Uyama, H; Kobayashi, S. Kinetics of the Ring-Opening Polymerization of 6-, 7-, 9-, 12-, 13-, 16-, and 17-Membered Lactones. Comparison of Chemical and Enzymatic Polymerizations *Macromolecules* **2002,** *35,* (4266-4270)

Duda, A.; Kowalski, A. Thermodynamica and Kinetics of Ring-Opening Polymerization in *Handbook of Ring-Opening Polymerization* Dubois, P.; Coulembier, O.; Raquez, J.-M. Wiley, Eds.; WILEY-VCH Verlag GmbH & Co. KGaA, Weinheim, **2009;** (6-7)

Duncan, R. K. The Wonders of Cellulose *Harpers Monthly Magazine,* September, **1906,** (573)

Duncan, R.K. The Chemistry of Commerce: A Simple Interpretation of Some New Chemistry In Its Relation to Modern Industry. **1907,** Harper and Brothers Publishers, New York and London

Duncan, R.K. Some Chemical Problems of Today. **1911,** Harper and Brothers Publishers New York and London

Dupret, I.; David, C.; Colpaert, M.; Loutz, J.-M.; Wauven, C. Biodegradation of poly(ester-urethane)s by a pure strain of micro-organisms *Macromol. Chem. Phys.* **1999,** *200,* (2508-2518)

Dusek, K.; Spirkova, M.; Havlicek, I. Network Formation of Polyurethanes Due to Side reactions *Macromolecules* **1990,** *23,* (1774-1781)

Ebbesmeyer, C. C.; Ingraham, W. J., Jr., Pacific Toy Spill Fuels Ocean Current Pathways Research *EOS, Transactions of the American Geophysical Union* **1994,** (37) 425-432

Ebbesmeyer, C. G.; Ingraham, Shoe Spill in the North Pacific *EOS, Transactions of the American Geophysical Union* **1992,** *73 (34),* 361-365

Ebbesmyer, C. C.; Ingraham, W. J. Jr.; Royer, T. C.; Grosch, C. E., Tub Toys Orbit the Pacific Subartic Gyre *EOS, Transactions of the American Geophysical Union* **2007,** *88, 1-4*

Ecomall. Degradable Plastics for Composting [Online] http://www.ecomall.com/greenshopping/biocycle.htm Accessed May 31st, 2016

Enquist-Newman M.; Faust, A. M.; Bravado, D. D.; Santos, C. N.; Raisner, R. M.; Hanel, A.; Sarvabhowman, P.; Le, C.; Regitsky, D. D.; Cooper, S. R.; Peereboom, L.; Clark, A.; Martinez, Y.; Goldsmith, J.; Cho, M. Y.; Donohoue, P. D.; Luo, L.; Lamberson, B.; Tamrakar, P.; Kim, E. J.; Villari, J. L.; Gill, A.; Tripathi, S. A.; Karamchedu, P.; Paredes, C. J.; Rajgarhia, V.; Kotlar, H. K.; Bailey, R. B.; Miller, D. J.; Ohler, N. L.; Swimmer, C.; Yoshikuni, Y. Efficient ethanol production from brown macroalgae sugars by a synthetic yeast platform *Nature* **2014**, *505*, (239-243)

Fan, D.; Dai, D.J.; Wu, H.-S. Ethylene Formation by Catalytic Dehydration of Ethanol with Industrial Considerations *Materials* **2013**, *6*, (101-115)

Fan, H.; Tekeei, A.; Suppes, G. J.; Hsieh F.-H. Rigid Polyurethane Foams made from High Viscosity Soy-Polyols *Journal of Applied Polymer Science* **2013**, (1623-1629)

Fasolka, M. J.; Mayes, A. M. Block Copolymer Thin Films: Physics and Applications *Annu. Rev. Mater. Res.* **2001**, *31*, (325-355)

Faÿ, F.; Renard, E.; Langlois, V.; Linossier, I.; Vallée-Rehel, K. Development of poly(ε-caprolactone-co-δ-valerolactone) as new degradable binder used for antifouling paint *European Polymer Journal* **2007**, *43*, (4800-4813)

Fernàndez, J.; Etxeberria, A.; Sarasua, J. Synthesis, structure, and properties of poly($_L$-lactide-co-ε-caprolactone) statistical copolymers *Journal of the Mechanical Behavior of Biomedical Materials* **2012**, *9*, (100-112)

Fetters, L. J.; Lohse, D. J.; Milner, S. T.; Graessley, W. W. Packing Length Influence in Linear Polymer Melts on the Entanglement, Critical, and Reptation Molecular Weights *Macromolecules* **1999**, *32*, (6847-6851)

Fetters, L. J.; Lohse, D. J.; Richter, D.; Witten, T. A.; Zirkel, A. Connection between Polymer Molecular Weight, Density, Chain Dimensions, and Melt Viscoelastic Properties *Macromolecules* **1994**, *27*, (4639-4647)

Freinkel, S. A Breif History of Plastic's Conquest of the World *Scientific American,* **2011**, (May 29th)

Funk, K.; Milford, J.; Simpkins, T. Waste Not, Want Not: Analyzing the Economic and Environmental Viability of Waste-to-Energy (WTE) Technology for Site-Specific Optimization of Renewable Energy Options NREL technical report (online) http://www.osti.gov/bridge accessed 2/25/2016

Furuhashi, Y.; Sikorski, P.; Atkins, E.; Iwata, T.; Doi, Y. Structure and Morphology of the Aliphatic Polyester Poly(δ-valerolactone) in Solution-Grown Chain-Folded Lamellar Crystals *Journal of Polymer Science B Polymer Physics* **2001**, *39*, (2622-2634)

Gimenez, J., Cassagnau, P., Michel, A. Bulk polymerization of ε-caprolactone: Rheological predictive laws. Journal of Rheology, **2000**, *44*, (527-547)

Glavas, L.; Olsén, P.; Odelius, K., and Albertsson, A.-C Achieving Micelle Control Through Core Crystallinity *Biomacromolecules* **2013**, *14*, (4150-4156)

Gordon, E. What's wrong with plastics *House Beautiful,* **1947,** October, 89 (10) p166

Goulet, L.; Prud'homme, R. E. Crystallization Kinetics and Melting of Caprolactone Random Copolymers *Journal of Polymer Science: Part B: Polymer Physics* **1990,** *28,* (2329-2352)

Green, S. K.; Patent, R. E.; Nikbin, N.; Williams, C. L.; Chang, C.-C.; Yu, J.; Gorte, R. J.; Caratzoulas, S.; Fan, W.; Vlachos, D. G.; Dauenhauer, P. J. Diels-Alder cycloaddition of 2-methylfuran and ethylene for renewable toluene *Applied Catalysis B:Environmental* **2016,** *180,* (487-496)

Gross, R. A.; Kumar, A; Kalra, B.; Dekhterman, A. Efficient Ring-Opening Polymerization and Copolymerization of ε-caprolactone and ω-pentadecalactone catalyzed by *Candida Antarctica* Lipase B. *Macromolecules.* **2000,** *33, (*6303-6309)

Grulke, E. A. in Brandrup, J.; Immergut, E. H., and Grulke, E. A. Polymer Handbook 4th Ed. John Wiley & Sons Inc. **1999**

Grünberg, L. *The Mystery of Values, Studies in Axiology,* Grünberg, C. and Grünberg, L. Eds. **2000,** Rodophi B.V. Amsterdam, Netherlands

Grundlinger, M.; Yasmin, S.; Lechner, B. E.; Geley, S.; Schretti, M.; Hynes, M.; Haas, H., et al. Fungal siderophore biosynthesis is partially localized in peroxisomes. *Mol Microbiol* **2013,** *88,* (862-875)

Guo, C.; Lin, Y.; Witman, M. D.; Smith, K. A.; Wang, C.; Hexemer, A.; Strzalka, J.; Gomez, E. D.; Verduzco, R. Conjugated Block Copolymer Photovoltaics with near 3% Efficiency through Microphase Separation *Nano Lett.* **2013,** *13,* (2957-2963)

Guo Q. and Groeninckx G., Crystallization Kinetics Poly(e-caprolactone) in Miscible Thermosetting Polymer Blends of Epoxy Resin and Poly (e-caprolactone), *Polymer*, **2001,** *42,* (8647-8655)

Gurusamy-Thangavelu, S. A.; Emond, S. J.; Kulshrestha, A.; Hillmyer, M. A.; Macosko, C. W.; Tolman, W. B.; Hoye, T. R. Polyurethanes based on renewable polyols from bioderived lactones *Polym. Chem.* **2012,** *3,* (2941)

Hager, R. *The Demon Under the Microscope* Random House, Inc. New York, USA, **2006**

Hall M.; Stueckler, C.; Hauer, B.; Stuermer, R.; Friedrich, T.; Breuer, M.; Kroutil, W.; Faber, K., Asymmetric Bioreduction of Activated C=C Bonds Using *Zymomonas mobilis* NCR Enoate Reductase and Old Yellow Enzymes OYE 1–3 from Yeasts. *European J Org Chem* **2008,** *2008,* (1511-1516)

Hamely, I. W.; Castelletto, V.; Castillo, R. V., Müller, A. J.; Martin, C. M., Pollet, E.; Dubois, P. Crystallization in Poly(L-Lactide)-b-poly(ε-caprolactone) Double Crystalline Diblock Copolymers *Macromolecules* **2005,** *38, (*463)

Hamely, I. W.; Parras, P.; Castelletto, V.; Castillo, R. V.; Müller, A. J.; Pollet, E.; Dubois, P.; Martin, C. M. Melt Structure and its Transformation by Sequential Crystallization of the Two Blocks within Poly(L-Lactide)-*block*-Poly(ε-Caprolactone) Double Crystalline Diblock Copolymers *Macromol. Chem. Phys.* **2006,** *207,* 941-953

Hammound, A. N.; Suthar, J.L. Characterization of Polybenzimidazole (PBI) Film at High Temperatures NASA Contractor Report # 189174, 1992

Handlin D, Trenor S, Wright K *Applications of Thermoplastic Elastomers Based on Styrenic Block Copolymers. Macromolecular Engineering,* (Wiley-VCH Verlag GmbH & Co. KGaA), **2007**, (2001-2031)

Harrane, A.; Leroy, A.;Nouailhas, H.; Garric, X.; Coudane, J.; Nottelet, B. PLA-based biodegradable and tunable soft elastomers for biomedical applications *Biomed. Mater.* **2011**, *6*, (1-11)

Helling, R. K.; Russel, D. A. Use of life cycle assessment to characterize the enviromental impacts of polyol production options *Green Chemistry* **2009**, *11*, (380-389)

Henton, D. E.; Gruber, P.; Lunt, J.; Randall, J. Polylactic Acid Technology in *Natural Fibers, Biopolymers, and Biocomposites* Mohanty, A. K.; Misra, M.; Drzal, L. T., Ed.; CRC: Boca Raton, Fl **2005**, **(**527-528)

Hermann, B.; Carus, M.; Patel, M.; Blok, K. Currrent policies affecting the market penetration of biomaterials *Biofuels, Bioprod. Bioref.* **2011**, *5*, (708-719)

Hernández, N.; Williams, C.; Cochran, E. The battle for the "green" polymer. Different approaches for biopolymer synthesis: bioadvantaged vs .bioreplacement *Org. Biomol. Chem.* **2014**, *12*, (2834-2849)

Hillmyer, M.A.; Tolman, W.B. Aliphatic polyester block polymers: renewable, degradable, and sustainable *Accounts of Chemical Research* **2014**, *47*, (2390-2396)

Hoffman, W. F. ; Scolnick, E.; Smith, R. L. HMG-COA Reductase Inhibitors US 4851436 1989

Hojabri, Leila; Kong, X.; Narine, S. Fatty Acid-Derived Diisocyante and Biobased Polyurethane Produced from Vegetable Oil: Synthesis, Polymerization, and Characterization *Biomacromolecules* **2009**, *10*, (884-891)

Hong, M.; Chen, E. Completely recyclable biopolymers with linear and cyclic topologies via ring-opening polymerization of γ-butyrolactone *Nature Chemistry* **2015**, *8*, (42-49)

Houk, K.N.; Jabbari, A.; Hall, H. K., Jr.; Alemán, C. Why δ-Valerolactone and γ-Butyrolactone Does Not *Journal of Organic Chemistry* **2008**, *73*, (2674-2678)

Howard, G. T. *International Biodeterioration and Biodegradation* **2002**, *49*, (245-252)

Ho, R.-M.; Hsieh, P.-Y.; Tseng, W.-H.; Lin, C.-C.; Huang, B.-H; Lotz, B. Crystallization-Induced Orientation of Poly(L-Lactide)-b-Poly(ε-Caprolactone) Diblock Copolymers *Macromolecules* **2003**, *36*, 9085-9092

Holmberg, A. L.; Reno, K. H., Wool, R. P.; Epps, T. H. Biobased building blocks for the rational design of renewable block polymers *Soft Matter* **2014**, *10*, (7405-7424)

Hopewell, J.; Dvorak, R.; Kosier, E. Plastics Recycling: Challenges and Opportunities *Philos. Trans. R. Soc. Lond. B Biol. Sci.* **2009,** *364,* (2115-2126)

Hyatt, J. W. Address of Acceptance, *Journal of Industrial and Engineering Chemistry* **1914,** *6(2),* (158-161)

Jackson, E. A.; Hillmyer, M. A. Nanoporous Membranes Derived from Block Copolymers: From Drug Delivery to Water Filtration *ACS Nano* **2010,** *4,* (3548-3553)

Jambunathan, P.; Zhang, K. Combining biological and chemical approaches for green synthesis of chemicals *Current Opinion in Chemical Engineering* **2015**, *10,* **(**35-41)

Jamshidi, K.; Hyon, S.-H, and Ikada, Y. Thermal Characterization of polylactides *Polymer* **1988,** *29*, (2229-2234)

Jasinska-Walc, L.; Bouyahyi, M.; Rozanski, A.; Gaf, R.; Hansen, M. R.; Duchateau, R. Synthetic Principles Determining Local Organization of Copolyesters Prepared from Lactones and Macrolactones *Macromolecules* Advanced online publication. **2015**, *48,* (502-510)

Jasinska-Walc, L.; Hansen, M. R.; Dudenko, D.; Rozanski, A.; Bouyahyi, M.; Wagner, M.; Graf, R.; Duchateau, R. Topological behavior mimicking ethylene-hexene copolymers using branched lactones and macrolactones *Polymer Chemistry* **2014**, *5,* **(**3306-310)

Jékely, G. The human genome sequence: a triumph of chemistry *EMBO reports* **2002***, 3,* (594-595)

Jeon, O.; Lee, S.-H. Kim, S. H.; Lee, Y. M.; Kim, Y. H. Synthesis and Characterization of Poly(L-Lactide)-Poly(ε-caprolactone) Multiblock Copolymers *Macromolecules* **2003,** *36,* (5585-5592)

Kable 2016, Coca-Cola's 100% Plant-Based Bottle, United States of America [Online] http://www.packaging-gateway.com/projects/-coca-cola-plant-based-bottle/ Accessed May 29th, 2016

Kamber, N. E.; Jeong, W.; Waymouth, R. M.; Pratt, R. C.; Lohmeijer, B. G. G.; Hedrick, J. L. Organocatalytic Ring-Opening Polymerization *Chem. Rev.* **2007**, *107,* (5813-5840)

Kanai, H.; Sullivan, V.; Auerbach, A. Impact Modification of Engineering Thermoplastics *Journal of Applied Polymer Science* **1994**, *53,* (527-541)

Kałużyński, K.; Penczek, S. Anionic Polymerization of 2-Oxo-1,2,3 λ5-dioxaphosphorinane. Thermodynamics *Makromol. Chem.* **1979**, *180,* (2289-2293)

Kataoka, K.; Harada, A.; Nagsaki, Y. Block copolymer micelles for drug delivery: design characterization, and biological significance *Advanced Drug Delivery reviews* **2001**, *47,* (113-131)

Keasbey, W.P. Did You Ever Wonder: What Bakelite Is and How It Got Its Name? *The Christian Science Monitor,* **1940**, Nov. 5th, (17)

Kiesewetter, M. K.; Scholten, M. D.; Kirn, N.; Weber, R. L.; Hedrick, J. L.; Waymouth, R. M. Cyclic Guanidine Organic Catalysts: What Is Magic About Triazabicyclodecene? *J Org Chem* **2009**, *74, (*9490-9496)

Kiesewetter, M. K.; Shin, E. J.; Hedrick, J. L.; Waymonth, R. M. Organocatalysis: Opportunities and Challenges for Polymer Synthesis *Macromolecules* **2010**, *43,* (2093-2107)

Kikuchi, H.; Uyama, H.; Kobayashi, S. Lipase-Catalyzed Ring-Opening Polymerization of Substituted Lactones *Polymer Journal* **2002**, *11,* (835-840)

Kim, J. K.; Park, D. J.; Lee, M. S.; Ihn, K. J. Synthesis and crystallization behavior of poly(L-Lactide)-block-poly(ε-caprolactone) copolymer *Polymer* **2001**, *42,* 7429-7441

Kinnaman, T.C. The economics of municipal solid waste management *Waste Management* **2009***,* *29,* (2615-2617)

Klug, Jörg; Commentary on Gáspár Jékly's article in EMBO reports, *EMBO reports* **2002**, *3,* (1004)

Kong, J. F.; Lipik, V.; Abadie, M. J.M.; Deen, G. R.; Venkatraman, Biodegradable elastomers based on ABA triblocks: influence of end-block crystallinity on elastomeric character S. S. *Polym. Int.* **2012,** *61,* (43-50)

Kowalski, A.; Duda, A.; Penczek, S. Kinetics and Mechnaism of Cyclic esters polymerization initiated with tin(II) octoate, 1 *Marcomol. Rapid Commun.* **1998**, *19,* (567-572)

Kraton Performance Polymers Inc. Product Families Kraton D SBS. http://www.kraton.com/products/Kraton_D_SBS.php.

Kraus, G.; Rollmann, K. W. The Entanglement Plateau in the Dynamic Modulus of Rubbery Styrene–Diene Block Copolymers. Significance to Pressure–Sensitive Adhesive Formulations *Journal of Applied Polymer Science* **1977**, *21,* (3311-3318)

Küllmer, K.; Kikuchi, H.; Uyama, H.; Kobayashi, S. Lipase-catalyzed ring-opening polymerization of α-methyl-δ-valerolactone and α-methyl-ε-caprolactone *Macromol. Rapid Commun.* **1998,** *19,* (127-130)

Labet, M.; Thielemans, W. Synthesis of polycaprolactone: a review. *Chem. Soc. Rev.* **2009**, *38,* (3484-38504)

Lea, W. R. Plastic incineration verses recycling: a comparison of energy and landfill cost savings *Journal of Hazardous Materials* **1996,** 47, (295-302)

Lebedev, B.V. Estropov, A.A. Thermodynamics of the Polymerization of Lactones *Dokl. Phys. Chem.* **1982,** *264,* (334)

Lebedev, B.V.; Bykova, T.A.; Kiparisova, E.G.; Belen'kaya, B. G.; Filatova, V. N. Thermodynamics of p-dioxanone, of its polymerization and of poly(p-dioxanone) at 0-450 K *Vysokomolekuliarnye soedineniia. Seriia A & Seriia B* **1995,** *37,* (187-196)

Lee, S.; Gillard, T. M.; Bates, F. S. Fluctuations, order, and disorder in short diblock copolymers *AIChE Journal,* **2013**, *59,* (3502-3513)

Lee, I.; Panthani, T. R.; Bates, F. S. Sustainable Poly(lactide-*b*-butadiene) Multiblock Copolymers with Enhanced Mechanical Properties. *Macromolecules* **2013**, *46*, (7387–7398)

Lee, J. M.; Subramani, S.; Lee, Y. S.; Kim, J. H. Thermal Decomposition Behavior of Blocked Diisocyanates Derived from Mixture of Blocking Agents *Macromolecular Research* **2005**, *13*, (427-434)

Leitão, M. L.; Pilcher, G.; Meng-Yan, Y., Brown, J. M.; Conn, A. D. Enthalpies of combustion of γ-butyrolactone γ-valerolactone, and δ-valerolactone *J. Chem. Thermodynamics* **1990**, *22*, (885-891)

Lewin, J. L.; Maerzke, K. A.; Schulz, N. E.; Ross, R. B.; Sipmann, J. I. Prediction of Hildebrand solubility parameters of acrylate and methacrylate monomers and their mixtures by molecular simulation *J. App. Sci.* **2010**, *116*, (1-9)

Li, Y.; Luo, X.; Hu, S. Bio-based polyols and polyurethanes Springer (Cham, Switerzerland), **2015**

Libiszowski, J.; Kowalski, A.; Szymanski, R.; Duda, A.; Taquez, J. M.; Degée, P.; Dubois, P. Monomer-Linear Macromolecules-Cyclic Oligomers Equilibria in the Polymerization of 1,4-Dioxan-2-one *Macromolecules* **2004**, *37*, (52-59)

Ligadas, G.; Ronda, J. C.; Galia, M.; Cadiz, V. Plant Oils as Platform Chemicals for Polyurethane Synthesis: Current State of the Art *Biomacromolecules* **2010**, *11*, (2825-2835)

Lin, J. O.; Chen, W.; Shen, Z.; Ling, J. Homo- and Block Copolymerizations of ε-Decalactone with L-Lactide Catalyzed by Lanthanum Compounds. *Macromolecules* **2013**, *46*, (7769–7776)

Liow, S.W.; Lipik, V.T.; Widjaja, L.K.; Venkatraman, S. S.; Abadie, M. J.M. Enhancing mechanical properties of thermoplastic polyurethane elastomers with 1,4-trimethylene carbonate, epsilon-caprolactone, and L-lactide copolymers via soft segment crystallization *eXPRESS Polymer Letters* **2011**, *5*, (897-910)

Lipik, V.T.; Widjaja, L. K.; Liow, S. S.; Venkatraman, S. S.; Abadie, M. J. M. Synthesis of biodegradable thermoplastic elastomers (BTPE) based on ε-caprolactione *eXPRESS Polymer Letters* **2010**, *4*, (32-38)

Lipik, V. T., and Abadie, M. J. M Synthesis of Block Copolymers of Varying Architecture Through Suppression of Transesterification during Coordinated Anionic Ring Opening Polymerization *International Journal of Biomaterials* **2012**, doi: 10.11555/2012/390947

Liu, H.; Zhang, J. Research Progress in Toughening Modification of Poly(lactic acid) *Journal of Polymer Science Part B Polymer Physics* **2011**, *49*, (1051-1083)

Liu, Q.; Jiang, L.; Shi, R.; Zhang, L. Synthesis, preparation, in vitro degradation, and application of novel degradable bioelaastomers—A Review *Progress in Polymer Science* **2012**, *37*, (715-765)

Lochee, Y.; Jhurry, D.; Bhaw-Luximon, A.; Kalangos, A. Biodegradable Poly(ester-ether)s: ring-opening polymerization of D,L-3-methyl-1,4-dioxan-2-ones using various initiator systems *Polym. Int.* **2010**, *59*, (1310-1318)

Lohmeijer, B. G. G.; Pratt, R. C.; Leibfarth, F.; Logan, J. W.; Long, D. A.; Dove, A. P.; Nederberg, F.; Choi, J.; Wade, C.; Waymonth, R. M.; Hedrick, J. L. Guanidine and Amidine Organocatalysts for Ring-Opening Polymerization of Cyclic Esters *Macromolecules* **2006**, *39*, (8574-8583)

Lomellini, P.; Rossi, A. G. Effect of compostion on the entanglement density in random copolymers *Makromol. Chem.* **1990**, *191*, (1729-1737)

Longley, R. I.; Emerson, W. S. β-Methyl-δ-Valerolactone *Organic Synthesis Coll.* **1963**, *4*, (677)

Lovinger, A. J.; Han, B. J.; Padden, F. J. Jr.; Mirau, P. A. Morphology and properties of Polycaprolactone-Poly(dimethyl siloxane)-Polycaprolactone Triblock copolymers *Journal of Polymer Science Part B Polymer Physics* **1993**, *31*, (115-123)

Lu, W.; Ness, J. E.; Xie, W.; Zhang, X.; Minshull, J.; Gross, R. A. Biosynthesis of Monomers for Plastics from Renwable Oils *JACS* **2010**, *132*, (15451-15455)

Ma S.M.; Li, J. W.; Choi, J. W.; Zhou, H.; Lee, K. K.; Moorthie, V. A.; Xie, X.; Kealey, J. T.; Da Silva, N. A.; Vederas, J. C.; Tang, Y., Complete reconstitution of a highly reducing iterative polyketide synthase. *Science* **2009**, *326*, (589-592)

MacDonald, J. P.; Parker, M. P.; Greenland, B. W.; Hermida–Merino, D.; Hamley, I. W.; Schaver, M. P. Tuning thermal properties and microphase separation in aliphatic polyester ABA copolyesters *Polymer Chemistry* **2015**, *6*, (1445-1453)

Maglio, G.; Migliozzi, A.; Palumbo, R. Thermal properties of di- and triblock copolymers of poly(L-lactide) with poly(oxyethylene) or poly(ε-caprolactone) *Polymer* **2003**, *44*, (369-375)

Mahoney, L.R.; Weiner, S.A.; Ferris, F.C. Hydrolysis of Polyurethane Foam Waste *Environmental Science Technology* **1974**, *8*, (135-139)

Makiguchi, K.; Satoh, T.; Kakuchi, T. Diphenyl Phosphate as an Efficient Cationic Organocatalyst for Controlled/Living Ring-Opening Polymerization of δ-Valerolactone and ε-Caprolactone *Macromolecules* **2011**, *44*, (1999-2005)

Makiguchi, K.; Ogasawara, Y.; Kikuchi, S.; Satoh, R.; Kakuchi, T. Diphenyl Phosphate as an Efficient Acidic Organocatalyst for Controlled/Living Ring–Opening Polymerization of Trimethylene Carbonates Leading to Block, End–Functionalized, and Macrocyclic Polycarbonates *Macromolecules* **2013**, *46*, (1772-1782)

Makiguchi, K.; Kikuchi, S.; Yanai, K.; Ogasawara, Y.; Sato, S.; Satoh, T.; Kakuchi, T. Diphenyl Phosphate/4– Dimethylaminopyridine as an Efficient Binary Organocatalyst System for Controlled/Living Ring–Opening Polymerization of L–Lactide Leading to Diblock and End–Functionalized Poly(L–Lactide)s *Journal of Polymer Science A: Polymer Chemistry* **2014**, *52*, (1047-1054)

Manzini, B.; Hodge, P.; Ben-Haida, A. Entropically–driven ring–opening polymerization of macrocyclic esters with up to 84–membered rings catalyzed by polymer–supported Candida antarctica *Polymer. Chem.* **2010**, *1*, (339-346)

Mark, H.F.; Remembering the Early Days of Polymer Science *Pioneers in Polymer Science* Seymour, R.B. Ed. **1989**, Kluwer Academic Publishers, Dordrecht, The Netherlands

Marlier, E. E.; Macaranas, J. A.; Marell, D. J.; Dunbar, C. R.; Johnson, M. A>; DePorre, Y.' Miranda, M. O.; Neisen, B. D.; Cramer, C. J.; Hillmyer, M. A.; Tolman, W. B. *ACS Catalysis* **2016**, *6,* (1215-1224)

Martello, M. T.; Burns, A.; Hillmyer, M. Bulk Ring-Opening Transesterification Polymerization of the Renewable δ-Decalactone Using an Organocatalyst. *ACS Macro Lett.*, **2012**, *1,* (131–135)

Martello, M. T.; Hillmyer, M. A. Polylactide-Poly(6-methyl-ε-caprolactone)-Polylactide Thermoplastic Elastomers *Macromolecules* **2011**, *44,* (8537-8545)

Martello, M. T.; Schneiderman, D. K.; Hillmyer, M. A.; Synthesis and Melt Processing of Sustainable Poly(ε-decalactone)-block-Poly(lactide) Multiblock Thermoplastic Elastomers *ACS Sustainable Chemistry and Engineering* **2014**, *2,* **(**2519-2526)

Martin V.J.; Pitera, D. D.; Withers, S. t.; Newman, J. D.; Keasling, J. D., Engineering a mevalonate pathway in *Escherichia coli* for production of terpenoids. *Nat Biotechnol* **2003**, *21,* (796-802)

Matsen, M.W. Effect of Architecure on the Phase Behavior of AB-Type Block Copolymer Melts *Macromolecules* **2012**, *45,* (2161-2165)

McDonough, W.; Braungart, M.; Anastas, Paul T.; Zimmerman, J. B. Peer Reviewed: Applying the Principles of Green Engineering to Cradle-to-Cradle Design *Environmental Science & Technology* **2003**, *37,* (434A-441A)

McNeil, I.C.; Leiper, H. A. Degredation Studies of Some Polyesters and Polycarbonates–2. Polylactide: Degredation Under Isothermal Conditions, Thermal Degradation Mechanism and photolysis of the Polymer *Polymer Degradation and Stability* **1985**, *11,* (309-326)

Miller, S. A. Sustainable Polymers: Opportunities for the Next Decade *ACS Macro Letters* **2013**, *2, (6),* (550-554)

Miranda, M. O.; DePorre, Y.; Vasquez-Lima, H.; Johnson, M. A.; Marell, D. J.; Cramer, C. J.; Tolman, W. B.; Understanding the Mechanism of Polymerization of ε-Caprolactone Catalyzed by Aluminum Salen Complexes *Inorganic Chemistry* **2013**, *52,* (13692-13701)

Monsanto House of the Future. Yesterland [Online] http://www.yesterland.com/futurehouse.html Accessed May 12th, 2017

Morris, J. Recycling verses incineration: an energy conservation analysis *Journal of Hazardous Materials* **1996**, *47,* (277-293)

Morton M Structure-Property Relations in Amorphous and Crystallizable ABA Triblock Copolymers. *Rubb Chem Technol* **1983**, *56, (1096-1110)*

Nakagawa, S.; Tanaka, T.; Ishizone, T.; Nojima, S.; Kamimura, K.; Yamaguchi, K. Nakahama, S. Crystallization behavior of poly(ε-caprolactone) chains confined in lamellar nanodomains *Polymer* **2014**, *55,* **(**4394-4400)

331

Nakajima-Kambe, T.; Shigeno-Akutsu, S.; Nomura, N.; Onuma, F.; Nakahara, T.; Microbial degradation of polyurethane, polyester polyurethanes, and polyether polyurethanes, *Appl. Microbiol. Bioechnol.* **1999,** *51,* (134-140)

Nakayama, Y.; Aihara, K.; Yamanishi, H.; Fukuoka, H.; Tanaka, R.; Zhengguo, C.; Shiono, T. Synthesis of Biodegradable Thermoplastic Elastomers from ε-Caprolactone and Lactide *Journal Polymer Science, Part A: Polymer Chemistry* **2015**, *53, (*489-495)

Nakayama A., Kawasake, N.; Arvanitoyannis, I.; Iyoda, J.; Yamamoto, N. Synthesis and Degradability of a Novel Aliphatic Polyester - Poly(β-methyl-δ-valerolactone-co-L-lactide). *Polymer* **1995,** 36, (1295-1301)

Neitzel, A. E.; Petersen, M. A.; Kokkoli, E.; Hillmyer, M. A.  Divergent Mechanistic Avenues to an Aliphatic Polyesteracetal or Polyester from a Single Cyclic Esteracetal *ACS Macro Lett.* **2014,** *3,* (1156-1160)

New York Times Editorial Board, How New York Can Put an End to The Plastic Bag 2016 [Online]    http://www.nytimes.com/2016/05/05/opinion/how-new-york-can-put-an-end-to-the-plastic-bag.html?_r=0  Accessed May 31st, 2016

Nicholson, J. L.; Leighton, G. R., Plastics come of Age *Harpers Weekly,* **1942**, August, (300-307)

Nishida, H.; Yamashita, M.; Endo, T.; Tokiwa, Y. Equilibrium Polymerization Behavior of 1,4-Dioxan-2-one in Bulk *Macromolecules* **2000**, *33,* (6982-6986)

NOAA Office of Response and Restoration, 2016 Great Pacific Garbage Patch [Online] https://marinedebris.noaa.gov/info/patch.html Accessed May 29th, 2016

Ocean Conservancy Stemming the Tide: Land-based strategies for a plastic-free ocean [Online] http://www.oceanconservancy.org/our-work/marine-debris/mckinsey-report-files/full-report-stemming-the.pdf Accessed January 15th, 2016

Oikawa, M.; Oikawa, H.; Ichihara, A. Reductive Opening of α-Methylspiroketals *Tetrahedron* **1995,** *51,* (6237)

Olsén P, Borke T, Odelius K, Albertsson AC  ε-Decalactone: A Thermoresilient and Toughening Comonomer to Poly(L-lactide). *Biomacromolecules* **2013,** *14,* (2883-2890)

Olsén, P.; Odelius, K.; Albertsson, A.-C. Thermodynamic Presynthetic Considerations for Ring-Opening Polymerization *Biomacromolecules* Article ASAP **2016**, *17, (*699-709)

Ooms, R.; Dusselier, M.; Geboers, J. A.; de Beeck, B. O.; Verhaeven, R.; Gobechiya, E.; Martens, J. A.; Redl, A.; Sels, B. F. Conversion of sugars to ethylene glycol with nickel tungsten carbide in a fed-batch reactor: high productivity and reaction network elucidation *Green Chem.* **2014,** *16, (*695-707)

Orjuela A.; Orjuela A.; Lira, C. T.; Miller, D. J. A novel process for recovery of fermentation-derived succinic acid: Process design and economic analysis. *Bioresour Technol.* **2013,** *139, (*235-241).

Our State Institutions XVII-The Manufactures of Albany, *New York Times,* January 19, **1872**

Paddon, C.J.; Westfall, P. J.; Pitera, D. J.; Benjamin, K.; Fisher, K.; McPhee, D.; Leavell, M. D.; Tai, A.; Main, A.; Eng, D.; Polichuck, D. R.; Teoh, K. H.; Reed, D. W.; Treynor, R.; Lenihan, J.; Jiang, H.; Fleck, M.; Bajad, S.; Dang, G.; Dengrove, D.; Diola, D.; Dorin, G.; Ellens, K. W.; Fickes, S.; Galazzo, J.; Gaucher, P.; Geistlinger, T.; Hepp, H. M.; horning, T.; Iqbal, T.; Kizer, L.; Lieu, B.; Melis, D.; Moss, N.; Regentin, R.; Secrest, S.; Tsuruta, H.; Vazquez, R.; Westblade, L. F.; Xu, L.; Yu, M.; Zhang, Y.; Zhao, L.; Lievense, J.; Covello, P. S.; Keasling, J. D.; Reiling, K. K.; Renninger, N. S.; Newman, J. D. High-level semi-synthetic production of the potent antimalarial artemisinin. *Nature* **2013,** *496, (*528-532)

Palaskar, D.; Boyer, A.; Cloutet, E.; Alfos, C.; Cramail, H. Synthesis of Biobased Polyurethane form Oleic and Ricinoleic Acids as the Renewable Resources via the AB-Type Self-Condensation Approach *Biomacromolecules* **2010,** *11, (*1202-1211)

Park S.J.; Kim, E. Y.; Noh, W.; Park, H. M.; Oh, Y. H.; Lee, S. H.; Song, B. K.; Jegal, J.; Lee, S. Y. Metabolic engineering of *Escherichia coli* for the production of 5-aminovalerate and glutarate as C5 platform chemicals. *Metab Eng* **2013,** *16, (*42-47)

Pawlik, H.; Prociak, A.; Influence of Palm Oil-Based Polyol on the Properties of Flexible Polyurethane Foams *J. Polym. Environ* **2012**, *20, (*438-445)

Perego, G.; Cella, G. D.; Bastioli, C. Effect of molecular weight and crystallinity on poly(lactic acid) mechanical properties *Journal of Applied Polymer Science* **1996,** *59, (1),* (37-43)

Persenaire, O.; Alexandre, M.; Degee, P.; Dubois, P. Mechanisms and Kinetics of Thermal Degredation of Poly(ε-Caprolactone) *Biomacromolecules* **2001**, *1,* (288-294)

Petrovic, Z. S.; Cvetkovic, I.; Hong, D.; Wan, X.; Zhang, W.; Abraham, T. W.; Malsam, J. Vegetable oil-based triols from hydrofomylated fatty acids and polyurethane elastomers *Eur. J. Lipid Sci. Technol.* **2010,** *112, (*97-102)

Petrovic, Z. S.; Cvetkovic, I.; Hong,D.; Wan, X.; Zhang, W.; Abraham, T.; Malsam, J. Polyester Polyols and Polyurethanes from Ricinoleic Acid *Journal of Applied Polymer Science* **2007**, *108,* (1184-1190)

Petrovic, Z. S.; Polyurethanes from Vegetable Oils *Polymer Reviews* **2008**, *48,* (109-155)

Pfeifer, B.A.; Admiraal, S. J.; Gramajo, H.; Cane, D. E.; Khosla, C., Biosynthesis of complex polyketides in a metabolically engineered strain of *E. coli. Science* **2001,** 291, (1790-1792)

Phillip, W. A.; O' Neill, B.; Rodwogin, M.; Hillmyer, M. A.; Cussler, E. L. Self-Assembled Block Copolymer Thin Films as Water Filtration Membranes *ACS Appl. Mater. Interfaces* **2010**, *2,* (847-853)

Pitet, L. M.; Amendt, M. A.; Hillmyer, M. A. Nanoporous Linear Polyethyene from a Block Polymer Precursor *J. Am. Chem. Soc.* **2010,** *132, (*8230-8231)

Pitt, C. G.; Gratzl, M. M.; Kimmel, G. L.; Surles, J.; Schindler, A. Aliphatic Polyesters II. The Degradation of Poly (D,L-lactide), Poly (ε-caprolactone), and Their Copolymers in Vivo *Biomaterials* **1981**, *2,* (215-220)

Plastics and a man named Yarsley. Epson and Ewell History Explorer [Online] http://www.epsomandewellhistoryexplorer.org.uk/Yarsley.html Accessed May 3rd, 2016

PlasticsEurope Plastics–the Facts 2014-2015 **http://www.plasticseurope.org/** (Accessed December 21, 2015)

Plastics the Facts 2015 [Online] http://www.plasticseurope.org/plastics-industry/market-and-economics.aspx Accessed May 15th, 2016

Posada, J.A.; Cardona, C. A.; Higuita, J. C.; Tamayo, J. A.; Pisarenko, Y. A. Design and economic analysis of the technological scheme for 1,3-propanediol production from raw glycerol. *Theor Found Chem Eng* **2013,** *47(3),* (239-253)

Pratt, R. C.; Lohmeijer, B. G. G.; Long, D. A.; Waymouth, R. M.; Hedrick, J. L. Triazabicyclodecene: A Simple Bifunctional Organocatalyst for Acyl Transfer and Ring-Opening Polymerization of Cyclic Esters *JACS*, **2006,** *128,* (4556-4557)

Qiu, X.; Zhou, Z.; Gobbi, G.; Redwine, O. Error Analysis for NMR Polymer Microstructure Measurement without Calibration Standards. *Anal. Chem.* **2009,** *81,* (8585-8589)

Reilly, J. A. Celluloid Objects: Their Chemistry and Preservation *Journal of the American Institute for Conservation,* **1991,** *30 (2),* (145)

Research and Markets Reports Engineering Plastics Market by Type, Applications and Geography-Trends and Forecasts (2013-2018) [Online] http://www.researchandmarkets.com/reports/3446120/ Accessed May 29th, 2016

Ro, D.K.; Paradise, E. M.; Ouellet, M.; Fisher, K. J.; Newman, K. L.; Ndungu, J. M.; Ho, K. A.; Eachus, R. A.; Ham, T. S.; Kirby, J.; Chang, M. C. Y.; Withers, S. T.; Shiba, Y.; Sarpong, R.; Keasling, J. D., Production of the antimalarial drug precursor artemisinic acid in engineered yeast. *Nature* **2006,** *440,* (940-943)

Robertson, J.D.; Patikarnmonthon, N.; Joseph, A. S.; Battaglia, G. Block Copolymer Micelles and Vesicles for Drug Delivery In *Engineering Polymer Systems for Improved Drug Delivery* Bader, R. A., and Putnam, D. A., Ed. John Wiley and Sons, **2014**

Rochman, C. M.; Browne, M. A.; Halpern, B. S.; Hentschel, B. T.; Hoh, E.; Karapanagioti, H. K.; Rios-Mendoza, L. M.; Takada, H.; Teh, S.; Thompson, R. C. Classify Plastics as Hazardous Waste Nature, **2013,** 494 (169-171)

Romer, J.R. The Evolution of SF's Plastic Bag Ban *Golden Gate University Environmental Law Journal* **2007,** *439,* (439-465)

Romer, J.R., Tamminen, L. M. Plastic Bag Reduction Ordinances: New York City's Proposed Charge on All Carryout Bags as a Model for U.S. Cities *Tulane Environmental Law Journal* **2014,** *27,* (237-275)

Rosendale, J. H., and Bates, F. S. Rheology of ordered and disordered symmetric poly(ethylenepropylene)-poly(ethylethyene) diblock copolymers *Macromolecules* **1990,** 23, (2329-2338)

Ryner, M.; Albertsson, A.-C. Resorbable and Highly Elastic Block Copolymers from 1,5-Dioxepan-2-One and L-Lactide with Controlled Tensile Properties and Hydrophilicity. *Biomacromolecules* **2002**, *3,* **(**601–608)

Ryynänen, T.; Nykänen, A., and Seppälä, J. V. Poly(CL/DLLA-b-CL) multiblock copolymers as biodegradable thermoplastic elastomers *eXPRESS Polymer Letters* **2008**, *2,* (184-193)

Sangjun, L.; Lee, K.; Kim, Y.-W.; Shin, J. Preparation and Characterization of a Renewable Pressure–Sensitive Adhesive System Derived from ε-Decalactone, L-Lactide, Epoxidized Soybean Oil, and Rosin Ester *ACS Sustainable Chemistry and Engineering* **2015**, *3,* **(**2309-2320)

Sanna T., Heikki, O. The Current Status and Future Expectations in Industrial Production of Lactic Acid by Lactic Acid Bacteria. **2013,** DOI: 10.5772/51282

Saralegi, A.; Rueda, L.; Fernandex-d'Arlas, B.; Mondragon, I.;Eceiza, A.; Corcuera, A., Thermoplastic polyurethanes from renewable resources: effect of soft segment chemical structure and molecular weight on morphology and final properties *Polymer International* **2013,** *62,* 1, (106-115)

Save, M.; Schappacher, M.; Soum, A. Controlled Ring–Opening Polymerization of Lactones and Lactides Initiated by Lanthanum Isopropoxide, 1 General Aspects and Kinetics *Macromol. Chem. Phys.* **2002,** *203,* (889-899)

Sawada, H. Thermodynamics of Polymerization. 1. *Journal of Macromolecular Science C: Polymer Reviews* **1969,** *3,* (313-396)

Schneiderman, D.K.; Hill, E. M.; Martello, M.T.; Hillmyer, M.A. Poly(lactide)-block-poly(ε-caprolactone-co-ε-decalactone)-block-poly(lactide) copolymer elastomers *Polymer Chemistry* **2015**, *6,* (3641-3651)

Schively, M. L.; Coonts, B. A.; Renner, W. D.; Southard, J. L., and Bennet, A. T. Physico-chemical characterization of a polymeric injectable implant delivery system *Journal of Controlled Release* **1995**, *33,* (237-243)

Schmalz H, Abetz V, Lange R Thermoplastic elastomers based on semicrystalline block copolymers. *Compos Sci Technol* **2003**, *63,* (1179-1186)

Schmidt, S.C.; Hillmyer, M.A. Morphological Behavior of Model Poly(ethylene-alt-propylene)-b-Polylactide Block Polymers *J. Poly. Sci. Part B: Polym. Phys.* **2002,** *40,* (2364-2376)

Schuessler, H. Where it Goes; Breaking Down All Those Computers: Glass Over Here, Plastic There *The New York Times* November 23, 2000

Schulze, Morgan, W.; McIntosh, Lucas D.; Hillmyer, Marc A.; Ldge, Timothy P. - High-Modulus, High-Conductivity Nanostructured Polymer Electrolyte Membranes via Polymerization-Induced Phase Separation *Nano Lett.,* **2014,** *14,* (122-126)

Shin, J.; Martello, M. T.; Shrestha, M.; Wissinger, J.E.; Tolman, W. B.; Hillmyer, M. A. Pressure-Sensitive Adhesives from Renewable Triblock Copolymers *Macromolecules* **2011,** *44,* (87-94)

Science: At Ithaca *Time Magazine,* **1924**, 4(12) September 22nd , (20)

Seefried, C.G.; Koleske, J.V.; Critchfield, F.E. Lactone Polymers. VIII. Dynamic Mechanical Properties of ε-Caprolactone and γ-(tert-butyl)-ε-Caprolactone Copolymers *Journal of Polymer Science Polymer Physics Edition* **1976,** *14,* (2011-2017)

Serpe, M. J.; Craig, S. L. Physical Organic Chemistry of Supramolecular Polymers *Langmuir,* **2007,** *23,* (1626-1634)

Shellenberger, M.; Nordhaus, T. The Death of Environmentalism: Global Warming Politics in a Post-Environmental World *Geopolitics, History and International Relations,* **2004,**

Shilna, I. and Nakata, K.; Medium–Sized Lactones In *Natural Lactones and Lactams: Synthesis, Occurrence and Biological Activity, Janecki, T., Ed.; Wiley:* Weinheim, Germany **2014** (193-227)

Shin, J.; Lee, Y.; Tolman, W.B.; Hillmyer, M. A. Pressure-Sensitive Adhesives from Renewable Triblock Copolymers *Macromolecules* **2011,** *4,* (87-94)

Simon, D.; Borreguro, A. M.; de Lucas, A.; Gutierrez, C.; Rodriquez, J.F. Sustainable Polyurethanes:Chemical Recycling to Get It E. Jimenz et al (eds.), *Enviroment and Climate Change 1.:Enviromental Chemistry of Pollutants and Wastes,* Hbd Env Chem **2015,** *32,* (229-260)

Simon, D.; Borreguero, A. M.; de Lucas, A.; Molero, C.; Rodriguez, J. F. Novel polyol initiator from polyurethane recyling residue *J. Mater. Cycles Waste Manag.* **2014,** *16,* (525-532)

Sobczak, M. Synthesis and Characterization of Polyurethane Based on Oligo(ε-caprolactone) Prepared by Free-Metal  Method *Journal of Macromolecular Science, Part A: Pure and Applied Chemistry* **2011,** *48,* **(**373-380)

Soetaert, W.; Vandamme, E. The impact of industrial biotechnology. *Biotechnol J* **2006,** *1(7-8),* (756-769)

Some Modern Inventions *The Washington Post,* **1909**, February 7th, (E4)

Sonnenschein, M. Polyurethanes: Science, Technology, Markets and Trends, John Wiley & Sons Inc. (Hoboken, NJ, US), **2015.**

Sonnenschein, M. F.; Lysenko, Z.; Brune, D. A.; Wendt, B. L.; Schrock, A. K. Enhancing polyurethane properties via soft segment crystallization *Polymer* **2005,** *46,* (10158-10166)

Stahl, A. G.; Development of a Modern Polymer Theory in *Pioneers in Polymer Science* Seymour, R.B. Ed. **1989,** Kluwer Academic Publishers, Dordrecht, The Netherlands

Staudinger, U.; Satapathy, B. K.; Thunga, M.; Weidisch, R.; Janke, A., and Knoll, K. Enhancement of mechanical properties of triblock copolymers by random copolymer midblocks *European Polymer Journal* **2007,** *43,* (2750-2758)

Staudinger, H. Über Polymerisation Berichte der deutschen chemischen Gesellschaft (A and B Serieze) **1920,** *12* (*6),* (1073-1085)

Steen, E.J.; Kang, Y.; Bokinsky, G.; Hu, Z.; Schirmer, A.; McClure, A.; del Cardayre, S. B.; Keasling, J. D. Microbial production of fatty-acid-derived fuels and chemicals from plant biomass *Nature* **2010**, *463, (*559-562)

Stockbridge, F. P. Harnessing Science to The Factory. *Popular Mechanics Magazine* **1914**, *21 (April)*, (474)

Storey, R. F.; Sherman, J. W. Kinetics and Mechanism of the Stannous Octoate-Catalyzed Bulk Polymerization of ε-Caprolactone *Macromolecules* **2002**, *35, (*1504-1512)

Storey, R. F.; Hoffman, D.C. Copolymerization of ε-caprolactone and δ-valerolactone *Mackromol. Chem. Marcomol. Symp.* **1991**, *42/43*, (185-193)

Suen, W.; Paul, C. W. A Spectroscopic Analysis of the Phase Evolution in Polyurethane Foams *Macromolecules* **2005**, *38,* (9192-9199)

Tabata K,; Hashimoto S. Production of mevalonate by a metabolically-engineered *Escherichia coli*. *Biotechnol Lett* **2004**, *26, (*1487-1491)

Tachibana, Y.; Kimura, S.; Kasuya, K. Synthesis and Verification of Biobased Terephthalic Acid from Furfural *Sci. Rep.* **2015**, *5,* (8249)

Takahashi, K.; Komine, K.; Yokoi, Y.; Ishihara, J.; Hatakeyama, S. Stereocontrolled Total Synthesis of (–)-Englerin A *Journal of Organic Chemistry* **2012**, *77,* (7364)

Tan, S.; Abraham, T.; Ference, D.; Macosko, C. W. Rigid polyurethane foams from a soybean oil-based Polyol *Polymer,* **2011**, *52,* (2840-2846)
3237)

Tanaka, T.; Yokaoyama, T.; Yamaguchi, Y. Quantitative Study on Hydrogen Bonding between Urethane Compond and Ethers by Infrared Spectroscopy *Journal of Polymer Science A-1* **1968**, *6,* (2137-2152)

Tang, D.; Macosko, C. W.; Hillmyer, M. A. Thermoplastic polyurethane elastomers from biobased poly(δ-decalactone) diols *Polym. Chem.* **2014**, *5,* (3231-3237)

Teuten, E. L.; Saquing, J. M.; Knappe, D. R. U.; Barlaz, M. A.; Jonsson, S.; Björn, A.; Rowland, S. J.; Thompson, R. C.; Galloway, T. S.; Yamashita, R.; Ochi, D.; Watanuki, Y.; Moore, C.; Viet, P. H.; Tana, T. S.; Prudente, M.; Boonyatumanond, R.; Zakaria, M. P.; Akkhavong, K.; Ogata, Y.; Hirai, H.; Iwasa, S.; Mizukawa, K.; Hagino, Y.; Imamura, A.; Saha, M.; Takada, H. Transport and release of chemicals from plastics to the environment and to wildlife *Phil. Trans. Royal Soc. B.* **2009**, *364,* (2027-2045)

Thakur, K. A. M.; Kean, R. T.; Hall, E. S.; Kolstad, J. J.; Lindgren, T. A.; Doscotch, M. A.; Siepmann, J. I.; Munson, E. J. High-Resolution ^{13}C and ^{1}H Solution NMR Study of Poly(lactide) *Macromolecules* **1997**, *30,* (2422-2428)

Thatte, S.; Datar, K.; Ottenbrite, R. M. Perpsectives On: Polymeric Drugs and Drug Delivery Systems *Journal of Bioactive and Compatible Polymers* **2005**, *20,* (585-601)

The Society of Plastics Industry, Inc. **2012** [report] Bioplastics Industry Overview Guide

The truth about plastics Gordon, E. (ed.) *House Beautiful,* **1947,** October, 89 *(10) 120-296*

Thompson, R. C.; Swan, S. H.; Moore, C. J.; vom Sall, F. S. Our plastic age *Phil. Trans. R. Soc. B* **2009,** *364,* (1973-1976)

Thompsan, R.C.; Swan, S. H.; Moore, C. J.; vom Sall, F. S.  Our Plastic Age *Phil. Trans. Soc. B.* **2009,** *364,* (1973-1976)

Tong, J.-D.; Jerôme, R. Dependence of the Ultimate Tensile Strength of Thermoplastic Elastomers of the Triblock Type on the Molecular Weight between Chain Entanglements of the Central Block. *Macromolecules* **2000,** *33,* (1479–1481)

Torlon® PAI Emco Industrial Plastics, Inc. 2016 [Online] http://www.emcoplastics.com/materials/torlon-pai/ Accessed May 4th, 2016

Trucost  and UNEP Valuing Plastic: the business case for measuring, managing, and disclosing plastic use in the consumer goods industry June 2014 [Online] www.trucost.com/published-research/134/**valuing-plastic** Accessed May 19th, 2016

Tseng H. C., Prather K. L. Controlled biosynthesis of odd-chain fuels and chemicals via engineered modular metabolic pathways. *Proc Natl Acad Sci USA* **2012,** *109,* (17925-17930)

Tseng, Y., Darling, S. B. Block Copolymer Nanostructures for Technology *Polymers* **2010**, *2,* (470-489)

Tsui, A.; Wright, Z. C.; Frank, C. W. Biodegradable Polyesters from Renewable Resources *Annu. Rev. Chem. Biomol. Eng.* **2013,** *4,* (143-170)

Turner, R.B.; Nichols, J.B.; Kuklies, R.A. The Influence of Viscosity on Cell Opening of a Flexible Molded Foam *Journal of Cellular Plastics* **1989,** *25,* (117-124)

U.S. Energy Information Administration Annual Energy Review 2011 [Online] http://www.eia.gov/totalenergy/data/annual/ Accessed May 1st, 2016

van der Mee, L; Helmich, F.; de Bruijn, R.; Vekemans, J. A. J. M.; Palamans, A. R. A.; Meijer, E. W. Investigation of Lipase-Catalyzed Ring-Opening Polymerizations of Lactones with Various Ring Sizes: Kinetic Evaluation *Macromolecules* **2006**, *39,* (5021-5027)

Veld, P. J.; Velner, E. M.; Van de Witte, P.; Hamhuis, J.; Dijkstra, P. J.; Feijen, J. Melt Block Copolymerization of ε-Caprolactone and L-Lactide *Journal of Polymer Science Part A. Polymer Chemistry*  **1997**, *35, (219-226)*

Versteegen, R. M.; Kleppinger, R.; Sijbesma, R. P.; Meijer, E. W. Properties and Morphology of Segmented Copoly(ether urea)s with Uniform Hard Segments *Macromolecules* **2006,** *39,* (772-783)

Vincent, P. I. A correlation between critical tensile strength and polymer cross-sectional area *Polymer* **1972,** *13, (*558-560)

Vion, J.-M.; Jérome, R.; Teyssié, P.; Aubin, M.; Prud'homme, R. E. Synthesis, Characterization, and Micibility of Caprolactone Random Copolymers *Macromolecules* **1986,** *19,* (1828-1838)

Wanamaker, C. L.; Bluemle, M. J.; Pitet, L. M.; O'Leary, L. E.; Tolman, W. B.; Hillmyer, M. A. Consequences of Polylactide Stereochemistry on the Properties of Polylactide-Polymenthide-Polylactide Thermoplastic Elastomers *Biomacromolecules* **2009,** *10,* (2904-2911)

Wanamaker, C. L.; O'Leary, L. E.; Lynd, N. A.; Hillmyer, M. A.; Tolman, W. B. Renewable-Resource Thermoplastic Elastomers Based on Polylactide and Polymenthide *Biomacromolecules* **2007,** *8,* **(**3634-3640)

Wanamaker, C. L.; Tolman, W. B.; Hillmyer, M. A. Hydrolytic Degradation Behavior of a Renewable Thermoplastic Elastomer *Biomacromolecules* **2009,** *10,* (443-448)

Wang, S.; Kesava, S. V.; Gomez, E. D.; Robertson, M. L. Sustainable Thermoplastic Elastomers Derived from Fatty Acid *Macromolecu*les **2013,** *46,* (7202-7212)

Wang, S.; Robertson, M. L. Thermodynamic Interactions between Polystyrene and Long–Chain Poly(n-Alkyl Acrylates) Derived from Plant Oils *ACS Applied Materials and Interfaces* **2015,** *1,* (12109-12118)

Wang, Y.; Hillmyer, M. A. Synthesis of Polybutadiene-Polylactide Diblock Copolymers Using Aluminum Alkoxide Macroinitiatiors. Kinetics and Mechanism *Macromolecules,* **2000,** *33,* (7395-7403)

Widin, J. M.; Schmitt, A. K.; Im, K.; Schmitt, A. L.; Mahanthappa, M. K. Polydispersity–Induced Stabilization of a Disordered Bicontinuous Morphology in ABA triblock copolymers, *Macromolecules,* **2010,** *43,* (7913-7915)

Widjaja, L. K.; Kong, J. F. Chattopadhyay, S.; Lipik, V. T.; Liow, S. S.; Abadie, M. J. M.; Venkatraman, S. S. Triblock copolymers of ε-caprolactone, trimethylene carbonate, and L-lactide: Effects of using random copolymer as hard-block *Journal of the Mechanical Behavior of Biomedical Materials* **2012,** *6,* (80-88)

Widjaja, L. K.; Kong, J. F.; Chattopadhyay, S.; Lipik, V.T.; Liow, S. S.; Abadie, M. J. M.; Venkatraman, S. S. Triblock copolymers of of ε-caprolactone, trimethylene carbonate, and L-lactide: Biodegradability and elastomeric behavior *Journal of Biomedical Materials Research A* **2011,** *99A,* (38-46)

Wijaya, Y. P.; Suh, D. J.; Jae, J. Production of renewable p-xylene from 2,5-dimethylfuran via Diels-Alder cycloaddition and dehydrative aromatization reactions over silica-aluminum aerogel catalysts *Catalyst Communications* **2015,** *5,* (12-16)

Williams, C. L.; Chang, C.-C.; Do, P.; Kikbin, N.; Caratzoulas, S.; Vlachos, D. G.; Lobo, R. F.; Fan, W.; Dauenhauer, P. J. Cycloaddition of Biomass-Derived Furans for Catalytic Production of Renewable p-Xylene *ACS Catal.* **2012,** *2,* (935-939)

Wolf, J. H.; Hillmyer, M.A.; Ordered Nanoporous Polycyclohexylethylene *Langmuir* **2003,** *19* (6553-6560)

Woods, G. *The ICI Polyurethanes Book 2<sup>nd</sup> Ed.* **1990**

World Economic Forum, Ellen MacArthur Foundation and McKinsey and Company, The New Plastics Economy Rethinking the Future of Plastics **2016**, http://www.ellenmacarthurfoundation.org/publications

Wu, Z.;  Wang, Z.; Wang, G.; Tan, T. Improved 1,3-propanediol production by engineering the 2,3-butanediol and formic acid pathways in integrative recombinant Klebsiella pneumoniae. *J Biotechnol* **2013**, *168(2),* (194-200)

Xiong, M.; Schneiderman, D.K., Bates, F.S.; Hillmyer, M.A.; Zhang, K.  Scalable production of mechanically tunable block polymers from sugar. Proceedings of the National Academy of Sciences, **2014**, *111,* (8357-8362)

Xu, C.; Arancon, R. A. D.; Labidi, J.; Luque, R. Lignin depolymerization strategies: toward valuable  chemicals and fuels *Chem. Soc. Rev.* **2014**, *43,* (7485-7500)

Xu P., Gu, Q.; Wang, W.; Wong, L.; Bower, A. G.; Collins, C. H.; Koffas, M. A. Modular optimization of multi-gene pathways for fatty acids production in *E. coli. Nat Commun* **2013**, *4,* (1409-1417)

Xu, Y.; Petrovic, Z.; Das, S.; Wilkes, G. L. Morphology and properties of thermoplastic polyurethanes with dangling chains in ricinoleate-based soft segments *Polymer* **2008**, *49,* (4248-4258)

Yanagishita, Y.; Kato, M.; Toshima, K.; Matsumura, S. Chemoenzymatic Synthesis and Chemical Recycling of Sustainable Polyurethanes *ChemSusChem* **2008**, *1,* (133-142)

Yang J.; Xian, M.; Su, S.; Zhao, G.; Nie, Q.; Jiang, X.; Zheng, Y.; Liu, W. Enhancing production of bio-isoprene using hybrid MVA pathway and isoprene synthase in *E. coli. PLoS One* **2012**, *7,* (27-34)

Yang, W.; Dong, Q.; Liu, S.; Xie, H.; Liu, L.; Li, Jinhui Recycling and disposal methods for polyurethane foam wastes  *Procedia Enviromental Sciences* **2012**, *16,* (167-175)

Yang, W.P.; Macosko, C. W.; Wellinghoff, S. T.; Thermal degredation of urethanes based on 4,4'-diphenylmethane diisocyanate and 1,4-butane diol (MDI/BDO) *Polymer* **1986,** *27,* (1235-1241)

Yao, K; Tang, C. Controlled Polymerization of Next-Generation Renewable Monomers and Beyond *Macromolecules* **2013**, *46,* (1689-1712)

Yarsley, V.E.; Couzens, E.G. *Plastics,* **1941**, Pelican Books, New York, USA

Yasmin S.; Alcazar-Fuoli, L.; Gründlinger, M.; Puempel, R.; Cains, T.; Blatzer, M.; Lopez, J. F.; Gimalt, J. O.; Bignell, E.; Haas, H. Mevalonate governs interdependency of ergosterol and siderophore biosyntheses in the fungal pathogen *Aspergillus fumigatus. Proc Natl Acad Sci USA* **2012***,* *109,* (E497-504)

Yeganeh, H.; Mehdizadeh, M. R. Synthesis and properties of isocyanate curable millable polyurethane elastomers based on castor oil as a renewable resource polyol *European Polymer Journal* **2004,** *40,* **(**1233-1238)

Yevstropov, A.A.; Lebedev, B.V.; Kulagina, T. G.; Calorimetric study of δ-Valerolactone, poly-δ-valerolactone and of the process of polymerization of δ-valerolactone in the 13.8 to 340 K temperature range *Vysokomolekuliarnye soedineniia. Seriia A* **1982,** *24,* (568-574)

Yevstroprov, A. A. Lebedev, B.V.; Kulagina, T.G.; Lyudvig, Ye. B.; Belenkaya, B.G., The thermodynamic properties of β-propiolactone, its polymer, and its polymerization in the 0-400 K range *Polym. Sci.* USSR, **1979,** *21,* (2249-2256)

Yilgör, I.; Yilgor, E.; Wilkes, G. L. Critical parameters in designing segmented polyurethanes and their effect on morphology and properties: A comprehensive review *Polymer* **2015,** *58,* (A1-A36)

Yim H.; Haselbeck, R.; Niu, W.; Pujol-Baxley, C.; Burgard, A.; Boldt, J.; Khandurina, J.; Trawick, J. D.; Osterhout, R. E.; Stephen, R.; Estadilla, J.; Teisan, S.; Schreyer, H. B.; Andrae, S.; Yang, T. H.; Lee, S. Y.; Burk, M. J.; Van Dien, S. Metabolic engineering of *Escherichia coli* for direct production of 1, 4-butanediol. *Nat Chem Biol* **2011,** *7, (*445-452)

Young, W.; Kuan, W., and Epps, T. H., III, Block Copolymer Electrolytes for Rechargeable Lithium Batteries *Journal of Polymer Science B: Polymer Physics* **2014,** *52,* (1-16)

Yu, J. M.; Dubois, P.; Jerome, R. Synthesis and Properties of Poly(isobornyl methacrylate (IBMA)-*b*-butadiene (BD)-*b*-IMBA Copolymers: New Thermoplastic Elastomers of a Large Service Temperature Range *Macromolecules* **1996,** *29, (*7316-7322)

Zalusky, A. S.; Olayo-Vales, R.; Wolf, J. H.; Hillmyer, M.A. Ordered Nanoporous Polymers from Polystyrene-Polylactide Block Copolymers *J. Am. Chem. Soc.* **2002,** *124,* (12761-12773)

Zhang, C.; Kessler, M. R. Bio-based Polyurethane Foam Made from Compatible Blends of Vegetable-Oil- Based Polyol and Petroleum-based Polyol *Sustainable Chemsitry and Engineering* **2015,** *3,* (743-749)

Zhang, C.; Madbouly, S.; Kessler, M. Bio-Based Polyurethanes Prepared from Different Vegetable Oils *ACS Applied Materials and Interfaces* **2015,** *7,* (1226-1233)

Zhang, D. Hillmyer, M. A.; Tolman, W. B. Catalytic Polymerization of a Cyclic Ester Derived from a "Cool" Natural Precursor *Biomacromolecules* **2005**, *6,* (2091-2095)

Zhang, L.; Jeon, H.; Malsam, J.; Herrington, R.; Macosko, C. Substtuting soybean oil-based polyol into ployurethane flexible foams *Polymer,* **2007,** *48,* (6656-6667)

Zhang, Z.; Grijpma, D. W.; Feijen, J.  Thermoplastic elastomers based on poly(lactide)-poly(trimethylene carbonate-co-caprolactone)-poly(lactide) triblock copolymers and their stereocomplexes  *Journal of Controlled Release* **2006,** *116,* (e29-e31)

Zhang, Z.; Grijpma, D. W.; Feijen, J. Triblock copolymers based on 1,3-Trimethylene Carbonate and Lactide as Biodegradable Thermoplastic Elastomers *Macromol. Chem. Phys.* **2004**, *205,* (867-875)

Zhao, J.; Hadjichristidis, N. Polymerization of 5-alkyl-δ-Lactones catalyzed by diphenyl phosphate and their sequential organocatalytic polymerization with monosubstituted epoxides *Polymer. Chem.* **2015,** *6,* (2659-2668)

Zhu, J.; Thakker, C.; San K.-Y.; Bennett, G. Effect of culture operating conditions on succinate production in a multiphase fed-batch bioreactor using an engineered Escherichia coli strain. *Appl Microbiol Biotechnol* **2011,** *92(3)*, (499-508)

Zlatanic, A.; Lava, C.; Zhang, W.; Petrovic, Z. S. Effect of Structure on Properties of Polyols and Polyurethanes Based on Different Vegetable Oils *Journal of Polymer Science Part B: Polymer Physics* **2004**, *42,* (809-819)